**TECHNICKÁ UNIVERZITA V LIBERCI**

**FAKULTA STROJNÍ**

**KATEDRA MATERIÁLU**

# DISERTAČNÍ PRÁCE

**2011**

**Ing. Nguyen Thang Xiem**

**TECHNICKÁ UNIVERZITA V LIBEREC**
**FAKULTA STROJNÍ**
**KATEDRA MATERIÁLU**

**STUDIJNÍ OBOR: 2303V002**
**STROJÍRENSKÁ TECHNOLOGIE**
**ZAMĚŘENÍ: MATERIÁLOVÉ INŽENÝRSTVÍ**

# POTENCIÁLNÍ VYUŽITÍ GEOPOLYMERNÍCH MATERIALŮ V OBLASTI ZPRACOVÁNÍ ODPADŮ

## THE POTENTIAL APPLICATIONS OF GEOPOLYMER MATERIALS IN WASTE PROCESSING

**ŠKOLITEL:** **Prof. Ing. Petr Louda, CSc.**

| **ROZSAH PRÁCE** | | |
|---|---|---|
| | POČET STRAN | 162 |
| | POČET OBRÁZKŮ | 120 |
| | POČET TABULEK | 27 |
| | POČET PŘÍLOH | |

## MÍSTOPŘÍSEŽNÉ PROHLÁŠENÍ

Prohlašuji, že:

Obsah disertační práce je mým vlastním dílem a neosahuje žádné informace, které by byly publikovány jinými autory než autory, kteří jsou uvedeni v odkazech. Žádná část práce nebyla využita pro jinou než tuto disertační práci.

Beru na vědomí, že Technická univerzita v Liberci (TUL) nezasahuje do mých autorských práv užitím mé disertační práce pro vnitřní potřebu TUL.

Užiji-li disertační práci nebo poskytnu-li licenci k jejímu využití, jsem si vědom povinnosti informovat o této skutečnosti TUL. V tomto případě má TUL právo ode mne požadovat úhradu nákladů, které vynaložila na vytvoření díla až do jejich skutečné výše.

Byl jsem seznámen s tím, že na mou disertační práci se plně vztahuje zákon č. 121/2000 Sb., 0 právu autorském, zejména §60 (školní dílo).

Datum: 11.2011

Ing. Nguyen Thang Xiem

## DECLARATION

1 hereby declare that:

To the best of my knowledge, the content of the thesis is original in my own work and contains no material which has been previously published by other people, except references that are stated. No part of this work has been submitted for the award of any other degree or diploma in any universities.

It is totally no problems in my copyright when this PhD-thesis work is used for internal purposes of Technical University of Liberec (TUL).

The thesis text, exclusive of tables, figures and appendices are applied to my PhD-dissertation in full with the notification of Copyright Act. No. 121/2000 Coll. and satisfied the Section 60 (School Work).

Date: 11.2011

Ing. Nguyen Thang Xiem

# ACKNOWLEDGMENT

The author is very grateful and many thanks to my supervisor Prof. Ing. Petr Louda, CSc for his guidance, supporting, advice, encouragement and the financial support throughout my study in more than three years.

I am also grateful to Doc. Ing. Dora Kroisová, PhD for the support to perform experiments during my work, help me edited and giving valuable feedback for my thesis.

The help provided by Prof. Ladislav Pešek of the Department of Materials Science, Faculty of Metallurgy, Technical University of Košice in Slovakia to obtain the complete impact and climate chamber testing for geopolymer mortar and concrete is also gratefully acknowledged.

I would like to respect Doc. Ing. Jan Jersák, CSc. for his helpful advice about testing the machinability of geopolymer mortar on the traditional machine.

I would like to respect my teachers in Department of Material Science, Faculty of Mechanical Engineering, Technical University of Liberec. They are so kind to me during my study here.

I would like to thank the financial support and contributions of the Project Ministry of Education of the European Social Fund (ESF) - Operational Program VaVpI under the project "Center for nano materials, advanced technology and innovation", CZ.1.05/2.1.00/ 01.0005 and by project "Innovation Research in Material Engineering" of PhD student Grant TUL.

I also would like to thank all colleagues and staffs in my department, including Ing. Pavel Kejzlar, Miss. Petra Zdobinská, Ing. Zbigniew Rozek, Ing. Petra Prokopčáková, Ph.D, Ing. Vladimír Nosek, Ing. David Pospíšil, Mr. Milan Vyvlečka, RNDr. Věra Vodičková, Ph.D., Ing. Adam Hotař, Ph.D, Ing. Pavel Hanus, Ph.D, Ing. Daniela Odehnalová, Mrs. Hana Šiftová, and young Vietnamese students who help me to do experiments and testing for my research.

Finally, I wish to thank all of my family back in Vietnam. These include my parents, my father in-law, my wife Huong and son Hung. If it were not for their dedication, endearing support, and personal sacrifices during the time I spent studying in here.

Thank you very much to all of the others whom I forget to mention specifically.

**Nguyen Thang Xiem**

Liberec, November 2011

# TABLE OF CONTENTS

# LIST OF FIGURES

# LIST OF TABLES

# PREFACE

Since the chemistry of geopolymer materials was discovered, many scientists have studied these new materials and investigated all properties of them as they apply to our live. Geopolymers have emerged as a promising new material for coatings and adhesives, a new binder for fiber composites, new cement for mortar or concrete and environmentally sustainable properties. Geopolymers have attracted the interest of scientists due to their excellent fire resistance, low density, low cost, low curing/hardening temperatures, easy processing, excellent mechanical properties, environmentally friendly nature, long-term durability, heavy metal ions fixation and acid resistance. The wide variety of potential applications of geopolymers as following: high-tech composites for aircraft interior and automobile, new ceramics, cements and concretes, matrices for hazardous waste stabilization, fire resistant materials and thermal insulation, sculpture and history of sciences.

From 2009, our laboratory realizes important research on the development, manufacture, behavior, and applications of waste materials (fly ash, stone powder and sand powder) based geopolymer mortar and concrete. In our study, we used the fly ash came from different sources of power plants in Czech republic. With silicon and alumina as the main constituents, fly ash has great potential as source material to make the binder necessary to manufacture mortar and concrete. Utilization of these materials may improve the microstructure, mechanical and durability properties of mortar and concrete, which are difficult to achieve by the use of pure Portland cement.

In this research, geopolymer resin was synthesized from shale fly dust burnt in rotary kiln (for 10 hours at 750 $^{o}$C) with Si/Al molar ratio of 2.0 with sodium hydroxide (NaOH) and sodium silicate ($Na_2SiO_3$). The purpose of this research is observing the influence of adding different kinds of fly ash, fibers in order to obtain the engineering properties (including compressive strength, impact energy, splitting tensile strength, flexural strength and modulus of elasticity) of geo mortar and concrete. Some values of these material properties are not independent but affect each other, and therefore a method for determining the input material properties is developed based on a previous experiment. The optimal curing conditions (both at elevated

temperature and at ambient conditions) and different curing time are investigated. In addition, preliminary study about the machinability of geopolymer material on the traditional machine are carried out and ability applications in industry.

We think that this study is necessary to offer such a work at the moment when the industry is changing so much. We are happy to participate and assist the industries to take the geopolymer concrete technology to the communities in construction applications. We hope that our work is a small step towards a broad vision to serve the communities for a better future.

***Key words:*** *fly ash, geopolymer mortar, geopolymer concrete, activator, commercial fibers, curing conditions, mechanicalproperty, microstructure.*

# PŘEDMLUVA

Od doby objevu chemie geopolymerů, mnozí vědci zkoumali tyto materiály a prověřovali všechny jejich vlastnosti a možné aplikace pro náš život. Geopolymery se ukázaly jako nový nadějný materiál pro nátěry a lepidla, nové pojivo pro vláknové kompozity, cement na maltu nebo beton s ekologicky přijatelnými vlastnostmi. Geopolymery přilákaly zájem vědců díky své vynikající požární odolnosti, nízké hustotě, nízkým nákladům, nízké teplotě vytvrzení, snadnému zpracování, výborným mechanickým vlastnostem, šetrnosti k životnímu prostředí, dlouhodobé životnosti, schopnosti fixovat ionty těžkých kovů a odolnosti vůči kyselinám. Spektrum potenciálních aplikací geopolymerů je velmi široké: high-tech kompozitní materiály pro letecký a automobilový interiér, nové keramiky, cementy a betony, matrice pro stabilizaci nebezpečných odpadů, ohnivzdorné materiály a tepelné izolace.

Od roku 2009, naše laboratoř provedla důležitý výzkum vývoje, výroby, chování a použití odpadů (popílek, kamenný prach a písek) v geopolymerní maltě a betonu. V naší studii jsme použili popílky pocházející z různých zdrojů, z různých elektráren v České republice. Popílek s křemíkem a hliníkem, coby hlavními složkami, má velký potenciál jako zdrojový materiál k přípravě pojiva potřebného k výrobě malty a betonu. Užití těchto materiálů může zlepšit mikrostrukturu a tak i mechanické vlastnosti a odolnost malty a betonu na hodnoty, kterých je jinak, u portlandského cementu, obtížné dosáhnout.

V tomto výzkumu byla geopolymerní pryskyřice syntetizována břidličným popílkem z rotační pece (na 10 hodin při 750 °C) s Si/Al o molárním poměru 2,0 s hydroxidem sodným (NaOH) a křemičitanem sodným ($Na_2SiO3$). Cílem tohoto výzkumu je sledování vlivu různých druhů přidaných popílků a vláken za účelem získání lepších mechanických vlastností (včetně pevnosti v tlaku, v tahu, v ohybu, rázové energie a modulu pružnosti) Geo malty a betonu. Některé hodnoty těchto vlastností nejsou nezávislé a vzájemně se ovlivňují. Proto metoda pro stanovení vlastností vstupního materiálu je založena na základě předchozího experimentu. Byly zkoumány optimální vytvrzovací podmínky (jak při zvýšené teplotě tak za normálních podmínek). Kromě toho je předběžně studována i obrobitelnost geopolymerních materiálů prováděná na tradičních strojích, a možná aplikace v průmyslu.

Myslíme si, že tuto studii je potřebné nabídnout v okamžiku, kdy se průmysl tolik mění. Jsme rádi, že se můžeme účastnit a pomáhat tak přiblížit společnosti využití technologie geopolymerního betonu ve stavebním průmyslu. Doufáme, že naše práce je první malý krok k naplnění vize lepší budoucnosti naší společnosti.

***Key words:*** *popílek, geopolymerní malta, geopolymerní beton, activátor, komerční vlákna, vytvrzení, mechanické vlastnosti, mikrostruktury.*

# Chapter 1

# INTRODUCTION

## 1.1 GENERAL

The most widely used construction material is concrete, commonly made by mixing Portland cement with aggregates (coarse and fine), chemical admixtures, mineral admixtures, and water [1]. Concrete has been the construction material used in the largest quantity for several decades. Today, the rate at which concrete is used is much higher than it was 40 years ago. The worldwide consumption of concrete is estimated to be about 11 billion tons every year. Due to increase in infrastructure developments, the demand for concrete would increase in the future [2-5].

There are at least three fundamental reasons to the most widely used concrete. First, concrete possesses excellent resistance to water. The second is the easy synthesis from many elements with different shapes and sizes. The third reason is that concrete is usually cheaper than steel, plastics or wood and the most available material on earth. The principal components for making concrete, namely aggregate, water, and Portland cement are relatively cheap and are commonly available in most parts of the world [3, 6].

The definitions of concrete from ASTM C 125 and ACI Committee 116 as following: *"Concrete is a composite material that consists essentially of a binding medium within which are embedded particles or fragments of aggregate. In hydraulic-cement concrete, the binder is formedfrom a mixture of hydraulic cement and water"* [3].

Aggregate is the granular material, such as sand, gravel, crushed stone, crushed blast-furnace slag and recycled concrete that is used with a cementing medium to produce either concrete or mortar. The term coarse aggregate refers to the aggregate particles larger than 4.75 mm, and the term fine aggregate (sand) refers to the aggregate particles smaller than 4.75 mm but larger than 75 p,m [3].

Mortar is a workable paste used to bind construction blocks together and fill the gaps between them. Modern mortar is typically made from a mixture of sand, cement or lime, and water. It is like concrete without a coarse aggregate [3].

Cement is a binder, a substance that sets and hardens independently, and can bind other materials together. The most commonly used hydraulic cement to product concrete is Ordinary Portland cement (OPC), which consists essentially of reactive calcium silicates; the calcium silicate hydrates formed during the hydration of Portland cement are primarily responsible for its adhesive characteristic, and are stable in aqueous environment. However, as we all know that the manufacture of OPC releases large amount of $CO_2$ (from 74% to 81% of the total CO2 emissions of concrete) to the atmosphere, because the process of chemical reaction creates CO2 from the calcinations of limestone (calcium carbonate - CaCO3) at very high temperatures (about 1450°C) with a source of silica according to the reaction:

3CaCO3 + SiO2 ^ CasSiO5 + 3CO2

The production of one ton of OPC emits approximately one ton of CO2 to the atmosphere, including 0.55 tons of chemical $CO_2$ and an additional 0.39 tons of $CO_2$ in fuel emissions for baking and grinding [3, 7-10]. Fig. 1.1 shows the projections for the global demand of the main binder OPC of concrete structures. Global demand will have increased almost 200% by 2050 from 2010 levels. This is particularly serious in the current context of climate change caused by carbon dioxide emissions worldwide, causing a rise in sea level and the occurrence of natural disasters and being responsible for a future meltdown in the world economy [11, 12].

Furthermore, each one of us and especially factories are generated large quantities of waste materials per day, such as: water, oils, solvents and solid waste (fly ash, glass, stone powder, mine tailings, etc). As a result, solid waste management has become one of the major environmental concerns in the world. Utilization of these materials not only help in getting them utilized in cement, mortar, concrete, and other building materials, it also helps in reducing the cost of manufacturing a product, and also has numerous indirect benefits such as saving in energy, and significantly reducing the emission of green - house gas $CO_2$ released from cement and concrete manufacturing. This is beneficial for resource conservation,

environmental protection and ecological damages caused by quarrying and exploitation of the raw materials for making cement [13, 14].

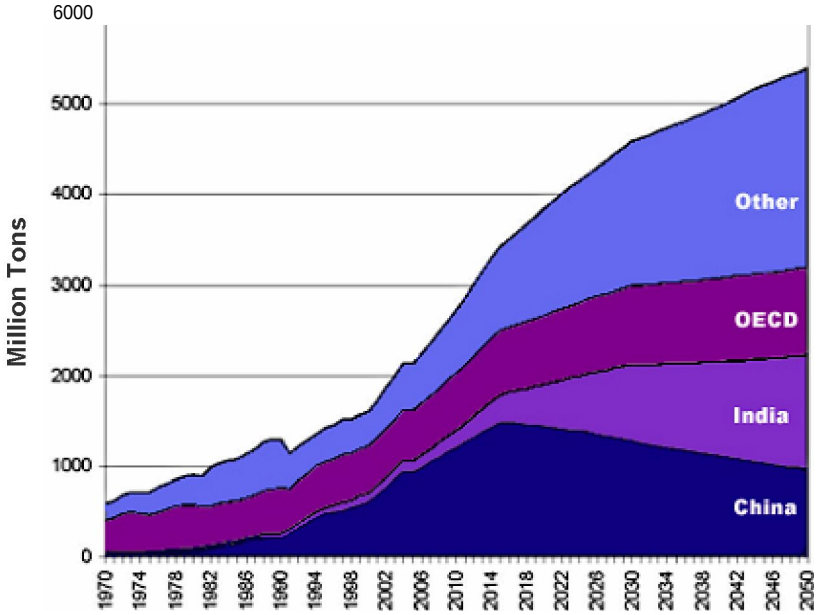


**Fig. 1.1** Global cement demand by region and country [15]

Recently, geopolymers have emerged as a promising new material with environmentally sustainable properties [7, 16, 17]. They are a new material for coatings and adhesives, a new binder for fiber composites, and new cement for concrete [18-20]. Geopolymer cements are a class of inorganic polymers formed by the reaction between an alkali-activated and an aluminosilicate source [19]. These materials have a structure that gives geopolymers properties which make them an ideal substitute for Ordinary Portland Cement (OPC) in a whole range of applications. Geopolymers possess many advantages comparing with OPC as the following:

- Abundant raw materials resources [8].
- Energy saving and environment protection: geopolymers do not require large energy consumption. Thermal processing of natural aluminosilicates at relative low temperature (600° to 800°) provides suitable geopolymeric raw materials, resulting in 3/5 less energy assumption than OPC [8, 19].
- Simple preparation technique: Geopolymer can be synthesized simply by mixing aluminosilicate reactive with alkaline solutions, then curing at room temperature [8].

- Excellent heavy metal immobilization [21, 22].
- High fire resistant (up to 1000 $^{o}$C) and high temperature stability, low shrinkage and low thermal conductivity [14, 20, 23, 24].
- Good volume stability, good acid resistance and salt solutions [14, 20, 25].
- Ultra-excellent durability and high compressive strength [8, 14, 20, 26].
- Quick solidification with high strength, high surface definition that replicates mould patterns [20, 26, 27].

Davidovits described four basic forms of silicoaluminate structures corresponding to Si:Al ratios of 1, 2, 3 and greater than 3 as poly(sialate), poly(sialate-siloxo), poly(sialate-disiloxo), and poly(sialate-multisiloxo) [19, 27]. In our study, recommended application of geopolymer cements were synthesized shale fly dust from rotary kiln. And the purpose of this thesis is research about the effect of adding fly ash and other waste materials on mechanical properties of geopolymer mortar and concrete.

## 1.2 AIMS OF THE RESEARCH

The present study dealt with the manufacture and structural applications of reinforced fly ash based geopolymer mortar and concrete. The aims of this study were:

- Analysis microstructure and chemical composition of pure geopolymer and fly ash.
- Mechanical properties of geopolymer mortar after modified fly ash particles by high temperature and milling.
- The optimum the percent values by mass of fly ash content in geopolymer mortar and concrete.
- The effect of curing different time and condition on mechanical properties of geopolymer mortar and concrete.
- The effect of high temperature on mechanical properties of geopolymer mortar and concrete.
- The effect of commercial fibers reinforced on the mechanical properties of geopolymer mortar.

- The effect of water and/or alkaline solution to liquids/fly ash ratio in geopolymer mortar and concrete.
- Durability/resistance to degradation: Acid sulfuric attack, freeze-thaw resistance, wet-dry. And effect of chemical reagent on the mechanical properties of pure geopolymer, mortar and concrete.
- The machinability of geopolymer mortar on the traditional machine.
- Ability applications in industry.

## 1.3 OUTLINE OF THE DISSERTATION

The dissertation is arranged as follows:

Chapter 1 describes a short introduction to the subject of thesis.

Chapter 2 describes the overview of the recent literature concerning the subject of thesis, including a brief literature review of geopolymer technology and fly ash.

Chapter 3 presents the geopolymer resin, characterization of fly ash and experimental part of the research including methods of calculations.

Chapter 4 describes the effect of types of fly ash, the ratio alkaline liquid and water, curing (times and conditions) on the mechanical properties of geopolymer mortar.

Chapter 5 investigates the effect of modified fly ash particles by wet milling and high temperature on the chemical composition, color, and particle size of fly ash and on the mechanical properties of geopolymer mortar.

Chapter 6 presents the optimum the percent values by mass of fly ash content in geopolymer mortar and concrete curing at room temperature.

Chapter 7 describes the effects of high temperature and environment conditions on mechanical properties of geopolymer mortar and concrete.

Chapter 8 describes the effects of commercial fibers on mechanical properties of geopolymer mortar and concrete. This chapter also provides the structure of geopolymer mortar, concrete and properties of fibers used in this study.

Chapter 9 presents the machinability of geopolymer material on the traditional machine and potential applications of geopolymer mortar or concrete in industries.

Chapter 10 presents the potential applications.

Chapter 11 presents the conclusion of the research and some recommendations for the directions of future research in the field of geopolymers.

# Chapter 2

# LITERATURE REVIEW

## 2.1 INTRODUCTION

There are three main purposes in preparing this chapter. First, it is provide background knowledge about structure, synthesis and chemistry of geopolymer materials. Second, it is introduce technologies to utilize fly ash into added-value products. One successful alternative would be to utilize fly ash in the production of geopolymers. Geopolymers are environmental friendly materials with properties comparable to that of Portland concrete. Finally, it is potential applications of geopolymers, especially cement for infrastructure and building applications.

## 2.2 GEOPOLYMER TERMINOLOGY

This section presents a brief literature review of geopolymer terminology and chemistry.

In 1979, the term "geopolymer" was first discovered to the chemical world by a French professor Joseph Davidovits [27], they are inorganic polymeric materials with a chemical composition similar to natural zeolite but containing an amorphous microstructure and possessing ceramic-like in their structures and properties [19, 28-30]. Geopolymer are synthesized and hardened at ambient pressure and temperature, so the science can produce artificial stone at a temperature below 100 $^{o}$C [31, 32]. This material (geopolymer cement) evolved into a mineral-based binder for use as a high strength industrial cement with significantly shorter cure times than OPC [19]. There are two main constituents of geopolymers, namely the source materials and the alkaline liquids. The source materials for geopolymers based on alumina-silicate should be rich in silicon (Si) and aluminium (Al) such as metakaolinite, slag, geological, blast furnace slag, fly ash, rice husk ash, etc. The choice of the source materials for making geopolymers depends on factors such as availability, cost, type of application, and specific demand of the end users. The most common alkaline liquid used in geopolymerization is a combination of sodium hydroxide (NaOH) or potassium hydroxide (KOH) and sodium silicate ($Na_2SiO_3$) or potassium silicate ($K_2SiO_3$) [33, 34].

To discuss the chemical structure of geopolymers, the term 'sialate' is an abbreviation for silicon-oxo-aluminate and is used here to describe the bonding of silicon and aluminium by bridging oxygen. And the term poly(sialate) was suggested as a descriptor of silico-aluminate structure of the type of material [19, 29, 35]. The amorphous to semi-crystalline three dimensional of sialate network consists of SiO4 and AlO4 tetrahedral which are linked alternately by sharing all the oxygens to create basic polymeric Si-O-Al bonds (see in Fig. 2.1) [19, 29], so Prof. Davidovits called it geopolymer. To balance the negative charge of $Al^{3+}$ in IV fold coordination, positive ions sodium (Na+), potassium (K+), lithium (Li+), calcium ($Ca^{2}$+), barium ($Ba^{2}$+), ammonium ($NH_4$+), hydronium ($H_3O$+) must be present in the structural spaces [19].

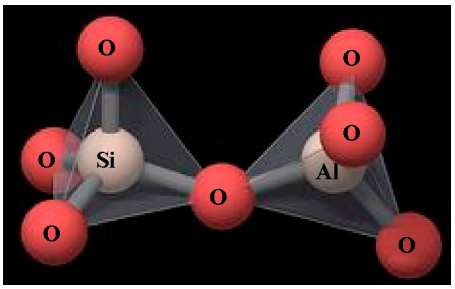


**Fig. 2.1** Tetrahedral configuration of sialate Si-O-Al-O; Si, Al atoms in white and O atoms in pink [19, 36]

Geopolymerization involves a chemical reaction between various aluminosilicate oxides $Al^{3}$+ in IV-V fold coordination with silicates, yielding polymeric Si-O-Al-O sialate bonds like the following:

$$2(Si2O5,AhO2) + K2(H_3SiO4)2 + Ca(H_3SiO4)2 \wedge (K2O,CaO)(8SiO2, 2AhO_3, nH2O) \quad (2\text{-}1)$$

Poly(sialates) are described by the following empirical formula [19, 27, 29, 37]:

$$M_n[- (SiO2)z - AlO2]n. wH2O , \quad (2\text{-}2)$$

where M is a monovalent cation such as potassium (K+) or sodium (Na+) , n is the degree of polycondensation and z is either 1, 2, 3 or >> 3. Poly(sialate) are described as chain and ring polymers with $Si^{4}$+ and $Al^{3}$+ in IV-fold coordination with oxygen and range in from amorphous to semi-crystalline.

Davidovits has also distinguished four types of polysialates according to the ratio Si:Al they are of the types:

| | | | |
|---|---|---|---|
| Poly(sialate): | $M_n$ - (- Si-O-Al-O-)n | M-PS | Si:Al=1:1 |
| Poly(sialate-siloxo) | Mn - (-Si-O-Al-O-Si-O-)n | M-PSS | Si:Al=2:1 |
| Poly(sialate-disiloxo) | Mn - (-Si-O-Al-O-Si-O-Si-O-)n | M-PSDS | Si:Al=3:1 |

Poly(sialate-multisiloxo), Si:Al >> 3:1, the polymeric structure results from the cross linking of poly(silicate) chains, sheets or networks with a sialate link (-Si-O-Al-O-) (2D or 3D cross-link).

Fig. 2.2 shows some examples of poly(sialate) molecular structures. The term poly(sialate) covers all geopolymers containing at least one (Na, K, Ca)-sialate unit and they involve at least four elementary units where z is 1, 2, 3 and higher. Geopolymerization forms aluminosilicate frameworks which are similar to those of rock-forming minerals. The structures shown in the figure below must be edited accordingly, with the exception of the sodalite ($Na_8Al_6Si_6O_{24}Cl_2$) framework. After dehydroxylation and dehydration, generally above 500 °C, geopolymers are becoming more and more crystalline with X-rays diffraction patterns and framework structures identical to their geological analogues [19].

z = 1 (Si:Al = 1)

Poly(sialate)

PS

*SOs* H AIO,

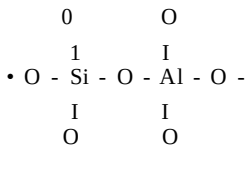


z = 2 (Si:Al = 2)

Poly(sialate-siloxo)

PSS

r f l

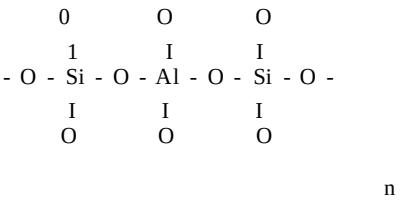


z = 3 (Si:Al = 3)

Poly(sialate-disiloxo)

PSDS

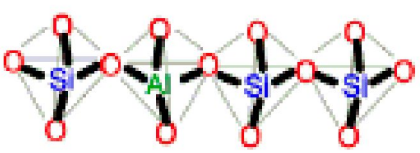


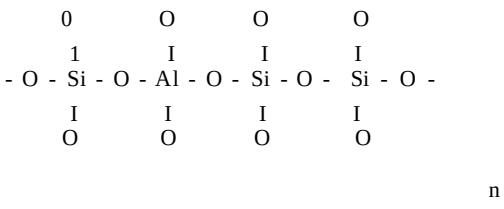

z > 3 (Si:Al > 3)

Sialate link

or Poly(sialate-multisiloxo)

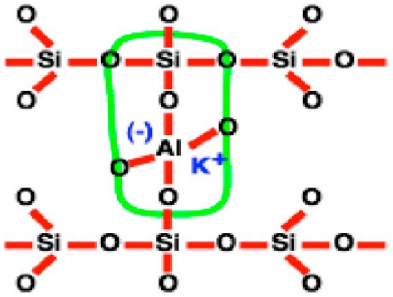


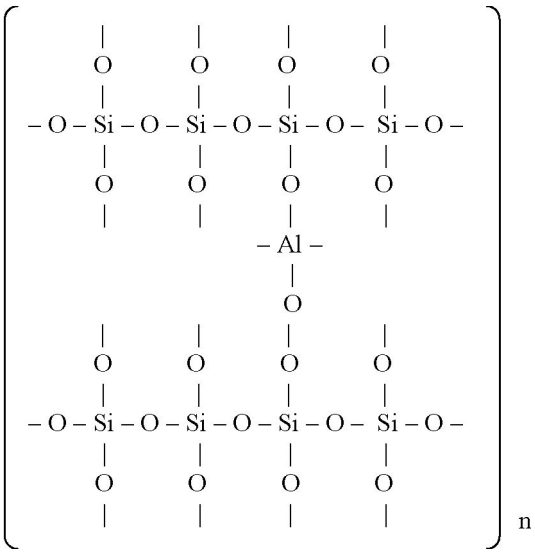


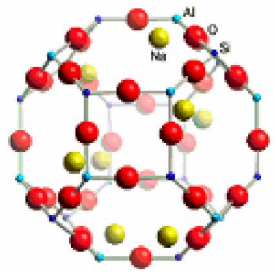

Sodium-Poly(sialate)
Na-PS (Sodalite)

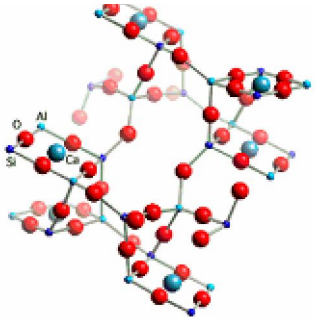

Calcium-Poly(disialate)
Ca-PS

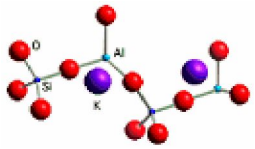

Potassium-Poly(sialate)
K-PS

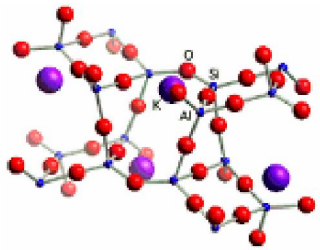

Potassium-Poly(sialate-disiloxo)
K-PSDS

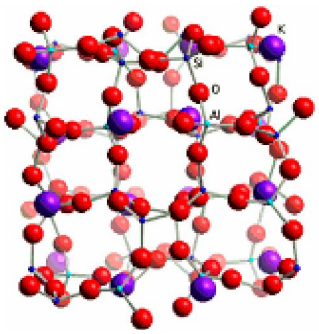

Potassium-Poly(sialate-siloxo)
K-PSS

**Fig. 2.2** Chemical structure of polysialates [19, 38]

## 2.3 THE GEOPOLYMERIZATION PROCESS

Many researches on the formation mechanism have been made since the invention of geopolymers, but only one formation mechanism was proposed by Prof. Davidovits. Because, geopolymerization is a complicated process, the exact process is not fully understood so far although the involved mechanism has been studied in the last 3 decades. Therefore, the understanding of geopolymerization process and its effective factors is useful for the application of geopolymeric materials. Davidovits explained that geopolymer synthesis consists of three steps dissolution of aluminosilicate under a strong alkali solution, reorientation of the free ion clusters, and polycondenzation but that each step includes many pathways [14, 39, 40].

The most proposed mechanisms for the geopolymerization process include the following four main stages [41, 42]:

(i) Dissolution of solid aluminosilicate sources in alkaline sodium silicate solution.

During this stage, Si and Al are transferred from the solid phase to the aqueous one. The dissolution results in the generation of soluble aqueous monomeric species of Si and Al. This type of dissolution is called congruent [14, 43]. For some researchers, the dissolution results in the release of oligomeric molecular units having composition, which is dependent on the type of the solid aluminosilicate raw material. This type of dissolution is called incongruent [19, 44]. There are not enough data to exclude either of the dissolution types. In the case of dissolution of industrial aluminosilicate minerals such as kaolin and feldspars, the incongruent type seems to be predominant. In the case of waste aluminosilicate materials with complex composition, the congruent type seems to be predominate [45].

(ii) Formation of Si and/or Si-Al oligomers in the aqueous phase.

In case of congruent type of dissolution, certain chemical reactions take place between the soluble aqueous monomeric species of Si and Al, resulting in the formation of the geopolymers precursors which are oligomeric species (polynuclear hydroxy-complexes) consisting of polymeric bonds of Si-O-Si and Si-O-Al type [46, 47].

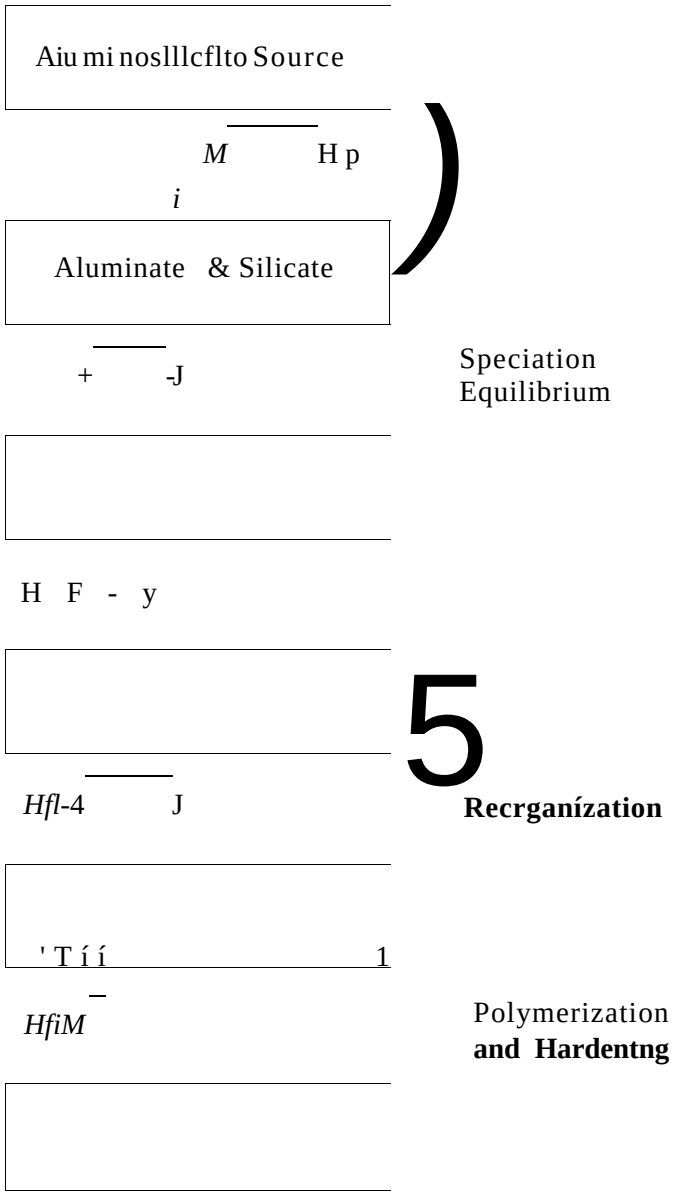


**Fig. 2.3** Conceptual model for geopolymerization [14]

(iii) Polycondensation of the oligomeric species or units in the aqueous phase to form an inorganic polymeric material [45].

(iv) The hardening of the gel that mean bonding of undissolved solid particles in the final geopolymeric structure [41, 45].

Fig. 2.3 presents a highly simplified reaction mechanism for geopolymerization. The reaction mechanism shown in the figure outlines the key processes occurring in the transformation of a solid aluminosilicate source into a synthetic alkali aluminosilicate.

Aluminosilicate materials containing aluminum in IV-fold coordination are necessary for the alkali activating process of geopolymerization. Should other coordinations of aluminum be present in the source materials for geopolymerization, the IV-fold aluminum will dominate the reaction and will be completely exhausted while aluminum (V) and aluminum (VI) remain unreacted unless converted to the less stable formation [48]. Aluminosilicates that are naturally occurring in the crust of the earth are the main sources of these materials, namely kaolinite, feldspars, mine tailings, volcanic ashes, as well as numerous other forms of minerals and clays. Other sources of materials that are rich in aluminum and silicon which can be used for geopolymerization include byproducts of industrial processes such as fly ash, which is the waste product of coal combustion plants, furnace slag, and construction residuals [49].

The process for the formation of the aluminum and silicon in IV-fold coordination typically follows one of two chemical processes. The most commonly applied method of obtaining these materials involves calcining aluminosilicate hydroxides such as kaolinite according to the reaction listed below [19, 29].

$$Si_2Al_2O5(OH)4 \text{ ^ } Al_2Si_2Oy + 2H_2O \quad (2\text{-}3)$$

In the studies, we represent the chemical structure of kaolinite and metakaolinite (main raw material for synthesizing geopolymer), were established to quantitatively analyze the formation process of a geopolymer.

*(a) Kaolinite*

The calcination of kaolinite process can complete itself at 600 $^{o}$C for 6 hrs [50]; between 600 and 750 $^{o}$C C for 10 hrs [51] or above 750 °C and can complete itself in only two hours dependence on source of materials [52]. The geopolymerization process itself is an exothermic polycondensation reaction involving alkali activation by a cation in solution. The reaction leading to the formation of a poly(sialate) geopolymer is described below [19, 53]:

$$(Al2Si2Oy)n + D \text{ ^ } O \xrightarrow{NaOH/\ KOH} - n(OH)3 - Si - O - Al(OH)3 \quad (2.4)$$

$$n(OH)3 - Si - O - \overset{(-)}{Al}(OH)3 \xrightarrow{NaOH/\ KOH} - (K+/Na+)(- \overset{i}{Si} - O - \overset{i\ (-)}{Al} - O)n + 3nH2O \quad (2.5)$$

O O

Orthosialate (K/Na)-Poly(sialate)

Additional amounts of amorphous silica must be present in order to form either the poly(sialate-siloxo) or poly(sialate-disiloxo) structures of geopolymers. The reaction for the poly(sialate-siloxo) formation is also provided as an illustration of how the two reactions differ [19, 53].

$$(Al_2Si_2O_y)_n + nSiO_2 + n\,\wedge O \xrightarrow{NaOH/K_o} n(OH)_3 - Si - O - Al - O - Si - (OH)_3 \quad (2\text{-}6)$$

$$n(OH)_3 - Si - O - \overset{(-)}{\underset{i}{Al}} - O - Si - (OH)^* \xrightarrow{NaOH/KOH} (K+/Na+)(- \underset{i}{Si} - O - \underset{i}{Al}^{(-)} - O - \underset{i}{Si} - O -)_n + nH_2O \quad (2\text{-}7)$$

Oligo(sialate-siloxo) (K/Na)-Poly(sialate-siloxo)

It has been assumed that the geo-chemical syntheses are carried out through hypothetical oligomers (dimer, trimer). Further polycondensation of these hypothetical building units provided the actual structures of three dimensional macromolecular edifice as presented from Equations (2-4) to (2-7) [19, 53].

*(b) Metakaolinite*

When kaolinite is heated to a temperature of 450 °C dehydroxylation occurs and the hydrated aluminosilicates are converted to materials consisting predominantly of chemically combined aluminium, silicon and oxygen. The rate at which water of crystallization is removed increases with increasing temperature and at 600 °C it proceeds to completion [54, 55].

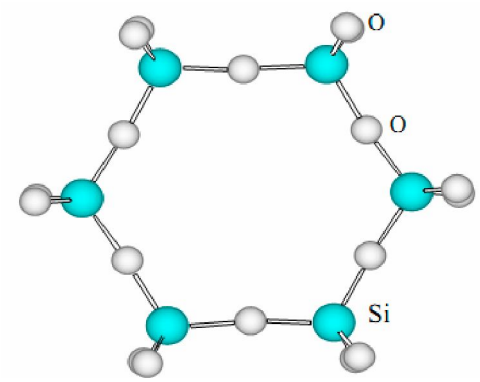


6-memner rings structure cluster of $SiO_4$ tetrahedral

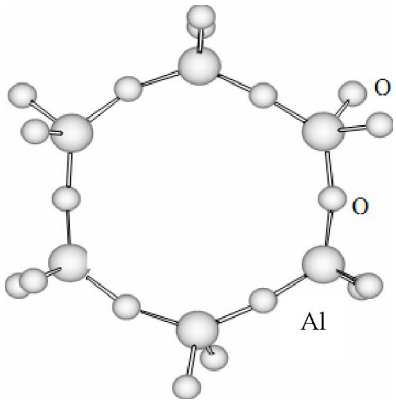


6-memner rings structure cluster of $SiO_4$ tetrahedral

**Fig. 2.4** Molecular structure representing model of metakaolinite [8]

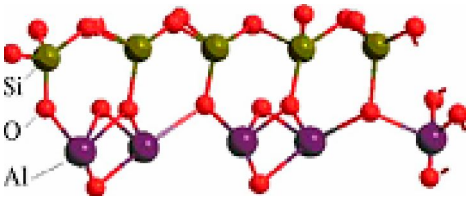


flfóCúitfUOliúiH

**decúnsLíLidLĭnn (I ljO,OE I',Níi ' J**

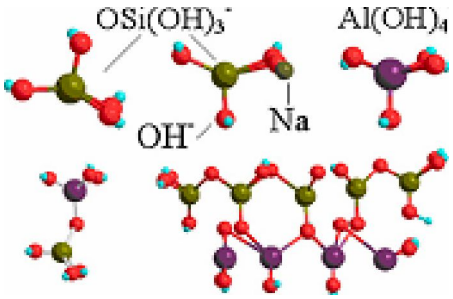


Si-O-Al opevníš residual parlicte

póly me rizali 011

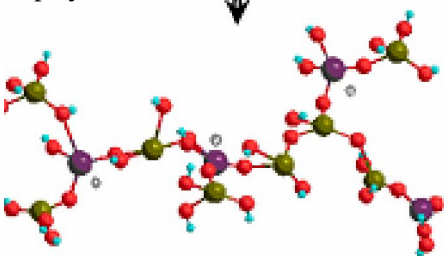

íjiiail cacenulaie gelí

stzbilization ^

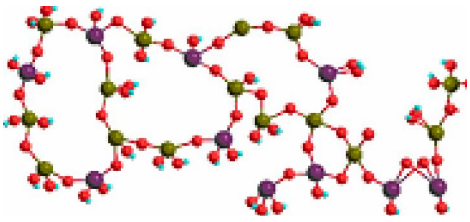

lar.EC nclworks

**Fig. 2.5** Sketch of the geopolymerization process of [56]

Metakaolinite is formed in kilns when kaolinite is heated at a temperature between 700 °C and 800 °C. The calcination of metakaolinite process can complete itself at 900 $^{o}$C for 6 hrs in China [56]; in France the temperature of calcinations from 700 to 750 $^{o}$C for 3 hrs [19]. The calcined product is cooled rapidly and ground to a fine powder. The metakaolinite formed in this way has a highly disorganized structure.

In Fig. 2.4 shows two 6-membered-ring molecular structural models that established to quantitatively analyze the formation process of a geopolymer. The dissolution of metakaolinite in alkaline solution is exothermic and the geopolymerization stages of alkaline - metakaolin can be supposed into three stages: (i) deconstruction, (ii) polymerization and (iii) stabilization as sketched in Fig. 2.5. However, these stages can hardly be separated clearly for they may occur simultaneously [14].

## 2.4 FLY ASH

The term fly ash is often used to describe any fine particulate material precipitated from the combustion of pulverized coal and is transported from the combustion chamber by exhaust gases. Fly ash generated in large quantities in coal based thermal power plants is a potential raw material for geopolymers due to the presence of silica and alumina bearing phases as major constituents [19, 57].

### 2.4.1 PRODUCTION OF FLY ASHES

Fly ash is produced by the combustion of finely ground coal injected at high speed with a stream of hot air into the furnace at electricity generating power plants. Typically, coal is pulverized and blown with air into the boiler's combustion chamber where it immediately ignites, generating heat and producing a molten mineral residue. On entry into the boiler, where the temperatures are usually around 1500 $^{o}$C, the coal in suspension is burnt instantaneously. The remaining matter present in the coal, such as shales and clays (essentially consisting of silica, alumina and iron oxide), melts whilst in suspension, and then on rapid cooling, as they are carried out by the flue gases [19, 57]. Fig. 2.6 presents the process example of coal ash generation from a pulverized coal firing boiler.

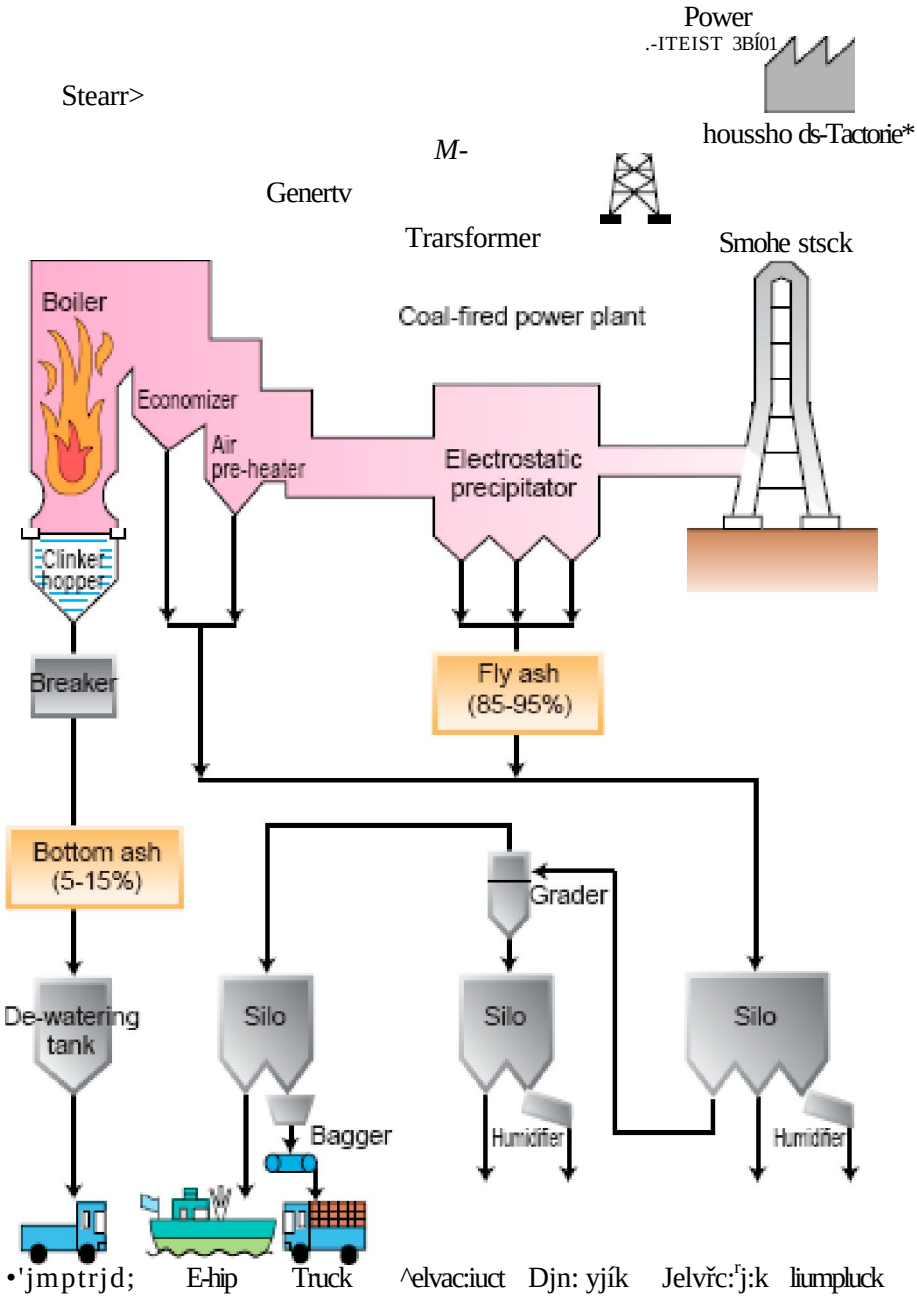


**Fig. 2.6** Coal ash generations from a pulverized coal-fired boiler [58]

There are two types of coal ash produced when coal is burnt in a modern pulverized fuel furnace, including fly ash and bottom ash. Fly ash is a ceramic waste material, obtained in huge quantities (comprises up to 90 % of the total ash) fine powder collected as the residue in the exhaust gases from the combustion chambers of the pulverized coal fired boilers at coal power plant stations [59]. The fly ash particle sizes range from less than 1 p,m to 150 p,m and are generally spherical in

shape (finer than Portland cement and lime) while the particle size of bottom ash of the furnace (10 %) is ranged from fine sand to coarse lumps [57, 60-62].

Depending upon the source and makeup of the coal being burned, the components of fly ash vary considerably. However, the chemical composition of all fly ash is very similar to that of Portland cement with mainly composed of the oxides of silicon ($SiO_2$), aluminium ($Al_2O_3$), iron ($Fe_2O_3$), and calcium (CaO), whereas magnesium (Mg), potassium (K), sodium (Na), titanium (Ti), and sulfur (S) are also present in a lesser amount. The major influence on the fly ash chemical composition comes from the type of coal. The combustion of sub-bituminous coal contains more calcium and less iron than fly ash from bituminous coal. The physical and chemical characteristics depend on the combustion methods, coal source and particle shape. The chemical compositions of various fly ashes show a wide range, indicating that there is a wide variations in the coal used in power plants all over the world [63, 64].

The color of fly ash is generally from tan to gray to black, depending on the amount of unburned carbon in the ash. The lighter color indicates the lower carbon content. Lignite or sub-bituminous fly ashes are usually light tan to buff in color, indicating relatively low amounts of carbon as well as the presence of some lime or calcium [57, 65].

According to the American Society for Testing Materials (ASTM C618) [66], the ashes containing more than 70 wt% $SiO_2$ + $Al_2O_3$ + $Fe_2O_3$ and being low in lime are defined as class F, while those with a $SiO_2$ + $Al_2O_3$ + $Fe_2O_3$ content between 50 and 70 wt% and high in lime are defined as class C [65, 67].

Fly ash has a number of useful applications that serves to utilize some of the large amounts being produced. Large quantities of power plant fly ash have to be dealt with in the Czech Republic every year (more than 10 million tons a year) [68].

Fly ash, bottom ash and other wastes from incinerators in the Czech Republic have been deposited in hazardous waste landfills for many years. In 1997 a decree of Law on wastes set a limit on the dioxin content in wastes of 10 p,g/kg. Wastes exceeding this limit would have to be stabilized and then deposited in a specialized hazardous waste only landfill. Simultaneously with the introduction of this law, the fees for depositing wastes on hazardous waste landfills increased significantly [69].

The sum of these measures have resulted in the operators of waste incinerators looking for ways to avoid paying these high landfill fees for fly ashes and for the means to avoid measurements of dioxins in fly ashes. So fly ashes have become one of the major environmental concerns in the world. Utilization of these materials help in reducing the cost of manufacturing a product and significantly reducing the emission of green - house gas $CO_2$ released from cement and concrete manufacturing. Some have expressed health concerns about this [57, 70].

### 2.4.2 APPLICATIONS OF FLY ASHES

Currently, over 40 percent of fly ashes are used annually in a variety of engineering applications [71-73]. Fly ashes have been used in several areas, such as: Portland cement concrete, soil and road base stabilization, bricks, flowable fills, grouts, structural fill and asphalt filler, etc [57, 73].

The fly ash is widely used as an additive in the cement, mortar and concrete building industry in the Czech Republic and worldwide [68, 73-76]. There are many advantages of incorporating fly ash into a cement concrete. Benefits to concrete vary depending on the type of fly ash, proportion used, other mix ingredients, mixing procedure, field conditions and placement. Some of the advantages of fly ash in concrete [57, 67, 77, 78]:

- Higher ultimate strength;
- Improved workability of the freshly mixed concrete;
- Corrosion resistance;
- Reduced bleeding;
- Reduced heat evolution during hydration;
- Reduced permeability;
- Increased resistance to sulfate attack;
- Increased resistance to alkali-silica reactivity;
- Reduced the production costs of concrete;
- Reduced shrinkage; and
- Increased durability.

Fly ash and lime can be combined with aggregate to produce a quality stabilized base course. These road bases are referred to as pozzolanic-stabilized mixtures. Typical fly ash contents may vary from 12 to 14 percent with corresponding lime contents of three to five percent. Portland cement may also be used in lieu of lime to increase early age strengths. The resulting material is produced, placed, and looks like cement stabilized aggregate base. Pozzolanic-stabilized mixture bases have benefits over other base materials [57, 65, 77]:

# Use of locally available materials;
# Good compaction;
# High internal angle of friction;
# Provides a strong, durable mixture;
# Increased energy efficiency;
# Easy and faster construction leads to reduction in construction cost;
# Suitable for using recycled base materials; and
# Can be placed with conventional equipment.

Fly ash can be used as a borrow material to construct fills and embankments. When fly ash is compacted in lifts, a structural fill is constructed that is capable of supporting highway buildings or other structures. Using fly ash in structural fills and embankments have several advantages over soil and rock [57, 65, 73]:

# Cost-effective where available in bulk quantities;
# Eliminates the need to purchase, permit, and operate a borrow pit;
# Can be placed over low bearing strength soils; and
# Ease of handling and compaction reduce construction time and equipment costs.

Fly ash is an influential agent for chemical and/or mechanical stabilization of soils. The properties of soil which can be change by using of fly ash are density, water content, plasticity, strength and compressibility performance of soils, hydraulic conductivity, and so on. Typical applications include: soil stabilization, soil drying, and control of shrink-swell. Fly ash provides the following benefits when used to improve soil conditions [57, 77]:

# Eliminates need for expensive borrow materials;

# Expedites construction by improving excessively wet or unstable sub grade;

# Reduces bulk density of soil and crust formation;

# Improves soil texture, water holding capacity and soil aeration;

# Provides micro nutrients like Fe, Zn, Cu, Mo, etc and provides macro nutrients like K, P, Ca, etc.

# By improving sub grade conditions, promotes cost savings through reduction in the required pavement thickness; and

# Can reduce or eliminate the need for more expensive natural aggregates in the pavement cross-section.

Other outlets for fly ash include the treatment of acid mine drainage [79-84], production of zeolites [76, 85], as a supplementary feedstock for cement production [86, 87] and application as bricks (both clay-fired and refractories) [88], as a filler in paint and organic-reactive dyes [77, 89-91].

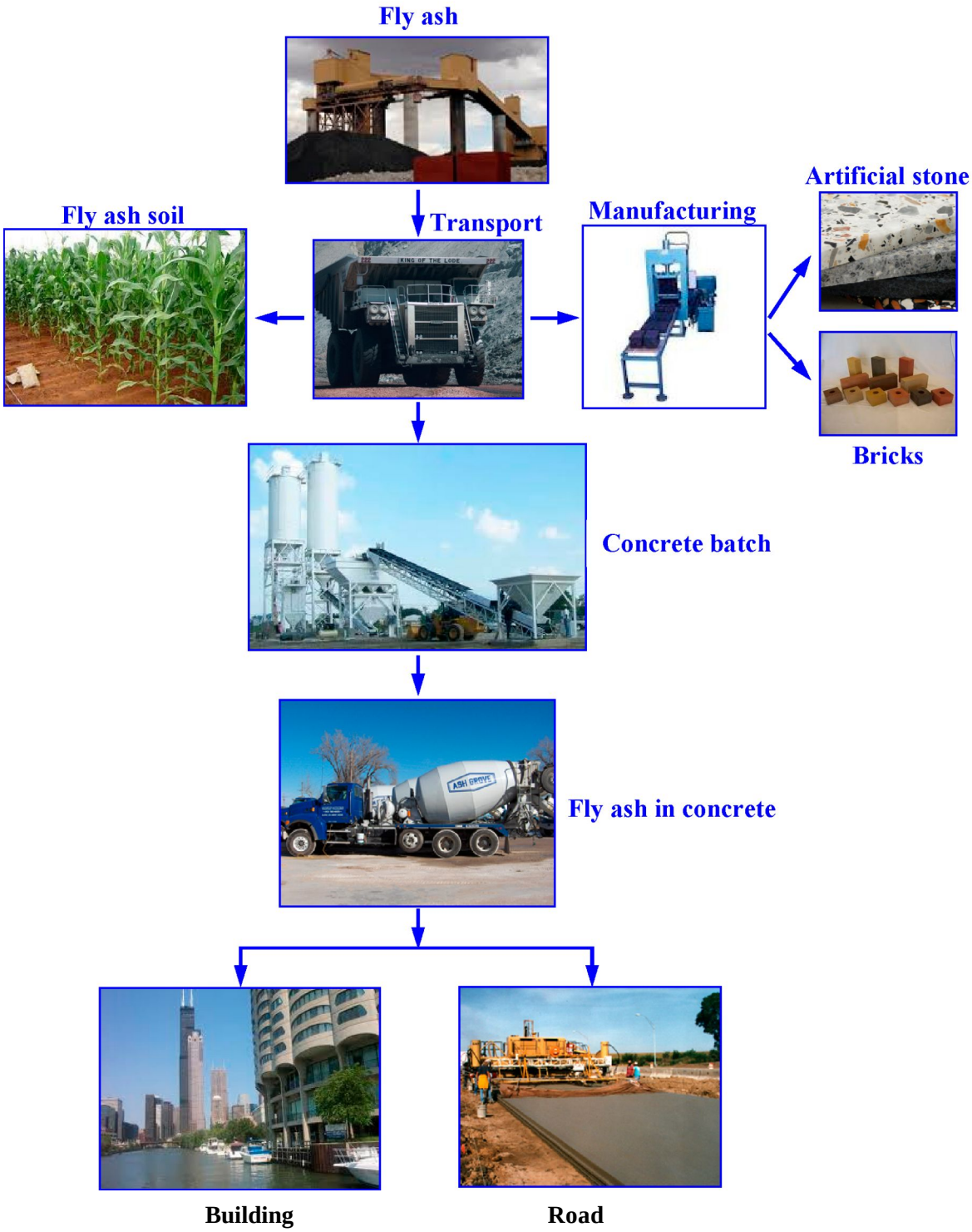


**Fig. 2.7** Applications of fly ashes

### 2.4.3 FLY ASHES BASED GEOPOLYMERS

One of the efforts to produce more environmentally friendly concrete is decrease the use of OPC by partially replacing the amount of cement in concrete with by products materials such as fly ash [92]. Fly ash, considered to be a waste material is rich in silica and alumina and hence can be used as a source material for manufacture of geopolymer binders [53]. These binders have been reported to achieve high early strength and better durability as compared to OPC based counterparts [93]. The spherical shape of fly ash often helps to improve the workability of the fresh concrete, while its small particle size also plays as filler of voids in the concrete, hence to produce dense and durable concrete [94].

In 1981, Forss had previously patented an alkaline-activated binder based on blast furnace slag and fly ash with the ratio of 2:1. The raw-material is also added in total 0.5 to 8 % by weight of sodium carbonate ($Na_2CO_3$) and/or sodium hydroxide (NaOH). Added in small amounts, the $Na_2CO_3$ and NaOH, separately or in combination, considerably shorten the hardening time of the concrete, yield excellent strengths, and made it possible to use cheap raw-materials [95]. Table 2.1 shows the results of binder after curing temperature at 70 $^{o}$C.

**Table 2.1** The result of binder based on fly ash (FA), slag (S) and slaked lime (SL) [95]

| Binder | Ligno-sulfonates [%] | Accelorator [% NaOH] | Water / cement ratio | Slump [cm] | Strengths [MPa] | | | |
|---|---|---|---|---|---|---|---|---|
| | | | | | 6 h | 9 h | 3 days | 7 days |
| 100% FA | 2.0 | 3.0 | 0.305 | 21 | 3 | 4 | 9 | 15 |
| 67% S, 33% FA | 1.5 | 3.0 | 0.310 | 20 | 0.1 | 0.2 | 2.0 | 5.0 |
| 90% S, 10% FA | 0.8 | 2.0 | 0.310 | 16 | 26 | 27 | 32 | 37 |
| 60% S, 30% FA, 10% SL | 1.5 | 3.0 | 0.315 | 17 | 33 | 52 | 57 | 60 |
| 53% S, 27% FA, 20% SL | 1.5 | 3.0 | 0.345 | 9 | 26 | 34 | 37 | 40 |
| 47% S, 23% FA, 30% SL | 1.5 | 3.0 | 0.360 | 17 | 20 | 26 | 32 | 35 |

In 1985, James Sawyer and Davidovits began product the Ca-based geopolymer cement introduced a hydraulic cement formed from a class C fly ash, an alkaline metal activator and citric acid [96]. Until 1992 the Materials Research Laboratory at Pennsylvania State University and University Park in United States (1992) were used some artificial pozzolanas (fly ash) that when mixed with lime, under hydrothermal conditions, also produced a new type of cementitious material. This was categorized as a new fly ash cement [97].

The similarity of some fly ashes to natural aluminosilicates (due to the presence of SiO2 and Al2O3 in the ash) has encouraged the use of geopolymerization as a possible technological solution in the making of special cements. The geopolymeric fly ash cement was used to replace Portland cement which has poor chemical resistance with a competitively priced, acid-stable cementitious material. Because the absence of calcium and the unique microstructure of geopolymeric fly ash cement provides good resistance to acidic environments [98, 99].

Van Jaarsveld and his team (1997) identified the potential use of waste materials such as fly ash, contaminated soil, mine tailings and building waste to immobilize toxic metals [35, 100, 101]. Other sdudy used fly ash as geopolymer powder and used highly alkaline solutions by combinations of NaOH with $Na_2SiO_3$ and KOH with $K_2SiO_3$. In this paper was found that the type of alkaline liquid is a notably factor affecting the mechanical strength, and that the combination of $Na_2SiO_3$ and NaOH gave the highest compressive strength. Mechanical strengths with values in the 60 MPa range were obtained after curing the fly ash at 85 $^oC$ for only 5 hours. In the bulk material, partially dissolved spheres with some mullite crystals on the surface can be found (see Fig. 2.8). The average molar ratios for the product of reaction is Si/Al = 1.5 and Na/Al = 0.48 [102].

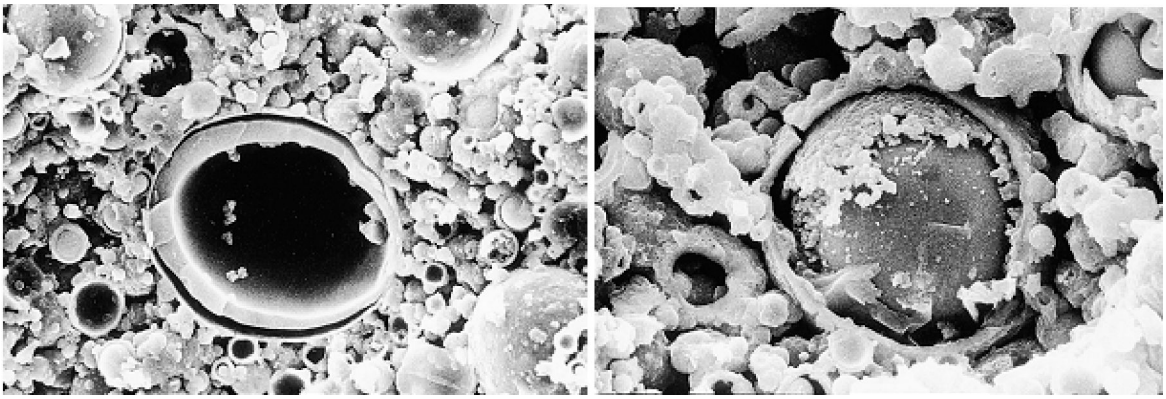

**Fig. 2.8** Activation with a activator/fly ash ratio of 0.25 for 24 h at 85 $^oC$ [102]

Van Jaarsveld investigated the effect of using different fly ashes on the setting characteristics of the geopolymer paste. Fly ash was obtained from different sources with variety of material parameters including water content, particle size, amorphous content, calcium content, alkali metal content, etc. It was also revealed that the calcium content of fly ash and the water/fly ash ratio played a significant role in strength development and final compressive strength as the

higher the calcium content resulted in faster strength development and higher compressive strength [103]. However, in order to obtain the optimal binding properties of the material, fly ash as a source material should have low calcium content and other characteristics such as unburned material less than 5 %, $Fe_2O_3$ content not higher than 10 %, 40 ^ 50 % of reactive silica content. Fig 2.9 shows that fly ashes are basically constituted by a major vitreous phase (halo registered between 29 = 20 $^{o}$ and 29 = 35 $^{o}$) and for some minor crystalline phases (quartz, mullite, hematite, magnetite and some CaO and $TiO_2$). All the fly ashes studied in this investigation had a very similar mineralogical composition.

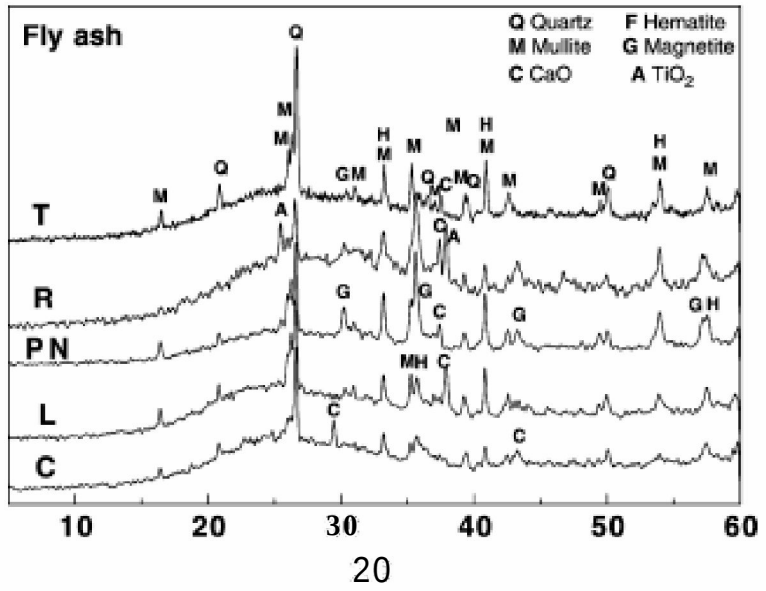


**Fig. 2.9** XRD patterns of fly ashes [104]

In Fig. 2.10 shows the granulometry distribution obtained by laser ray diffraction. Both methods give similar results with the highest amount of particles sized lower than 45 ^m. In addition, the alkaline activation process of the fly ashes it was very important to know the percentage of 'reactive silica' because reactive silica is the part of fly ash reacting with the alumina and the alkalis for giving place the cementitious. The compressive strength of ash mortars with low silica content was investigated about 60 ^ 66 MPa after curing at 1 day [104, 105].

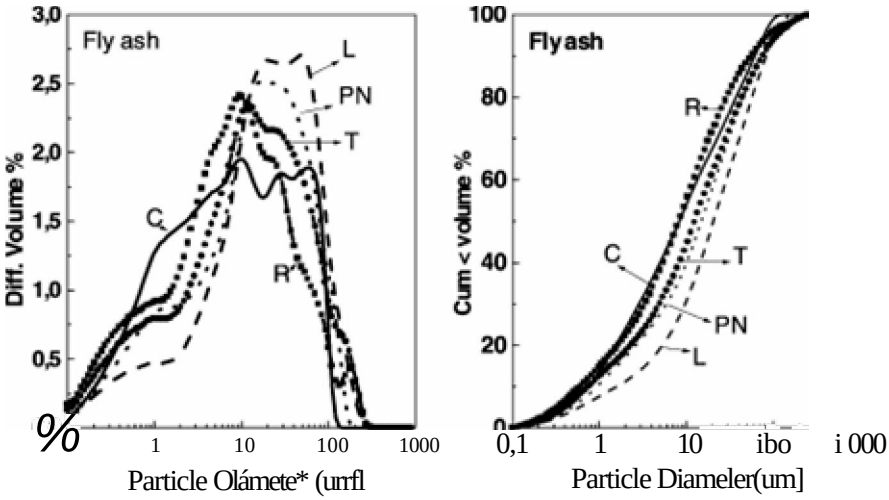


**Fig. 2.10** Granulometry distribution by laser rays diffraction [104]

Gourley, Swanepoel, Phair and Bakharev also developed that the presence of calcium in fly ash in significant quantities could interfere with the polymerization setting rate and alters the microstructure. Therefore, it appears that the use of Low Calcium (Class F) fly ash is more preferable than High Calcium (Class C) fly ash as a source material to make geopolymers [106-109].

Mingyu and his colleagues was synthesized of geopolymers at ambient temperature by using fly ash as the main starting material, zeolite or bentonite as the supplementary material, and NaOH and CaO together as activators. They demonstrated that the concentration of NaOH solution plays the most important role on the strength of the fly ash-based geopolymers, whereas the function of calcium oxide is also significant. Fig. 2.11 shows the secondary electron image of the matrix containing zeolite and bentonite, which demonstrates that although some un-reacted fly ash particles still exist in the sample and some discontinuous network products between the fly ash particles. However, zeolite used as a supplementary material may involve the process of geopolymerization to form a stable zeolitic structure and improve the properties of the fly ash based geopolymer [110].

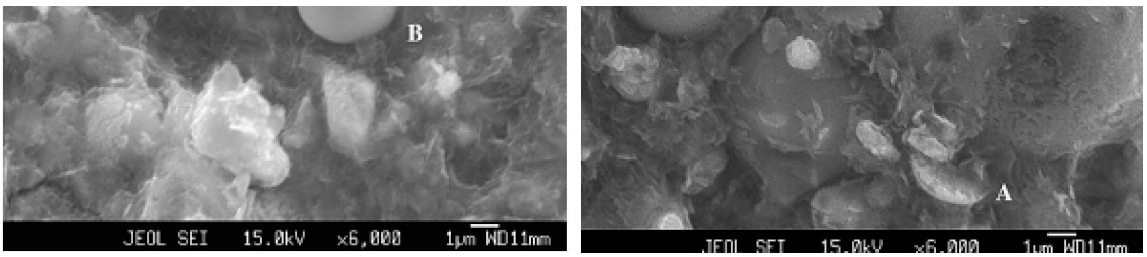


**Fig. 2.11** SEM images of the matrix containing zeolite (left) and bentonite (right) [110]

In 2011, Paulo and his team investigated basic sodalite, $Na_8[AlSiO_4]6(OH)_22H_2O$, cubic, P43n, (also known as hydroxysodalite hydrate). It was prepared by the alkaline activation of amorphous aluminosilicate glass, obtained from the phase separation of Class F fly ash. The sample was subjected to a process similar to geopolymerization, using high concentrations of a NaOH solution at 90 $^oC$ for 24 hrs [111].

# Chapter 3

# EXPERIMENTAL METHODS

This Chapter describes all the experimental details of our work. The experimental procedures in this study are divided into four sections as following: (i) The chemical composition and shape forming of materials (i.e., powder binder, fly ashes, aggregates, and reinforcements) in order to enhance properties and performance. (ii) The second section deals with process of control, which includes orchestration of the procedures of production (e.g., mixing techniques and curing conditions) to obtain the desired product. (iii) The third section discusses materials testing and equipments used, the need for improved testing procedures to permit better decision making throughout the production process. (iv) The fourth section describes calculation methods and determines the appropriate mixture proportions of geopolymer mortar and concrete.

## 3.1 MATERIALS

### 3.1.1 RAW MATERIALS

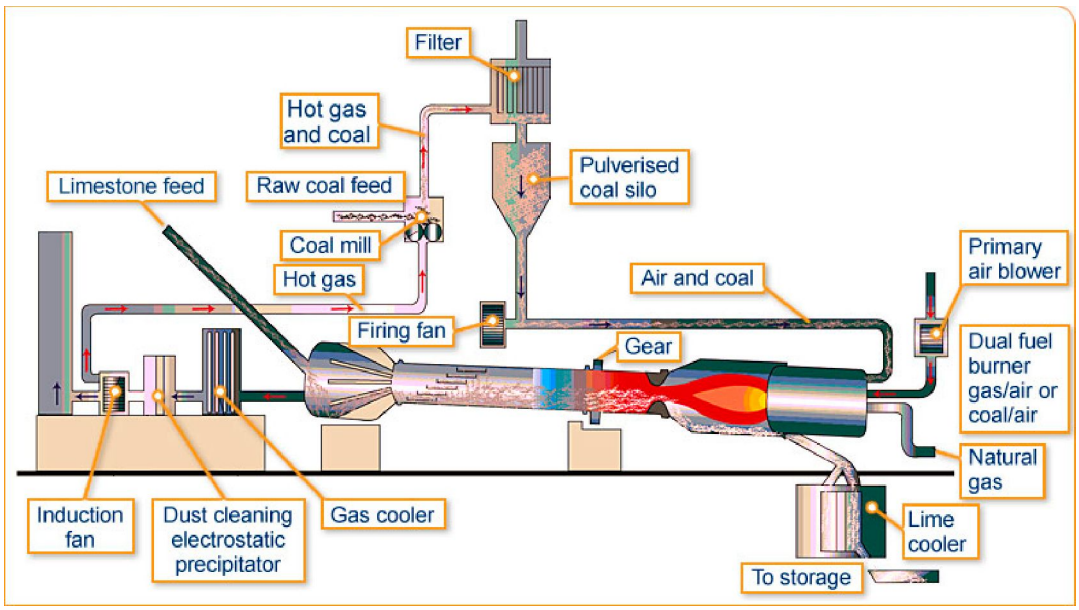


**Fig. 3.1** Structure diagram of rotary kilns [112]

Any material that contains mostly Silicon (Si) and Aluminium (Al) in amorphous form is a possible source material for the manufacture of geopolymer. Several minerals and industrial by-product materials have been investigated in the past.

Metakaolinite or calcined kaolin, natural Al-Si minerals, combination of calcined mineral and non-calcined materials, combination of fly ash and metakaolinite and combination of granulated blast furnace slag and metakaolinite have been studied as source materials.

Metakaolinite is preferred by the niche geopolymer product developers due to its high rate of dissolution in the reactant solution, easier control on the Si/Al ratio and the white color. However, for making concrete in a mass production state, metakaolinite is expensive to produce in large volumes because it has to be calcined at temperatures around 500 ^ 700 $^{o}$C for few hours. In this respect using waste materials such as fly ash is economically advantageous.

In the present experimental work, source fly dust obtained from České lupkové závody, Inc. in Czech Republic with the specific surface area was 20.8 m /g and the mean particle size was $d_{50}$ = 4.2 p,m and $d_{90}$ = 9.3 p,m, was used as the powder binder. Fig. 3.1 shows the structure diagram of rotary kilns. The chemical compositions of the fly dust from rotary kiln, as determined by X-ray diffraction (XRD) analysis, are given in Table 3.1. Through the analysis of XRD we can observe that the material is mainly composed of kaolinite with low amount of quartz (1% mass fraction) and anatase of shale fly dust as impurities. The calcium oxide content in this case is very low. During passing of fly dust through in rotary kiln it partly dexydroxylated with 30 ^ 70 % lose of kaolinitic structure. Calcination shale clay residues from dust filters for 10 hours at 750 $^{o}$C in a bath oven transformation to metakaolinite were utilized in the production geopolymer cement with a molar Si:Al ratio of 2:0.

**Table 3.1** Chemical composition of fly dust as determined by XRD

| Compound | $Al_2O_3$ | $SiO_2$ | Fe2O3 | SO3 | CaO | LOI |
|---|---|---|---|---|---|---|
| Percent composition [% mass] | 41.6 | 52.6 | 2.6 | 1.1 | 0.8 | 1.3 |

The Scanning Electron Microscopy (SEM) image of fly dust is shown in Fig. 3.2. The particle shapes of the fly dust were generally sharp and point. It can be seen very good from the Table 3.1 that $Al_2O_3$ and $SiO_2$ are two the main components in production geopolymer cement.

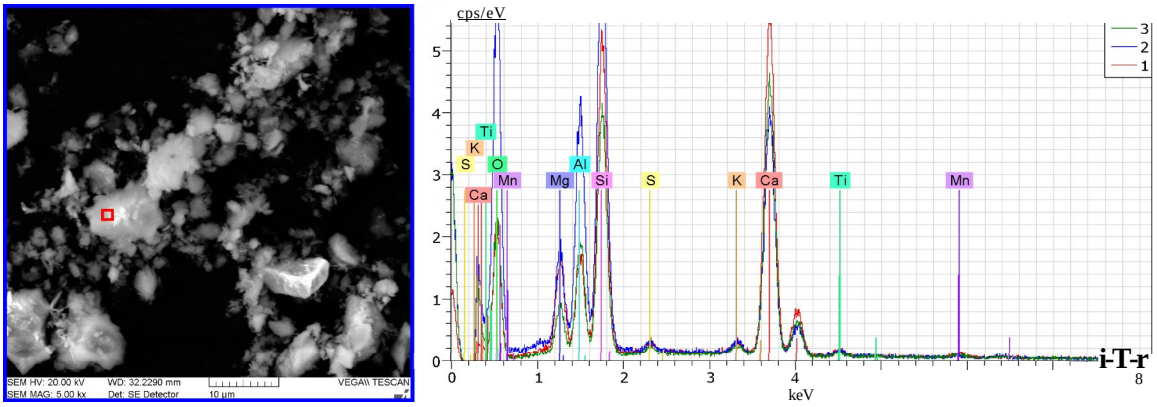


**Fig. 3.2** SEM image and EDX of geopolymer cement

### 3.1.2 GEOPOLYMER RESIN

Each mixture geopolymer resin contained only ground aluminosilicate fly dust as the powder binder and various combinations of four activators: sodium silicate ($Na_2SiO_3$) or potassium ($K_2SiO3$) and sodium (NaOH) or potassium (KOH). In this study, we mixed $Na_2SO_3$ solution with NaOH solution to produce alkaline silicate solution with modulus 1.50. The ratio of $H_2O/Na_2O$ used for was 12. Pure geopolymer samples for mechanical properties tests, SEM and EDX were prepared with mass ratio of activator/powder equal to 4:5. This is a condition for easy production derived to achieve a flow similar to that of the paste used commercial Portland cement.

The microstructure of pure geopolymer matrix were analyzed by mean SEM, EDX TESCAN VEGA 3XM microscope (Fig. 3.3) and mapping of individual elements in the same image on Appendix A, corresponds to a Si/Al and Na/Al molar ratio of 2.0 and 0.8 respectively, that is poly(sialate-siloxo) [19].

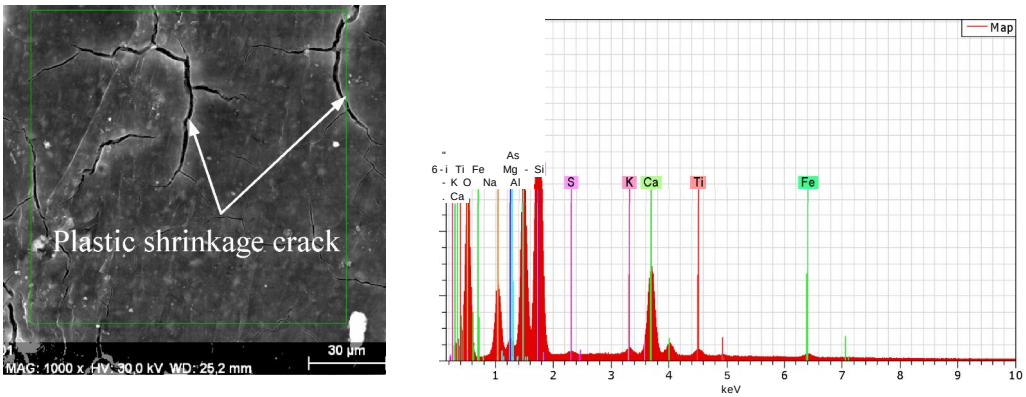


**Fig. 3.3** SEM and EDX mapping of an individual geopolymer matrix

The potential applications of geopolymers are summarized in Table 3.2. The atomic ratio Si:Al in the poly(sialate) structure determines the properties and application fields.

**Table 3.2** Applications of geopolymers [19]

| Si: Al ratio | Applications |
|---|---|
| 1 | Bricks, ceramics, fire protection |
| 2 | Low CO2 cements, concrete, radioactive and toxic waste encapsulation |
| 3 | Heat resistance composites, foundry equipments, fiber glass composites |
| > 3 | Sealants for industry |
| 20 < Si/Al < 35 | Fire resistance and heat resistance fiber composites |

### 3.1.3 AGREGATES

#### *3.1.3.1 CHARACTERIZA TION OF FLY ASH*

Fly ash is a good source material for making geopolymer owing to its high content of silica and alumina [104, 113, 114]. The fly ash geopolymer can totally substitute the use of normal Portland cement. Six different fly ashes commercially available for use in mortar and concrete were chosen for this study. The fly ashes selected represent a wide range of chemical and physical properties, and were obtained from sources distributed in Czech Republic. The fly ashes were already classified into 6 names of city and coded such as: K1 (Kotel 1 Plzeň), K3 (Kotel 3 Plzeň), K6 (Komořany), K6_LF (Komořany Látkový Filtr), PRT (Pražská Teplárenská), OPE (Elna Opatovice). They have many different colors like brown, light grey to black due to its chemical compositions and contaminants. Fly ash particles are generally sharp, pointed, and spherical in shape and range in size from 1 (xm to 30 (xm.

Fly ash can be used to manufacture blended cement. In this study, fly ash can be used to produce modified concrete by adding it during the mixing process. Research carried out in past 40 years or so shows that the incorporation of fly ash into concrete has certain advantages and some disadvantages. Incorporation of fly ash into concrete can improve the workability due to the spherical shape and glassy surface of fly ash particles. By replacing cement with fly ash, the cost of concrete can be reduced, since fly ash costs low than cement. Because fly ash is an industrial by product, it lowers the energy demand in producing concrete. In addition, incorporating fly ash into concrete can reduce the hydration heat of fresh concrete and is good for mass concrete structures [40].

The disadvantages of fly ash concrete are low early age strength and longer initial setting time due to the low reactivity of fly ash. Much research has been carried out to improve the reactivity by chemically activating [115]. One method is to add an alkali activator such as 1 or 2 % NaOH or KOH into concrete mix. Another is to use lime to mix with fly ash for a few days before incorporating the fly ash into the concrete mix. Recently, some studies using a mechanical method to wet grind or mill fly ash to "activate" its reactivity have been conducted and some promising results have been obtained [116, 117]. The normal replacement of cement by fly ash is around 25 to 30 % by weight. However, in high-volume fly ash concrete, fly ash content up to 60 % is reached [118].

### *3.1.3.2 AGGREGATES*

Approximately three-quarters of the volume of concrete is occupied by aggregate. It is inevitable that a constituent occupying such a large percentage of the mass should contribute important properties to both the fresh and hardened product. Not only may the aggregate limit the strength of concrete but also the aggregate properties greatly influent the durability and structural performance of concrete [119, 120].

Aggregate was originally viewed as an inert material and act as filler material in cement mortar or concrete can be divided into coarse aggregate and fine aggregate. Aggregate of size less than 4.75 mm are usually considered as fine aggregate (sand) and these larger than 4.75 mm, as coarse aggregate [3, 119].

**Fig. 3.4** Find sand (left) and coarse aggregate (right)

Aggregates were currently used by the local concrete industry in Czech Republic. Coarse aggregates were obtained in crushed form; majority of the particles were of gravel-type with the size particles ranging from 4.0 to 8.0 mm. The fine sand was obtained from the sand dunes in uncrushed form and particles range in diameter from 0.063 mm to 2.0 mm. All aggregates were in saturated surface dry condition. Fig. 3.4 shows the aggregates used in our study.

## 3.2 FABRICATION OF THE GEOPOLYMER MORTAR - CONCRETE

Several series of samples were prepared to test the influential variables on the compressive strength of hardened geopolymer. The variables include modulus and content of the mixed alkali activator and the sample curing conditions. The technology of sample preparation is as follows. At first, the geopolymer resin was prepared by mixing the alkaline activator with the raw materials. The liquid and solid components were mixed about 5 minutes at room temperature until the solution homogenized. Next, the geopolymer resin mixture was mixed with different fly ash and aggregates (coarse and/or fine) content. The mixing was done in an air conditioned room at approximately 23 $^{o}$C ± 2 $^{o}$C until the well homogenized mixture (about 5 minutes). Directly after mixing, the fresh mortar and concrete was poured in the plastic moulds and vibrated for 2 minutes on the vibration table to remove air voids. Specimens were covered with a plastic bag for 24 hrs after casting. Compressive strength testing of mortar was performed as per AS 1012.9 using (046 x 92) mm diameter cylindrical moulds. ASTM C39 was conducted for compressive strength tests of hardened concrete, using (0100 x 200) mm cylinder moulds. Three cylinders of each sample were tested, with the experimental values being averaged. Testing of the flexural strength indices of the specimens was conducted on (40 x 40 x 160) mm samples in accordance to ASTM C348 - 08.

There are two ways to curing these samples:

(i) These samples were cured at room temperature for 3 days after casting. Next, the samples were removed from the moulds and left in laboratory ambient conditions until the day of test. The sample ages for the latter tests were 7, 14, and 28 days.

(ii) All the mixtures were cured in an oven without delay time at the specific curing temperature for 24 hr and 48 hr ranging from 60 $^{o}$C ^ 90 $^{o}$C. Samples were demoulded after

the curing process in the oven and continued curing ambient condition for 2 days. Figs. 3.5 ^ 3.10 show the processing of mixing and curing of geopolymer concrete.

**Fig. 3.5** Pour the activator liquid (left) and raw materials (right) into the component

**Fig. 3.6** The well homogenized mixture (left) and pour fly ash (right) into the component

**Fig. 3.7** Combination of both fine sand (left) and coarse aggregate (right) into the mixture

**Fig. 3.8** Fresh materials for placing (left) and test slump (right)

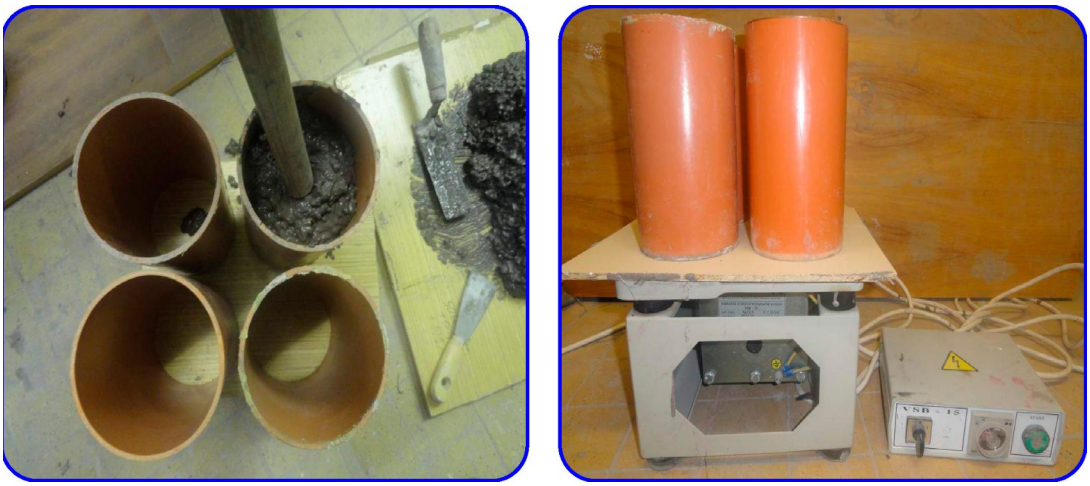

**Fig. 3.9** Compaction the materials into moulds (left) and vibration (right)

The fresh fly ash-based geopolymer concrete was dark in color and shiny in appearance (see Fig. 3.8 left). The mixtures were usually cohesive. The workability of the fresh concrete was measured by means of the conventional slump test (Fig. 3.8 right).

**Fig. 3.10** Specimens curing at room temperature (left) and curing at high temperature (right)

## 3.3 TESTING

### 3.3.1 TEST SLUMP

The slump test is performed on newly mixed geopolymer concrete. The slump of the concrete is checked in accordance with Test Method for Slump of Hydraulic-Cement Concrete - C143/C143M [121]. A sample of freshly mixed concrete is placed in a mould shaped as the frustum of a cone, 300 mm in height, 100 mm in diameter at the top, and 200 mm in diameter at the bottom, see Fig. 3.11. To conduct a slump test, first moisten the slump test mould and place it on a flat, nonabsorbent, moist, and rigid surface. Then hold it firmly to the ground by foot supports. Next, fill the mould completely and remove the mold immediately in one move. Measure and record the slump as the vertical distance from the top of the mold to average concrete level is shown in Fig. 3.8 [40].

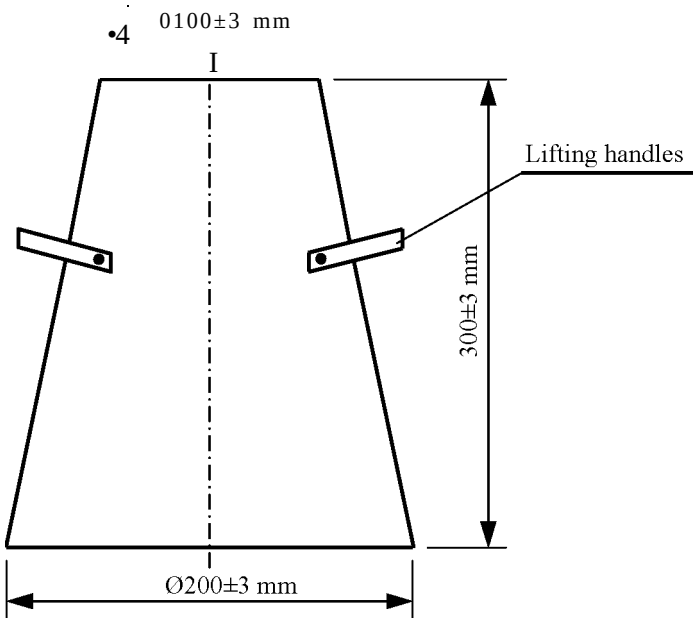


**Fig. 3.11** The mould used in test slump

### 3.3.2 TEST FLEXURAL STRENGTH

The authors are used the Standard Test Method for Flexural Strength of Concrete (Using Simple Beam with Third-Point Loading) - ASTM C78/C78M - 10 and the Standard Test Method for Flexural Strength of Hydraulic-Cement Mortars - ASTM C348 - 08. These methods are used to determine of the flexural strength of concrete and hydraulic cement mortar by the use of a simple beam with third-point loading [122, 123]. The flexural tests are conducted over a simply supported a cross-head speed of 2.0 mm/min and span length of 120 mm with a center-point load on Universal Testing Machine INSTRON Model 4202 (maximum load of the sensor: 10 kN) ambient condition temperature about 23 ± 2 $^{o}$C and relative humidity 65 % (Fig. 3.12). The flexural strength (modulus of rupture) of geopolymer mortar and concrete is determined from the average of four specimens.

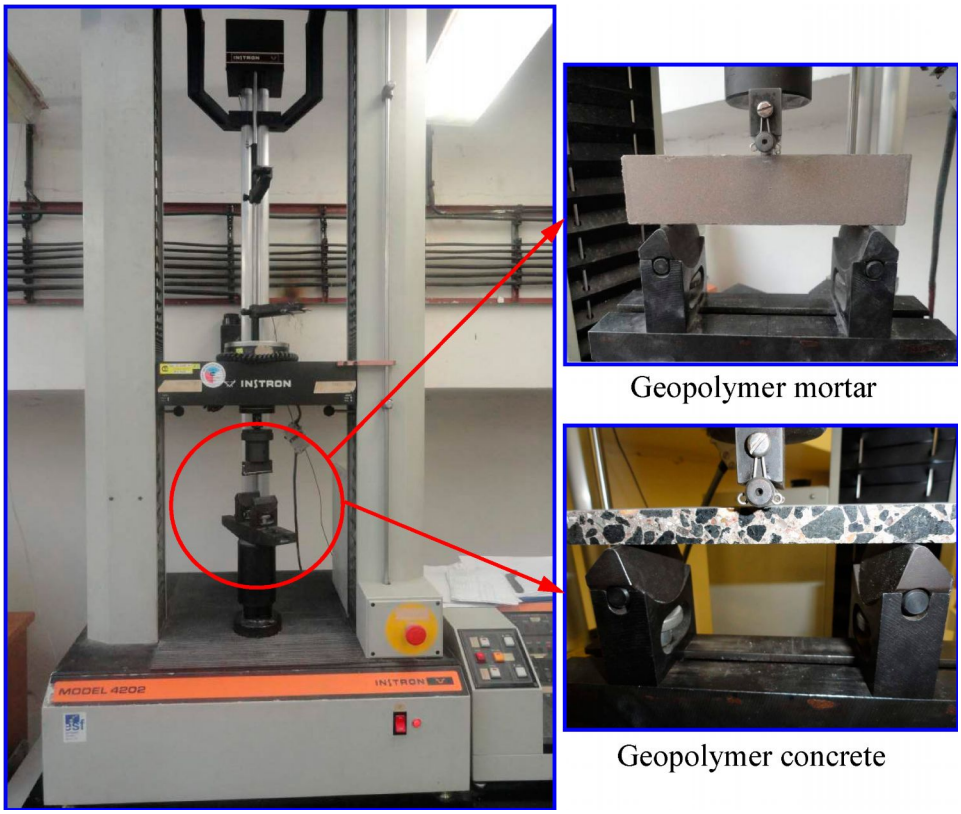


**Fig. 3.12** Universal Testing Machine - Instron Model 4202

### 3.3.2 TEST COMPRESSIVE STRENGTH

The compressive strength of geopolymer mortar and concrete is measured on a VEB Werktoff Prufmaschinen Leipzig, 500 kN, ambient condition temperature about 23 ± 2 $^{o}$C and relative humidity 65 % (Fig. 3.13). The samples are cured and tested in accordance with the Standard Practice for Making and Curing Concrete Test Specimens in the Field - ASTM C 31/C 31M - 03a and the Methods of testing concrete - Determination of the compressive strength of concrete specimens - AS 1012.9 - 1999 [124, 125]. Values are the averages of four separate tests. Data that deviated more than 10 % were eliminated.

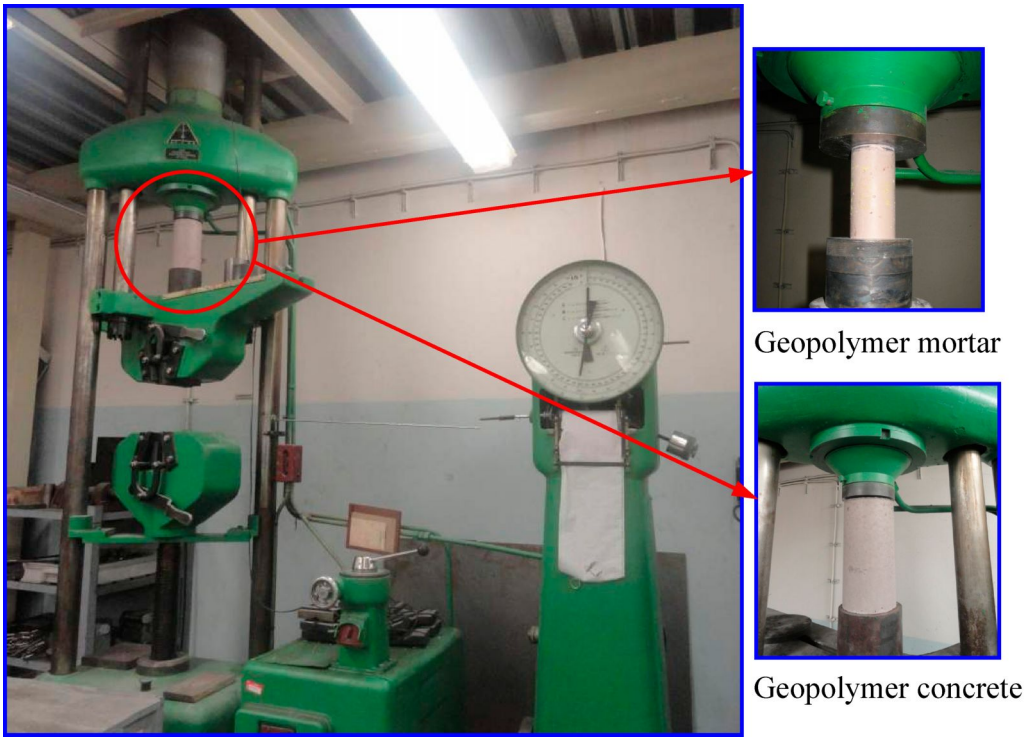


**Fig. 3.13** Universal Testing Machine - Werktoff Prufmaschinen Leipzig, 500 kN

### 3.3.3 CHARPY IMPACT TESTING

Impact testing machine and specimens are shown in Fig. 3.14

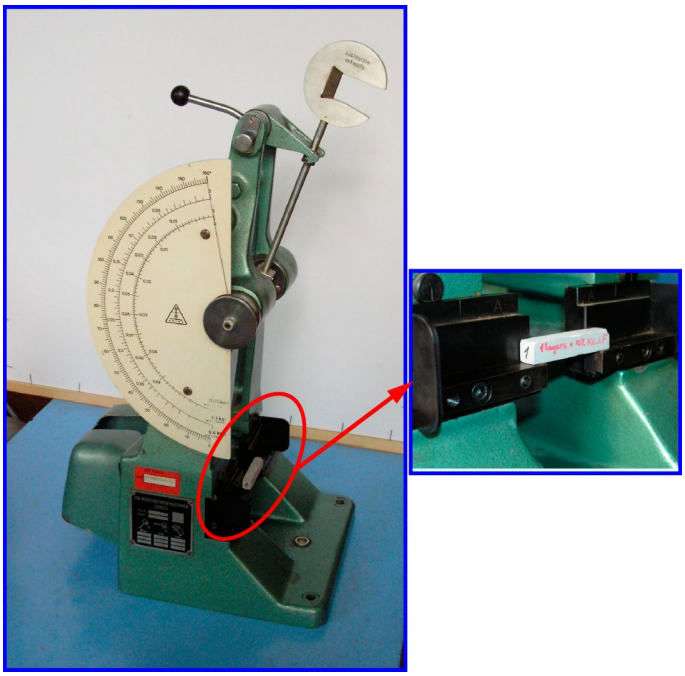

**Fig. 3.14** Impact testing machine - Werktoff Prufmaschinen Leipzig, 0.05 kpm

According to the standard specimen size for Charpy impact testing in the Standard Test Methods and Definitions for Mechanical Testing of Steel Products - ASTM A370 - 07a is (10 x 10 x 55) mm [126] and the Standard Test Method for Low Strain Impact Integrity Testing of Deep Foundations - ASTM D5882 - 07 (Fig. 3.20) [127]. The impact testing of geo mortar are measured on a VEB Werktoff Prufmaschinen Leipzig, 0.05 kpm of Technical University of Košice, ambient condition temperature about 23 ± 2 $^{o}$C and relative humidity 65 %. This method is used to determine the amount of energy absorbed of geo mortar during fracture and the quantitative result needed to measure the toughness of this material and the yield strength.

### 3.3.4 DRYING FURNACE

Curing at elevated temperatures was done in dry curing in the laboratory furnace (Fig. 3.15). With electronically controlled APT.line™ preheating chamber assuring temperature accuracy. The samples are cured at temperature ranging from 60 °C to 90 °C for 24 hrs and 48 hours.


**Fig. 3.15** Drying furnace ED 23

### 3.3.5 OVEN

All samples after curing at room temperature for 28 days are heated in the oven ranging from 200 $^{o}$C to 1000 $^{o}$C at a heating rate of 5 K/min and with a soak time of 1 hour at the maximum temperature and finally cooled in the furnace with opening gate for 24 hrs. Fig. 3.16 shows geopolymer mortars heating at 1000 $^{o}$C.

**Fig. 3.16** Oven

### 3.3.6 MICROSTRUCTURE OF GEO SAMPLES

In this study, the authors are used a scanning electron microscope (SEM) and Energy Dispersive X-ray Analysis (EDX) on TESCAN VEGA 3XM microscope to analysis the structure and chemical compositions of particles, geopolymer resin, fibers (Fig. 3.17 left). Examination of the geopolymer material was made on the SEM with the dispersive radiation spectrometer at the maximum magnification of 2500x, using the secondary electron detection, and the Esprit 1.8 software, using 30 kV acceleration voltages.

**Fig. 3.17** TESCAN VEGA 3XM microscope (left) and optical microscope NIKON EPIPHOT 200 (right)

In addition, geopolymer mortar and concrete are also investigated about the adhesion between geo matrix and particle on optical microscope NIKON EPIPHOT 200 (macroscopic observation) and used the software NIS Elements to take pictures (Fig. 3.17 right).

### 3.3.7 ENVIRONMENTAL CHAMBER

**Fig. 3.18** Climate chamber LIEBISCH KB 300 of Technical University of Košice

The authors are used the environmental test chamber to test the effects of moisture (relative humidity) conditions on geopolymer mortar, concrete and a slightly effect on the mechanical properties and structure of geopolymer materials (Fig. 3.18). The cycles are stopped after 28 days curing (about 120 cycles).

### 3.3.8 HARDNESS TESTING

The authors are used MH 180 Portable Leeb Hardness Tester to measure the hardness of geopolymer mortar presented in Fig. 3.19. This equipment can test any angle, even upside down. The hardness scales are convertable among hardness units: HRB (Rockwell Hardness B Scale), HRC (Rockwell Hardness C Scale), HV (Vicker), HB (Brinell), HS (Shore), HL (Leeb).

The basic principle of this equipment is to use an impact body of certain weight impacts against the testing surface under certain test force, then measure the impacting velocity and the rebounding velocity of the impact body respectively when the spherically test tip is located 1 mm above the testing surface.

The calculation formula is as follows:

$$HL = \frac{VB}{VA} \text{x} 1000 \qquad (3\text{-}1)$$

Where: HL - Leeb hardness value

VB - Rebounding velocity of the impact body

VA - Impacting velocity of the impact body


**Fig. 3.19** MH 180 Portable Leeb Hardness Tester

### 3.3.9 PLANETARY BALL MILL

This equipment is used to making particles from micro to nano size (Fig. 3.20). Designed for a broad range of applications and ideally suited for loss-free grinding down to a fineness as small as 100 nm. The comminution takes place primarily through the high-energy impact of grinding balls. To achieve this, the grinding bowl, containing the material to be ground and grinding balls, rotates around its own axis on a main disk rotating in the opposite direction. At a certain speed, the centrifugal force causes the ground sample material and grinding balls to bounce off the inner wall of the grinding bowl, cross the bowl diagonally at an extremely high speed, and impact on the material to be ground on the opposite wall of the bowl.


**Fig. 3.20** Planetary ball mill of Fritsch Pulverisette 7

### 3.3.10 THE TYPES OF MOULDS

There are four types of moulds used:

(i) ASTM C 470/C 470M was conducted for compressive strength tests of hardened concrete, using (0100 x 200) mm cylinder plastic moulds (Fig. 3.21 left).

(ii) Compressive strength testing of geo mortar was performed as per AS 1012.9 using (046 x 92) mm diameter cylindrical plastic moulds (Fig. 3.21 right).

**Fig. 3.21** Moulds to making geopolymer concrete (left) and mortar (right) for compressive strength testing

(iii)Testing of the flexural strength indices of the specimens were conducted on (40 x 40 x 160) mm samples in accordance to ASTM C78/C78M - 10 and ASTM C348 - 08.

**Fig. 3.22** Moulds to making geopolymer concrete and mortar for flexural strength testing

## 3.4 CALCULATION METHODS

### 3.4.1 COMPRESSIVE STRENGTH

Compressive tests were performed according of the European Standard EN 12390-3: 2009. Three samples of each formulation were tested and the average data were reported. The loading was displacement-controlled at a constant rate of 2.4 mm/min for all the tests.

The compressive strength of mortar ($f_{cm}$) was calculated using equation:

$$f_{cm} = \frac{F}{A} \tag{3-2}$$

Where:

$f_{cm}$ is compressive strength, MPa;

$F_{max}$ is the maximum applied load indicated by the testing machine, N;

$A_c$ is the original cross-sectional area of a specimen in a compression test, mm

At least two cylinders are test at the same age and the average strength is reported as the test result to the nearest 0.1 MPa.

### 3.4.2 FLEXURAL STRENGTH

The flexural strength is expressed as Modulus of Rupture in MPa and is determined by standard test method ASTM C 293 (Using Simple Beam with Center Point Loading) and AASHO T17. The flexural strength was calculated from this test, the flexural strength was calculated using:

$$R, = \frac{3F_{max} L}{2bh^2} \tag{3-3}$$

Where:

$R_{mo}$ is the flexural strength, MPa;

$F_{max}$ is the maximum applied load indicated by the testing machine, N;

b is the average width of specimen, mm;

h is the average depth of specimen, mm;

L is span length, mm.

### 3.4.3 MODULUS OF ELASTICITY OF GEOPOLYMER CONCRETE

From 2005 - 2007, the model proposed by Fernandez et al. [128], Sofi et al. [129] and Hardjito et al. [1] were determined the modulus of elasticity ($E_c$) of geopolymer concrete by testing cylinder specimens. There were some variations in these reported test results in terms of the ingredients of the test specimens and the test methods used. The test results of Fernandez et al. [128] were measured in accordance with the Spanish Standard UNE 83316. These specimens were made using low-calcium fly ash, 12.5 molar NaOH, $Na_2SiO_3$ with $SiO_2$ to $Na_2O$ ratio of 3.4, coarse and fine aggregates. While the test specimens of Sofi et al. [129] were also used low-calcium fly ash from three different sources, slag containing 40% CaO by mass and a combination of NaOH or KOH and $Na_2SiO_3$ as the alkaline liquid.

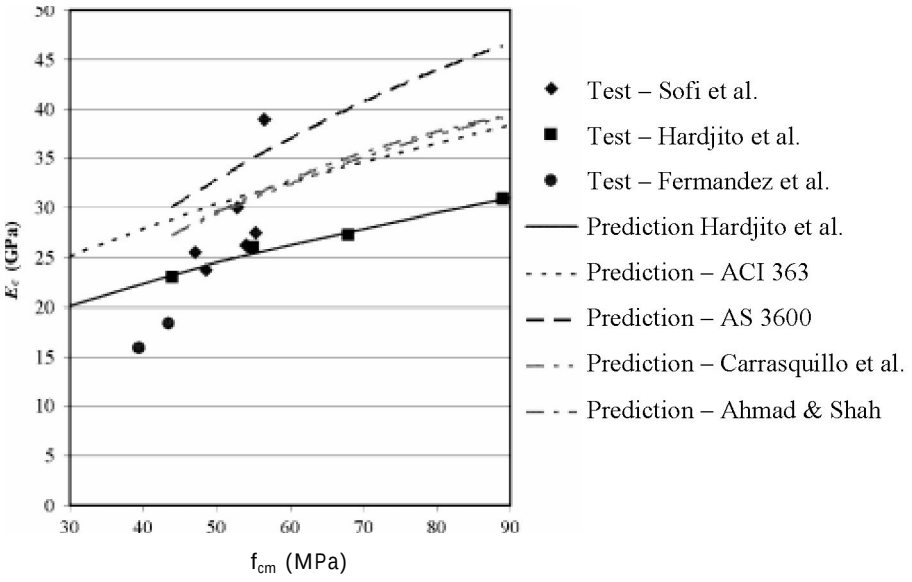


**Fig. 3.23** Modulus of elasticity of geopolymer concrete [130]

The specimens did not have any coarse aggregates except the one corresponding to compressive strength of 39 MPa. And the test specimens by Hardjito et al. [1] also used low-calcium fly ash, 14 molar NaOH, $Na_2SiO_3$ with $SiO_2$ to $Na_2O$ ratio of 2.0, and coarse and fine aggregates. The type of coarse aggregates used in these specimens was granite. The test data of Sofi et al. [129] and Hardjito et al. [1] were measured in accordance with the Australian Standard 1012.17 [131].

It is known that the mechanical properties of geopolymer vary with the chemical composition (fly ash, alkaline and aggregates) of the product obtained after the reaction. It was found in the previous studies [128, 129] that geopolymer showed different mechanical properties depending on the kind of fly ash, the type and concentration of the alkaline used. Usually a higher concentration of the alkaline dissolves a higher proportion of the fly ash particles. Fig. 3.23 shows the results of elastic modulus of geopolymer concrete and compared with the predictions by different empirical equations.

While the modulus of elasticity of concrete varies depending on the paste and the type of aggregates, simplified empirical equations in terms of concrete compressive strength (fcm) and concrete density (p) are often used for normal weight concretes. The values of the modulus of elasticity calculated by the empirical equations are compared with the test results of geopolymer concrete. Some empirical equations proposed for OPC concrete with Equations (3-4) ^ (3-7) and Equation (3.8) for geopolymer concrete are given below:

American Concrete Institute ACI 363 [132]:

$$E_c = 3\,3\,2\,0\,\wedge + 6900 \tag{3-4}$$

Australian Standard AS 3600, within an error of ± 20 % [133]:

$$E_c = 0.043\rho^{1.5}\sqrt{f_{cm}} \tag{3-5}$$

Carrasquillo et al. [134]:

$$E_c = (3320\sqrt{f_{cm}} + 6900)\left(\frac{\rho}{2320}\right)^{1.5} \tag{3-6}$$

Ahmad and Shah [135]:

$$Ec = 3.38p^{25} f)°\text{-}^{65}.10\text{-}^{5} \quad (3\text{-}7)$$

Hardjito et al.[1]:

$$E_c = 2\ 7\ 0\ 7\ 7 + 5300 \quad (3\text{-}8)$$

The prediction equations for the modulus of elasticity of OPC concrete recommended by the AS 3600 [133], Carrasquillo et al. [134] and Ahmad and Shah [135] are functions of the density and the compressive strength of concrete. The equation proposed by Hardjito et al. [1] for geopolymer concrete is similar to that given by the ACI 363 [132] with different values of the constants. These equations are relatively simple to use since they are expressed as function of concrete compressive strength only. The trend lines through the predicted values of the test results by the five equations (3-4) ^ (3-8) are shown in Fig. 3.23. It can be seen that the equations of the ACI 363, AS 3600, Carrasquillo et al. and Ahmad and Shah overestimate most of the test results of geopolymer concrete [132-135]. The prediction of the modulus of elasticity by Equation (3-8) is close to the test results and this equation is used to calculate the modulus of elasticity of geopolymer concrete, presented in this study.

### 3.4.4 INDIRECT TENSILE STRENGTH

The splitting tensile strength ($f_{ct}$) of the IPC mixes was experimentally measured following the procedure prescribed by AS 1012.10. The values of splitting tensile strength of geopolymer concrete depend on the basis of their correlation to compressive strength ($f_{cm}$). There is an agreement on the increasing of splitting tensile strength with the increase in compressive strength of geopolymer concrete.

The modulus of splitting tensile strength of geopolymer concrete was calculated using equation [136]:

$$7 = 0\ .\ 4\ 7 \quad , \text{MPa} \quad (3\text{-}9)$$

Where: the value of compressive strength of concrete from 10 MPa to 65 MPa are applied.

### 3.4.5 THE MECHANISM OF PLASTIC SHRINKAGE AFTER CASTING

Several types of shrinkage can occur in a concrete, including thermal shrinkage, plastic shrinkage, autogenous shrinkage, chemical shrinkage, and drying shrinkage. In this study, the authors focus on plastic shrinkage and dry shrinkage [137].

Fresh concrete just after it has been placed has little strength. Water can move relatively freely in what is still a fluid suspension. Water, the least dense component of the mixture, tends to move upwards towards the surface as heavier materials move down during compaction. The upward movement of water is known as bleeding [138].

Many factors affect plastic shrinkage cracking, in particular the evaporation of water can be lost at the plastic concrete surface. Plastic shrinkage is mainly a physical action and is caused by surface tension forces. As the surface dries, menisci are formed between the solid particles and therefore capillary tension forces act [139]. The magnitude of the shrinkage is affected by the amount of water lost from the surface which is governed by the temperature, wind speed, and ambient relative humidity [137, 138, 140].

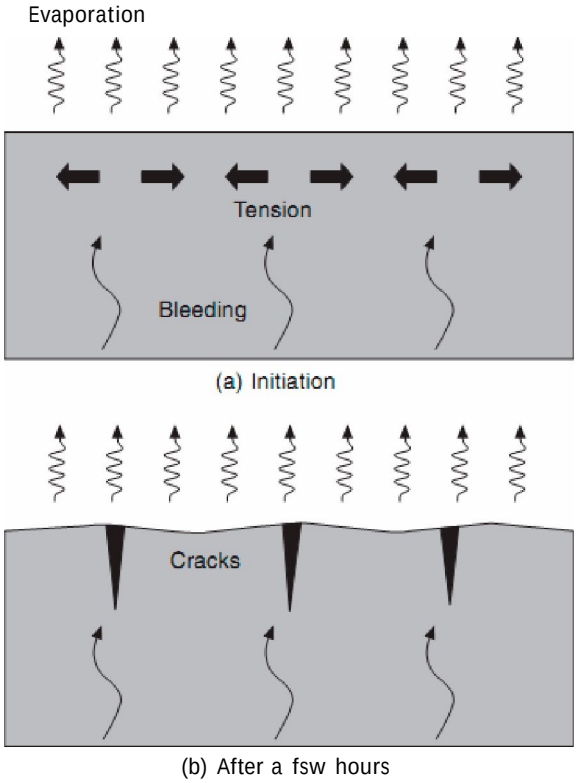


**Fig. 3.24** Process of plastic shrinkage cracking (initiation and final state) [138]

The surface layer of concrete tries to shrink but is restrained by underlying layers that are not subject to the same reduction in volume. Restraint can also be partly provided by the reinforcement and friction at the surface of the formwork or sub base. The result of the restraint is that tensile stresses develop in the surface layer. As the concrete is still in a plastic state and has very little strength, cracks develop at the surface. The phenomenon is analogous to the drying shrinkage of clays [137, 138]. The process is illustrated in Fig. 3.24, the upper part showing initiation and the lower the condition after a few hours. Admixtures profoundly alter the chemical forces acting between the cementitious, fibers and fine particles within the concrete. The rheological behavior as well as setting times can be significantly altered. It is therefore important to assess the mix design for its bleeding capacity and set time and plan accordingly. Mixes using water reducers for instance may bleed less and therefore be prone to plastic shrinkage.

*(i) Weight loss:*

Equation (3-9) was used to calculate weight loss $w_L$ (%) for each specimen [141]

$$w_L = \frac{w_o - w}{w_o} \times 100, \% \qquad (3\text{-}10)$$

Where: $w_o$ is the initial mass and $w_t$ is the remaining mass at any given time, t. All results are the average of four replicates.

*(ii) Shrinkage after casting:*

Length (L): $$S_L = \frac{SLO - SL}{S_{Lo}} \times 100, \% \qquad (3\text{-}11)$$

Diameter (D): $$S_D = \frac{SDO - SD}{S_{Do}} \times 100, \% \qquad (3\text{-}12)$$

Where: $s_{Lo}$ is the initial length and $s_{Lt}$ is the remaining length at any given time, t;

$S_{Do}$ is the initial diameter and $s_{Lt}$ is the remaining diameter at any given time, t;

# Chapter 4

# EFFECTS OF SALIENT PARAMETERS ON COMPRESSIVE STRENGTH OF FLY ASH BASED GEOPOLYMER MORTAR

## 4.1 INTRODUCTION

Many investigators have studied the use of fly ash in cement production as an additive material. The purpose of this research was concerned about the development, manufacture and applications of waste materials, especially fly ash based geopolymer mortar and concrete. So in order to attain optimal strength levels, it was necessary to conduct numerous trials to determine the appropriate mixture proportions.

There are many parameters effect on the mechanical properties of fly ash based geopolymer mortar are investigated. The parameters considered are as follows:

(i) Ratio of alkaline liquid-to-fly ash, by mass;

(ii) Type of fly ash;

(iii) Concentration of activator solution;

(iv) Curing conditions (time and temperature);

(v) Percentage of aggregates (coarse and fine sand)

(vi) Rest period prior to curing;

(vii) Water content of mixture;

(viii) Mixing Time.

The focus of this chapter was the optimal ratio of alkaline liquid-to-fly ash, type of fly ash, curing conditions and percentage of aggregates. In all, some primary mixtures of geopolymer mortar were made to study the effect of various parameters. Four specimens for each of the mixtures were made. The details of these mixtures have been described in the remaining chapters. In addition, a number of supplementary mixtures were also made and tested. The details of these supplementary mixtures are given in Appendix A.

Section 4.2 of the Chapter describes the effect of the different types of fly ash on the mechanical properties of geopolymer mortar. The chemical composition and characteristics of fly ashes were investigated. Structures of fly ash specimens were collected from different thermal power plants in Czech Republic.

The effect of alkaline liquid and water on the compressive strength of geopolymer mortar are presents in section 4.3. The chapter ends with section 4.4, where curing conditions of geopolymer mortar ranging from 60 to 90 $^{o}$C for 24 hrs to 72 hrs and rest period 2 days in ambient condition are investigated.

## 4.2 EFFECT OF THE DIFFERENT TYPES OF FLY ASH

### 4.2.1 CHARACTERIZATION OF FLY ASH

SEM was used for measurement of the structure and morphology of the original fly ash. The SEM images (Figs. 4.1 ^ 4.6) present the original fly ash of a series of different sizes particles. All fly ash particles are generally sharp, pointed, and spherical in shape. SEM show that the OPE and PRT fly ashes are finer than other kinds and K6 fly ash has the very coarse particles in all fly ashes.

*(i) Fly ash K1*

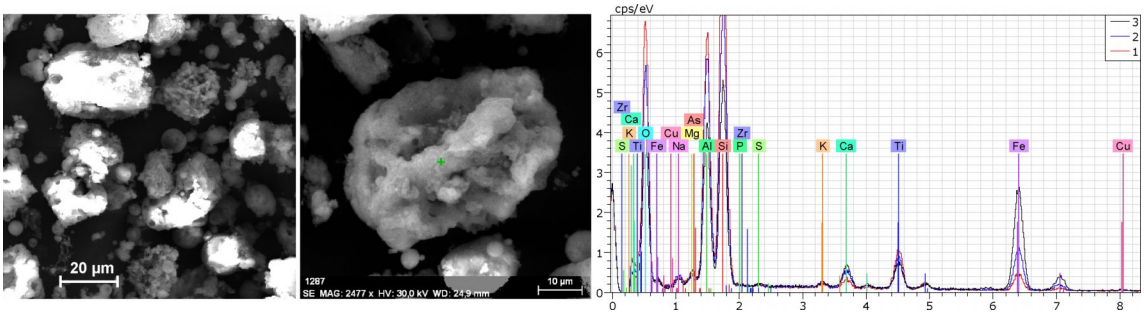


**Fig. 4.1** SEM photographs and corresponding energy spectrum of fly ash K1

*(ii) Fly ash K3*

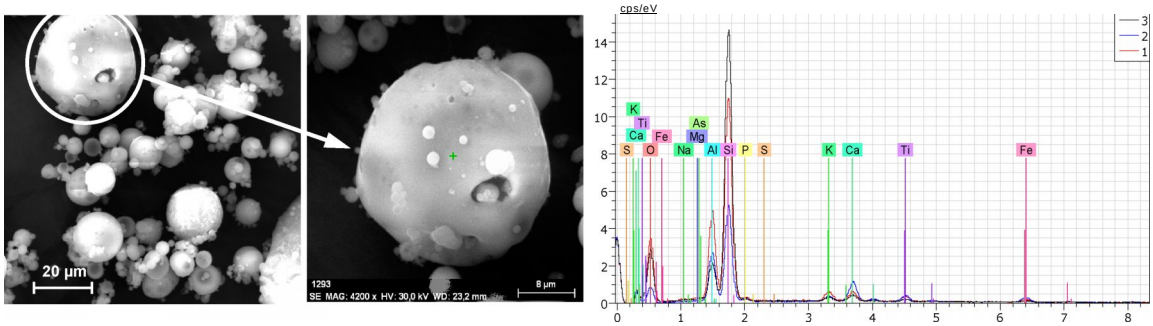


**Fig. 4.2** SEM photographs and corresponding energy spectrum of fly ash K3

(iii) Fly ash K6

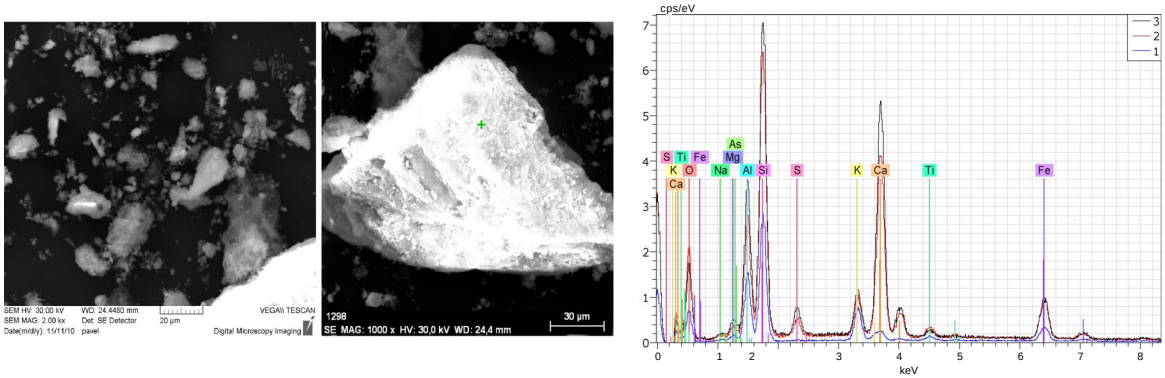


**Fig. 4.3** SEM photographs and corresponding energy spectrum of fly ash K6

*(iv) Fly ash K6 LF*

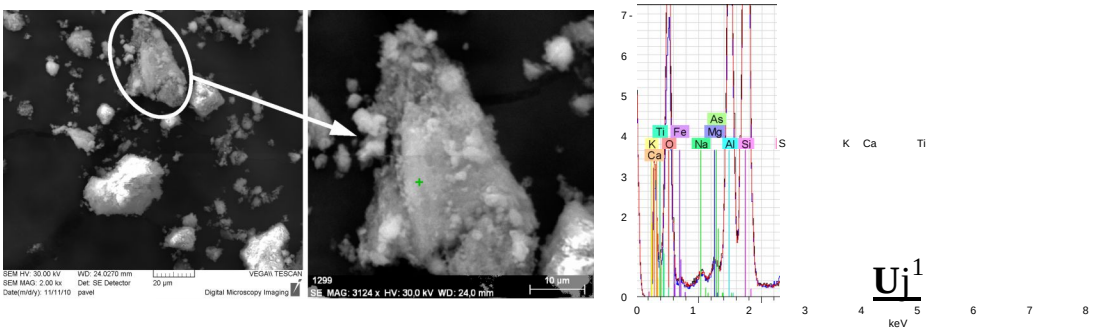


**Fig. 4.4** SEM photographs and corresponding energy spectrum of fly ash K6_LF

*(v) Fly ash OPE*

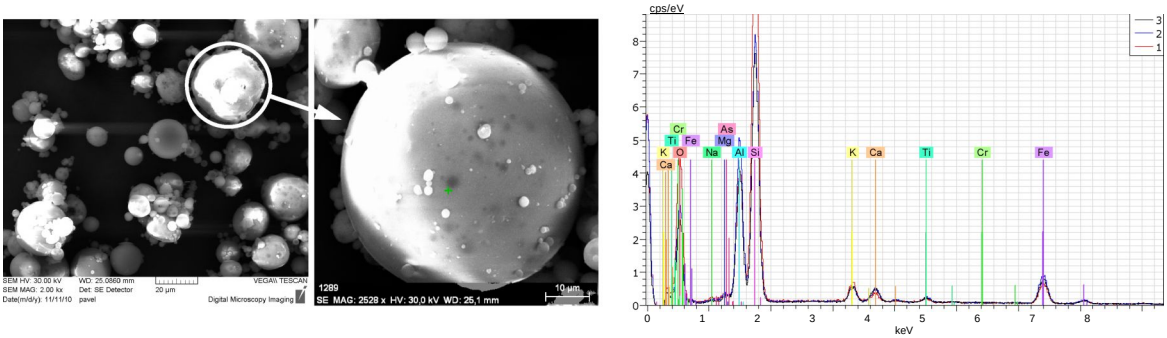


**Fig. 4.5** SEM photographs and corresponding energy spectrum of fly ash OPE

*(vi) Fly ash PRT*

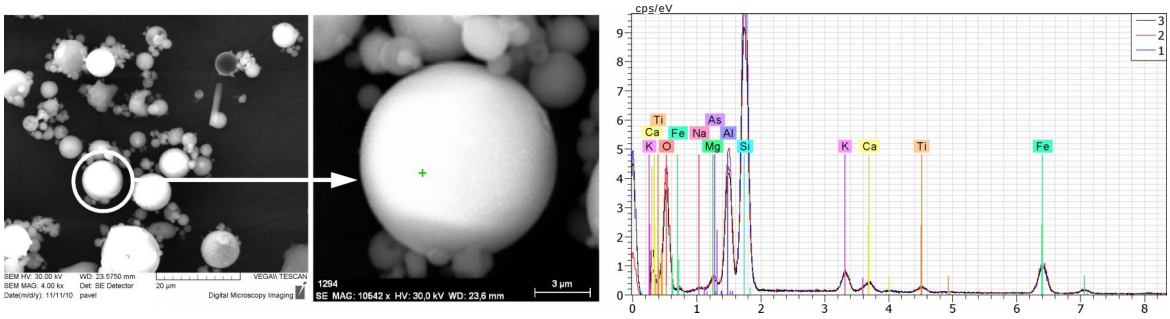


**Fig. 4.6** SEM photographs and corresponding energy spectrum of fly ash PRT

Table 4.1 shows the summary chemical composition of all fly ashes.

**Table 4.1** The summary chemical composition of all fly ashes

| Atomic [%] | K1 | K3 | K6 | K6_LF | OPE | PRT |
|---|---|---|---|---|---|---|
| O | 53.80 | 53.84 | 55.43 | 52.81 | 52.65 | 55.06 |
| Na | 1.84 | 0.35 | 0.42 | 1.81 | 0.47 | 0.77 |
| Mg | 1.06 | 0.10 | 0.80 | 0.97 | 0.43 | 1.17 |
| Al | 14.27 | 9.74 | 10.00 | 14.73 | 12.64 | 10.89 |
| Si | 20.25 | 30.57 | 20.81 | 23.97 | 28.54 | 25.17 |
| P | 0.09 | 0.82 | - | - | - | - |
| S | 0.19 | 0.12 | 0.92 | 0.39 | - | - |
| K | 0.25 | 0.93 | 2.42 | 0.41 | 1.27 | 1.70 |
| Ca | 0.94 | 2.11 | 6.60 | 1.69 | 0.97 | 0.93 |
| Ti | 1.95 | 0.76 | 0.42 | 0.57 | 0.41 | 0.53 |
| Fe | 4.72 | 0.57 | 2.04 | 2.57 | 2.44 | 3.68 |
| **As** | 0.15 | 0.10 | 0.14 | 0.09 | 0.11 | 0.10 |
| **Cu** | 0.16 | - | - | - | - | - |
| **Zr** | 0.34 | - | - | - | - | - |
| **Cr** | - | - | - | - | 0.08 | - |

## 4.2.2 EXPERIMENTAL

The experimental results are presented the effects of type of fly ash on the compressive strength of geopolymer mortar. The compositions of the geopolymer mortars are shown in Table 4.2. Each of the compressive strength testing corresponds to the mean value of the compressive strengths of four test mortar cylinders (0 46 x 92) mm in a series.

**Table 4.2** Composition of fresh geopolymer mortar mixes by extra water

| Type of fly ash | Materials | | | | | Curing | | | | Age at test [days] |
|---|---|---|---|---|---|---|---|---|---|---|
| | Mixtures No | Fly ash [%] | Geo cement [%] | Activator [%] | Extra water [%] | Time [hours] | | Temp [$^{o}$C] | | |
| PRT | MT-1 | 10 | 50 | 40 | - | 24, | 48 | 60, | 70 | 2 |
| | MT-2 | 20 | 43.5 | 34 | 2.5 | 24, | 48 | 60, | 70 | 2 |
| | MT-3 | 30 | 35 | 28 | 7.0 | 24, | 48 | 60, | 70 | 2 |
| | MT-4 | 40 | 27 | 21 | 12 | 24, | 48 | 60, | 70 | 2 |
| OPE | ME-1 | 10 | 50 | 40 | - | 24, | 48 | 60, | 70 | 2 |
| | ME-2 | 20 | 43.5 | 34 | 2.5 | 24, | 48 | 60, | 70 | 2 |
| | ME-3 | 30 | 35 | 28 | 7.0 | 24, | 48 | 60, | 70 | 2 |
| | ME-4 | 40 | 27 | 21 | 12 | 24, | 48 | 60, | 70 | 2 |
| K1 | MK1-1 | 10 | 50 | 40 | - | 24, | 48 | 60, | 70 | 2 |
| | MK1-2 | 20 | 43.5 | 31.5 | 5.0 | 24, | 48 | 60, | 70 | 2 |
| | MK1-3 | 30 | 35 | 25 | 10 | 24, | 48 | 60, | 70 | 2 |
| | MK1-4 | 40 | 27 | 19 | 16 | 24, | 48 | 60, | 70 | 2 |
| K3 | MK3-1 | 10 | 50 | 40 | - | 24, | 48 | 60, | 70 | 2 |
| | MK3-2 | 20 | 43.5 | 31.5 | 5.0 | 24, | 48 | 60, | 70 | 2 |
| | MK3-3 | 30 | 35 | 28 | 7.0 | 24, | 48 | 60, | 70 | 2 |
| | MK3-4 | 40 | 27 | 21 | 12 | 24, | 48 | 60, | 70 | 2 |
| K6_LF | MLF-1 | 10 | 50 | 40 | - | 24, | 48 | 60, | 70 | 2 |
| | MLF-2 | 20 | 39.5 | 33 | 7.5 | 24, | 48 | 60, | 70 | 2 |
| | MLF-3 | 30 | 33 | 26 | 12 | 24, | 48 | 60, | 70 | 2 |
| | MLF-4 | 40 | 22 | 18 | 20 | 24, | 48 | 60, | 70 | 2 |
| K6 | MK6-1 | 10 | 50 | 40 | - | 24, | 48 | 60, | 70 | 2 |
| | MK6-2 | 20 | 39.5 | 33 | 7.5 | 24, | 48 | 60, | 70 | 2 |
| | MK6-3 | 30 | 33 | 26 | 12 | 24, | 48 | 60, | 70 | 2 |
| | MK6-4 | 40 | 22 | 18 | 20 | 24, | 48 | 60, | 70 | 2 |

Effects of salient parameters on compressive strength of fly ash based geopolymer mortar

### 4.2.3 RESULTS

The experimental shows that geopolymer mortar are prepared with 10 ^ 30 wt% of fly ash exhibited acceptable flowability while more than 40 wt% fly ash containing mortars were stiff and difficult to pack into the plastic moulds.

Geopolymer mortars with varying levels of fly ash were prepared and their mechanical properties studied. The linear regressions of compressive strength value of geopolymer mortar are exhibited on Figs. 4.7 and 4.8. The results indicate that compressive strength of mortar is a strong relationship between types of fly ash, particle size, and percentage of fly ash in the mixtures. When comparing the compressive strength values of geopolymer mortars which obtained the same percentage fly ash content and curing conditions it can be seen that fly ash PRT in the ratio of 10, 20, 30, and 40% after curing at 70 $^{o}$C for 24 hrs and 48 hrs gives the higher compressive strength and the hardness than mortars produced with other blended fly ash. It has lower particle size than other kinds of fly ash. This result is the same with other researches [142-145]. Because fines fly ash content fulfils a void-filling role, and aids cohesion and finishability [138]. And the test results showed that, with increasing fly ash content causes a decrease in compressive strength of geopolymer mortar.

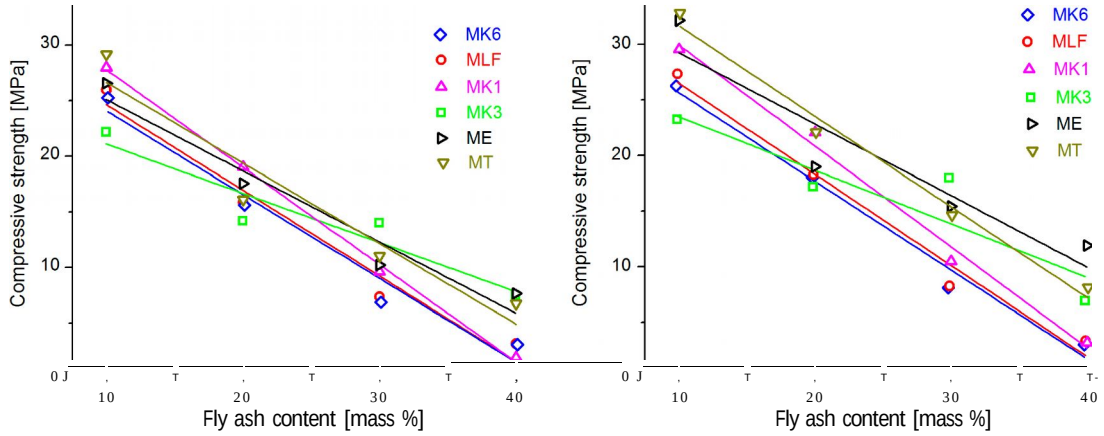


**Fig. 4.7** Compressive strength of geopolymer mortar samples after curing in the oven at 60 $^{o}$C for 24 hrs (left) and 48 hrs (right)

In additions, the compressive strength of mortar also depended on curing time and curing temperature. When the curing time and temperature increase, the compressive strength also increases. With curing temperature in range of 60 to 90 °C, within time in 5 to 72 hrs (we will

detail discuss in section 4.4), the compressive strength of mortar can be obtained about 25 to 39 MPa.

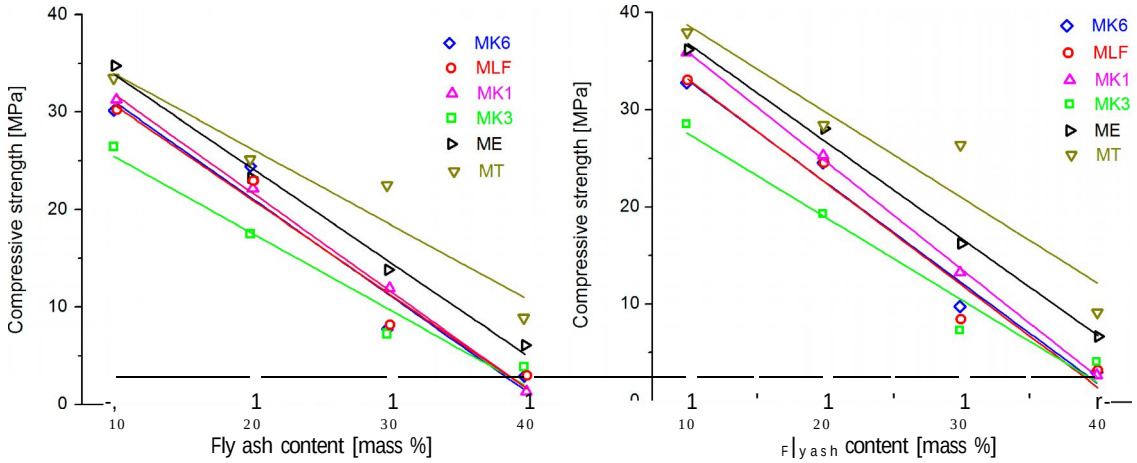


**Fig. 4.8** Compressive strength of geopolymer mortar samples after curing in the oven at 70 °C for 24 hrs (left) and 48 hrs (right)

Mechanical properties of the geopolymer mortars cured 60 and 70 °C are summarized in Table 4.3. Geopolymer mortar curing at 60 and 70 °C for 24 hrs is given in Appendix B.

**Table 4.3** Properties of geopolymer mortar produced by fly ash cured at 60, 70 °C for 48 hrs

| Type of fly ash | Mixture No | 60 °C, 48 hrs | | | 70 °C, 48 hrs | | |
|---|---|---|---|---|---|---|---|
| | | Density $\rho$ [kg/m$^3$] | Hardness [HV] | Compressive strength [MPa] | Density $\rho$ [kg/m$^3$] | Hardness [HV] | Compressive strength [MPa] |
| PRT | MT-1 | 1712 | **321** ± 5 | **32.92** ± 0.1 | 1615 | **385** ± 5 | **38.02** ± 0.7 |
| | MT-2 | 1520 | **262** ± 2 | **22.21** ± 0.2 | 1520 | **296** ± 12 | **28.47** ± 0.8 |
| | MT-3 | 1518 | **184** ± 5 | **14.77** ± 0.4 | 1430 | **258** ± 8 | **26.43** ± 0.6 |
| | MT-4 | 1515 | **157** ± 4 | **8.27** ± 1.0 | 1390 | **169** ± 8 | **9.17** ± 0.4 |
| OPE | ME-1 | 1573 | **333** ± 11 | **32.21** ± 5.5 | 1560 | **354** ± 14 | **36.28** ± 3.7 |
| | ME-2 | 1423 | **241** ± 10 | **18.99** ± 0.3 | 1480 | **305** ± 13 | **28.16** ± 4.9 |
| | ME-3 | 1403 | **192** ± 10 | **15.43** ± 6.7 | 1430 | **242** ± 9 | **16.32** ± 6.9 |
| | ME-4 | 1411 | **159** ± 3 | **11.9** ± 4.6 | 1350 | **148** ± 8 | **6.78** ± 1.0 |
| K1 | MK1-1 | 1696 | **315** ± 5 | **29.48** ± 1.2 | 1541 | **327** ± 2 | **35.76** ± 0.3 |
| | MK1-2 | 1532 | **271** ± 4 | **21.98** ± 0.3 | 1461 | **270** ± 4 | **25.15** ± 0.3 |
| | MK1-3 | 1519 | **259** ± 7 | **10.42** ± 2.3 | 1390 | **181** ± 3 | **13.11** ± 0.8 |
| | MK1-4 | 1269 | **233** ± 8 | **3.12** ± 0.1 | 1301 | **134** ± 2 | **2.54** ± 0.1 |

| | | | | | | | |
|---|---|---|---|---|---|---|---|
| K3 | MK3-1 | 1676 | **288** ± 7 | **23.09** ± 2.5 | 1520 | **361** ± 2 | **28.66** ± 0.5 |
| | MK3-2 | 1550 | **303** ± 3 | **17.07** ± 0.1 | 1450 | **256** ± 2 | **19.40** ± 0.6 |
| | MK3-3 | 1500 | **293** ± 4 | **17.86** ± 0.2 | 1390 | **184** ± 3 | **7.40** ± 0.3 |
| | MK3-4 | 1401 | **181** ± 4 | **6.80** ± 0.2 | 1371 | **173** ± 3 | **4.15** ± 0.1 |
| K6_LF | MLF-1 | 1595 | **270** ± 5 | **27.27** ± 0.7 | 1564 | **334** ± 5 | **33.03** ± 1.0 |
| | MLF-2 | 1488 | **214** ± 3 | **18.21** ± 1.1 | 1448 | **227** ± 5 | **24.51** ± 0.4 |
| | MLF-3 | 1381 | **157** ± 4 | **8.22** ± 1.0 | 1376 | **166** ± 4 | **8.40** ± 0.4 |
| | MLF-4 | 1305 | **125** ± 8 | **3.31** ± 0.2 | 1306 | **125** ± 5 | **3.14** ± 0.1 |
| K6 | MK6-1 | 1647 | **270** ± 5 | **26.21** ± 1.7 | 1627 | **340** ± 6 | **32.76** ± 0.8 |
| | MK6-2 | 1557 | **214** ± 3 | **17.97** ± 0.8 | 1523 | **231** ± 12 | **24.53** ± 1.5 |
| | MK6-3 | 1447 | **160** ± 9 | **8.06** ± 0.7 | 1411 | **144** ± 4 | **9.73** ± 0.5 |
| | MK6-4 | 1305 | **128** ± 10 | **2.96** ± 0.3 | 1278 | **133** ± 10 | **2.98** ± 0.2 |

## 4.3 EFFECT OF ALKALINE LIQUID AND WATER

In OPC mortar and concrete, water in the mixture chemically reacts with the cement to produce a paste that binds the aggregates. In contrast, the water in fly ash-based geopolymer mortar and concrete mixtures does not cause a chemical reaction. Experience showed that water content in the geopolymer concrete mixture affected the properties of concrete in the fresh state as well as in the hardened state. Because the excess water in fresh mixtures which reduces the concentration of activator, the chemical reaction that occurs in geopolymers produces water that is eventually expelled from the binder, leads to a reduced geopolymerization reaction and thus lowers compressive strength.

In this section, authors were concerned about 3 types of fly ash PRT, OPE and K6_LF. In order to investigate the effect of alkaline liquid and water content in the mixture, the mixtures were divided into two sets. In the first set, the mixtures were mixed with the same components in section 4.2 by extra water (see Table 4.2). And the second set presents the details of the mixtures by adding alkaline are given in Table 4.4 and already classified into 3 coded such as: MT', ME' and MLF'. The ratio of $H_2O/Na_2O$ and concentrations of NaOH liquid (in Molars) used for this study was 12 and 14 M, respectively.

| | | | Materials | | Curing | |
|---|---|---|---|---|---|---|
| | | | [%] | Alkaline [%] | Time [hours] | Temp [$^{o}$C] |
| | | | 50 | 40 | 24, 48 | 70 |
| PRT | MT'-2 | 20 | 43.5 | 36.5 | 24, 48 | 70 |
| | MT'-3 | 30 | 35 | 35 | 24, 48 | 70 |
| | MT'-4 | 40 | 27 | 33 | 24, 48 | 70 |
| | MT'-5 | 50 | 17 | 33 | 24, 48 | 70 |
| OPE | ME'-1 | 10 | 50 | 40 | 24, 48 | 70 |
| | ME'-2 | 20 | 43.5 | 36.5 | 24, 48 | 70 |
| | ME'-3 | 30 | 35 | 35 | 24, 48 | 70 |
| | ME'-4 | 40 | 27 | 33 | 24, 48 | 70 |
| | ME'-5 | 50 | 17 | 33 | 24, 48 | 70 |
| K6_LF | MLF'-1 | 10 | 50 | 40 | 24, 48 | 70 |
| | MLF'-2 | 20 | 39.5 | 40.5 | 24, 48 | 70 |
| | MLF'-3 | 30 | 33 | 38 | 24, 48 | 70 |
| | MLF'-4 | 40 | 22 | 38 | 24, 48 | 70 |
| | MLF'-5 | 50 | 9 | 41 | 24, 48 | 70 |

Figs. 4.9 ^ 4.11 show that water and/or alkaline solution has a significant effect on the compressive strength of geopolymer mortar.

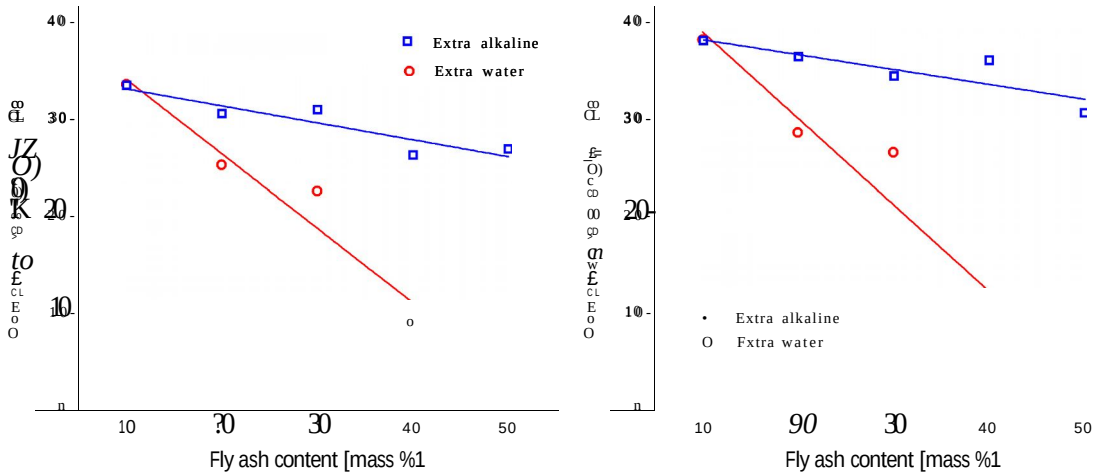


**Fig. 4.9** Compressive strength of fly ash PRT based geopolymer mortar after curing at 70 $^{o}$C for 24 hrs (left) and 48 hrs (right)

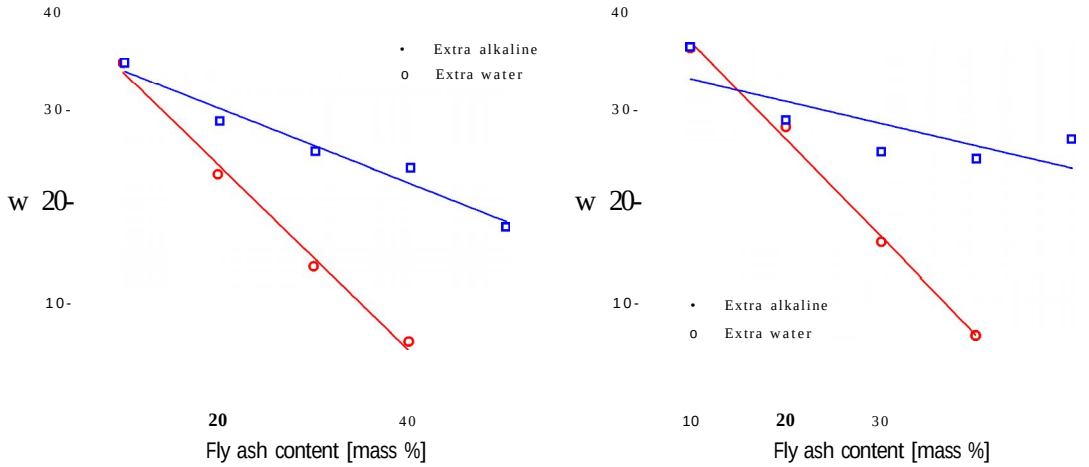


**Fig. 4.10** Compressive strength of fly ash OPE based geopolymer mortar after curing at 70 °C for 24 hrs (left) and 48 hrs (right)

It can be seen that increasing the percentage of fly ash from 10 to 40 % and adding water is significant reduce the compressive strength of samples, which exhibited nearly 24 % with PRT, 19 % with OPE and 90 % with K6_LF when curing in the oven at 70 $^{o}$C for 48 hrs. While the compressive strength values of geopolymer mortar with extra alkaline is slightly decrease with increasing fly ash content until 50 %. These results are very important for our future research to make specimens and using only alkaline solution for fresh mixtures.

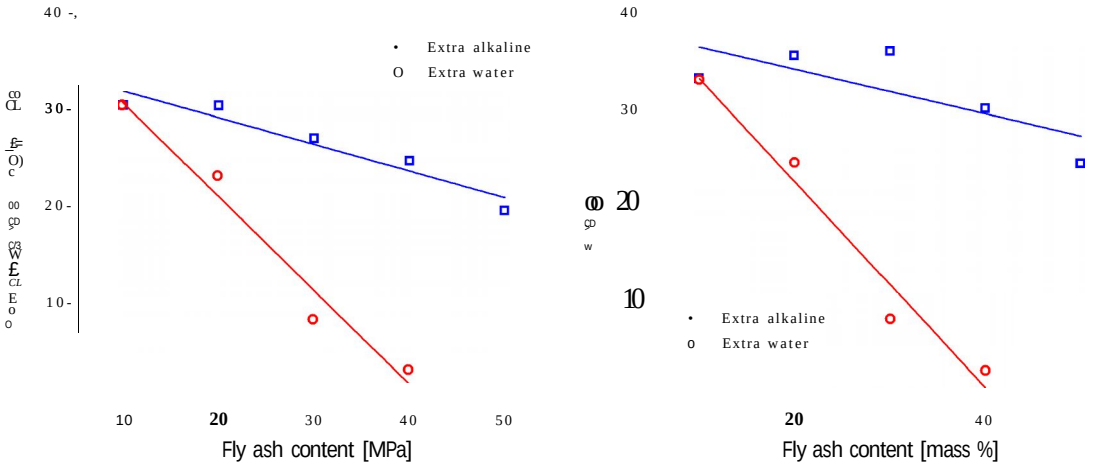


**Fig. 4.11** Compressive strength of fly ash K6 LF based geopolymer mortar after curing at 70 $^{o}$C for 24 hrs (left) and 48 hrs (right)

Compressive strength and density of the geopolymer mortars cured 70 $^{o}$C for 24 hrs and 48 hrs are summarized in Table 4.5. The table shows that increasing fly ash content can reduce the density of geopolymer mortar.

**Table 4.5** Properties of fly ash based geopolymer mortar with adding alkaline after curing at 70 °C for 24 hrs and 48 hrs

| Type of fly ash | Mixture No | 24 hours | | 48 hours | |
|---|---|---|---|---|---|
| | | Density p [kg/m$^3$] | Compressive strength [MPa] | Density p [kg/m$^3$] | Compressive strength [MPa] |
| PRT | MT'-1 | 1773 | **33.43** ± 3.7 | 1615 | **38.02** ± 0.7 |
| | MT'-2 | 1636 | **30.51** ± 7.1 | 1610 | **36.36** ± 1.6 |
| | MT'-3 | 1637 | **30.91** ± 6.8 | 1583 | **34.35** ± 5.5 |
| | MT'-4 | 1631 | **26.24** ± 5.0 | 1541 | **35.99** ± 4.4 |
| | MT'-5 | 1609 | **26.84** ± 1.0 | 1521 | **30.57** ± 15.8 |
| OPE | ME'-1 | 1679 | **34.79** ± 2.2 | 1564 | **36.28** ± 3.7 |
| | ME'-2 | 1602 | **28.76** ± 3.0 | 1520 | **28.77** ± 3.2 |
| | ME'-3 | 1593 | **25.61** ± 4.1 | 1501 | **25.48** ± 1.5 |
| | ME'-4 | 1490 | **23.92** ± 3.2 | 1431 | **24.75** ± 5.0 |
| | ME'-5 | 1510 | **17.87** ± 4.1 | 1463 | **26.39** ± 5.5 |
| K6_LF | MLF'-1 | 1631 | **30.32** ± 1.6 | 1564 | **33.03** ± 1.0 |
| | MLF'-2 | 1562 | **30.27** ± 4.4 | 1452 | **35.40** ± 1.6 |
| | MLF'-3 | 1561 | **26.92** ± 0.9 | 1442 | **35.86** ± 2.6 |
| | MLF'-4 | 1531 | **24.57** ± 6.8 | 1441 | **29.98** ± 4.9 |
| | MLF'-5 | 1517 | **19.44** ± 5.2 | 1437 | **24.30** ± 5.9 |

## 4.4. EFFECT OF CURING ON THE COMPRESSIVE STRENGTH OF GEOPOLYER MORTAR

Although fly ash based geopolymer mortar can be cured in ambient conditions, heat curing is generally recommended. Both curing time and curing temperature influence the compressive strength of geopolymer mortar and concrete. This section, fresh geopolymer mortar was mixed from 10 % fly ash (K6_LF, OPE, and PRT) together 80 % geopolymer resin.

### 4.4.1 CURING TIME

The curing time is illustrated in Fig. 4.12. The tests cylinders from mixtures MLF-1, ME-1 and MT-1 were heat cured at 70 °C in a furnace and continued curing at ambient temperature

for 2 days. The curing time varied from 5 hrs to 72 hrs. Longer curing time improved the polymerization process resulting in higher compressive strength. The rate of increase in strength was rapid up to 24 hrs of curing time.

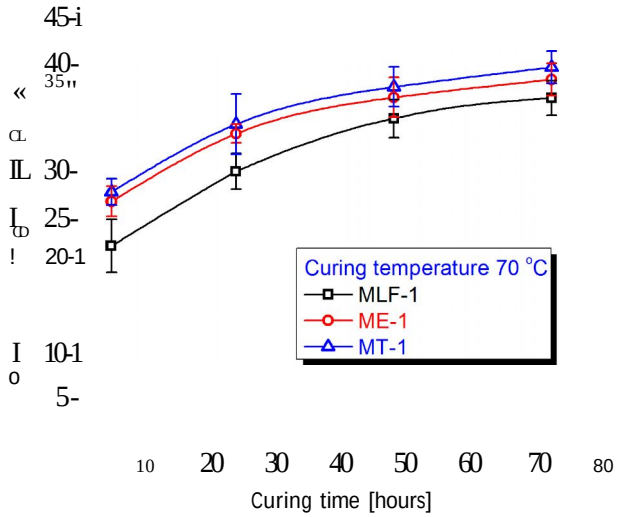


**Fig. 4.12** Effect of curing time on compression strength of geopolymer mortar

### 4.4.2 CURING TEMPERATURE

Fig. 4.13 shows the effect of curing temperature on the compressive strength of geopolymer mortar. The tests cylinders from mixtures MLF-1, ME-1 and MT-1 were heat cured in a furnace for 48 hrs and continued curing at ambient temperature for 2 days. Higher curing temperature resulted in larger compressive strength, although an increase in the curing temperature beyond 70 °C did not increase the compressive strength substantially. Based on these test trends, a curing temperature of about 70 °C is recommended.

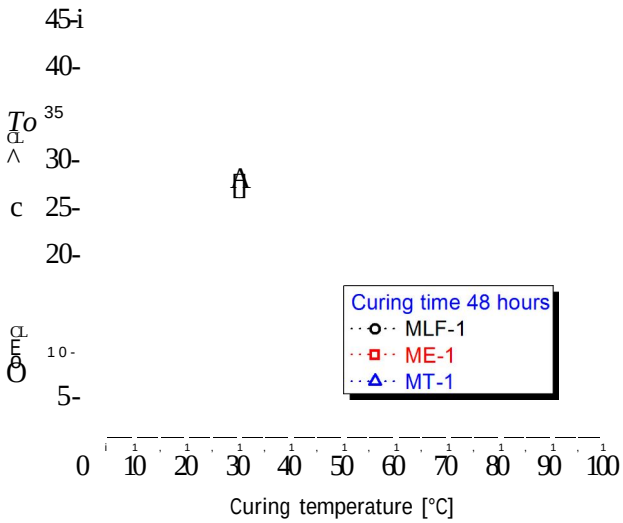


**Fig. 4.13** Effect of curing temperature on compression strength of geopolymer mortar

## 4.5. CONCLUSIONS

The following conclusions were drawn from this chapter on geopolymer mortar:

(i) It was detemined that the most important parameter is particle size on mechanical properties of geopolymer mortar. The microstructure of fly ash support compressive strength value due to their shape and size differences. The mortar obtained from the geopolymer resin with fineness PRT fly ash (10 %, 38.02 MPa) after curing 70 $^{o}$C for 48 hrs gives better mechanical strength than using other fly ashes.

(ii) The compressive strength of specimens with extra alkaline was slightly reduced with increasing fly ash content until 50 %, while using extra water was decreased too much about 90 % mechanical properties of geopolymer mortar.

(iii) Increase in compressive strength was also observed with increase in curing time. However when curing time was increased from 48 hrs to 72 hrs, there was not much variation in compressive strength.

(iv) We can be seen that fly ash is just an industrial waste many types of chemical substances might get mixed with it and may cause significant changes in reactions. For example calcium reacts very fast with Si and Al produced by dissolution during geopolymerization [56]. So fly ash based geopolymer mortar or concrete is more environmental friendly and has the potential to replace ordinary cement concrete in many applications.

# Chapter 5

# EFFECTS OF MODIFIED FLY ASH PARTICLES BY WET MILLING AND HIGH TEMPERATURE ON THE PROPERTIES OF GEOPOLYMER MORTAR

## 5.1. INTRODUCTION

There are several references that describe the influence of mechanical activation of fly ash on the mechanical properties of geopolymers [146-148]. In this Chapter, the influence of mechanical activation of fly ash via ball milling process and high temperature on the chemical composition, color, particle size of fly ash and on the mechanical properties of geopolymer has been investigated. We are divided into two sections as following:

(i) In first section, fly ash was mechanically activated through particle size refinement from micro to nano scale by milling 1 hr to 5 hr in wet conditions. The milled fly ash was then mixed with geopolymer resin in water dispersion form and in the form of dried particles after evaporation of water. Significant increase in compression strength was observed for dried milled fly ash geopolymers whereas significant loss in compression strength was observed for water dispersion fly ash geopolymers. The improvements in physical properties were found to be associated with microstructural changes that resulted from the enhanced geopolymerization in mechanically activated samples from dried fly ash due to more reactive surface of fly ash particles after milling.

(ii) The purpose of this section is whitening the fly ash by high temperature to compete with other filler materials. And compared influence of adding fly ash before and after modified by high temperature in order to obtain the compressive strength and the hardness of geopolymer mortar is investigated.

## 5.2. INFLUENCE OF MODIFIED FLY ASH PARTICLES BY WET MILLING

Mixture MK1-1 (see Table 4.2) is being studied to determine the relationships existing between the physical and chemical properties of the powder and its sinterability. Mechanical activation through ball milling offers the possibility to alter the reactivity of solids through physicochemical changes in bulk and surface but without altering the overall chemistry of the material [149]. Ball milling results in modification of the fly ash by transforming the micro sized fly ash into nanostructured fly ash. Particle size distribution measurements have been made on the virgin powders, ball milled powder. The smooth, glassy and inert surface of the fly ash can be altered to a rough and more reactive by this technique.

### 5.2.1 EXPERIMENTAL

Mechanical activation of fly ash was carried out using a high-energy planetary ball mill of Fritsch Pulverisette 7 in a sintered corundum container of 80 ml capacity using zirconia balls of 3 mm under wet condition in distilled water for 1, 2, 3, 4, and 5 hours. The ball mill was loaded with ball to powder weight ratio of 10:1. The rotation speed of the planet carrier was 850 rpm. In this mechanical treatment, powder particles are subjected to a severe plastic deformation due to the repetitive compressive loads arising from the impacts between the balls and the powder. The milled sample powder was taken out at a regular interval of every 1 hour of milling to test for particle size distribution on Malvern Zetasizer Nano based on dynamic light scattering principle. The dispersion medium was deionised water. The dispersion was ultrasonicated for 5 min with Bandelin ultrasonic probe before characterization. Refractive index of 1.55 was used for fly ash to calculate particle size. Later the size and dimensions of fresh as well as ball milled fly ash were examined by means of Scanning Electron Microscope TS5130-Tescan SEM at 30 KV accelerated voltage.

The technology of sample preparation is as follows. At first, the geopolymer resin was prepared by mixing the alkaline activator with the raw materials. The liquid and solid components were mixed about 5 minutes at room temperature until the solution homogenized. Next, the geopolymer resin mixture was mixed with fly ash in two ways. On one way wet milled dispersion of fly ash in water was directly mixed with geopolymer resin

without evaporating the excess water in dispersion. While on other way the excess water from wet milled dispersion of fly ash was evaporated first and then the dried nano particles of fly ash were mixed with geopolymer resin. The mixing was done in an air conditioned room at approximately 23 $^{o}$C until the well homogenized mixture (about 5 minutes). Directly after mixing, the fresh mortar was poured in the moulds and vibrated for 2 minutes on the vibration table to remove air voids. These samples were cured at room temperature for 3 days after casting. Next, the samples were removed from the moulds and left in laboratory ambient conditions till 7, 14, and 28 days. Fig. 5.1 shows the detail procedure of geopolymer preparation.

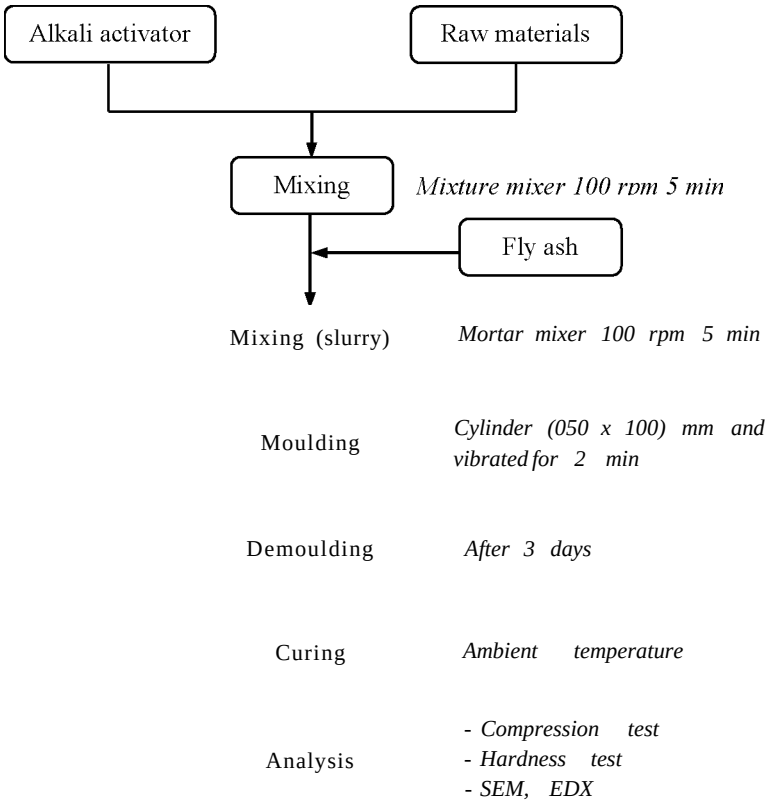


**Fig. 5.1** Geopolymer preparation procedure

### 5.2.2 EFFECT OF BALL MILLING ON PARTICLE SIZE DISTRIBUTION

Fig. 5.2a shows the particle size distribution curves of the unmilled and fly ashes milled for different time 1, 2, 3, 4 and 5 hr. The rate of particle size reduction was greatest during the initial 1hr of milling during which the characteristic particle diameter Z-average reduced from 3547 nm to 989 nm .The particle size gradually decreased with milling time and reached to

493 nm after 5 hrs of wet milling as shown in Figs. 5.2b and 5.2c. This shows that the main influence of the mechanical activation of fly ash is to decrease particle size rather than change mineralogical content.

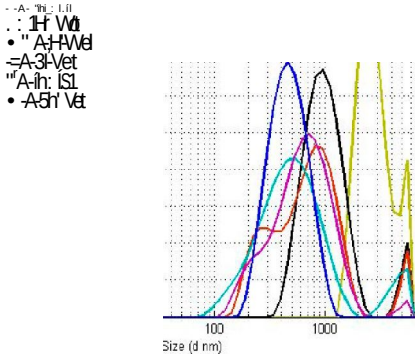


(a) Unmilled and milled fly ash

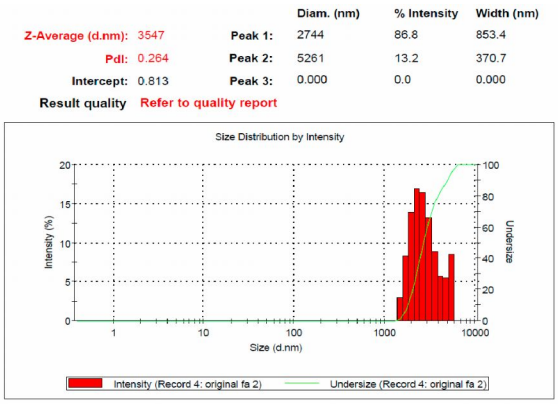


(b) Unmilled fly ash

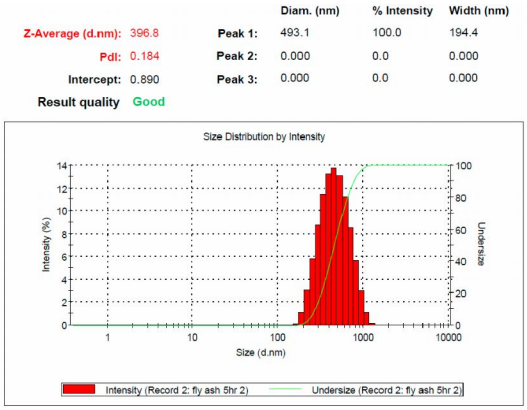


(c) Milled fly ash after 5 hr

**Fig. 5.2** Particle size distributions of unmilled and milled fly ash

Fig. 5.3 shows SEM image of unmilled and milled fly ash particles.

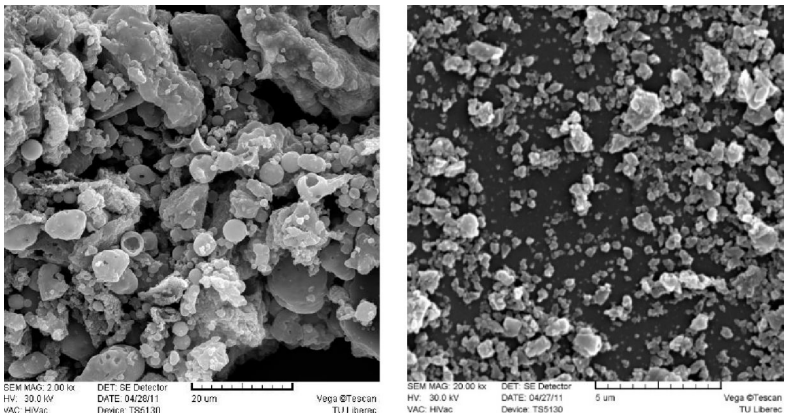

Unmilled original fly ash Milled fly ash

**Fig. 5.3** SEM image of unmilled and milled fly ash

It clearly shows that milling destroys a large proportion of the spherical morphology of the unmilled original fly ash. However, the spherical morphology of the unmilled fly ash was not fully destroyed and there is some agglomeration of the fine grained particles.

### 5.2.3 EFFECT OF MECHANICAL ACTIVATION ON COMPRESSION STRENGTH OF GEOPOLYMER

Fig. 5.4 left shows significant improvement in compression strength of geopolymers made from wet milled fly ash which was dried before mixing with geopolymer resin as compared to unmilled fly ash. One of the reasons for improved compressive strength in mechanically activated fly ash mixtures is the high rate of geopolymerization in the sample. Mechanical activation increases the reactivity of the fly ash causing faster dissolution of the fly ash and rapid setting. Fast setting is the result of improved dissolution of the fly ash into alkaline liquid; leading to improved polymerization and hardening of the gel phase and thus developing compact structure within the geopolymer.

On the other hand sharp reduction in compression strength was observed for the geopolymers made from wet milled fly ash which was not dried before mixing with geopolymer resin as compared to unmilled fly ash geopolymer. The loss of compression strength is due to the excess water present in wet milled fly ash dispersion which reduces the concentration of sodium hydroxide. The less concentration of sodium hydroxide leads to reduced geopolymerization reaction and thus lowers compressive strength.

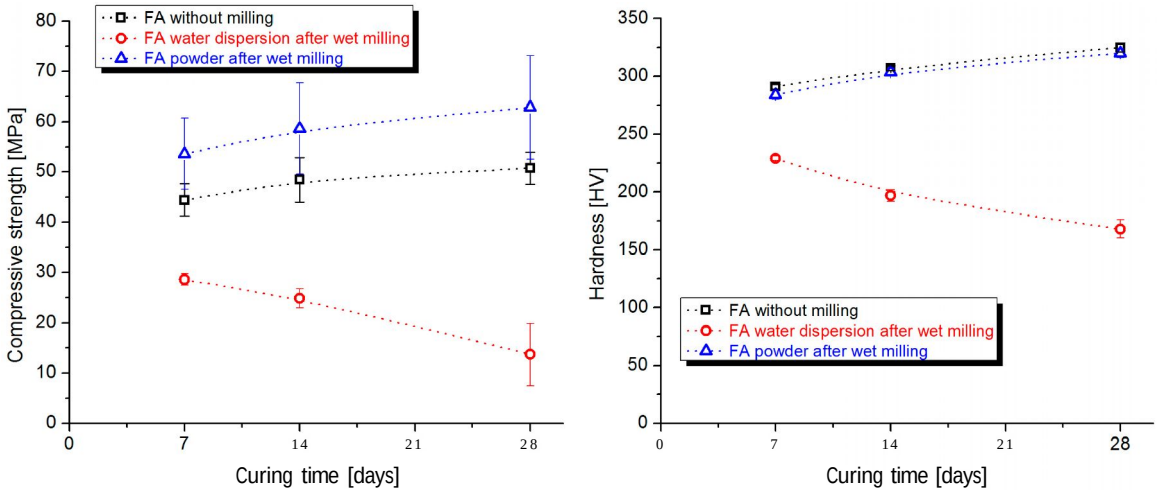


**Fig. 5.4** Effect of mechanical activation of fly ash on the compression strength (left) and the hardness (right) of geopolymer mortar

However, Fig. 5.4 right shows that the local hardness of geopolymer mortar is not improve comparing with unmilled fly ash.

### 5.2.4 EFFECT OF MECHANICAL ACTIVATION ON PHYSICAL PROPERTIES OF GEOPOLYMER

The physical properties of the geopolymers were tested for unmilled fly ash and milled fly ash both in dispersion and powder form and shown in table 2. The 10 MPa increase in compression strength was observed for the geopolymers made from nano particles of wet milled fly ash in all 7, 14 and 28 days of ambient curing as compared to the geopolymers made from microparticles of unmilled fly ash. Whereas significant loss of 30 ^ 35 MPa in compression strength was observed for the geopolymers made from water dispersion of wet milled fly ash as compared to those of unmilled fly ash. The same trend was observed in case of density for all types of geopolymers. However lower value of hardness was observed for mechanically activated fly ash than unmilled fly ash geopolymers.

**Table 5.1** The properties of 10 % fly ash (FA) (unmilled and milled) based geo mortar after curing at room temperature

| Properties | Time [days] | FA unmilled | FA after with milling | FA after with milling and drying |
|---|---|---|---|---|
| Compressive strength [MPa] | 7 | **44.41** ± 3.2 | **28.59** ± 1.1 | **53.56** ± 7.1 |
| | 14 | **48.42** ± 4.4 | **24.88** ± 1.9 | **58.61** ± 9.1 |
| | 28 | **50.72** ± 3.2 | **13.69** ± 6.2 | **62.80** ± 10.3 |
| Hardness [GPa] | 7 | **291** ± 2 | **229** ± 2 | **284** ± 4 |
| | 14 | **307** ± 2 | **197** ± 5 | **304** ± 3 |
| | 28 | **325** ± 4 | **168** ± 8 | **320** ± 4 |
| Density [g/cm$^3$] | 7 | 1.73 | 1.61 | 1.77 |
| | 14 | 1.72 | 1.57 | 1.77 |
| | 28 | 1.71 | 1.55 | 1.76 |
| Grain size [nm] | | 3547 | 298.4 | 298.4 |

The obtained fly ash dispersion from wet milling was directly added in geopolymers and the samples were cured at room temperature for 7, 14 and 28 days. But significant reduction in compression strength was observed as compared with original fly ash geopolymers due to presence of free water which reduced geopolymerisation rate. However when fly ash was

dried, it resulted into improved compression strength of geopolymer mortars. After 28 days, compression strength was 62 MPa as compared with 50 MPa of original fly ash geopolymer mortars.

### 5.2.5 CONCLUSIONS

Mechanical activation of fly ash in a planetary ball mill with milling media to powder ratio of 10:1 leads to a reduction of particle size and change in particle shape but little change in mineralogical composition. Geopolymer mortar made with mechanically activated fly ash cured at ambient temperature leads to an increase in compressive strength of 10 MPa when compared with geopolymer made from unmilled fly ash. The main contribution to increased compressive strength of the geopolymer is attributed to reduction of particle size and change in morphology allowing a higher dissolution rate of the fly ash particles. Mechanically activation of fly ash can be seriously considered as a viable method to achieve ambient temperature curing of geopolymers.

## 5.3. INFLUENCE OF MODIFIED FLY ASH PARTICLES BY HEATING

Every day, the world is generated large quantities of waste materials, such as: water, oils, solvents and solid waste (fly ash, glass, stone powder, mine tailings, etc). Fly ash has emerged as a material with high potential applications in construction because it has a chemical composition similar to Portland cement, cheep material, low density, good dispersion and fluidity [150, 151]. However, the scope application of fly ash is very limited due to fly ash is grey or black in color; using only to product where color is not important. For this reason, a heating method was necessary to be developed to increase the whiteness of fly ash.

The purpose of this research is whitening the fly ash to compete with other filler materials. And compared the influence of adding fly ash before and after modified by high temperature in order to obtain the compressive strength and the local hardness of geopolymer mortar is investigated. Experimental results show that high temperature are effective methods to purify fly ash, high whiteness of the particle which increased with the calcination temperature and slightly reduced the local hardness of geopolymer mortar.

### 5.3.1 EXPERIMENTAL

Fly ashes are heated to improve the whiteness at certain temperature using a furnace. Around 1 kg fly ashes were heated in a furnace to 200 $^{o}$C, 400 $^{o}$C, 600 $^{o}$C, 800 $^{o}$C and 1000 $^{o}$C at a heating rate of 5 K/min and with a soak time of 1 hour at the maximum temperature and finally annealed down to room temperature. The exact weight of fly ashes before and after heating was measured by using an analytical balance with a resolution of 0.1mg.

After modification fly ash particles at 1000 $^{o}$C, they were used to making geopolymer mortar; the technology of preparation was the same with section 5.2. The samples were kept at room temperature until the time of testing. The details of the mixtures are given in Table 4.4 and mixtures MLF'-2, MLF'-3, MLF'-4 and MLF'-5 were used to investigate the mechanical properties of geopolymer based fly ash after modified by high temperature.


**Fig. 5.5** The heating of fly ashes using a furnace

### 5.3.2 RESULTS

Fig. 5.6 shows that the weight loss of fly ash samples at temperature below 200 $^{o}$C is small (less than 0.2 %), it indicates that as-received fly ash samples are relatively dry. When fly ash samples are further heated, the weight loss will be increased and the maximum of weight loss is at around 1000 $^{o}$C.

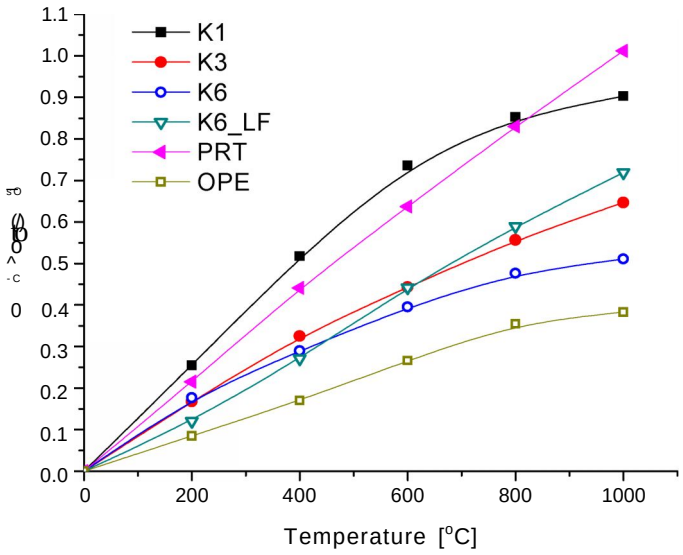


**Fig. 5.6** The weight loss as a function of heating temperature

Figs. 5.7 ^ 5.9 show the photographs and SEM of fly ash before and after heating at 1000 °C. After heating at high temperature, fly ash particles may suffer sever degradation, pitting, buckling, and breakage, which all can eventually regression the mechanical property of matrix. The obvious color difference can be observed by a naked eye. The SEM photographs and corresponding energy spectrum of all types of fly ash before and after heating at 1000 °C are given detail on Appendix C. Table 5.2 shows the summary chemical composition of fly ashes after heating at 1000 °C.

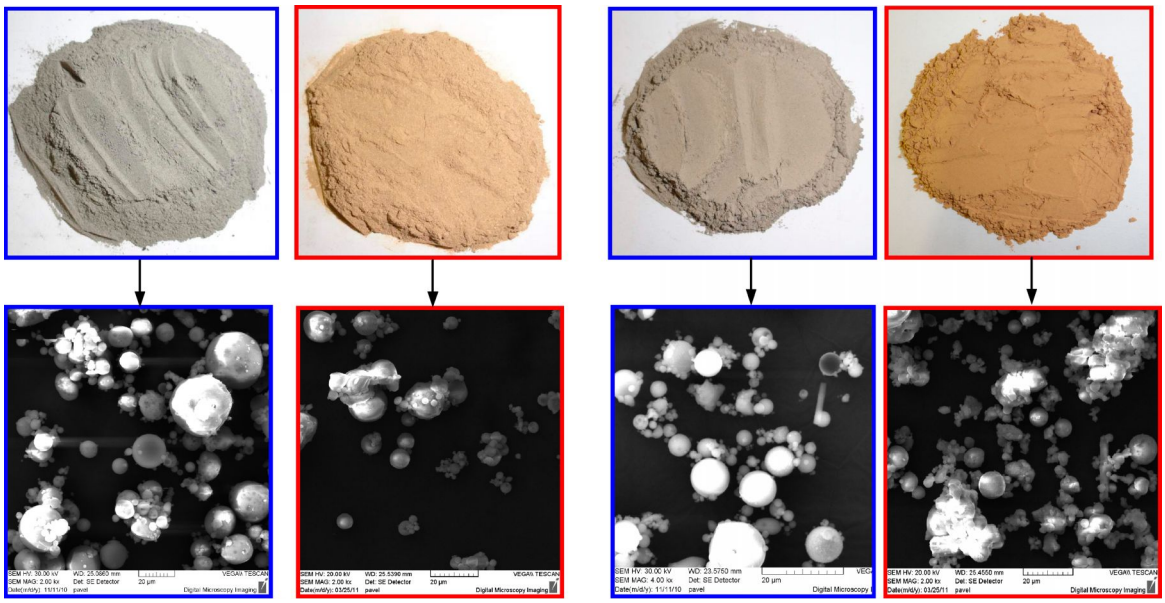

**Fig. 5.7** The photograph and SEM of OPE and PRT before (grey) and after heating at 1000°C (brown)

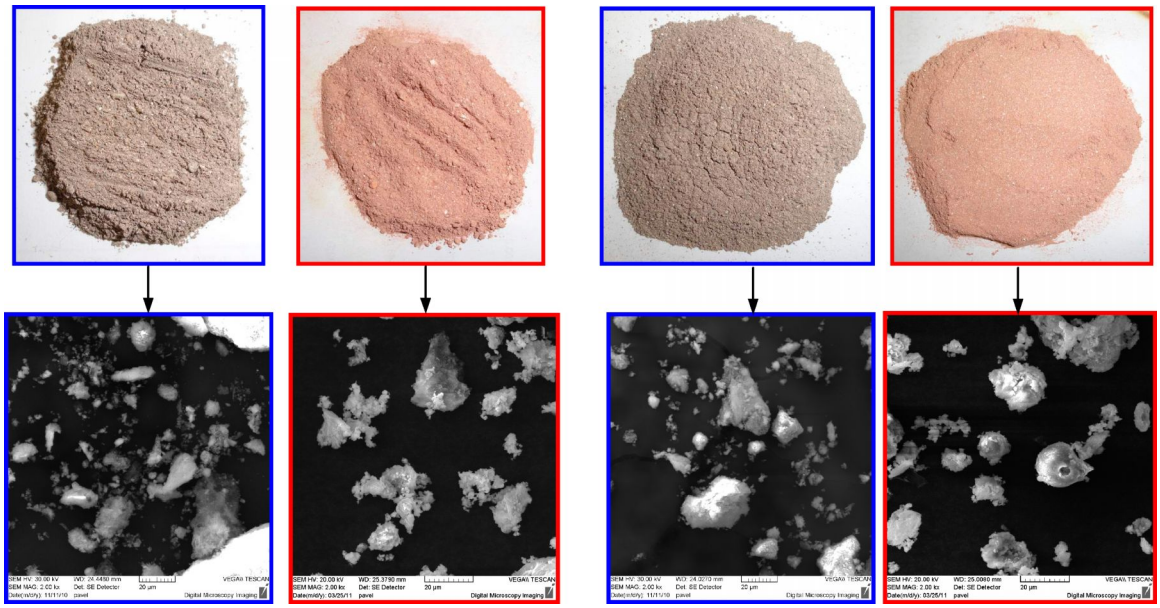

**Fig. 5.8** The photograph and SEM of K6 and K6_LF before (grey) and after heating at 1000$^{o}$C (red)

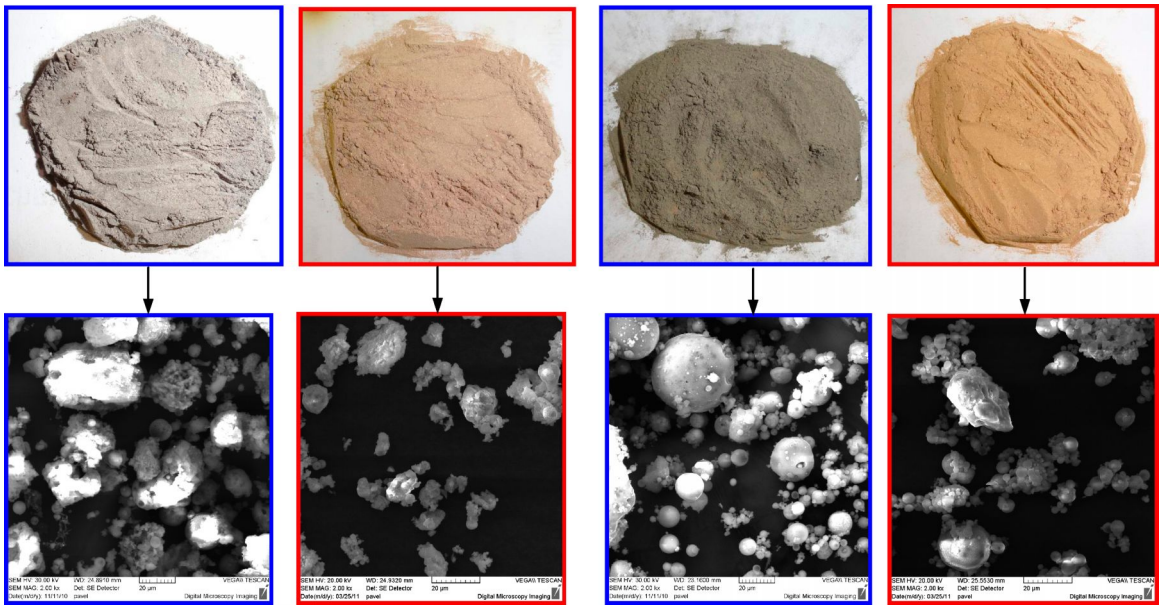

**Fig. 5.9** The photograph and SEM of K1 and K3 before (grey) and after heating at 1000 $^{o}$C (dark yellow)

**Table 5.2** The calcinations dependent composition of fly ashes after heating at 1000 °C

| Atomic [%] | PRT | OPE | K1 | K3 | K6 | K6_LF |
|---|---|---|---|---|---|---|
| Na | 0.63 | 0.61 | - | 1.22 | 0.99 | 0.32 |
| Mg | 0.70 | 0.53 | - | 0.36 | 0.56 | 1.16 |
| Al | 4.50 | 13.88 | 20.99 | 16.82 | 18.70 | 14.07 |
| Si | 33.56 | 22.47 | 17.01 | 25.22 | 17.96 | 21.29 |
| K | 0.83 | 1.42 | 0.52 | 0.58 | 1.20 | 0.80 |
| Ca | 1.06 | 4.64 | 0.35 | 0.79 | 0.65 | 10.13 |
| Ti | 0.50 | 1.06 | 7.50 | 1.59 | 1.40 | 1.08 |
| Fe | 1.76 | 8.78 | 1.24 | 1.85 | 2.02 | 8.19 |
| As | 0.03 | 1.29 | 0.49 | 0.49 | 0.58 | 0.80 |
| Zr | - | 0.08 | 0.59 | 0.98 | 0.48 | 0.69 |
| Cu | - | - | 0.80 | - | - | 1.08 |
| O | 56.43 | 45.24 | 50.51 | 50.09 | 55.45 | 40.39 |

In Figs. 5.10 ^ 5.12 present the photomacrographs of geopolymer mortar based on 40 % fly ash OPE, PRT, K6_LF before and after modified particles by heating at 1000 °C.

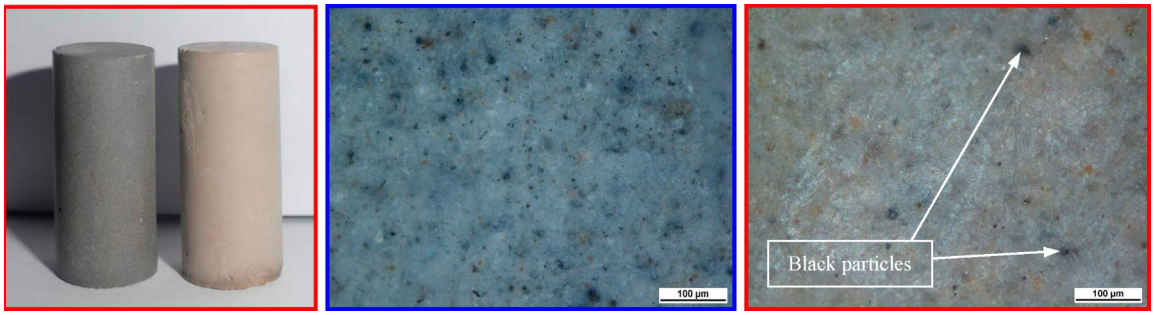


**Fig. 5.10** Photomacrographs geopolymer mortar based on fly ash OPE before (left) and after heating at 1000 °C (right)

In the photomacrographs indicate that the color of geopolymer mortar after heating at 1000 °C is brighter than unmodified powder. Because after heating the fly ash at 1000 °C removed unburnt carbon from black particles. Furthermore the oxidation of iron from magnetite ($Fe_3O_4$), wuestite (FeO), and/or other sources to hematite ($Fe_2O_3$) (see Equations 5-1 to 5-3) took place especially on the surface.

$$3FeO + \wedge O2 \text{—} Fe3O4 \quad (5\text{-}1)$$

$$2Fe3O4 + \wedge O2 \text{ —} 3Fe2O3 \quad (5\text{-}2)$$

$$6FeO + 1.5\ O2 \ \text{—}\ 3\ Fe2O3 \qquad (5\text{-}3)$$

However in geopolymer mortar based fly ash modified at 1000 $^{o}$C have still black particle, it may be because a heterogeneous mixture of geopolymer cement and some powder of fly ash unburnt carbon.

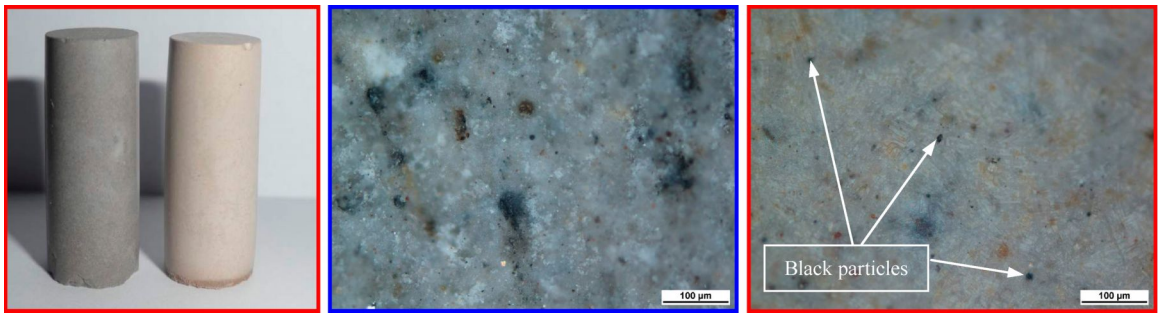


**Fig. 5.11** Photomacrographs geopolymer mortar based on fly ash PRT before (left) and after heating at 1000 $^{o}$C (right)

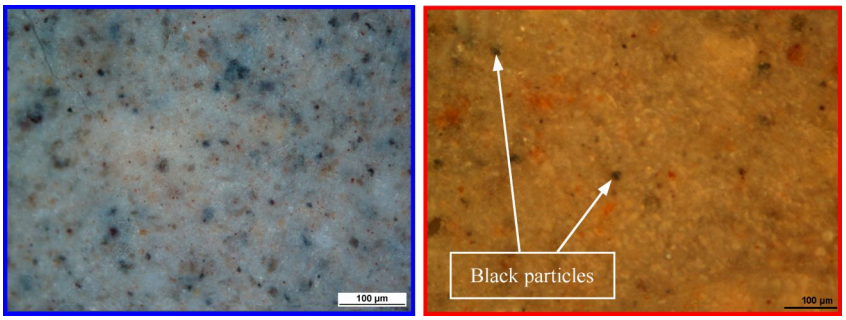


**Fig. 5.12** Photomacrographs geopolymer mortar based on fly ash K6_LF before (left) and after heating at 1000 $^{o}$C (right)

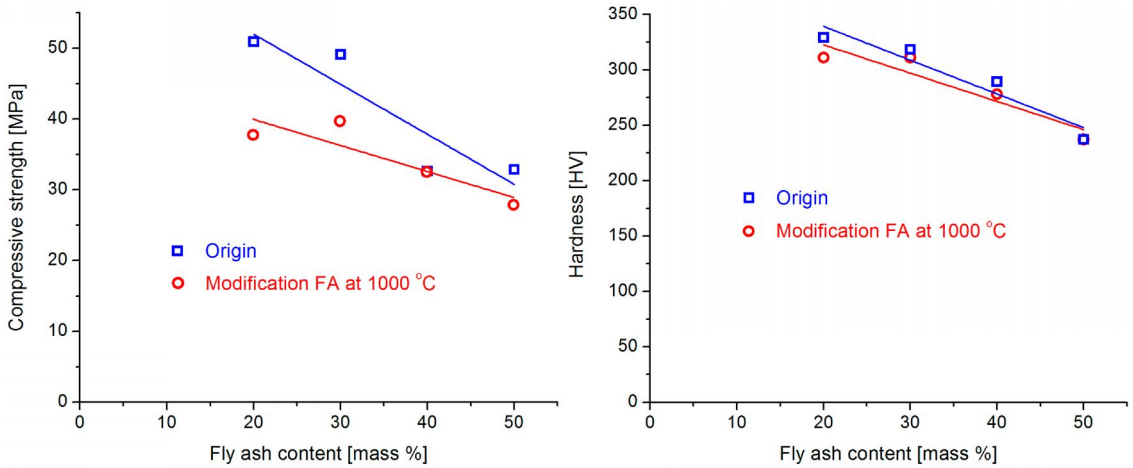


**Fig. 5.13** Compressive strength (left) and hardness (right) of geopolymer mortar based on fly ash K6_LF before and after heating at 1000 $^{o}$C

**Table 5.3** Mechanical properties of geopolymer mortar before and after modified K6_LF fly ash particles at 1000 $^{o}$C

| Mixture No | Types of fly ash | Time [days] | Density [kg/m$^3$] | Hardness [HV] | Compressive strength [MPa] |
|---|---|---|---|---|---|
| MLF'-2 | Origin | 7 | 1774 | **267** ± 2 | **41.69** ± 1.9 |
| | | 14 | 1726 | **305** ± 10 | **48.10** ± 5.4 |
| | | 28 | 1624 | **330** ± 11 | **50.93** ± 5.1 |
| | Modified FA at 1000 $^{o}$C | 7 | 1850 | **245** ± 2 | **33.29** ± 1.9 |
| | | 14 | 1758 | **285** ± 12 | **35.72** ± 4.4 |
| | | 28 | 1615 | **311** ± 8 | **37.72** ± 4.8 |
| MLF'-3 | Origin | 7 | 1776 | **259** ± 6 | **36.11** ± 3.4 |
| | | 14 | 1684 | **306** ± 8 | **44.78** ± 4.2 |
| | | 28 | 1622 | **319** ± 8 | **49.10** ± 5.7 |
| | Modified FA at 1000 $^{o}$C | 7 | 1878 | **254** ± 7 | **24.89** ± 1.9 |
| | | 14 | 1752 | **302** ± 8 | **32.91** ± 5.9 |
| | | 28 | 1678 | **311** ± 8 | **39.69** ± 5.3 |
| MLF'-4 | Origin | 7 | 1721 | **186** ± 7 | **28.86** ± 5.8 |
| | | 14 | 1671 | **225** ± 3 | **31.91** ± 4.0 |
| | | 28 | 1607 | **290** ± 6 | **32.61** ± 5.5 |
| | Modified FA at 1000 $^{o}$C | 7 | 1851 | **219** ± 4 | **28.18** ± 1.2 |
| | | 14 | 1769 | **247** ± 6 | **30.37** ± 1.0 |
| | | 28 | 1651 | **278** ± 7 | **32.51** ± 1.6 |
| MLF'-5 | Origin | 7 | 1658 | **153** ± 4 | **27.21** ± 6.7 |
| | | 14 | 1639 | **204** ± 5 | **31.60** ± 2.7 |
| | | 28 | 1567 | **238** ± 3 | **32.85** ± 1.7 |
| | Modified FA at 1000 $^{o}$C | 7 | 1852 | **112** ± 3 | **21.68** ± 1.4 |
| | | 14 | 1699 | **223** ± 10 | **23.33** ± 1.7 |
| | | 28 | 1629 | **237** ± 6 | **27.84** ± 1.3 |

This high processing temperature can have significant influence on the final properties of the geopolymer mortar. Fig. 5.13 presents the compressive strength and the hardness of geopolymer mortar based on fly ash K6_LF unmodified and modified particles by heating at

1000 $^{o}$C. After heating fly ash particles at 1000 $^{o}$C, the compressive strength of samples can be reduced slightly but not much.

From Table 5.3 it can also be seen that the density of specimens after modified fly ash at 1000 $^{o}$C is higher than origin fly ash, because they tend to absorb water more than origin. In general both unmodified and modification fly ash gave the same effect on the geopolymer mortar and have the similar pattern of mechanical properties as function of fly ash content that was decreased with increasing of fly ash content.

### 5.2.5 CONCLUSIONS

The purpose of this research is used the method of calcination temperature to whitening the fly ash to compete with other filler materials. It is evident from the above observations that the high temperature has considerable effect on the surface morphology and pitting of the fly ash particles. The study where used fly ash particles as filler, the particles after heated at high temperature will soften and may have adverse effect on the structural and reduced mechanical properties of the geopolymer mortar. Thus, authors recommended this method use in sculpture, architecture, especially where color is more important than the mechanical properties.

# Chapter 6

# OPTIMAL FLY ASH CONTENT IN GEOPOLYMER MORTAR AND CONCRETE

## 6.1. INTRODUCTION

Concrete is the most commonly used construction material. Its use by communities across the globe is second only to water [19, 152]. Geopolymeric binders appear to be an alternative to OPC, due to high mechanical performances and environmental advantages [153]. However the cost of geopolymer binders is still higher than OPC, it is one of the major factors explaining why this new product is not yet a current alternative. So the purpose of this chapter was reduced the cost of geopolymer binders by increasing fly ash content but mechanical properties of mortar and concrete is still good enough to meet essential requirements of industries.

In order to determine the optimal proportion of fly ash content in mortar and concrete, the influences of ratio of fly ash / geopolymer cement (FA / GC), effects of fly ash on mechanical properties (compressive strength, flexural strength, modulus of elasticity) of mortar and concrete were investigated in this chapter.

## 6.2. GEOPOLYMER MORTAR

Test specimens were made using geopolymer mortar from mixture MLF'-2 to MLF'-4 are given in Table 4.4, and adding mixtures from MLF'-6 to MLF'-10. The details of these mixtures are given in Table 6.1.

### 6.2.1 EXPERIMENTAL

Compressive strength testing of mortar was performed on cylinder specimens (046 x 92) mm and testing of the flexural strength indices of the specimens was conducted on (40 x 40 x 160) mm. These samples were cured at room temperature for 7, 14 and 28 days. And we used the standard specimen size (10 x 10 x 55) mm according to ASTM 370 for charpy impact testing, these samples used to determine impact strength, they were cured at room temperature for 28 days before testing.

**Table 6.1** Composition of fresh geopolymer mortar K6_LF mixes by adding alkaline

| Mixtures No | Materials | | | |
|---|---|---|---|---|
| | Fly ash [%] | Geo cement [%] | Alkaline [%] | Fine sand [%] |
| MLF'-2 | 20 | 39.5 | 40.5 | - |
| MLF'-3 | 30 | 33 | 38 | - |
| MLF'-4 | 40 | 22 | 38 | - |
| MLF'-6 | 25 | 28 | 38 | 9 |
| MLF'-7 | 25 | 23 | 35 | 17 |
| MLF'-8 | 25 | 18 | 32 | 25 |
| MLF'-9 | 25 | 12 | 33 | 30 |
| MLF'-10 | 25 | 8 | 31 | 36 |

### 6.2.2 RESULTS

Fig. 6.1 presents linear regression of a fictitious compressive strength and a fictitious flexural strength against ratio of FA / GC. This figure shows that mechanical properties of geopolymer mortar, compressive and flexural strength, are dependent on the ratio of FA / GC which decreasing strength is associated with increasing the ratio of FA / GC.

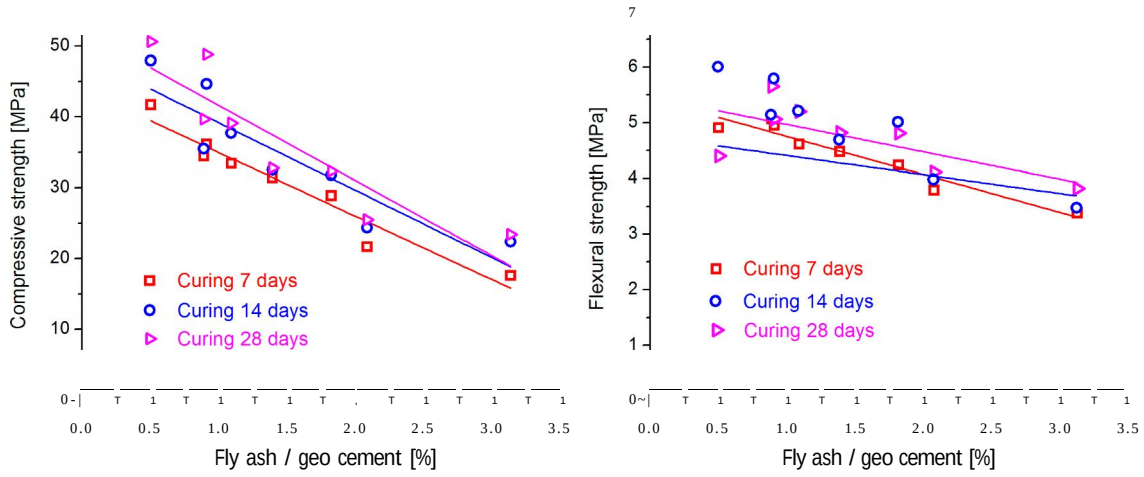


**Fig. 6.1** Compressive strength (left) and flexural strength (right) of geopolymer mortar

Table 6.2 presents the summarized results of geopolymer mortar. The mean values of virtual compressive strength, modulus of elasticity and flexural strength are completed with standard deviations, marked with ± sign. It can be seen from Fig. 6.1 and Table 6.2 that the ratio FA / GC of 0.5 (that mean FA = 20 % in mass) is given the results higher than other ratio.

**Table 6.2** Mechanical properties of geopolymer mortar cured at room temperature

| J71UJIC111 Co | Time [days] | Mixtures No | | | | | | | |
|---|---|---|---|---|---|---|---|---|---|
| | | MLF'-2 | MLF'-3 | MLF'-4 | MLF'-6 | MLF'-7 | MLF'-8 | MLF'-9 | MLF'-10 |
| Density [kg/m$^3$] | 7 | 1774 | 1776 | 1721 | 1867 | 1874 | 1802 | 1701 | 1781 |
| | 14 | 1726 | 1684 | 1671 | 1816 | 1731 | 1700 | 1651 | 1684 |
| | 28 | 1624 | 1622 | 1607 | 1745 | 1694 | 1682 | 1620 | 1610 |
| Compressive strength [MPa] | 7 | **41.69**±1.9 | **36.11**±3.4 | **28.86**±5.8 | **34.44**±2.6 | **33.39**±3.6 | **31.43**±1.5 | **21.66**±0.7 | **17.61**±1.4 |
| | 14 | **48.10**±5.4 | **44.78**±4.2 | **31.91**±4.0 | **35.63**±4.4 | **37.82**±4.7 | **32.64**±3.4 | **24.52**±3.4 | **22.54**±2.2 |
| | 28 | **50.93**±5.1 | **49.10**±5.7 | **32.61**±5.5 | **39.97**±2.4 | **39.39**±1.9 | **33.06**±0.7 | **25.78**±1.9 | **23.71**±0.7 |
| Flexural strength [MPa] | 7 | **4.91**±0.6 | **4.95**±0.48 | **4.24**±0.2 | **5.07**±0.5 | **4.61**±0.49 | **4.48**±0.52 | **3.79**±0.12 | **3.38**±0.05 |
| | 14 | **6.02**±0.52 | **5.81**±0.16 | **5.03**±0.25 | **5.16**±0.14 | **5.23**±0.23 | **4.71**±0.33 | **4.00**±0.05 | **3.49**±0.09 |
| | 28 | **4.40**±0.32 | **5.06**±0.57 | **4.81**±0.45 | **5.65**±0.34 | **5.20**±0.42 | **4.82**±0.19 | **4.11**±0.17 | **3.82**±0.19 |
| Elastic modulus of flexion [MPa] | 7 | **1366**±120 | **1365**±179 | **1325**±131 | **1027**±140 | **1358**±80 | **1219**±30 | **1164**±45 | **1064**±26 |
| | 14 | **1418**±133 | **1307**±92 | **1328**±83 | **1290**±140 | **1418**±43 | **1265**±103 | **1141**±9 | **1122**±51 |
| | 28 | **1476**±160 | **1515**±188 | **1413**±85 | **1361**±218 | **1504**±111 | **1347**±93 | **1370**±142 | **1201**±92 |
| Relative deformation [%] | 7 | 0.95 | 1.09 | 0.95 | 1.15 | 1.07 | 0.86 | 1.11 | 0.97 |
| | 14 | 1.38 | 1.23 | 1.10 | 1.39 | 1.01 | 0.92 | 0.86 | 1.01 |
| | 28 | 0.91 | 1.04 | 1.09 | 1.32 | 1.19 | 0.66 | 0.88 | 0.99 |
| Impact energy [mJ/cm$^2$] | 28 | **62.87**±3.62 | **53.59**±3.62 | **49.04**±2.34 | **51.67**±5.00 | **55.25**±4.84 | **57.92**±3.26 | **55.16**±5.79 | **48.38**±4.61 |

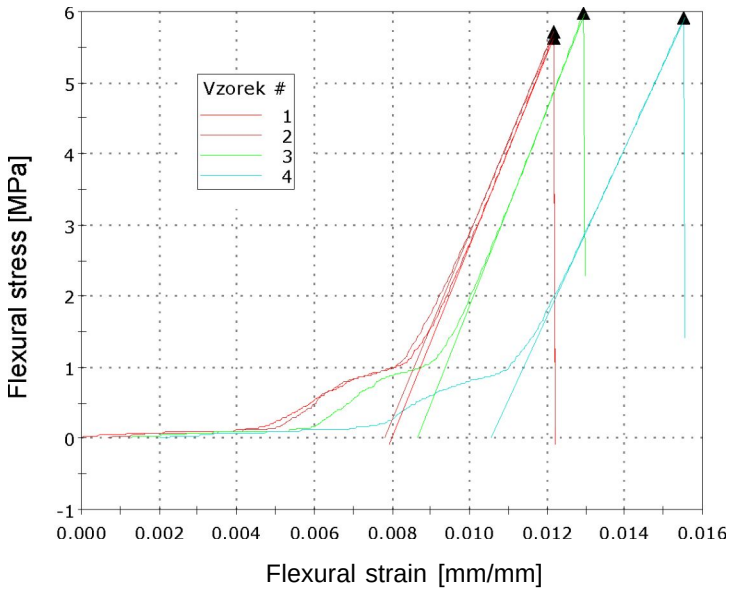


**Fig. 6.2** Typical stress and strain curve in flexure of geopolymer mortar MLF'-3

Typical diagram of flexural tests of geopolymer mortar MLF'-3 curing at room temperature for 14 days is show on Fig. 6.2. As can be seen that the linear parts of the cures is very short and slope, they present very typical behavior of brittle materials and hardening.

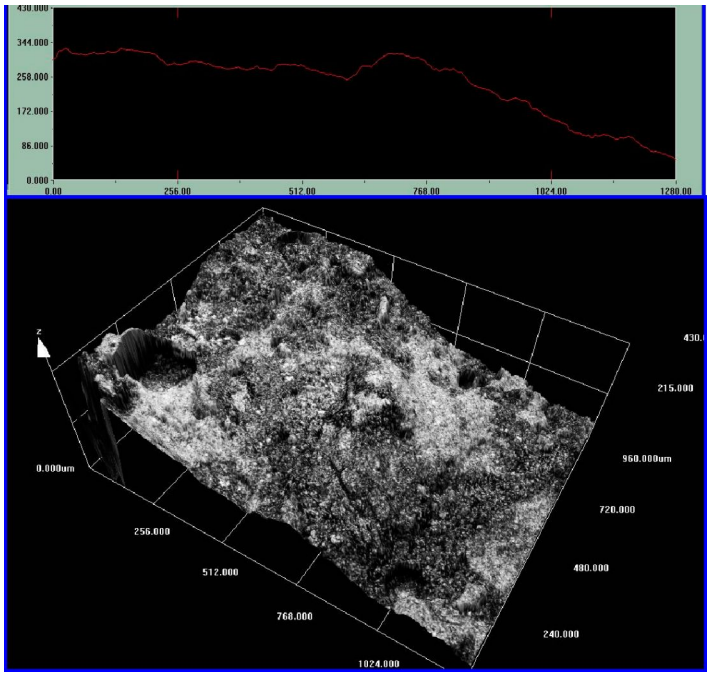


**Fig. 6.3** The LEXT OLS4000 Measuring Laser Confocal Microscope of geopolymer mortar MLF'-3

The surface roughness profile of geopolymer mortar is measured by the LEXT OLS4000 with 3D display, image provide level differences on the surface of the specimen are given in Fig. 6.3.

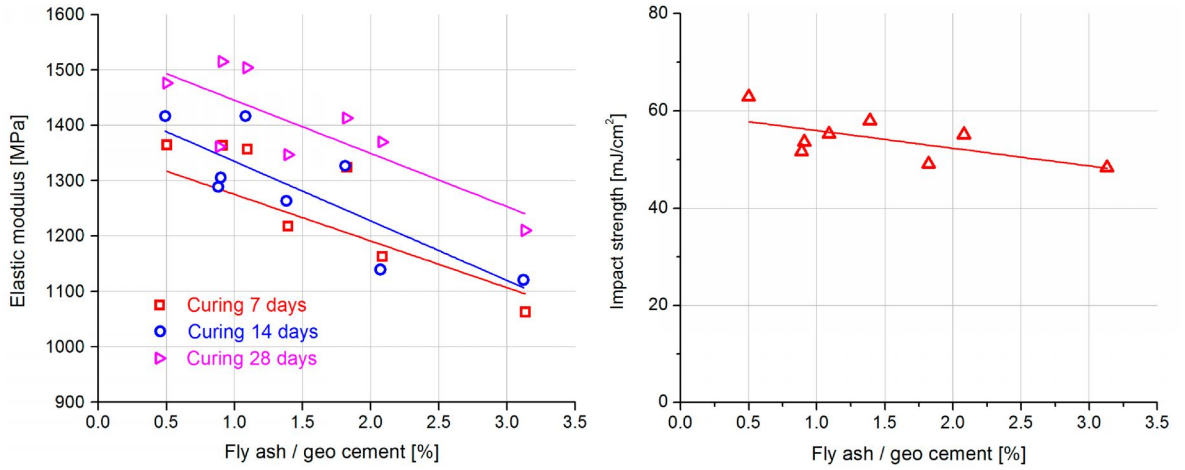


**Fig. 6.4** Modulus of elasticity (left) and Impact strength (right) of geopolymer mortar

The impact strength test was performed taking average three samples from each mixture after curing 28 days. The results of tests are plotted as Fig. 6.4. Impact strength and Modulus of elasticity increased with the reducing the ratio FA / GC. And it can be seen that increasing in curing time from 7 to 28 days is increases the elastic modulus.

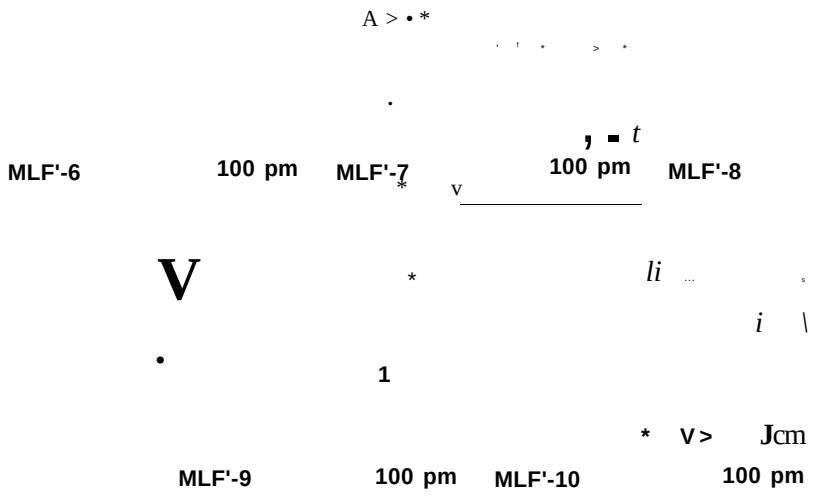


**Fig. 6.5** Surface of geopolymer mortar with mixtures MLF'-6 to MLF'-10

## 6.3. GEOPOLYMER CONCRETE

### 6.3.1 EXPERIMENTAL

Six mixtures were made to study the effect of ratio FA / GC on the mechanical properties of geopolymer concrete. The details of these mixtures are given in Table 6.3, and the properties of the mixtures are presented in Table 6.4. The authors were used fly ash K6_LF for all experimental, because the researches are supported this kind of fly ash in Komořany.

**Table 6.3** Composition of fresh geopolymer concrete mixes

| Mixture No | Materials | | | | | |
|---|---|---|---|---|---|---|
| | Fly ash [%] | Geo cement [%] | Alkaline [%] | Fine sand [%] | Coarse aggregate [%] | Extra water [%] |
| M1 | 20 | 10 | 8.5 | 19 | 38 | 4.5 |
| M2 | 15 | 13 | 11 | 19 | 38 | 4 |
| M3 | 15 | 13 | 15 | 19 | 38 | - |
| M4 | 10 | 15 | 18 | 19 | 38 | - |
| M5 | 10 | 15 | 18 | 9 | 48 | - |
| M6 | 10 | 9 | 14 | 9 | 58 | - |

Compressive strength testing of geopolymer concrete was performed on cylinder specimens (0100 x 200) mm, slump test, the elastic modulus and modulus of splitting tensile strength of geopolymer concrete was calculated using Equations (3-8) and (3-9). These samples were cured at room temperature for 7, 14 and 28 days.

### 6.2.2 RESULTS

The results show that samples cured in the laboratory ambient were measured after 7, 14, 28, and 90 days. After 28 days value of strength is higher than value after curing 7 days presented in Fig. 6.6. For strength development in time is for cured samples at room temperature typical long time period to reach the final physical-mechanical characteristics. Therefore was measurement focused on compressive strengths after 7, 14, 28 and 90 days, however the results of samples cured at room temperature from 28 days to 90 days was lightly increased or remained unaltered.

**Fig. 6.6** Compressive strength (left) and Modulus of elasticity (right) of geopolymer mortar

From the Fig. 6.6, it can be seen that the above mentioned results of mixtures M1 and M2 is smaller than other mixtures, because of added water in these mixtures to investigate the effect of water on the mechanical properties of geopolymer concrete, details of these mixtures are given in Table 6.3.

The slump test was chosen to measure the workability of the fresh state concrete. Slump test is useful in detecting the variations in the uniformity of a concrete mixture [154]. It can be seen from Table 6.4 that slump values increased as the content of water or alkaline liquid in the mixtures increased, it is one of major effect on the compressive strength of geopolymer concrete.

Fig. 6.6 shows that the results of the compressive strength of mixture M5 is higher than other mixtures, after 90 days curing at room temperature the mixture M5 present the compressive strength approximately 32 MPa and elastic modulus about 21 GPa.

Table 6.4 shows the values of elastic modulus and splitting tensile strength of samples from mixtures M1 to M5. As expected, the modulus of elasticity increased as the compressive strength of concrete increased.

**Table 6.4** Mechanical properties of geopolymer concrete cured at room temperature

| Properties | Time [days] | Mixture No | | | | | |
|---|---|---|---|---|---|---|---|
| | | M1 | M2 | M3 | M4 | M5 | M6 |
| Slump [mm] | | 235 | 230 | 205 | 205 | 195 | 210 |
| Density [kg/m$^3$] | 7 | 2112 | 2135 | 2195 | 2222 | 2250 | 2250 |
| | 14 | 2073 | 2104 | 2168 | 2230 | 2153 | 2233 |
| | 28 | 2057 | 2093 | 2146 | 2167 | 2164 | 2176 |
| | 90 | 1999 | 2033 | 2003 | 1984 | 2035 | 2104 |
| Compressive strength [MPa] | 7 | **6.58**±0.4 | **7.25**±0.5 | **20.85**±2.5 | **19.23**±0.7 | **26.61**±2.7 | **22.18**±2.5 |
| | 14 | **7.13**±0.3 | **9.12**±0.9 | **24.76**±1.5 | **26.44**±0.9 | **28.03**±3.6 | **27.76**±5.1 |
| | 28 | **8.94**±0.4 | **9.75**±0.2 | **29.76**±0.6 | **28.11**±1.8 | **31.49**±1.9 | **28.61**±2.0 |
| | 90 | **9.09**±0.4 | **10.05**±0.5 | **29.96**±1.2 | **28.41**±1.4 | **31.97**±1.4 | **29.88**±0.7 |
| Modulus of Elasticity in compression [GPa] | 7 | **12.24** | **9.76** | **17.89** | **17.27** | **19.77** | **18.36** |
| | 14 | **12.53** | **11.52** | **19.21** | **19.72** | **20.17** | **20.09** |
| | 28 | **13.39** | **12.03** | **20.63** | **20.19** | **21.06** | **20.32** |
| | 90 | **13.46** | **12.27** | **20.68** | **20.27** | **21.18** | **20.66** |
| Splitting tensile strength [MPa] | 7 | **1.03** | **0.68** | **1.46** | **1.40** | **1.64** | **1.51** |
| | 14 | **1.07** | **0.85** | **1.59** | **1.64** | **1.68** | **1.68** |
| | 28 | **1.20** | **0.90** | **1.73** | **1.69** | **1.77** | **1.70** |
| | 90 | **1.21** | **0.92** | **1.73** | **1.69** | **1.78** | **1.73** |

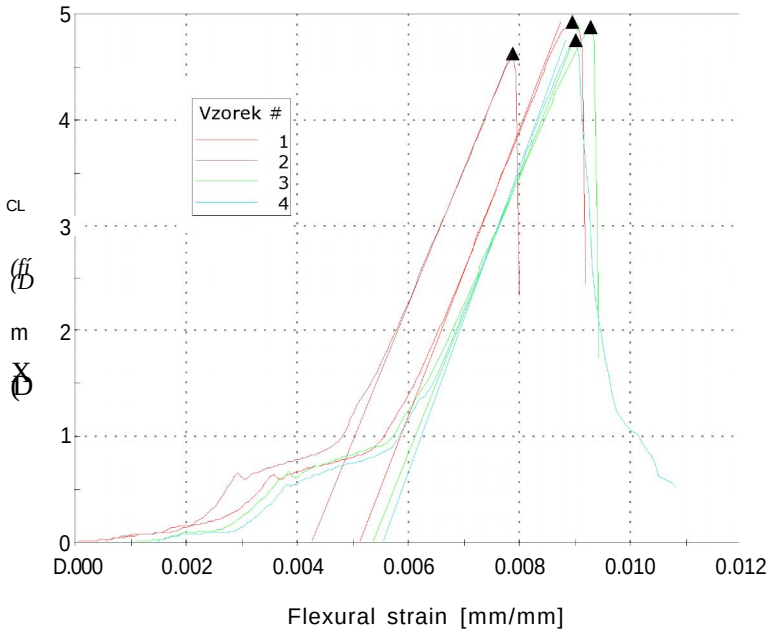


**Fig. 6.7** Typical stress and strain curve in flexure of geopolymer concrete M5 after curing at room temperature for 7 days

Mixture M5 was used in this section to investigate the flexural strength of geopolymer concrete. The samples were cured in the ambient temperature for 7, 14 and 28 days. The test results are presented in Table 6.5 and Fig. 6.8. The results show that the flexural strength of geopolymer concrete increases with age in the order of about 30 % from 7 days to 14 days and remained almost constant after that.

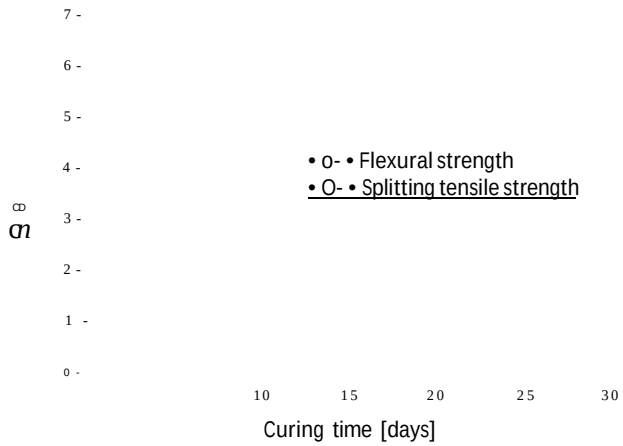


Fig. 6.8 Flexural strength and splitting tensile strength of geopolymer concrete M5

**Table 6.5** Flexural strength of geopolymer concrete M5 cured at room temperature

| Mixture | Flexural strength $R_{mo}$ [MPa] | | | Relative deformation [%] | | |
|---|---|---|---|---|---|---|
| | 7 days | 14 days | 28 days | 7 days | 14 days | 28 days |
| M5 | **4.80** ± 0.13 | **6.88** ± 0.98 | **7.09** ± 0.58 | 0.81 | 1.14 | 0.71 |

Fig. 6.8a shows that the type of geopolymer concrete fracture was examined the same with ASTM C 39-03, "Standard Test Method for Compressive Strength of Cylindrical Concrete Specimens". The broken of samples exhibits normally the conical fracture typical of cylinders.

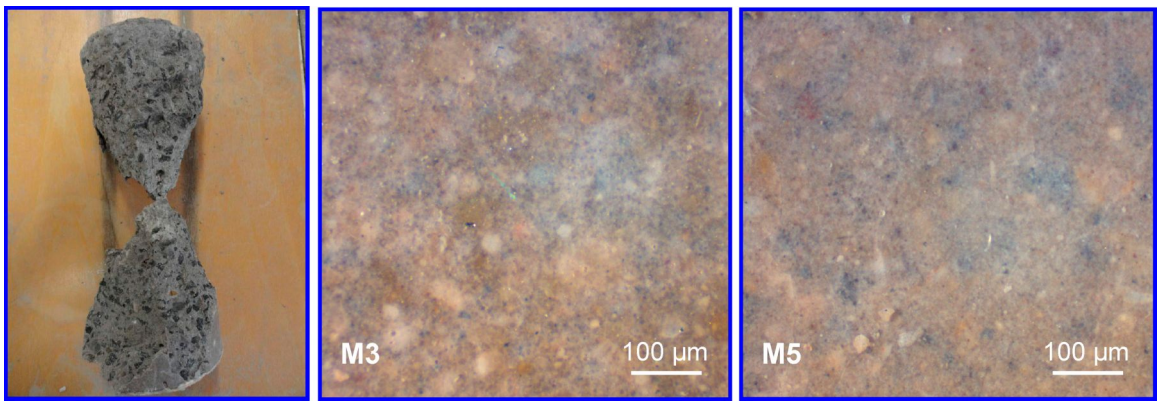


(a) (b) (c)

**Fig. 6.8** Type of fracture (a) and surface of geopolymer concrete with mixtures M3 (b) and M5 (c)

## 6.4. CONCLUSIONS

The results show that fly ash based geopolymer mortar and concrete has excellent the mechanical properties and is suitable for structural applications. Eight mixtures of mortar and six of concrete were evaluated the mechanical properties of specimens depend on the ratio of fly ash / geopolymer cement, aggregate content, the concentration of alkaline, and with age of samples after casting. The strengths will be increase when increasing curing time. Two optimal mixtures MLF'-2 and M5 were identified, they given the highest value comparing with other mixtures of mortar and concrete. Results show that the geopolymer concrete can be produced with of 32 MPa at 90 days. The test results confirmed that the mechanical properties of the geopolymer mixtures tested are competitive with those of OPC concrete [155].

# Chapter 7

# EFFECTS OF HIGH TEMPERATURE AND ENVIRONMENTAL CODITIONS ON MECHANICAL PROPERTIES OF GEOPOLYMER MORTAR AND CONCRETE

## 7.1 INTRODUCTION

Fly ash based geopolymer concrete can sustain when exposed to exposed to considerably high temperature. While OPC concrete degrades and degenerates at high temperature, it has been found from different study that fly ash geopolymer concrete can maintain its desired compressive strength even at 400 degree centigrade. Strength starts dropping once temperature crosses 400 centigrade and remains almost constant at higher temperatures [156].

Beside, environmental conditions (water, acid, ice) are also important, they are direct effect on the mechanical, chemical and physical properties of geopolymer mortar and concrete. In this chapter, the basic processes will be described, and then typical test results will be presented to illustrate of the various parameters.

## 7.2 EFFECT OF HIGH TEMPERATURE

### 7.2.1 EXPERIMENTAL

Test specimens were used eight mixtures of mortar and six mixtures of concrete to test high temperature. The details of mixtures are given in Tables 6.1 and 6.3. This chapter, we used cylinder specimens (0100 x 200) mm and (0 46 x 92) mm to determine the compressive strength mortar and concrete after heating high temperature. All samples after curing at room temperature for 28 days are heated in the oven ranging from 200 $^{o}$C to 1000 $^{o}$C at a heating rate of 5 K/min and with a soak time of 1 hour at the maximum temperature and finally cooled in the furnace with opening gate for 24 hours. The weight loss and shrinkage of specimen were also investigated.

### 7.2.2 RESULTS

Figs. 7.1 ^ 7.5 show geopolymer mortars after heating from 200 $^{o}$C to 1000 $^{o}$C. It easy to see by a naked eye that branched cracks appear over the whole surface of the samples after heating up to 600 $^{o}$C, that is causes the mechanical properties of geopolymer mortar and concrete significantly reduce after thermal exposure up to high temperature.

**Fig. 7.1** The samples after heated in the oven at 1000 $^{o}$C (left) and 800 $^{o}$C (right)

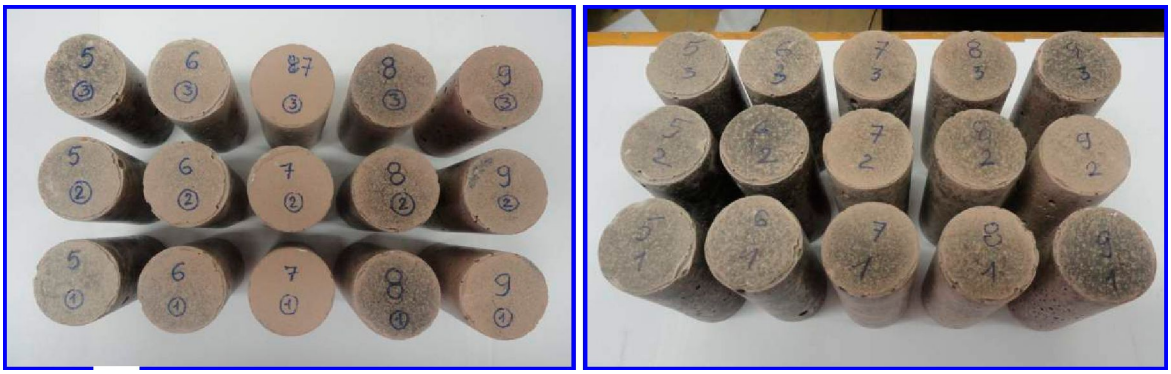

**Fig. 7.2** The samples after heated in the oven at 600 $^{o}$C (left) and 400 $^{o}$C (right)

**Fig. 7.3** The samples after heated in the oven at 200 $^{o}$C

**Table 7.1** Summary some properties of geopolymer mortar after heating at high temperature

| Temperature [$^{o}$C] | J71UJJC1 UCS | Mixtures No | | | | | | | |
|---|---|---|---|---|---|---|---|---|---|
| | | **MLF'-2** | **MLF'-3** | **MLF'-4** | **MLF'-6** | **MLF'-7** | **MLF'-8** | **MLF'-9** | **MLF'-10** |
| 1000 | WL [%] | 20.96 | 21.69 | 19.33 | 22.51 | 21.70 | 20.05 | 19.20 | 18.37 |
| | SD [%] | 6.86 | 7.88 | 9.15 | 5.51 | 4.54 | 2.94 | 2.24 | 1.88 |
| | SL [%] | 4.72 | 6.98 | 7.69 | 6.20 | 5.08 | 4.54 | 3.53 | 2.48 |
| | fcm [MPa] | **6.57**±0.6 | **5.75**±0.5 | **5.46**±0.4 | **2.92**±0.2 | **3.10**±0.4 | **2.65**±0.3 | **2.74**±0.3 | **2.54**±0.1 |
| | [HV] | **200**±4 | **151**±6 | **142**±7 | **105**±3 | **131**±14 | **102**±18 | **108**±15 | **124**±4 |
| | P [kg/m$^3$] | 1491 | 1597 | 1639 | 1612 | 1653 | 1467 | 1519 | 1481 |
| 800 | WL [%] | 21.80 | 20.92 | 20.31 | 22.52 | 21.68 | 210.4 | 19.69 | 20.65 |
| | SD [%] | 8.40 | 9.10 | 8.97 | 5.73 | 3.16 | 3.33 | 2.09 | 1.51 |
| | SL [%] | 7.30 | 8.58 | 7.39 | 4.57 | 4.02 | 3.45 | 3.05 | 2.19 |
| | fcm [MPa] | **5.30**±0.6 | **4.79**±0.2 | **4.28**±0.2 | **6.77**±0.6 | **7.54**±1.5 | **4.66**±1.3 | **4.85**±1.7 | **3.39**±0.1 |
| | [HV] | **201**±20 | **171**±8 | **133**±2 | **202**±20 | **184**±14 | **147**±12 | **129**±9 | **119**±9 |
| | P [kg/m$^3$] | 1590 | 1628 | 1687 | 1566 | 1586 | 1455 | 1473 | 1503 |
| 600 | WL [%] | 20.85 | 20.24 | 19.47 | 22.18 | 19.54 | 17.97 | 19.52 | 17.89 |
| | SD [%] | 3.93 | 3.38 | 3.33 | 2.57 | 1.10 | 1.60 | 0.87 | 1.86 |
| | SL [%] | 3.38 | 2.81 | 2.37 | 1.79 | 1.29 | 1.53 | 1.22 | 0.59 |
| | fcm [MPa] | **12.00**±0.3 | **11.14**±0.6 | **9.85**±0.3 | **8.29**±1.0 | **10.20**±0.3 | **7.22**±0.6 | **7.63**±0.2 | **7.34**±0.2 |
| | [HV] | **214**±8 | **183**±8 | **164**±8 | **207**±21 | **200**±8 | **188**±1 | **205**±8 | **230**±9 |
| | P [kg/m$^3$] | 1401 | 1379 | 1397 | 1437 | 1484 | 1397 | 1458 | 1505 |

| | | | | | | | | | |
|---|---|---|---|---|---|---|---|---|---|
| 400 | WL [%] | 18.97 | 20.60 | 18.10 | 22.43 | 20.80 | 20.24 | 19.78 | 19.68 |
| | SD [%] | 2.71 | 2.67 | 2.82 | 2.15 | 1.04 | 2.64 | 1.48 | 1.86 |
| | SL [%] | 2.59 | 2.37 | 1.89 | 1.78 | 1.78 | 1.44 | 1.71 | 1.44 |
| | fcm [MPa] | **15.48**±0.9 | **15.21**±1.4 | **13.82**±1.4 | **14.82**±1.6 | **15.96**±3.9 | **11.17**±1.2 | **11.18**±0.5 | **9.92**±0.4 |
| | [HV] | **222**±12 | **210**±13 | **197**±4 | **207**±12 | **292**±19 | **251**±9 | **254**±18 | **273**±4 |
| | P [kg/m$^3$] | 1407 | 1404 | 1424 | 1446 | 1534 | 1413 | 1468 | 1491 |
| 200 | WL [%] | 7.77 | 8.97 | 8.57 | 9.09 | 7.86 | 8.61 | 8.58 | 9.46 |
| | SD [%] | 0.96 | 1.25 | 0.91 | 0.61 | 0.61 | 0.66 | 0.52 | 0.71 |
| | SL [%] | 0.38 | 0.58 | 0.37 | 0.43 | 0.24 | 0.33 | 0.29 | 0.35 |
| | fcm [MPa] | **35.04**±1.6 | **34.40**±2.6 | **29.85**±0.2 | **28.05**±0.8 | **21.85**±2.7 | **19.16**±5.1 | **20.65**±4.1 | **13.88**±1.9 |
| | [HV] | **324**±9 | **309**±17 | **277**±12 | **245**±12 | **228**±9 | **227**±8 | **234**±8 | **211**±8 |
| | P [kg/m$^3$] | 1472 | 1470 | 1451 | 1598 | 1660 | 1551 | 1605 | 1620 |

$f_c$m - Compressive strength, [MPa] SL - Shrinkage in length, [%] HV - Hardness, [HV]

WL - Weight loss, [%] $S_D$ - Shrinkage in diameter, [%] P - Density, [kg/m$^3$]

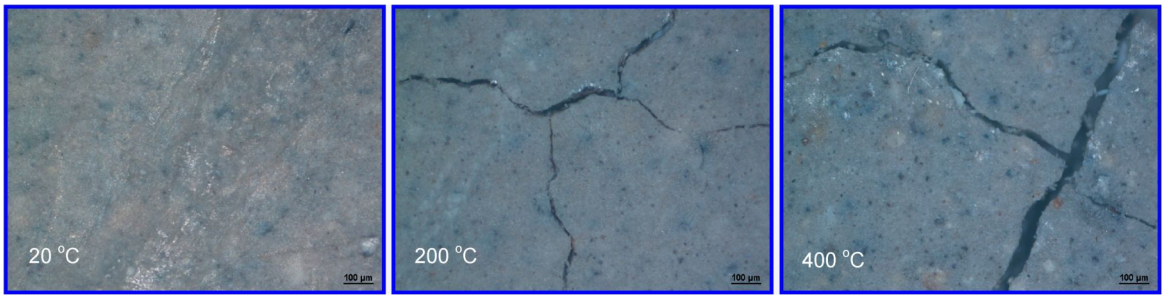


**Fig. 7.4** The surface of samples MLF'-2 after curing at 20 °C and heated at 200 °C, 400 °C

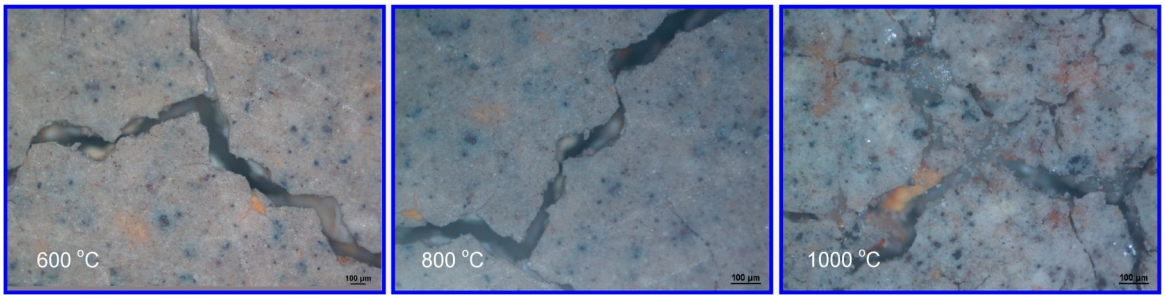


**Fig. 7.4** The surface of samples MLF'-2 after heating from 600 °C to 1000 °C

The distance cracks are increased and made many branch cracks on the surface of samples when increasing the heating temperature (see in Figs. 7.3 and 7.4) and up to 1000 °C the adhesion between geopolymer, fly ash and fine aggregate is not good. The behaviors also look like the same with geopolymer concrete, however the cracks of concrete are smaller than mortar cause much coarse aggregate content lead to reduce shrinkage and weight loss. And when comparing macrostructure of sample MLF'-3 with image of mixture MLF'-10 heated at 800 °C, the cracks occurring in samples MLF'-3 (without fine sand) is bigger than MLF-10 (Fig. 7.5).

The weight loss, shrinkage and compressive strength of geopolymer mortar and concrete were determined during the experiment and the detail results show in Table 7.1. It can see from Fig. 7.5 that the weight loss of mortar is increased about 20 % when the temperature up to 400 °C and remained up to 1000 °C, while concrete is also increased but smaller than mortar approximately 12 % at 1000 °C.

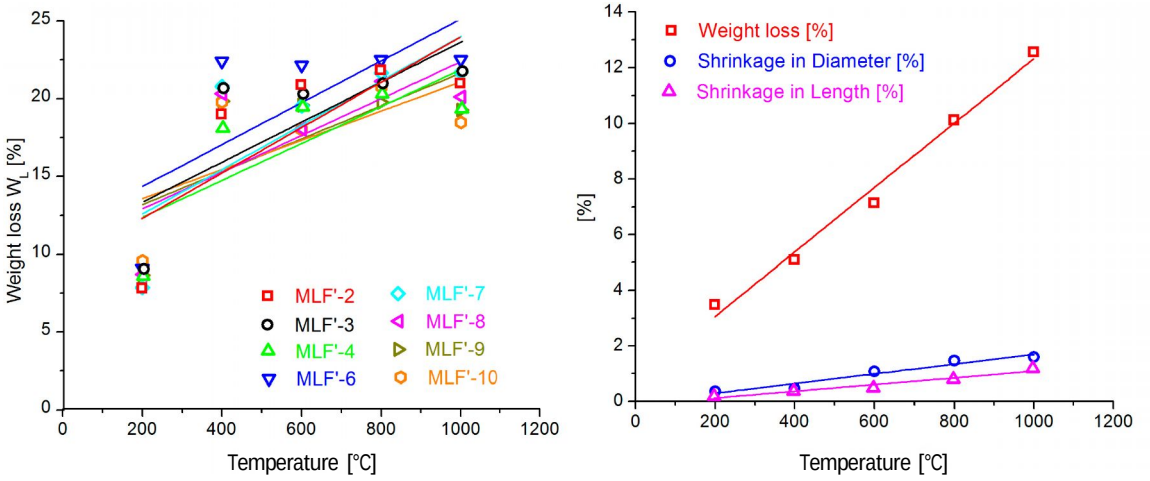


**Fig. 7.5** The weight loss of mortar (left), the weight loss and shrinkage of concrete (right) after heating from 200 °C to 1000 °C

**Table 7.2** Summary properties of concrete M5 after heating at high temperature

| Properties | Temperature [°C] | | | | |
|---|---|---|---|---|---|
| | 200 | 400 | 600 | 800 | 1000 |
| $w_L$ [%] | 3.49 | 5.10 | 7.14 | 10.12 | 12.56 |
| SD [%] | 0.36 | 0.46 | 1.08 | 1.47 | 1.60 |
| SL [%] | 0.20 | 0.38 | 0.50 | 0.81 | 1.20 |
| P [kg/m$^3$] | 2082 | 2053 | 2039 | 1997 | 1957 |
| $f_{cm}$ [MPa] | **29.10**±1.9 | **16.23**±1.5 | **11.46**±0.8 | **8.16**±0.7 | **5.24**±0.1 |
| Ec [GPa] | 19.90 | 16.21 | 14.46 | 13.03 | 11.50 |
| $f_{ct}$ [MPa] | 2.16 | 1.61 | 1.35 | 1.14 | 0.92 |

$E_c$ - Young's modulus in compression $f_{ct}$ - Splitting tensile strength

Shrinkages in length and in diameter (Figs. 7.5 and 7.6) are the reduction in volume which is primarily caused by loss of water contained in the alkaline and burnt some particles on the surface of samples during the heating process. Percentage of shrinkage of samples was also depended about temperature and aggregates content. While the aggregate plays the important role in affecting shrinkage of concrete. Indeed, most aggregates restrain concrete shrinkage because they are less elastic than the cement paste to which they are bonded. Concretes with

higher aggregate contents shrink substantially less than cement-rich mixes all else being equal [138, 156].

Davidovits had given the concept that the smaller drying shrinkage strain of fly ash-based geopolymer concrete may be explained by the block polymerization. According to this concept, the Si and Al atoms in the fly ash are not entirely dissolved by the alkaline liquid. The polymerization that takes place only on the surface of the atoms is sufficient to form the blocks necessary to produce the geopolymer binder. Therefore, the insides of the atoms are not destroyed and remain stable, so that they can act as micro-aggregates in the system and this could increase the aggregate content in concrete [156-158]. The below Fig. 7.7 shows the shrinkage of fly ash geopolymer mortar after heated at 800 $^{o}$C.

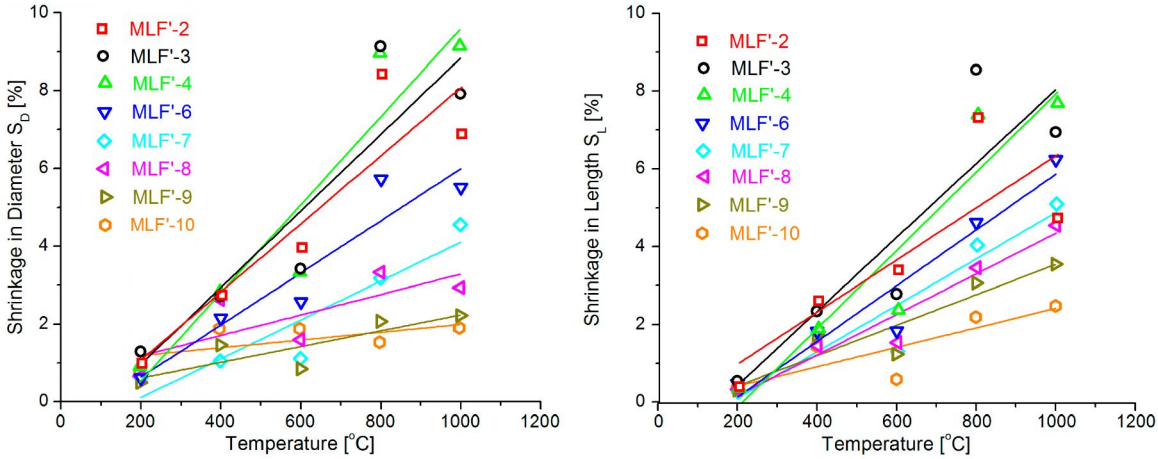


**Fig. 7.6** Shrinkage in Diameter (left) and in Length (right) of mortar at high temperature

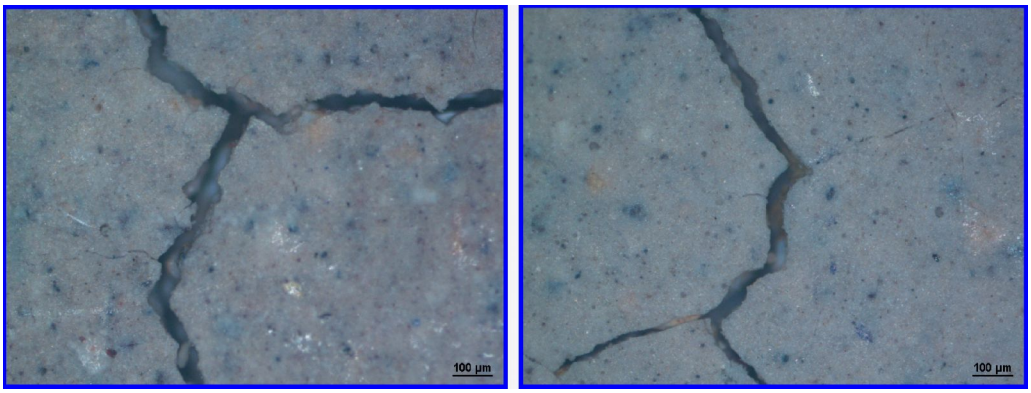


**Fig 7.7** Influence of sand on the shrinkage performance after heated at 800 $^{o}$C: 0 % (left) and 50 % (right)

Fly ash based geopolymer mortar and concrete can sustain when exposed to considerably high temperature. It can see from Fig. 7.8 that the highest compressive strength is obtained when the temperature is 200 $^{o}$C, but they exhibit a decreasing tendency afterwards. The strength starts dropping once temperature over 400 $^{o}$C and slightly reduces at higher temperatures. The lowest values of the residual strength were observed in the temperature range of 600 to 800 $^{o}$C; they were due to the presence of the melt that started forming. While OPC concrete degrades and degenerates at high temperature, it has been found from different study that fly ash geopolymer concrete can maintain its desired compressive strength even at 400 $^{o}$C [156], the residual strengths of the OPC concrete are very low, on the order a few MPa.

In Table 7.2 presents the modulus of elasticity and plitting tensile strength after drying high temperature. The compressive strength can be reduced slightly with increasing high temperature, but these samples were stilled stable at 1000 $^{o}$C.

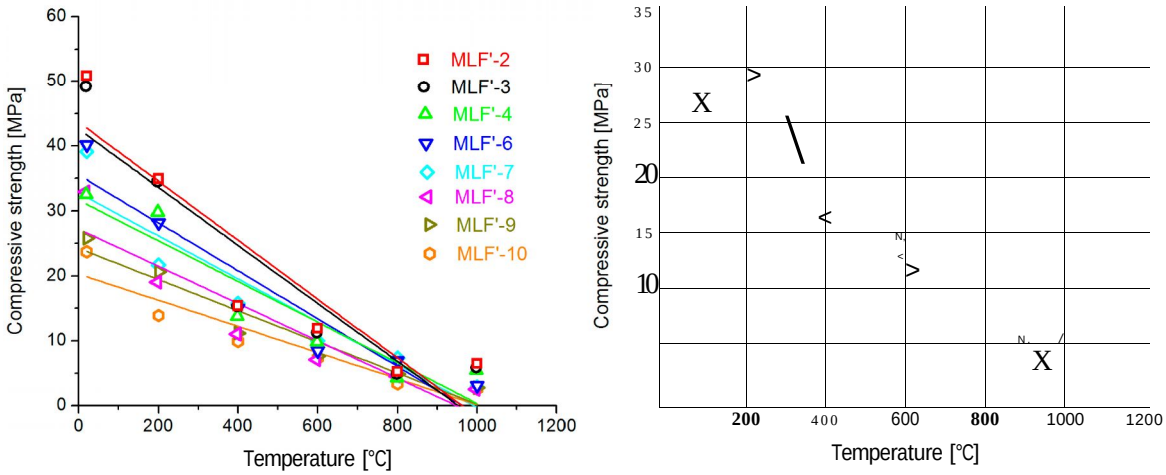


**Fig. 7.8** Influence of high temperature on the compressive strength of mortar (left) and concrete (right)

## 7.3 EFFECT OF ENVIRIONMENTAL CONDITIONS

### 7.3.1 FREEZE - THAW / WET - DRY TEST

*7.3.1.1 FREEZE - THAW*

The samples are first saturated with water and then frozen at -15 $^{o}$C for 1 day. For the next day, the samples are taken from the freezer and immediately put in water without thawing. The cycles are stopped after 28 days (this is sufficient for regular laboratory testing). One

measures the compressive strength and compares with the initial strength after 28 days curing at room temperature.

*7.3.1.2 WET - DRY*

The samples are first saturated with water and then dried at 70 $^{o}$C for 1 day. For the next day, the samples are taken from the furnace and immediately put in water without cooling. The cycles are stopped after 28 days (this is sufficient for regular laboratory testing). One measures the compressive strength and compares with the initial strength after 28 days curing at room temperature.

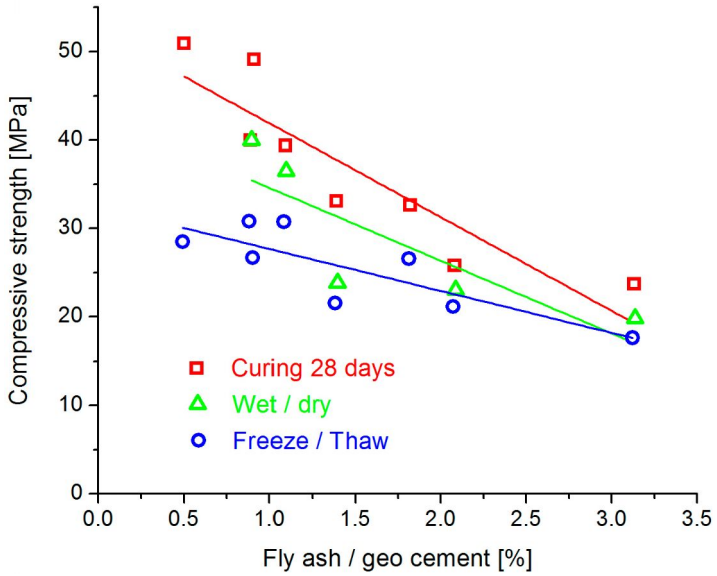


**Fig. 7.9.** Compressive strength of geopolymer mortar after freeze/thaw and wet/dry cycle, comparison with initial strength at 28 days

After freeze-thaw and wet-dry test were determined water absorption, weight loss, shrinkage and compressive strength of geopolymer mortar. Fig. 7.9 shows the results obtained from mixtures MLF'-2 to MLF'-10 samples subjected to the environments together with the control samples test at 28 days. This figure presents the results of geopolymer mortar for 3 environments such as ambient conditions, freeze-thaw, and wet-dry. The effects of freeze-thaw cycling were stronger than wet-dry and the compressive strength of MLF'-7 was reduced about 45 % and in wet-dry test was 8 %. It is easy to see that, mixtures (MLF'-2 to 4) without sand are significantly effected by environments on the properties when compared with mixtures MLF'-6 to MLF'-10. And the results for the freeze-thaw cycles in Table 7.3 show that the weight of samples is increased that mean geopolymer mortar absorption water

about 1.5 %. At the end of the analyzing micrograph, we observed that the micro cracking with effect of freeze-thaw and wet/dry on the surface of geopolymer mortar (see Fig. 7.16).

### 7.3.2 ACID RESISTANCE TEST

Acid resistance test was conducted on geopolymer mortar. In this study, the specimens were soaked in sulfuric acid solution with selected concentrations ranging from 1% to 3% with the measured pH about 1.0. The test specimens were immersed in sulfuric acid solution in a container (see Fig. 7.10). In each case, three samples were immersed in the sulfuric acid solutions until 28 days. The acid resistance of geopolymer mortar was then evaluated based on the change in compressive strength and the change in mass after acid exposure.

**Fig. 7.10** Acid resistance test

We can see from Fig. 7.11 left and right that the appearance of these white zones is probably related to two causes: first, by extracting unstable aluminum, i.e. Al-end units with non-bridging oxygens; second, by formation of a zeolitic structure, which causes strength loss depending on the acid concentration [159]. The process similarly occurs with nitric acid, but there were little effects on the structure of geopolymer mortar when samples were immersed in the chloric-acid solution.

**Table 7.3** Summary properties of geopolymer mortar after testing freeze / thaw

| Properties | Mixtures No | | | | | | | |
|---|---|---|---|---|---|---|---|---|
| | **MLF'-2** | **MLF'-3** | **MLF'-4** | **MLF'-6** | **MLF'-7** | **MLF'-8** | **MLF'-9** | **MLF'-10** |
| WL [%] | -1.40 | -1.62 | -1.51 | -1.01 | -0.68 | -1.06 | -0.86 | -1.14 |
| SD [%] | 0.05 | 0.08 | 0.68 | 0.18 | 0.35 | 0.45 | 0.20 | 0.24 |
| SL [%] | 0.04 | 0.22 | 0.15 | 0.10 | 0.23 | 0.14 | 0.37 | 0.08 |
| fcm [MPa] | **28.43**±3.8 | **26.60**±2.4 | **26.50**±2.6 | **30.72**±2.8 | **30.68**±4.5 | **21.47**±5.1 | **21.09**±3.4 | **17.53**±4.3 |
| [HV] | **308**±8 | **280**±2 | **278**±8 | **266**±9 | **253**±7 | **246**±10 | **248**±10 | **245**±13 |
| P [kg/m3] | 1609 | 1588 | 1593 | 1777 | 1808 | 1711 | 1730 | 1768 |

**Table 7.4** Summary properties of geopolymer mortar after testing wet / dry

| Properties | Mixtures No | | | | |
|---|---|---|---|---|---|
| | **MLF'-6** | **MLF'-7** | **MLF'-8** | **MLF'-9** | **MLF'-10** |
| WL [%] | 12.87 | 12.03 | 11.61 | 11.11 | 12.17 |
| SD [%] | 0.51 | 0.56 | 0.50 | 0.40 | 0.38 |
| SL [%] | 0.40 | 0.57 | 0.48 | 0.41 | 0.28 |
| fcm [MPa] | **39.81**±5.4 | **36.28**±3.2 | **23.64**±3.1 | **22.83**±3.4 | **19.60**±1.8 |
| [HV] | **285**±11 | **281**±4 | **267**±7 | **262**±17 | **261**±2 |
| P [kg/m3] | 1537 | 1586 | 1503 | 1549 | 1561 |

**Fig. 7.11** Effect of 3 % sulfuric acid (left), 5 % chloric acid (middle), 5 % nitric (right) on the surface of geopolymer

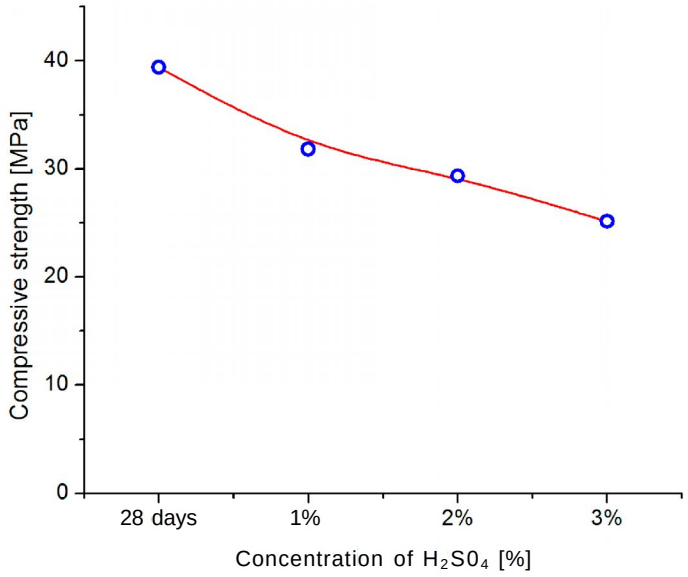


**Fig. 7.12** Compressive strength of MLF'-7 curing ambient temperature at 28 days and immersion in $H_2SO_4$ solutions for 28 days

The concentration of $H_2SO_4$ solution was also significantly effect on the compressive strength of mortar, if increasing the concentration was reduced the strength and concomitant the weight loss of samples was also increased.

Fly ash-based geopolymer concrete had been proved by many studies to provide better resistance against aggressive environment. The report of Wallah and Rangan was calculated the geopolymer concrete exposed to 0.5 % concentration of $H_2SO_4$ acid solution the compressive strength decreased about 20 % after one year exposure. This value was about 52 % and 65 % respectively for geopolymer concrete exposed to 1 % and 2 % concentration

[160]. Song and his colleagues suggested that the reduction in compressive strength was in the range of 32 to 37 % after 56 days of exposure to 10 % $H_2SO_4$ acid solution [161].

### 7.3.3 CLIMATE CHAMBER TEST

The environmental test chamber was realised after 28 days (about 120 cycles).

Conditions: distilled water, cyclic changes of temperature and humidity (see graph in Fig. 7.14)

In this section, we were trial with mixtures from MLF'-6 to MLF'-10, pure geopolymer and concrete M3 and M5.

The experimental was culculated gravimetric assessment and analysis macrostructure of samples.

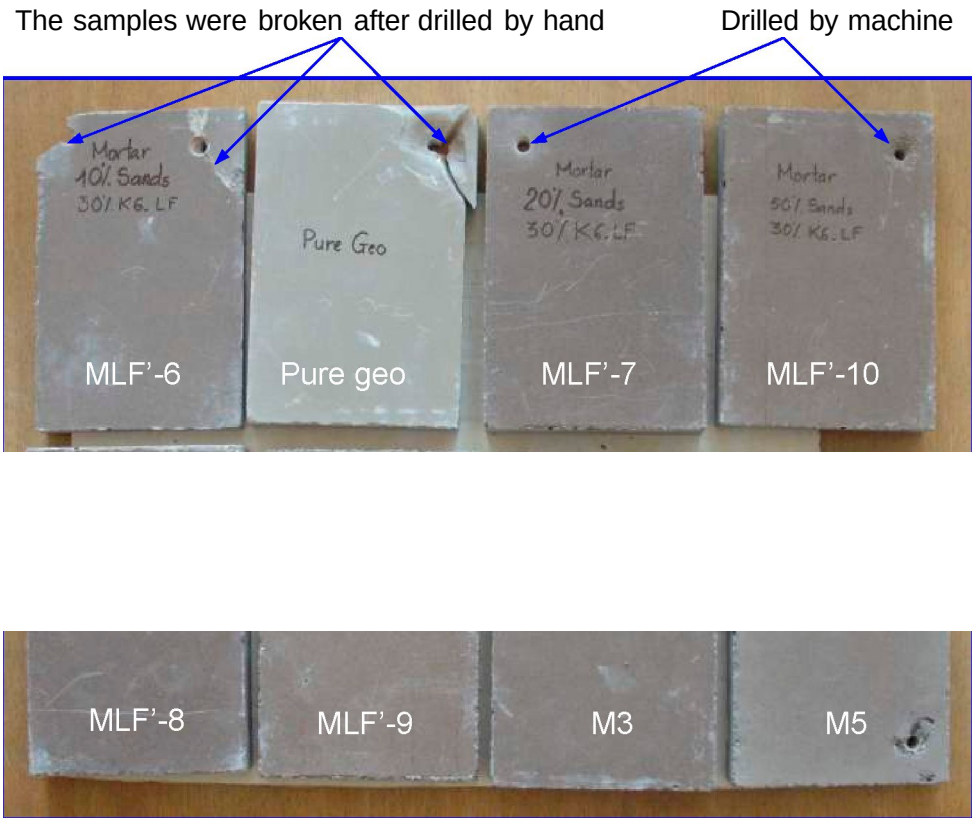


**Fig. 7.13** Samples before test climate chamber

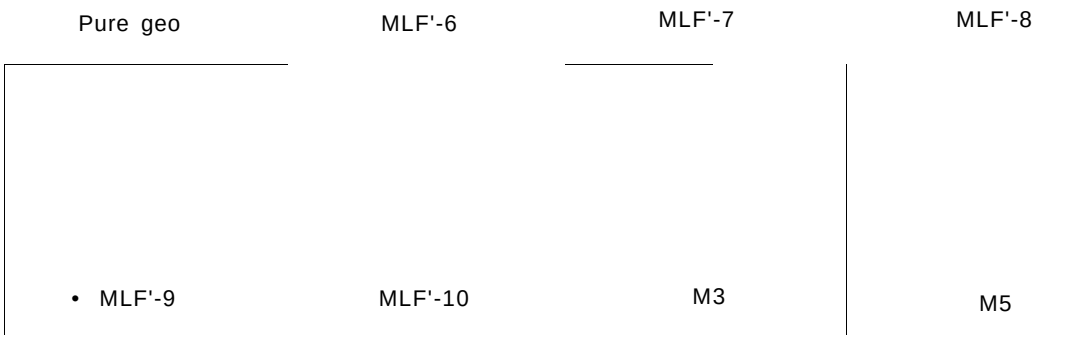


**Fig. 7.14** Geopolymer samples surface before test climate chamber (magnification of 63x)

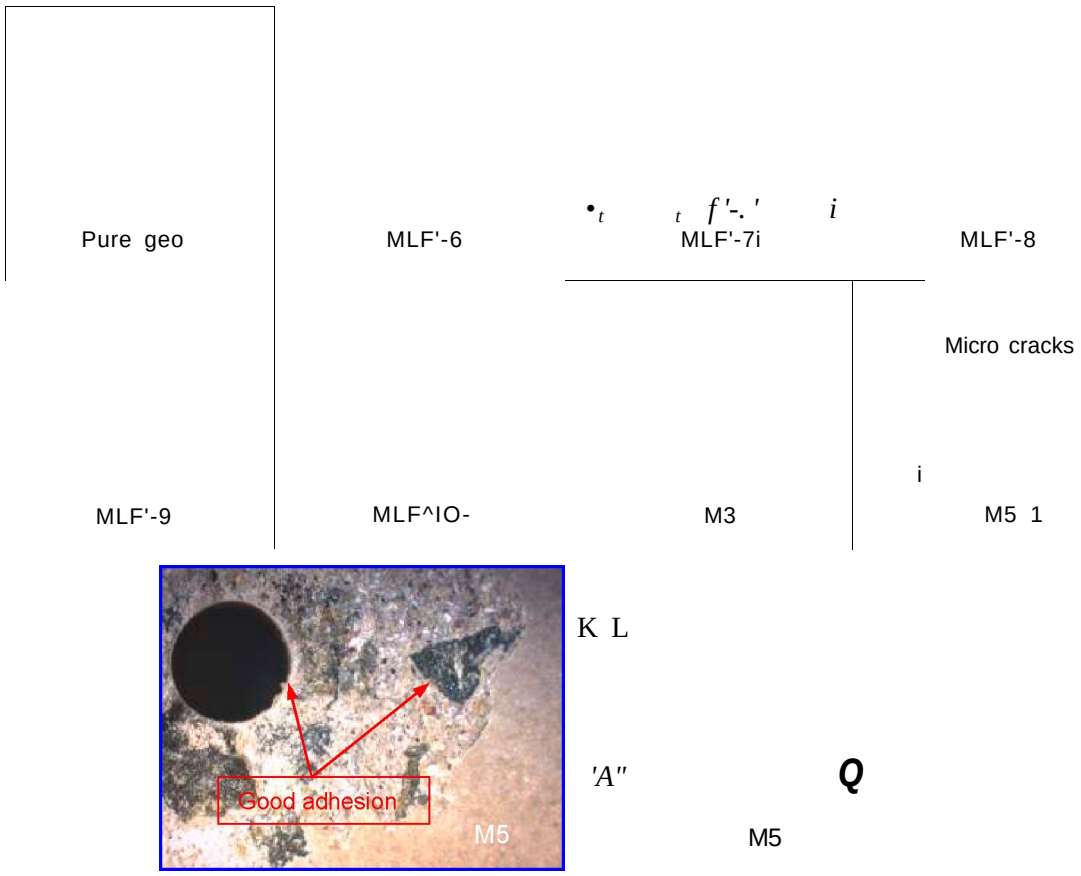


**Fig. 7.15** The photographs of geopolymer samples surface before test climate chamber (magnification of 63x)

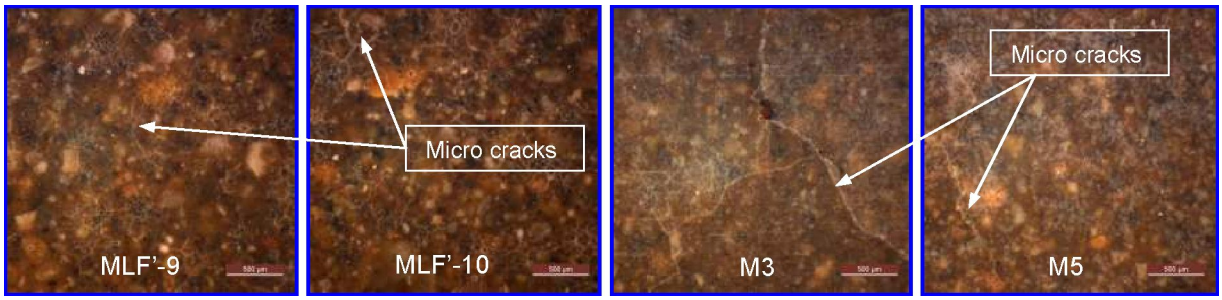


**Fig. 7.16** The photographs of geopolymer samples after testing climate chamber

**Table 7.5** Gravimetric evaluation of geopolymer mortar and concrete before and after exposure 28 days (120 cycles 50 °C / 100 % R.h., 120 cycles 20 °C / 60 % R.h.)

| Mix | $^{m}$O [g] | m30 [g] | Am [g]* | Am [%] | |
|---|---|---|---|---|---|
| Pure geo | 465.4 | 471.9 | - 6.5 | - 1.39 | ** |
| MLF'-6 | 297.2 | 303.3 | - 6.1 | - 2.05 | *** |
| MLF'-7 | 531.5 | 528.8 | 2.7 | 0.51 | |
| MLF'-8 | 556.2 | 548.6 | 7.6 | 1.37 | |
| MLF'-9 | 418.3 | 417.8 | 0.5 | 0.12 | |
| MLF'-10 | 448.6 | 436.6 | 12 | 2.67 | |
| M3 | 498.2 | 498.7 | - 0.5 | - 0.10 | |
| M5 | 545.8 | 535.8 | 10 | 1.83 | |

* Weight loss, respectively (-) increment in grams

** Sample pure geopolymer cracked and separated across the width in the 13$^{th}$ day exposure, respectively after 48 cycles.

*** Sample MLF'-6 cracked and separated in the second circuit substrate day of exposure, respectively after 4 cycles.

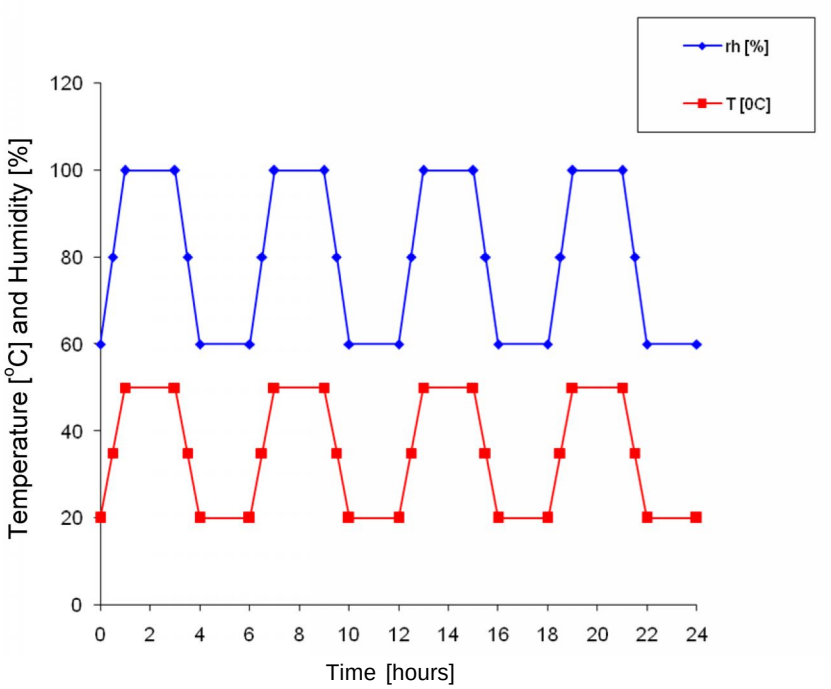


**Fig. 7.17** Cyclic test geopolymer mortar and concrete (4 temperature and 4 humidity cyclic/24 hrs)

## 7.4 CONCLUSIONS

The results show that the aggregate (coarse and fine) are significantly influence on the strength, shrinkage of geopolymer concrete and mortar. In this research, concrete are made from coarse aggregate (4 ^ 8 mm) lead to extensive cracking of geopolymer. Kong and his colleagues observed the behavior geopolymer concrete under elevated temperature, the larger aggregate (>10 mm) were more stable [162]. And the ratio of fly ash to alkaline liquid was also effect the general strength and fire resistance of geopolymer. It was found that the fly ash-based geopolymer displayed increase in strength after temperature exposure [163]. Moreover, the intrinsic chemistry of the geopolymer binder does not require the retention of water or hydration within gel phases to maintain structural integrity of the binder in fire processing [164], so geopolymer mortar and concrete can applied in places or equipments requiring high degrees of fire resistance.

For freeze-thaw and dry-wet tests, mixtures MLF'-6 to MLF'-10 and M5 were used. After 28 days, the environments were significantly influence on the compressive strength, weight loss, shrinkage, and microstructure of geopolymer mortar and concrete.

The sulfuric acid resistance of fly ash-based geopolymer mortar was studied for mixture MLF'-7. The concentration of sulfuric acid solution was 1 %, 2 % and 3 % for soaking specimens. The sulfuric acid was also effect on the compressive strength, change in mass and microstructure of samples. However, the sulfuric acid resistance of geopolymer mortar is significantly better than that of OPC mortar as reported in earlier studies.

# Chapter 8

# EFFECTS OF COMMERCIAL FIBERS REINFORCED ON THE MECHANICAL PROPERTIES

## 8.1 INTRODUCTION

The use of fibers in brittle matrix materials has a long history going back at least 3500 years when sun-baked bricks reinforced with straw were used to build the 57 m high hill of Aqar Quf near Baghdad [32]. In more recent times, short fibers have been known and used for many decades to reinforced brittle materials like cement [165]. Currently, there are various types of fiber available for commercial use, the basic types being glass [166], carbon [166], polypropylene [167], nylon [168] and some natural fibers [168] (coconut, jute, rice straw, sugar cane, wood, banana, etc.). All previous research has been concerned with short random fibers reinforced concrete and mortar. When combined with short fibers reinforced concrete, the results showed that concrete has increases its mechanical (tensile or flexural strength and durability) and control cracking (Fig. 8.1) compared to unreinforced concrete [166-168].

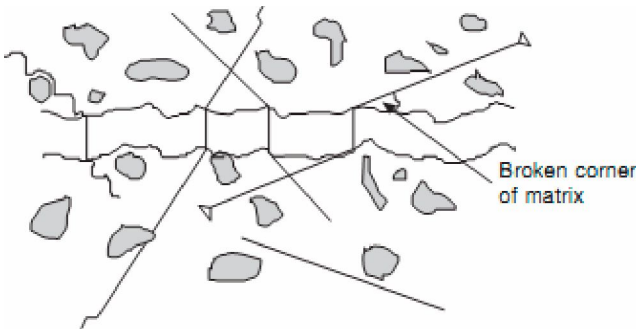


**Fig. 8.1** Cracked short fiber composite containing N fibers per unit area and showing change in fiber orientation at a crack [32]

In this chapter, we used basalt and Isover granulate fibers as a filler in geopolymer mortar and concrete. These fibers have some advantage properties including low cost, light weight, good chemical resistance, high-performance insulation materials (thermal and sound), stable in the alkaline environment of concrete and resistant to plastic shrinkage cracking. Especially, the fiberization process is more environmentally safe than other fibers. Further, they have no toxic reaction with air or water, and are noncombustible and non explosion proof. Nevertheless, Isover granulate also has some disadvantages including poor fire resistance, a low modulus of elasticity [169, 170].

At the present time, there are no reports about basalt and Isover granulate reinforced geopolymer mortar and concrete. The present chapter compares the mechanical properties of geopolymer mortar and concrete reinforced with short random commercial fibers and with unreinforced geopolymer mortar and concrete. Preliminary, the results showed a significant increase in the flexural strength and the hardness of mortar and concrete containing different percentages of fibers studied.

## 8.2 EXPERIMENTAL

The fly ash K6_LF used in this chapter and the mixture MLF'-2 of mortar and M5 of concrete were used to reinforce different volume fractions ranging from 0.2 to 4 % of Isover granulate and basalt fiber from 0.2 to 2 %, respectively with dimension mentioned in Table 8.1. Tensile strength, Young's modulus and elongation of fibers were investigated as following:

A single filament of each kind of fiber was separated with a magnifier and prepared on a punched mounting tab. The single filament test piece was bonded by adhesive so as to let the length specified gauge length under the condition to make the filament straight along the center line of the mounting tab. This was evaluated in accordance with Japanese Industrial Standard (JIS R 7601) [11]. Tensile strength and Young's modulus were calculated from the load-elongation records and the cross-sectional area measurements. The specimen is shown in Fig. 8.2.

The samples were tested by the machine Instron LaborTech 2.050 (maximum load of sensor: 5 N).

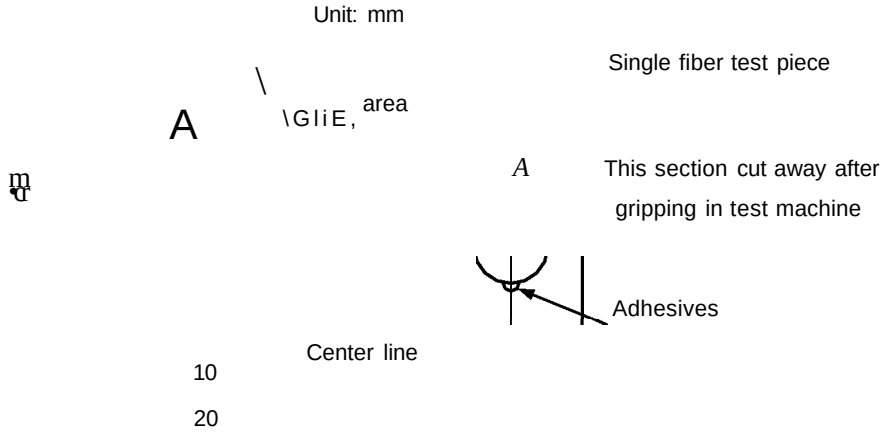


**Fig. 8.2** Mounting tab for single filament testing

The technology of sample preparation is as follows. After the mixture homogenized with fly ash, geopolymer resin and aggregates, the fibers were added, and the mixer was allowed to run for another 5 minutes. Directly after mixing, the fresh mortar was poured into the moulds with dimension (40 x 40 x 160) mm in accordance to ASTM C348 and vibrated for 2 minutes on the vibration table to remove air voids. These samples were cured at room temperature for 3 days after casting. Next, the samples were removed from the moulds and left in laboratory ambient conditions until the day of the test. The sample ages for the latter tests were 7, 14, and 28 days.

## 8.3 RESULTS

Properties of commercial fibers are illustrated in Table 8.1 and Fig. 8.3 displays SEM images of the fibers.

**Table 8.1** Main properties of short basalt fiber (3.2 mm) and Isover granulate fiber

| Fiber | D [Rm] | Density [kg/m$^3$] | Length [mm] | Modulus [GPa] | Tensile [MPa] | Elongation [%] | k [W/(m.K)] |
|---|---|---|---|---|---|---|---|
| Basalt BCF13-2520tex-KV12 | 13 | 2670 | 3.2±0.5 | 64 | 2563 | 3.98 | 0.031-0.038 |
| Basalt Isover granulate AO 204 | 7 | 2880 | 1.0-5.0 | - | 0.146 | 2.3 | 0.044 |

D - Diameter, [p,m] k - Thermal conductivity

The initial density of specimens containing Isover granulate and basalt fibers was less than that of mixes without any fibers. Tables 8.2 and 8.3 show that the density of specimens is significantly decreased when increased the percentage of fibers reinforced with geopolymer mortar. The weight change of mortar was mainly due to the dehydration of cement paste.

**Table 8.2** The flexural properties of short basalt fiber (3.2 mm) reinforced geopolymer mortar after curing at room temperature

| Percentage of fiber | Time [days] | Density P [kg/m$^3$] | Flexural strength $R_{mo}$ [MPa] | Young's modulus Ec [MPa] | Relative deformation £ [%] |
|---|---|---|---|---|---|
| Without fiber | 7 | 1774 | **4.91** ± 0.6 | **1366**±120 | 0.95 |
| | 14 | 1726 | **6.02** ± 0.52 | **1418**±133 | 1.38 |
| | 28 | 1624 | **4.40** ± 0.32 | **1476**±160 | 0.91 |
| 0.2 % | 7 | 1783 | **5.28** ± 0.5 | **1404** ± 57 | 1.16 |
| | 14 | 1740 | **5.80** ± 0.6 | **1576**±112 | 1.14 |
| | 28 | 1694 | **4.66** ± 0.5 | **1422** ± 59 | 0.89 |
| 0.5% | 7 | 1763 | **5.23** ± 0.3 | **1442** ± 55 | 0.87 |
| | 14 | 1740 | **6.67** ± 0.9 | **1498** ± 92 | 1.16 |
| | 28 | 1693 | **4.41** ± 0.8 | **1510**±297 | 0.91 |
| 1% | 7 | 1777 | **5.39** ± 0.4 | **1432**±173 | 1.14 |
| | 14 | 1622 | **5.52** ± 0.7 | **1228**±103 | 1.29 |
| | 28 | 1579 | **5.81** ± 0.4 | **1458**±122 | 1.05 |
| 2% | 7 | 1700 | **5.76** ± 0.4 | **1293**±115 | 0.98 |
| | 14 | 1609 | **6.88** ± 0.7 | **1353**±169 | 1.52 |
| | 28 | 1571 | **6.91** ± 0.6 | **1171**± 28 | 1.38 |

Figs. 8.3 and 8.4 show a flexural strength and flexural modulus comparison graph between the commercial fibers studied. According to the results, by increasing the amount of fibers in the matrix the flexural strength of specimens reduced. Also, it is clear that the flexural strength of specimens increased by increasing the curing time at room temperature. When the curing time was increased (particularly from 14 to 28 days), the flexural strength of the geopolymer mortar of the specimens without fibers was significantly reduced by 27 % (6.02 to 4.40 MPa).

**Table 8.3** The flexural properties of Isover granulate fiber reinforced geopolymer mortar after curing at room temperature

| Percentage of fiber | Time [days] | Density P [g/cm3] | Flexural strength Ro [MPa] | Flexural modulus E [MPa] | Relative deformation £ [%] |
|---|---|---|---|---|---|
| Without fiber | 7 | 1774 | 4.91 ± 0.6 | 1366±120 | 0.95 |
| | 14 | 1726 | 6.02 ± 0.52 | 1418±133 | 1.38 |
| | 28 | 1624 | 4.40 ± 0.32 | 1476±160 | 0.91 |
| 0.2 % | 7 | 1796 | 5.95 ± 0.2 | 1382±75 | 1.19 |
| | 14 | 1762 | 6.45 ± 0.3 | 1513±113 | 1.28 |
| | 28 | 1725 | 6.51 ± 0.1 | 1655±275 | 1.06 |
| 0.5% | 7 | 1840 | 6.24 ± 0.4 | 1404 ± 6 | 1.23 |
| | 14 | 1811 | 6.27 ± 0.2 | 1758±226 | 0.78 |
| | 28 | 1719 | 5.15 ± 0.8 | 1573±218 | 0.99 |
| 1% | 7 | 1761 | 6.10 ± 0.3 | 1236±196 | 1.64 |
| | 14 | 1745 | 6.50 ± 0.4 | 1339±69 | 1.85 |
| | 28 | 1718 | 6.95 ± 0.2 | 1149±236 | 2.01 |
| 2% | 7 | 1810 | 5.33 ± 0.3 | 1206±123 | 1.29 |
| | 14 | 1734 | 5.76 ± 0.7 | 1273 ± 34 | 1.51 |
| | 28 | 1711 | 6.89 ± 0.8 | 1316±118 | 1.32 |
| 3% | 7 | 1733 | 5.38 ± 0.4 | 1193±52 | 1.46 |
| | 14 | 1708 | 5.89 ± 0.4 | 1178±31 | 1.84 |
| | 28 | 1684 | 5.89 ± 0.5 | 1294± 53 | 1.60 |
| 4% | 7 | 1722 | 4.80 ± 0.3 | 1341± 45 | 0.90 |
| | 14 | 1597 | 4.92 ± 0.3 | 1118±34 | 1.46 |
| | 28 | 1569 | 5.17 ± 0.3 | 1176±113 | 1.66 |

The results of geopolymer mortar containing 0 %, 1 % Isover granulate and 2 % basalt fibers are shown in Tables 8.2 and 8.3. The flexural strength of unreinforced and synthetic reinforced geopolymer mortar is compared. Commercial fibers reinforced geopolymer mortars are express higher value of mechanical properties than unreinforced mortar. The test results showed similar the flexural strength of 2 kind fibers reinforcement of mortar after curing 28 days at room temperature. An increase in the flexural strength of 37 % with Isover

granulate reinforcement and 36 % increasement for basalt reinforcement is observed when compared to unreinforced geopolymer mortar.

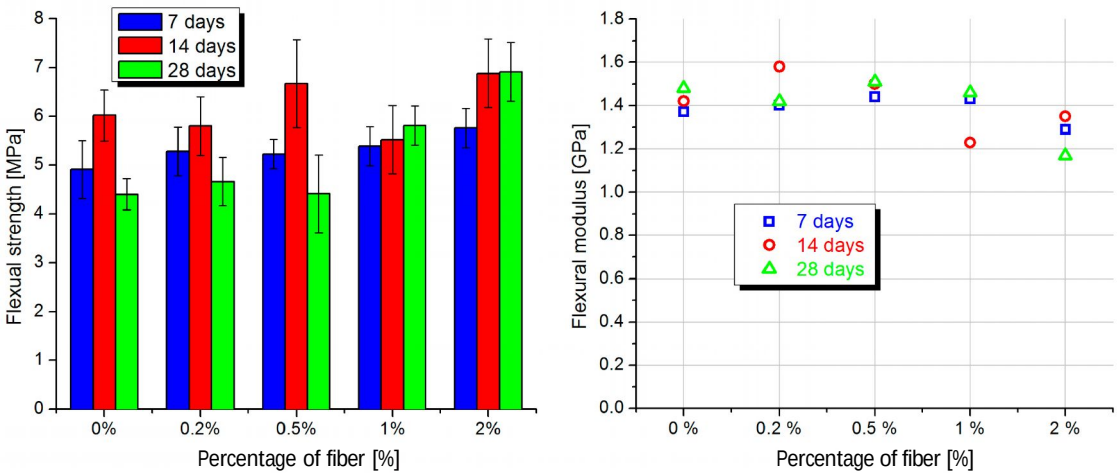


**Fig. 8.3** The flexural strength (left) and flexural modulus (right) of short basalt fiber reinforced geopolymer mortar

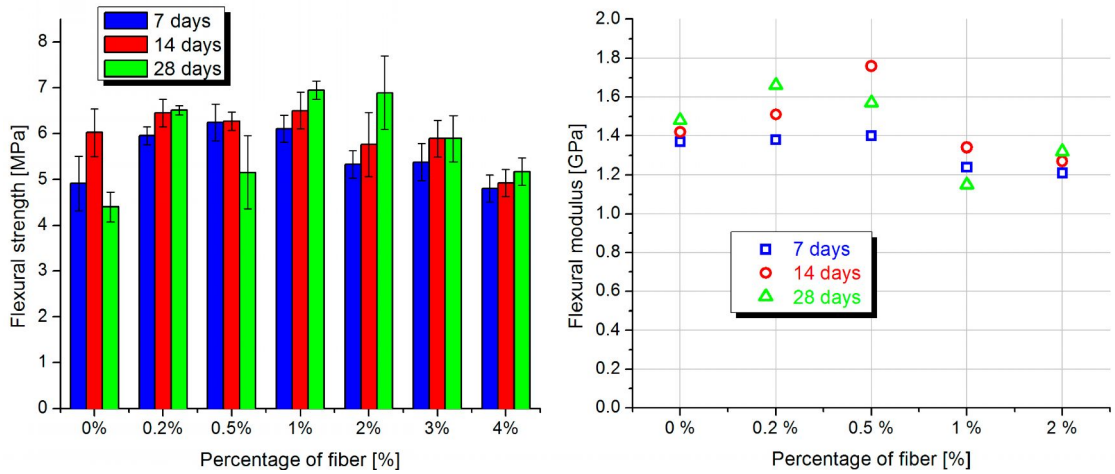


**8.4** The flexural strength and flexural modulus of Isover granulate fiber reinforced geopolymer mortar

The specimens after testing are presented in Fig. 8.5. This picture shows that commercial fibers were mixed and well homogenized with geopolymer resin.

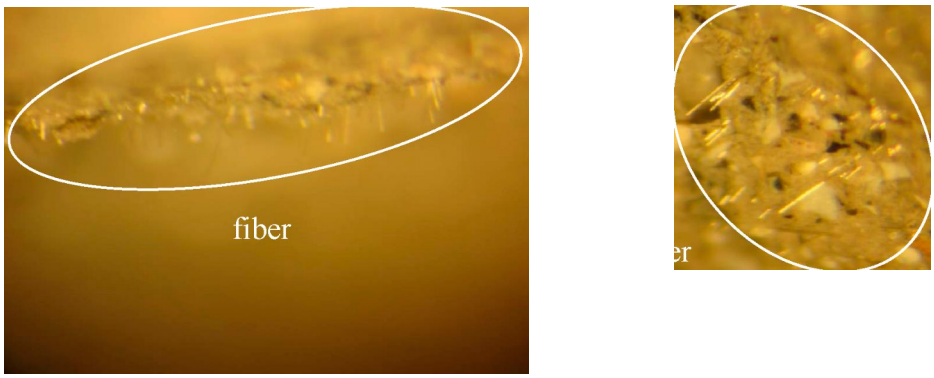


**Fig. 8.5** The macrostructure (magnification 50x) of fibers reinforced geopolymer mortar, left: 1 % Isover granulate, right: 2 % basalt

Fig. 8.6 shows the variation of Vickers hardness depending on the fibers content and curing time of geopolymer mortar. Isover granulate (1 %) fiber reinforced mortar exhibits the highest hardness of 3.30 GPa compared to 3.08 GPa of the unreinforced sample.

Generally the addition of commercial fibers in mortar can lead to the improved local hardness.

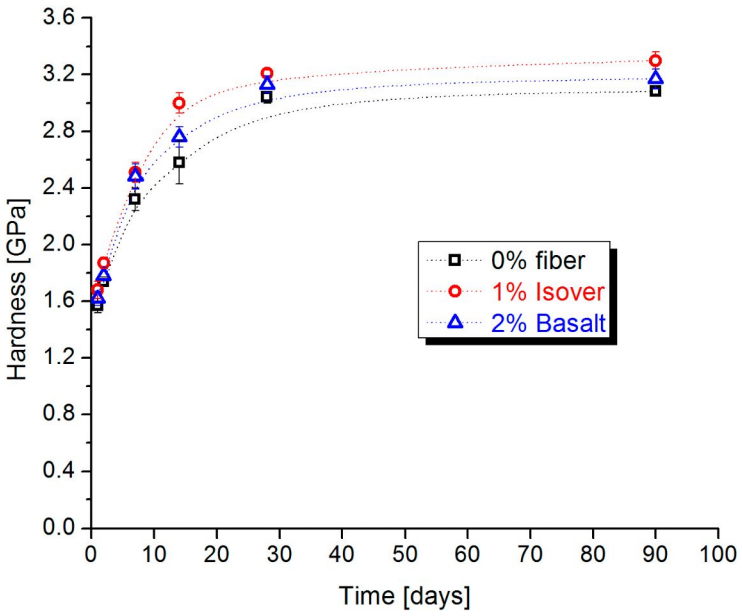


**Fig. 8.6** The hardness of fibers reinforced geopolymer mortar with function of time and fibers content

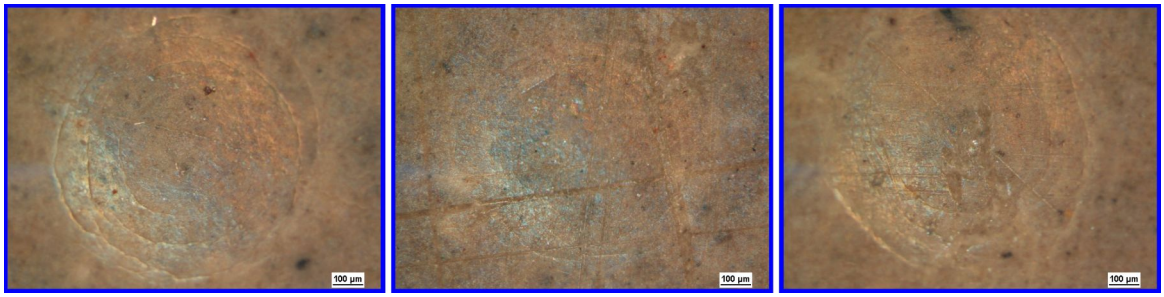

**Fig. 8.7** The surface of the geopolymer mortar after pressing, left: 0 %, 1 % Isover granulate, right: 2 % basalt fiber

**Table 8.4** Flexural properties of concrete M5 reinforced with 1 % Isover granulate and 2 % basalt fiber

| Properties | 0 % | | 1 % Isover granulate | | 2 % basalt | |
|---|---|---|---|---|---|---|
| | 7 days | 14 days | 7 days | 14 days | 7 days | 14 days |
| $\rho$ [kg/m3] | 2250 | 2153 | 2208 | 2136 | 2110 | 2069 |
| $R_{mo}$ [MPa] | **4.80** ± 0.13 | **6.88** ± 0.98 | **5.52**±0.2 | **6.98**±0.3 | **5.61**±0.2 | **6.73**±0.4 |
| s [%] | 0.81 | 1.14 | 0.8 | 1.19 | 0.93 | 0.94 |

$R_{mo}$ - Flexural strength, [MPa] s - Relative deformation, [%]

The results of geopolymer concrete M5 containing 0 %, 1 % Isover granulate and 2 % basalt fibers are shown in Table 8.4. It is easy to see that the flexural strengths of concrete reinforced with basalt and Isover granulate are almost unchanged when comparing with concrete unreinforced fiber, only density is lightly decreased about 4 %.

## 8.4 CONCLUSIONS

In this chapter, the effect of commercial fibers content on the mechanical properties of the geopolymer mortar and concrete was investigated and the following conclusions were derived:

- The percentage of fibers content in mortar has been optimized.
- Mechanical properties of mortar can be improved by the addition of short basalt and Isover granulate fibers, while concrete was not increased the flexural strength.

- The density of specimens was slightly decreased when increasing the percentage of fibers reinforced with geopolymer mortar and concrete.

- Isover granulate fiber displays to be an excellent reinforcement for mortar increasing the hardness, flexural results and very easy homogeneous mixing with geopolymer resin.

- The durability of commercial fibers is important for reinforcement mortar and can be improved by stabilization of micro-cracks and reduced shrinkage.

# Chapter 9

# MACHINABILITY OF GEOPOLYMER MORTAR

## 9.1 INTRODUCTION

The term machinability is a relative measure of how easily a material can be machined acceptable surface finish [171]. Materials with good machinability require little power to cut, can be cut quickly, easily obtain a good finish, and do not wear the tooling much [172].

Machinability can be difficult to predict because machining has so many variables. Two sets of factors are the condition of work materials and the physical properties of work materials [171].

The condition of the work material includes eight factors: microstructure, grain size, heat treatment, chemical composition, fabrication, hardness, yield strength, and tensile strength [171]. The microstructure, grain size, chemical composition, and the hardness will be discusses in this chapter.

There are many methods (drilling, grinding, turning, milling, etc) to evaluate machinability of material. In this research, we were concerned about drilling method to measure cutting force, time cutting, and cutting conditions of geopolymer mortar based fly ash, stone powder and shale powder.

## 9.2 EXPERIMENTAL

The processing to make specimens is described in chapter 3. All samples had a cylindrical shape with a diameter $D_o$ = 120 mm and a length $l_o$ = 45 mm (Fig. 9.1). We used 3 kinds of powder (fly ash K6_LF, stone and shale) as a filler to produce geopolymer mortar. Test specimens were made using geopolymer mortar from mixture MLF'-4 are given details in Table 4.4.


(a) (b) (c)

**Fig. 9.1** Geo mortar with different fillers: a) fly ash, b) stone powder, c) shale powder

## 9.3 RESULTS

### 9.3.1 MATERIALS

Table 9.1 shows the summary chemical composition of stone and shale particles, fly ash K6_LF are given in Table 4.1.

**Table 9.1** The chemical composition of stone and shale particles

| Atomic [%] | O | Na | Al | Si | K | Ca | Mn | Fe |
|---|---|---|---|---|---|---|---|---|
| Stone | 70.48 | 1.68 | 12.21 | 11.31 | 3.31 | 0.37 | 0.11 | 0.53 |
| Shale | 69.03 | 15.82 | 12.89 | 0.23 | 0.71 | 0.20 | 0.24 | 0.86 |

The SEM images (Figs. 9.2) present the fly ash, stone and shale powder of different sizes particles. All particles are generally sharp and pointed in shape. The SEM shows that the stone particles are bigger than fly ash and shale.

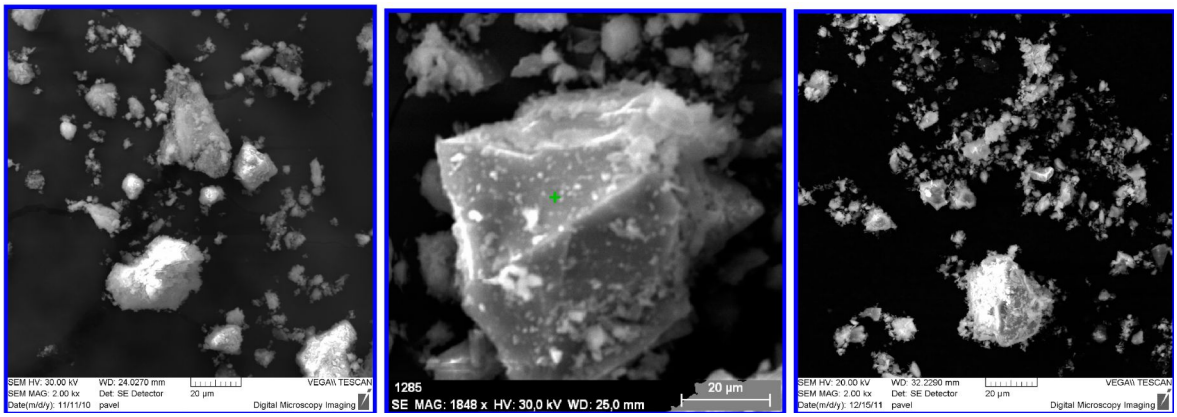


(a) (b) (c)

**Fig. 9.2** SEM images of fly ash K6_LF (a), stone (b) and shale (c)

Figs. 9.3, 9.4 and 9.6 illustrate the SEM image and EDX of a polished cross-section of the fly ash, stone powder and shale based geopolymer. The results of EDX investigations highlighted are summarized in Table 9.2. The main components of fly ash geopolymer are $Al_2O_3$ and $SiO_2$. In this study, the mole ratio of Si to Al directly determines the molecular configuration types of the products type at Si/Al = 7, 10, 8 respectively fly ash, stone and shale geopolymer. With this type geopolymer are obvious excellent fire-resistance and high bonding [19, 53]. Thus, the mole ratio of Si to Al is one very key parameter for the synthesis of geopolymer with fly ash, stone and shale powder.

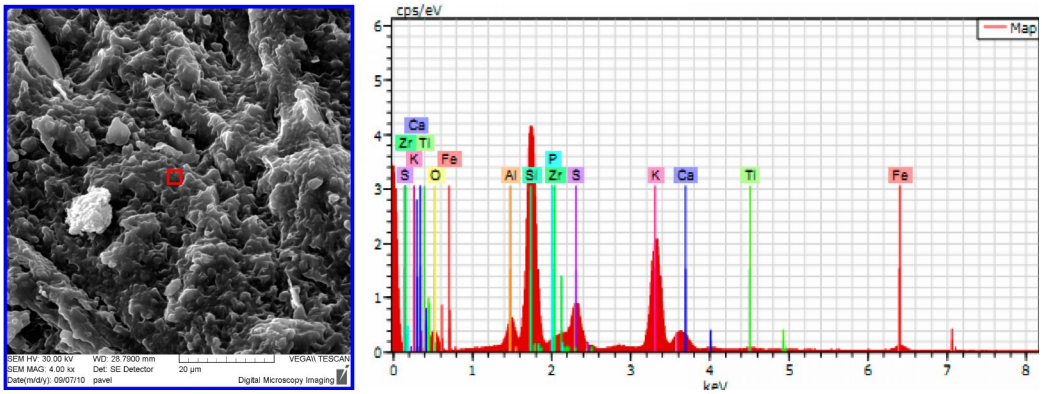


**Fig. 9.3** SEM image and EDX of fly ash geopolymer

**Table 9.2** Quantitative elemental analysis data of fly ash, stone and shale based geopolymer

| Atomic [%] | O | Al | Si | P | S | K | Ca | Ti | Fe | Zr | Na |
|---|---|---|---|---|---|---|---|---|---|---|---|
| Fly ash | 57.43 | 3.02 | 21.71 | 0.10 | 5.07 | 10.23 | 1.34 | 0.16 | 0.59 | 0.36 | - |
| Stone | 62.77 | 2.60 | 24.66 | 0.76 | - | 8.11 | - | - | 0.20 | 0.27 | 0.64 |
| Shale | 63.78 | 2.38 | 18.65 | 2.90 | - | 11.99 | - | - | - | 0.31 | - |

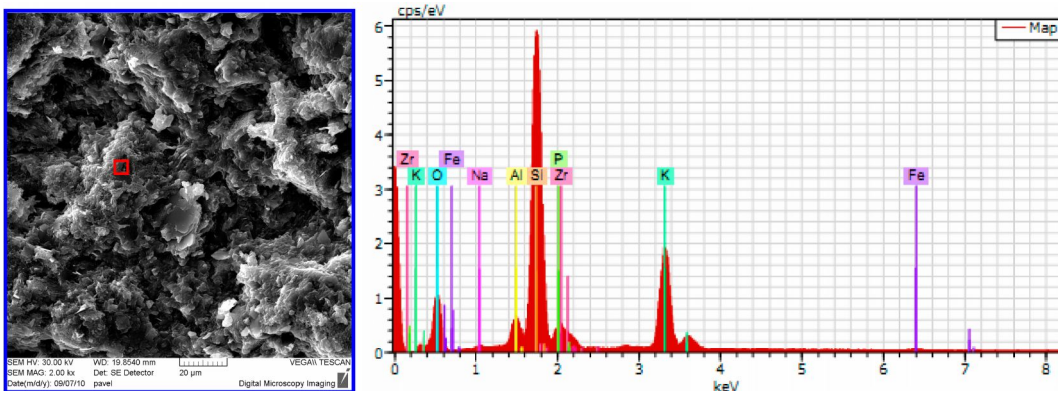


**Fig. 9.4** SEM image and EDX of stone geopolymer

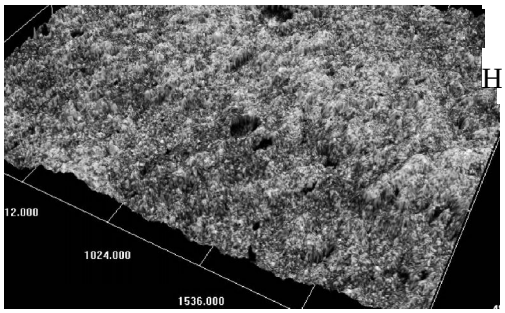


**Fig. 9.5** The LEXT OLS4000 Measuring Laser Confocal Microscope of stone geopolymer

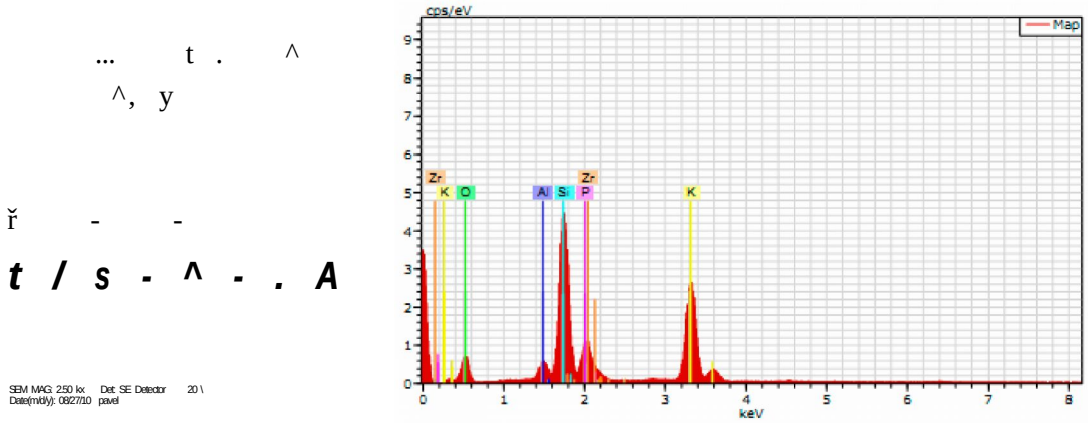


**Fig. 9.6** SEM image and EDX of shale geopolymer

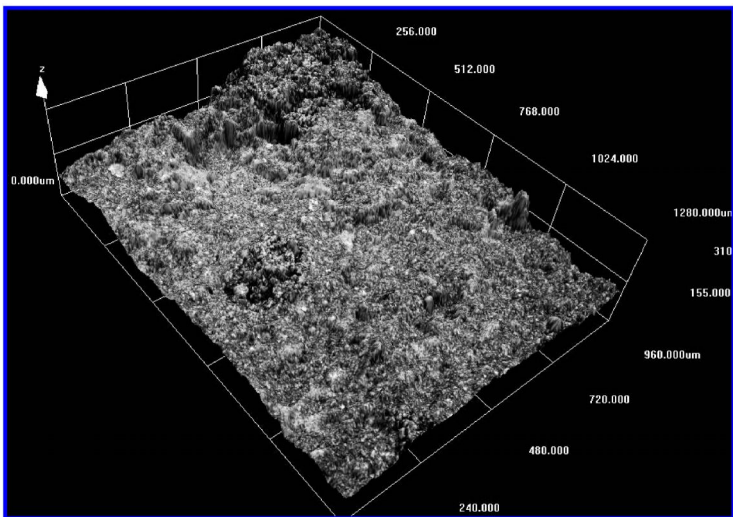


**Fig. 9.7** The LEXT OLS4000 Measuring Laser Confocal Microscope of shale geopolymer

## 9.3.2 QUANTIFYING MACHINABILITY

*9.3.2.1 EVALUATION OF THE DURABILITY OF TOOL*

*Equipment and tools:*

Used machine: Radial drilling machine VR 4.

Used tools: twist drill with diameter 0 D = 8 mm, TiN coated Ro.

All samples were processed on the machine without added liquid.

The selected tool wear criterion, in order to avoid tool breakages, was VB^- = 0.5 mm (VB - the average wear land width)

The samples were cut on the machine under the same cutting conditions:

- Cutting speed : $V_c$ = 1.13 m/min, n = 45 turns/min
- Shift : f = 0.025 mm/turn
- Drilling into the full material

For each sample was used for a new drill

During processing, chips always formed as the fine dust (Fig. 10.8), that were identical in all samples

**Fig. 9.8** Chips of fly ash based geopolymer mortar

Wear the edges of the auger was almost identical for all samples - abrasive wear (Fig. 9.9)

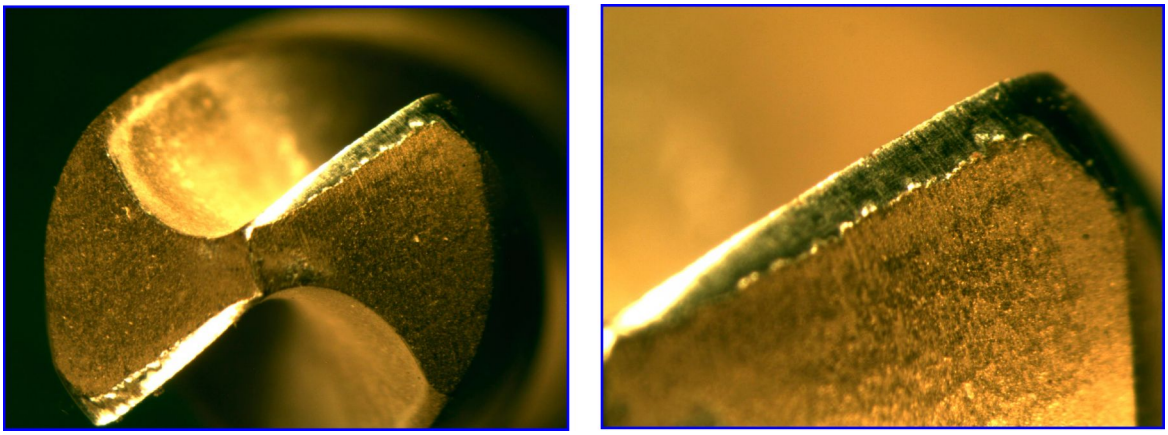

**Fig. 9.9** Wear of the auger blades (geo mortar with fly ash filler)

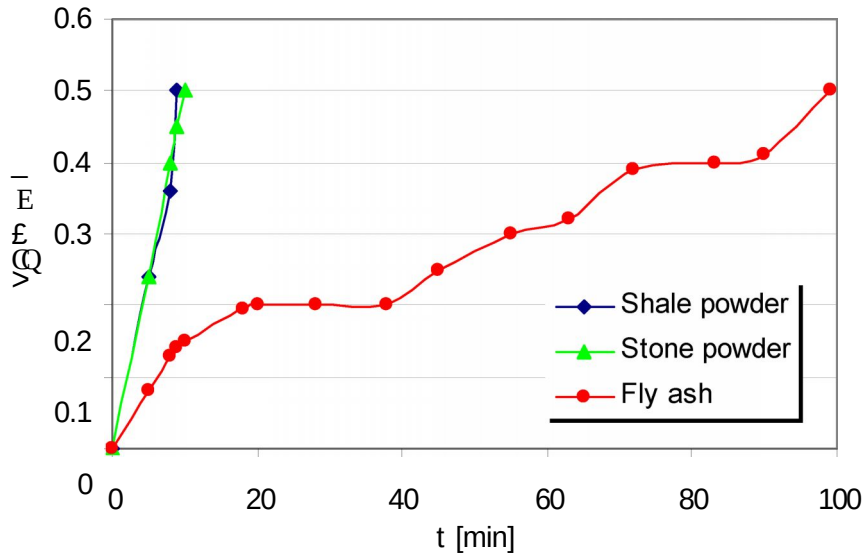


**Fig. 9.10** The time course of cutting edge wear

Fig. 9.10 shows geopolymer mortar with fly ash filler is the best tool life under the same cutting conditions. Geopolymer mortar with stone and shale filler expresses very low durability. Geopolymer mortar with fly ash filler has 10 times higher durability than geopolymer mortar with stone and shale filler. Geopolymer mortar with stone and shale filler shows very abrasive effects. It was done only approximately measurements without repetition (experimental duration about 4 hours).

### *9.3.2.2 EVALUATION OF CUTTING FORCE IN DRILLING*

*Cutting force during machining:*

Used machine: Radial drilling machine VR 4.

Used tools: twist drill with diameter 0 D = 8 mm, TiN coated Ro (sharpened).

All samples were processed on the machine without added liquid.

The samples were cut on the machine under the same cutting conditions:

- Cutting speed : $V_c$ = 1.13 m/min, n = 45 turns/min
- Shift : f = 0.025 mm/turn
- Drilling into the full material

A new drill was used for each sample.

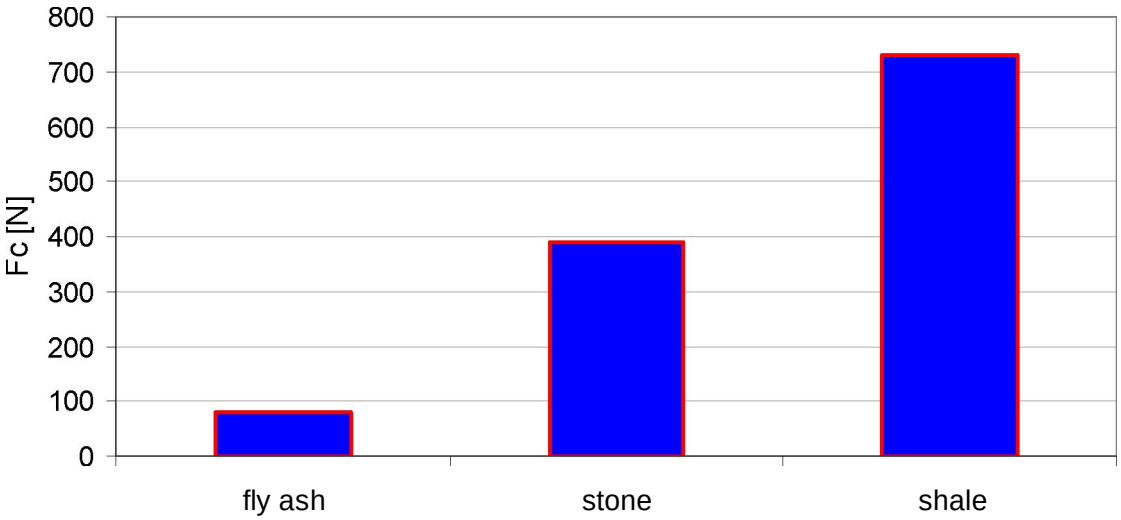


**Fig. 9.11** Comparison of cutting force Fc

Fig. 9.11 shows that geopolymer mortar with shale filler need the largest cutting force during machining by drilling. Medium needed for cutting force of geopolymer mortar with stone filler. The smallest cutting force is the geopolymer mortar with fly ash filler. It was done only approximately measurements without repetition (experimental duration about 1 hour).

*9.3.2.3 EVALUA TION OF THE EFFECTS OF CUTTING CONDITIONS FOR DRILLING*

Effects of cutting speed and shift were assessed on the durability

Only tested - geo mortar with fly ash filler.

Used machine: Radial drilling machine VR 4.

Used tools: twist drill with diameter 0 D = 8 mm, TiN coated Ro.

The selected tool wear criterion, in order to avoid tool breakages, was VB^ = 0.5 mm (VB - the average wear land width).

Experiments in which the cutting forces were determined and made with drill sharpening.

All samples were processed on the machine without added liquid.

The samples were cut on the machine under the cutting conditions as following:

- First set of measurements with shift f = 0.025 mm/turn:

  + Cutting speed $v_{c1}$ = 1.13 $m.min^{-1}$ ($n_1$ = 45 $min^{-1}$)

    $v_{c2}$ = 3.14 $m.min^{-1}$ ($n_2$ = 125 $min^{-1}$)

    $v_{c3}$ = 6.28 $m.min^{-1}$ ($n_3$ = 250 $min^{-1}$)

  + Drilling into the full material

- Second set of measurements with shift f = 0.063 mm/turn:

  + Cutting speed $v_{c1}$ = 1.13 $m.min^{-1}$ ($n_1$ = 45 $min^{-1}$)

    $v_{c2}$ = 3.14 $m.min^{-1}$ ($n_2$ = 125 $min^{-1}$)

    $v_{c3}$ = 6.28 $m.min^{-1}$ ($n_3$ = 250 $min^{-1}$)

  + Drilling into the full material

- Third set of measurements with shift f = 0.16 mm/turn:

  + Cutting speed $v_{c1}$ = 1.13 $m.min^{-1}$ ($n_1$ = 45 $min^{-1}$)

    $v_{c2}$ = 3.14 $m.min^{-1}$ ($n_2$ = 125 $min^{-1}$)

    $v_{c3}$ = 6.28 $m.min^{-1}$ ($n_3$ = 250 $min^{-1}$)

  + Drilling into the full material

When cutting speed or shift was changed, we used a new drill

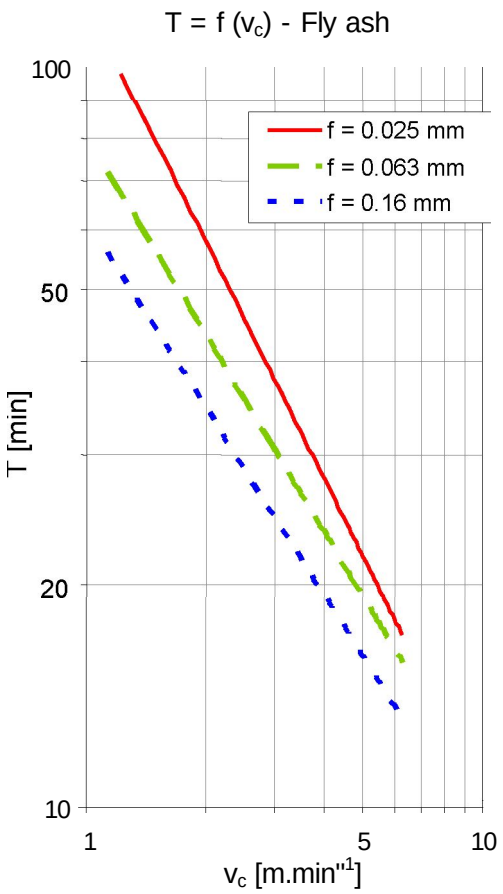


**Fig. 9.12** Dependence of durability for cutting speeds for three different shifts - geopolymer mortar with fly ash filler

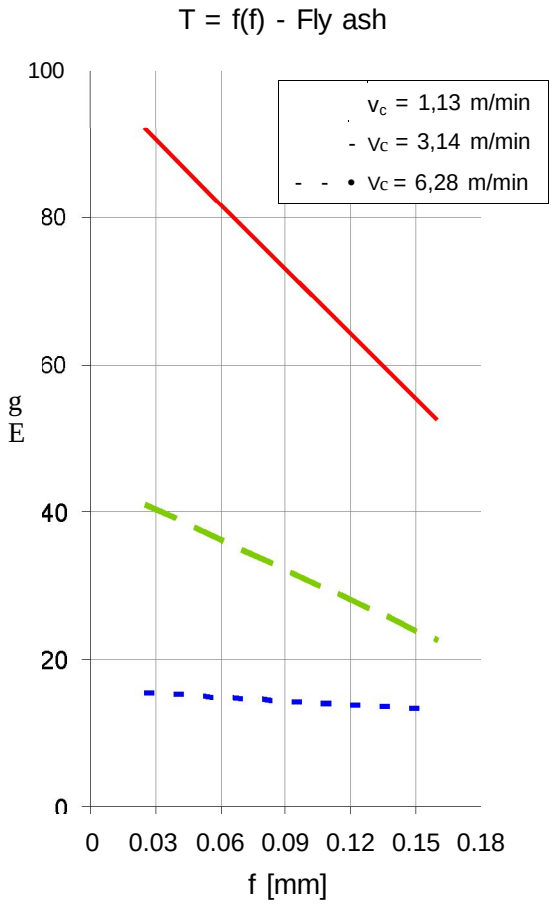


**Fig. 9.13** Dependence of durability for shift for three different cutting speeds - geopolymer mortar with fly ash filler

Fig. 9.12 shows that increasing cutting speed is decreases tool life. This chart shows three lines of constant displacements, where the highest durability is with the constant shift of 0.025 mm.

Fig. 9.13 shows a very significantly effect of cutting speed on tool life, it is also clear that at high cutting speed ($v_c$ = 6.28 m-min$^{-1}$) the change of the shift value has the minimal influence on the tool life. But the change of shift at low cutting speed ($v_c$ = 1,13 m-min$^{-1}$) has far more significantly effect on tool life, thus with increasing value of shift with low cutting speed, tool life decreases rapidly.

The effects of cutting speed and shift to the $F_c$ were assessed while experiments.

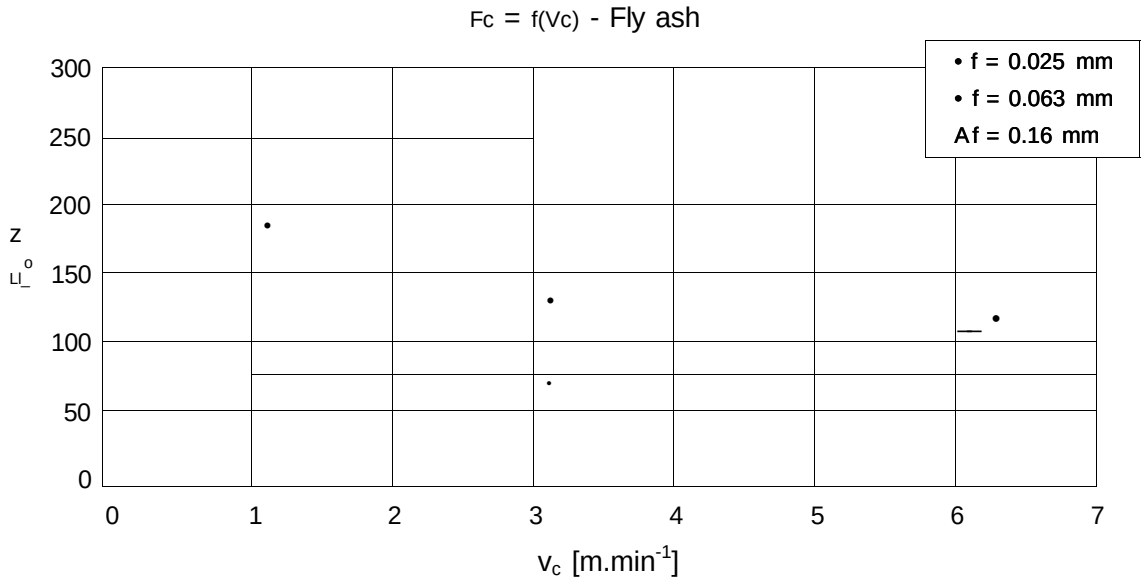


**Fig. 9.14** Dependence of cutting force on the cutting speed for three different shifts - geopolymer mortar with fly ash filler

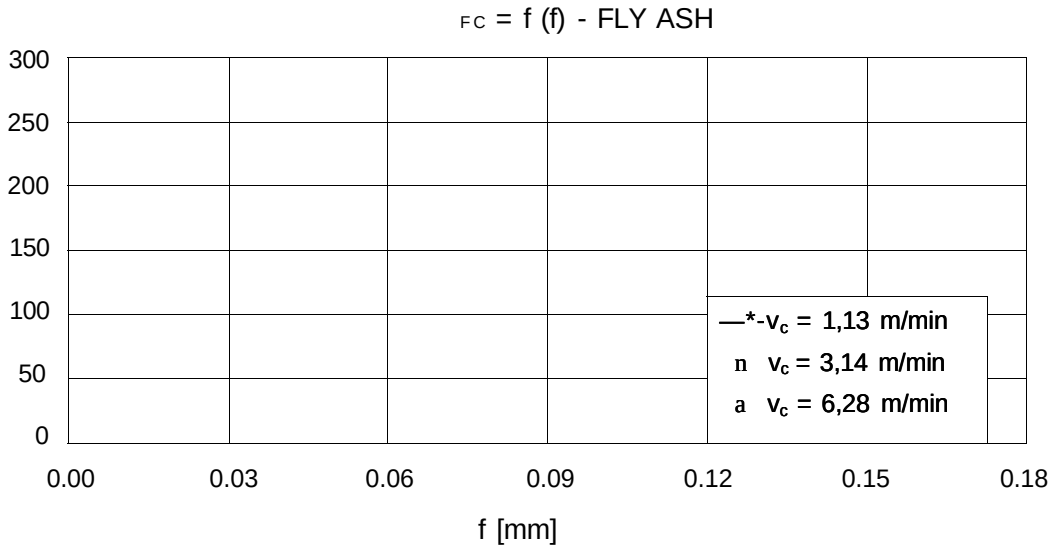


**Fig. 9.15** Dependence of cutting force on the shift for three different cutting speeds - geopolymer mortar with fly ash filler

Fig. 9.14 shows that increasing cutting speed gradually decreases the value of cutting forces. This is most pronounced in case of the line with constant shift f = 0.16 mm/turn and f = 0.063 mm/turn.

Fig. 9.15 shows that increasing shift increases the value of cutting forces. This progression is evident in all curves of constant cutting speeds.

## 9.4 CONCLUSIONS

In order to clarify the machinability of fly ash, stone and shale powder based geopolymer mortar in drilling; drilling tests were performed with TiN coated Ro. The tool wear, tool life, cutting force and others were investigated practically and these results were discussed. The results can be summarized as follows:

Geopolymer mortar with fly ash filler had 10 times higher durability than geopolymer mortar with stone and shale filler.

The temperatures generated and cutting force of fly ash based geopolymer mortar in the drilling process were smaller than stone and shale filler.

The results show that the machinability of fly ash based geopolymer is less wear on the tools and easier machining. It is an advantage to apply fly ash based geopolymer in industries.

# Chapter 10

# POTENTIAL APPLICATIONS

The atomic ratio Si:Al in the poly(sialate) structure determines the properties and application fields. In my thesis, recommended application of geopolymer resin was synthesized shale fly dust from rotary kiln (for 10 hours at 750 $^{o}$C) with Si/Al molar ratio of 2.0 with sodium hydroxide (NaOH) and sodium silicate ($Na_2SiO_3$). From 2009 to present, we have been produced some productions that are made mainly from fly ash as following:

# Bricks, ceramic tiles, artificial stone

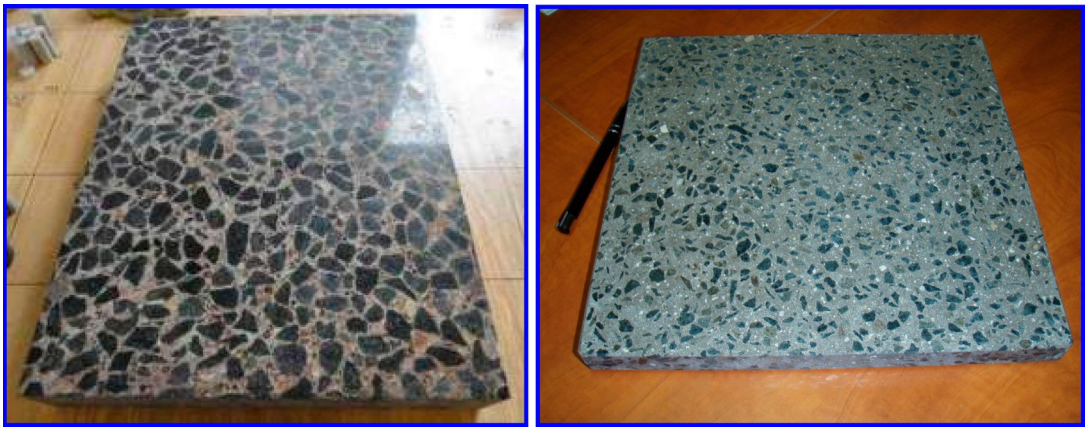

**Fig. 10.1** Artificial stone

# Backfilling the road and embankment


**Fig. 10.2** Backfilling the road by fly ash based geopolymer concrete in United Energy company

# We have been used pure geopolymer and fly ash based geopolymer mortar for fire resistant coatings for some materials, such as: polystyrene, wood, plastic, and concrete.

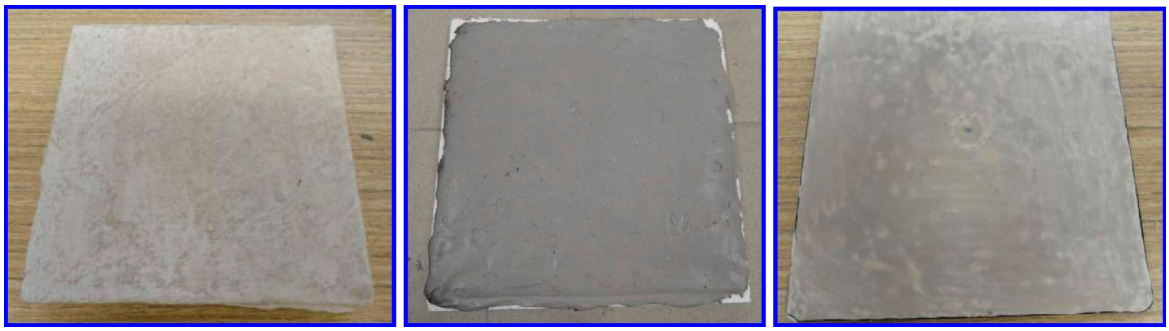

(a) (b) (c)

**Fig. 10.3** Polystyrene coated by pure geopolymer (a), geopolymer mortar (b) and plastic coated by pure geopolymer (c)

**Fig. 10.4** Portland concrete coated by pure geopolymer before (left) and after heated 600 $^{o}$C

(a) (b)

**Fig. 10.5** Geopolymer composite reinforced basalt fabric fiber, box (200 x 200 x 200) mm (a) (b) Heating 300 $^{o}$C and loading 1.5 kg


**Fig. 10.6** The box heated by flame up to 374 $^{o}$C

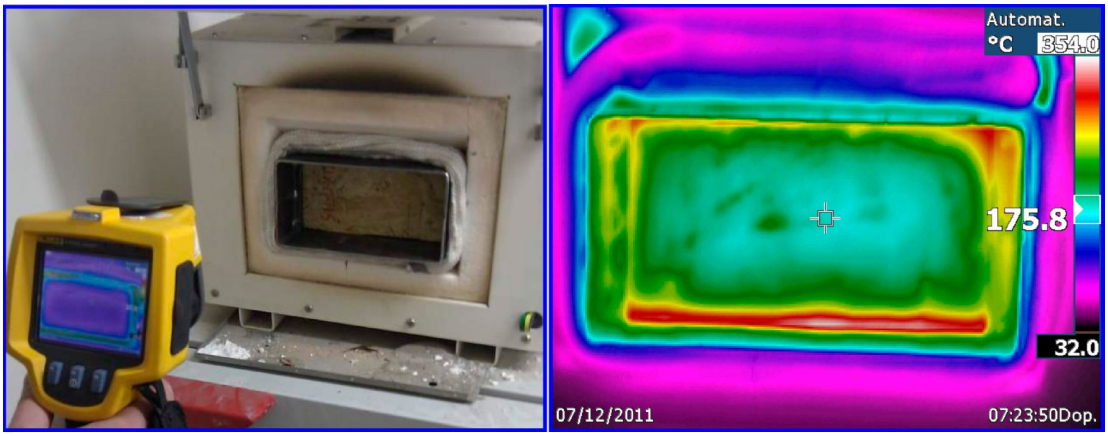


**Fig. 10.7** Wood coated by geopolymer mortar before (left) and after heated 354 °C in the oven, outside only 175.8 °C

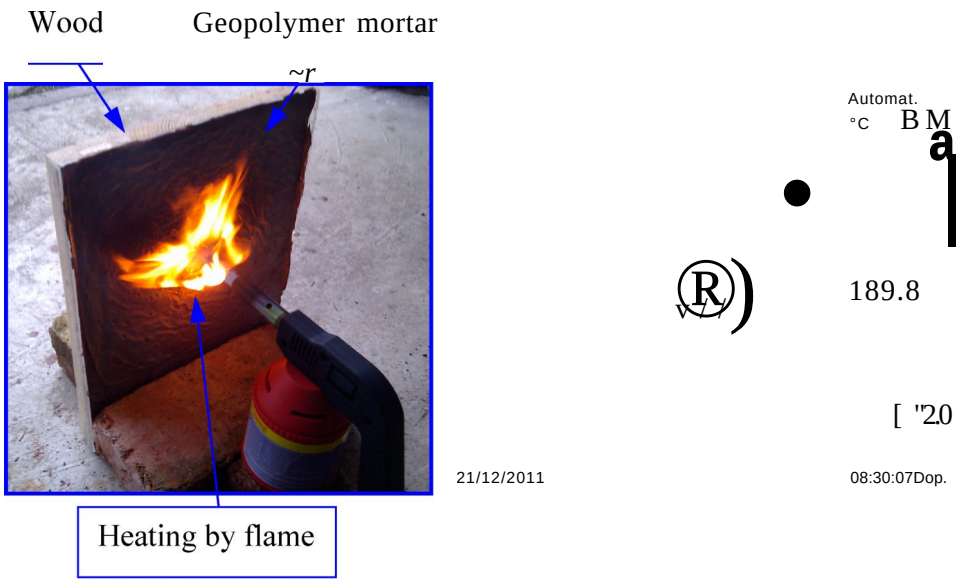


**Fig. 10.8** Wood coated by geopolymer mortar heating by flame (left) and measured local temperature (right)

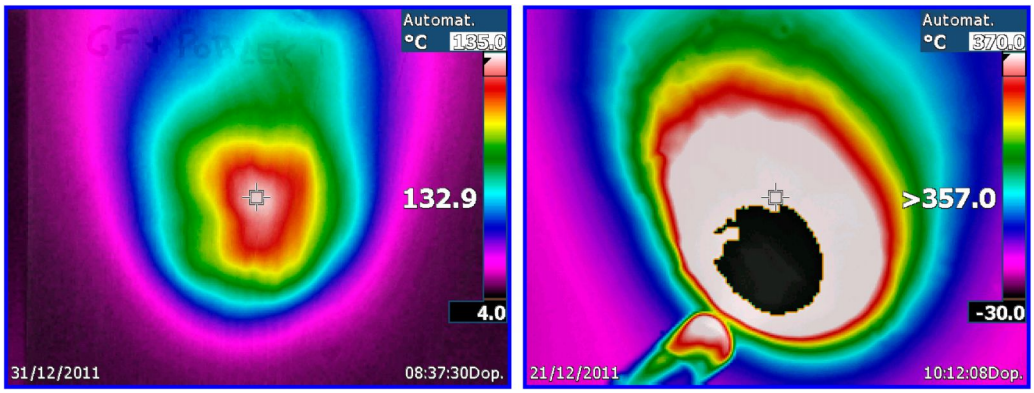


**Fig. 10.9** Measured local temperature of wood coated geopolymer mortar

# Tanks to contain acid solution


**Fig. 10.10** Tank made from geopolymer mortar

# Optimal colors

**Fig. 10.11** Geopolymer mortar with different colors

# Logo of Technistone Company

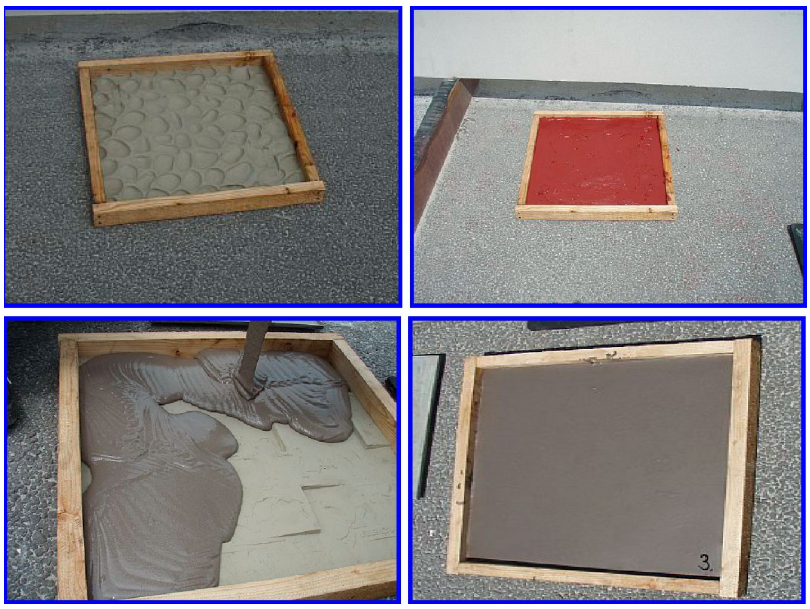

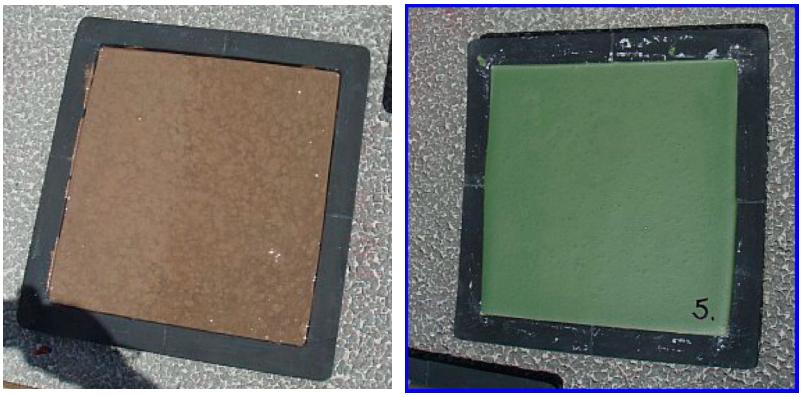


**Fig. 10.12** Samples made from fly ash + stone powder + geopolymer

# They can be used for repairing in the ancient and modern architecture.

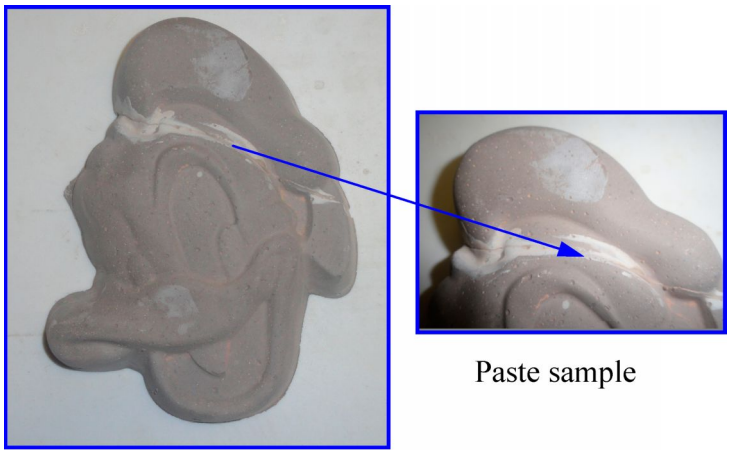


**Fig. 10.13** Preparing a samplee

# Beside, geopolymers can be used in radioactive waste stores because geopolymers are inorganic polymers suitable for incapsulating radioactive wastes so as to enable their safe and long-term storage [173].

# Geopolymer can be applied in nuclear power plants and other buildings in the radiological industry, such as fire resistant walls and fire doors.

# In metallurgy industry: direct molten systems, transferred ladles.

# Structural surfaces like floor and storage areas as well as runways have also been proposed and the feasibility of the latter was investigated by Malone [174].

# Chapter 11

# CONCLUSIONS AND FUTURE WORKS

## 11.1 CONCLUSIONS

In this research, geopolymer binders were synthesized from shale fly dust from rotary kiln with a molar Si:Al ratio of 2.0 combined with alkaline silicate solution ($Na_2SO_3$ + NaOH) and using geopolymer binders to produce geopolymer mortar and concrete. Geopolymer binders have many advantages in comparison with than OPC, due to their excellent fire resistance, excellent mechanical properties, environmentally friendly nature and good acid resistance. However the cost of geopolymer mortar and concrete especially geopolymer cement and alkaline is still high, so the main purpose of this study was reduced the cost of geopolymer binders by additive more waste material as fly ash, stone with rich content of Si and Al and extra water in the mixtures but mechanical properties of mortar and concrete is still good enough to meet essential requirements of industries.

Results show that the mechanical properties of geopolymer mortar and concrete are dependant on the chemical composition, types of fly ashes, ratio fly ash / geopolymer cement, curing conditions, addition fibers and other fillers. Using SEM/EDX analysis was carried out to analysis the shape, chemical composition of fly ash particles and microstructure of geopolymers. We can easy see that the strength of geopolymers after milling fly ash and combination with commercial fibers is higher than unmilled fly ash particles and without fibers. They are analyzed detailed as follows:

The chemical composition and properties of all types of fly ash coming from many power station of Czech Republic were investigated. They are different color brown, light grey to black due to its chemical compositions and contaminants. Fly ash particles are generally sharp, pointed, and spherical in shape and range in size from 1 (xm to 30 (xm. From chapter 6 to 10, the authors were used K6_LF to study, because United Energy Company were supported this material for our research. When fly ashes were combined with geopolymer resin, fly ash PRT

based geopolymer (finest particles) are gave the highest results as we can see in Figs. 4.7 and 4.8.

We were recognized that extra water lead to decrease amount of alkaline and in the mixtures was significantly reduced the mechanical properties of geopolymer mortar from 30 % to 80 % with the same curing conditions and components see Table 4.3. The compressive strength of geopolymer mortar were also strongly influenced by both curing time and curing temperature. As the curing temperature in the range of 30 $^{o}$C to 90 $^{o}$C increases, the compressive strength of fly ash-based geopolymer mortar also increases about 40 % see Fig. 4.13. Based on these test trends, a curing temperature of about 70 $^{o}$C is recommended. In additions, curing time with ranging from 5 to 72 hrs, the rate of increase in strength was rapid up to 48 hrs of curing time (Fig. 4.12). Therefore, heat curing time need not be more than 48 hrs in practical applications for fly ash based geopolymer mortar.

The scope application of fly ash is very limited due to fly ash is grey or black in color. For this reason, a heating method (1000 $^{o}$C) is necessary to increase the whiteness of fly ash. However, the particles after heated 1000 $^{o}$C are reduced mechanical properties of the geopolymer mortar about 20 %. Thus, authors recommended this method use in sculpture, architecture, especially where color is more important than the mechanical properties.

Modification of fly ash particles from micro to nano scale by milling method is significantly increase about 20 % the compressive strength of fly ash based geopolymer with the same component.

The ratio of fly ash / geopolymer cement of 2.0 content in the mixtures of geopolymer mortar give the mechanical properties (50.93 MPa of compressive strength after curing at room temperature for 28 days) higher than other ratio see Table 6.2. And the compressive strength concrete of mixture M5 of 32 MPa (10 % fly ash + 15 % geopolymer cement + 18 % alkaline + 9 % fine sand + 48 % coarse aggregate) is higher than other mixtures (Fig. 6.6). And the slump value of the fresh fly-ash-based geopolymer concrete increases with the increase of extra water or alkaline added to the mixture lead to reduce the mechanical properties of concrete.

For each type of test, after 28 days the compressive strength did not change significantly.

The effect of high temperature on the mechanical properties of geopolymer mortar and concrete are investigated. After heating up to 600 $^{o}$C (Figs. 7.1 and 7.2), the branched cracks appear over

the whole surface of the samples. Compressive strength of samples is strongly reduced after 400 $^{o}$C approximately 70 %, 50 % respectively mortar and concrete, and slightly reduces up to 1000 $^{o}$C (Fig. 7.8). The weight loss of mortar is increased about 20 % when the temperature go up to 400 $^{o}$C and remained up to 1000 $^{o}$C, while concrete is also increased but smaller than mortar about 12 % at 1000 $^{o}$C. Increasing the percentage of fine sand of mortar or coarse aggregate of concrete will be reduced the shrinkage and micro-cracks.

For environmental conditions testing, geopolymer mortars were immersed in sulfuric acid solution with selected concentrations ranging from 1% to 3% with the measured pH about 1.0. The weight loss, shrinkage and compressive strength are investigated. The concentration of H2SO4 solution has significantly effect on the compressive strength of mortar and concrete, increasing the concentration 3 % is reduced the strength about 38 % and concomitant the weight loss of samples is also increased. And the effects of freeze-thaw testing are also reduced about 45 % and 8 % in wet-dry of the compressive strength of geopolymer mortar.

Optimal percentage of Isover granulate (1 %) and basalt (2 %) fibers reinforced geopolymer mortar are given highest results of the flexural properties, however concrete is still remained. After curing at room temperature for 28 days, the flexural strength of geopolymer mortar is increased 37 % with Isover granulate reinforcement and 36 % increasement for basalt reinforcement is observed when compared to unreinforced geopolymer mortar.

The machinability of fly ash based geopolymer mortar is good with small temperatures generated, cutting force and high durability.

## 11.2 FUTURE WORKS

At the present, we have many projects to develop and applied geopolymer in some places in Czech Republic. In the next time, we will continue the study as following:

Reducing the cost of geopolymer mortar and concrete by using different waste materials as sand powder, stone powder.

Addition some materials in the mixture of geopolymer with the purpose is reduce the plastic shrinkage and increasing strength as super plastic, additives, etc.

Finding another fiber to increase the mechanical properties, reduce the cost and density.

The research will be concerning about physical and chemical properties geopolymer in concrete and optimal fly ash / geopolymer cement and other fillers.

Continuing apply the milling method to modify fly ash particles to improve the mechanical properties of geopolymer mortar and concrete.

Concerning applies geopolymer mortar and concrete in place that need high fire resistant and thermal insulation, such as: fire door, fire wall, etc.

We believe that geopolymer may apply in building and other fields. And utilization of these materials is the energy and resource saving process and it is also indirectly reduce the emission of green - house gas $CO_2$ released from cement manufacturing. This is beneficial for resource conservation and environmental protection.

# REFERENCES


[1] Hardjito D., et al., *The stress-strain behaviour of fly ash-based geopolymer concrete.* Developments in mechanics of structures and materials, p. 831-834, 2005.

[2] Sandor P., *Concrete materials: Properties, Specifications and Testing* 1992: Noyes, United States, 641.

[3] Kumar M. P., P. J. M. M., *Concrete: Microstructure, Properties, and Materials*, 2006, United States, 647.

[4] Ramachandran V. S., B. J. J., *Handbook of analytical techniques in concrete science and technology*, 2001: Noyes, United States, 964.

[5] Pierre, C. A., *Binders for Durable and Sustainable Concrete:* Taylor & Francis, 529, 2008.

[6] Skalny, J., *High strength concrete.* Annual Review of Materials Science. 17: p. 35-56, 1987.

[7] Hardjito D., R. B. V., *Development and properties of low-calcium fly ash-based geopolymer concrete:* Australia, p. 103, 2005.

[8] Zongjin L., et al., *Development of sustainable cementitious materials.* International Workshop on Sustainable Development and Concrete Technology, China, p. 55-76, 2004.

[9] Flower D., S.J., *Green house gas emissions due to concrete manufacture.* Inter J Life Cycle Assess 12, p. 282-288, 2007.

[10] Gartner, E., *Industrially interesting approaches to low - $CO_2$ cements.* Cement Concrete Research. 34, p. 1489-1498, 2004.

[11] *IPCC, Intergovernmental Panel on Climate Change.* 4th Assessment report. In: ParryML, editor. Assessment of observed changes and responses in natural and managed systems. Climate change 2007: impacts, adaptation and vulnerability. Contribution of working group II to the 4th assessment report of the Intergovernmental Panel on Climate Change. Cambridge Univ. Press: p. 79-131, 2007.

[12] Stern, N., *Stern review on economics of climate change.* Cambridge University. Press, 2006.

[13] Rafat, S., *Waste Materials and By-Products in Concrete.* 2008: Springer, German.

[14] Duxson P., et al., *Geopolymer technology: the current state of the art.* Journal Material Science. 42: p. 2917-2933, 2007.

[15] Taylor M., et al., *Energy Efficiency and $CO_2$ Emissions from the Global Cement Industry.* IEA-WBCSD workshop, 2006.

[16] Palomo, A., *Alkaline activation of metakaolin and calcium hydroxide mixtures: influence of temperature, activator concentration and.* Materials Letters. 47: p. 55-62, 2001.

[17] Rangan, R.V., *Low-calcium fly ash based geopolymer concrete.* Concrete construction Engineering handbook, New York 2007. 2nd ed.

[18] Shuzheng Z., et al., *Novel modification method for inorganic geopolymer by using water soluble organicpolymers.* Lsevier B.V. 58(7-8): p. 1292 - 1296, 2004.

[19] Davidovits, J., *Geopolymer chemistry & application,* ed. Second. 2008: Institute Géopolymer - France. 587.

[20] Duxson P., et al., *The role of inorganic polymer technology in the development of 'green concrete.* Cement and Concrete Research. 37: p. 1590 - 1597, 2007.

[21] Provis J. L., et al., *Geopolymers for immobilization of $Cr^{6}$+, $Cd^{2}$+, and $Pb^{2+}$.* Hazardous Materials. 157: p. 587-598, 2008.

[22] Provis J. L., et al., *The role of sulfide in the immobilization of Cr(VI) in fly ash geopolymers.* Cement and Concrete Research. 38: p. 681-688, 2008.

[23] Duxson P., et al., *Thermal conductivity of metakaolin geopolymers used as a first approximation for determining gel interconnectivity.* Ind. Eng. Chem. Res. 45(23): p. 7781 - 7788, 2006.

[24] Cheng T. W., et al., *Fire-resistant geopolymer produced by granulated blast furnace slag.* Minerals Engineering 16: p. 205-210, 2003.

[25] Palomo A., et al., *Chemical stability of cementitious materials based on metakaolin.* Cement Concrete Research. 29 (7): p. 997 - 1004, 2004.

[26] Lee W. K. W., et al., *The effect of ionic contaminants on the early-age properties of alkali-activated fly ash-based cements.* Cement Concrete Research. 32 (4): p. 577 - 584, 2006.

[27] Davidovits, J., *Chemistry of Geopolymeric Systems, Terminology.* 2nd International conference 'Géopolymere': p. 9 - 40, 1999.

[28] Pereira, C. F., *Waste stabilization/solidification of an electric arc furnace dust using fly ash-based geopolymers.* Fuel. 88: p. 1185-1193, 2009.

[29] Davidovits, J., *Geopolymers: Inorganic polymeric new materials.* Journal of Thermal Analysis. 37: p. 1633 - 1656, 1991.

[30] Davidovits, J., *30 Years of Successes and Failures in Geopolymer Applications - Market trends and Potential breakthroughs.* Geopolymer 2002 Conference: Melbourne, Australia, 2002.

[31] Carlos A. R. R., et al., *A comparative study of two methods for the synthesis o f f l y ash-based sodium and potassium type zeolites.* Fuel. 88: p. 1043-1416, 2009.

[32] Newman J., B. S. C., *Advanced Concrete Technology Processes.* 2003, Elsevier. p. 699.

[33] Lioyd, N. A., *Geopolymer concrete with fly ash.* 2nd International Conference on Sustainable Construction Materials and Technologies. 3: p. 1493 - 1504, 2010.

[34] Ahmed, M. F., *Compressive Strength and Workability Characteristics of Low-Calcium Fly ash-based Self-Compacting Geopolymer Concrete.* World Academy of Science, Engineering and Technology 74, 2011.

[35] Van J., et al., *The effect of composition and temperature on the properties o f f l y ash- and kaolinite-based geopolymers.* Chemical Engineering Journal 89: p. 63 - 73, 2002.

[36] *Chemical properties of quartz.* [cited 2011 20 October]; Available from: http://www.quartzpage.de/gen_chem.html.

[37] Davidovits, J., *Geopolymer chemistry and sustainable Development. The Poly(sialate) terminology: a very useful and simple model.* The International Workshop on Geopolymer Cements and Concrete for the promotion and understanding of green-chemistry, Australia, 2005.

[38] Duxson P., et al., *Structural ordering in geopolymers derived from metakaolin.* Geopolymer chemistry and sustainable Development. 21-25, Australia, 2005.

[39] Davidovits, J. *About geopolymerization.* [cited 2011 October 22 ]; Available from: http://www.geopolymer.org/science/about-geopolymerization.

[40] Zongjin Li, et al., *Advanced Concrete Technology:* John Wiley & Sons, Canada, 2011.

[41] Mustafa, A. B. A. M., *Mechanism and Chemical Reaction of Fly Ash Geopolymer Cement- A Review* Journal of Asian Scientific Research. 1: p. 247-253, 2011.
[42] Panagiotopoulou Ch., et al., *Dissolution of aluminosilicate minerals and by-products in alkaline media.* Materials Science. 42: p. 2967-2973, 2007.
[43] McCormick A. V., et al., *Evidence from alkali-metal NMR spectroscopy for ion pairing in alkaline silicate solutions.* Physical Chemistry 93: p. 1737-1742, 1989.
[44] Aagard P., et al., *Thermodynamic and kinetic constraints on reaction rates among minerals and aqueous solutions.* Science. 282: p. 237-285, 1982.
[45] Dimas D., et al., *Polymerization in sodium silicate solutions: a fundamentalprocess in geopolymerization technology.* Materials Science. 44: p. 3719-373, 2009.
[46] Panias D., et al., *Effect of synthesis parameters on the mechanical properties of fly ash-based geopolymers.* Colloids and Surfaces A: Physicochemical and Engineering Aspects. 301: p. 246-254, 2007.
[47] Phair, J. W., *Effect of the silicate activator pH on the microstructural characteristics of waste-based geopolymers.* International Journal of Mineral Processing. 66: p. 121-143, 2002.
[48] Duxson P., et al., *Effect of Alkali Cations on Aluminum Incorporation in Geopolymeric Gels.* Industrial Engineering Chemistry Research. 44: p. 832-839, 2005.
[49] Hua X., *Effect of Source Materials on Geopolymerization.* Industrial Engineering Chemistry Research. 42: p. 1698-1706, 2003.
[50]. Madani, A., et al., *Silicon-29 and aluminum-27 NMR study of zeolite formation from alkali-leached kaolinites: influence of thermal preactivation.* . Physical Chemistry. 94: p. 760-765, 1990.
[51] Bortnovsky, O., et al., *Structure and stability of geopolymers synthesized from kaolinitic and shale clay residues.* Geopolymer, green chemistry and sustainable development solutions. The World Congress Geopolymer 2005, Sain-Quentin: p. 81-84, 2005.
[52] Amándio, T. P., *Optimised Conditions for the Obtaining of Metakaolin.* Materials Science Forum. 514 - 516: p. 1536-1540, 2006.
[53] Davidovits, J., *Geopolymer Chemistry and Properties* First European Conference on Soft Mineralurgy, France, 1988.
[54] *ECCI, New pozzolanic materials for the concrete industry. UK, 1993.*
[55] Highley, D. E., *China clay. MineralDossier No. 26. HMSO, London, 1984.*
[56] Xiao Y., et al., *Geopolymerization process of alkali-metakaolinite characterized by isothermal calorimetry.* Thermochimica Acta 493: p. 49-54, 2009.
[57] *American Coal Ash Assosiation, Fly Ash Facts for Highway Engineers, p. 81.* 2003.
[58] *Environment technology Development.* [cited 2011 23 October]; Available from: http ://www.jcoal.or.jp/overview_en/kankyou. html.
[59] Ashby, J. B., *Fly Ash and Its Use in Concrete.* The Concrete Institute of Australia, Sydney, Australia, 1990.
[60] Fansuri, H., *Suitability Of Coal Fly Ashes To Aggregate Manufacture From Coal Fly Ash By Sintering.* 11th APCChE Congress, Kuala Lumpur, 2006.
[61] Potgieter, J. H., et al., *Alternative procedure for classification of fly ash particle size fractions.* Proceedings of the international ash utilisation symposium, USA, 2003.
[62] Hewlett, P. C., *Lea's Chemistry of cement and concrete,* ed. 4: Oxford: Elsevier, Butterworth-Heinemann. 1087, 2004.
[63] Malhotra, V. M., *Fly Ash in Concrete.* CANMET, 1994.

[64] *Managing Coal Combustion Residues in Mines, Committee on Mine Placement of Coal Combustion Wastes, National Research Council of the National Academies, 2006.*

[65] Ahmaruzzaman, M., *A review on the utilization of fly ash.* Progress in Energy and Combustion Science. 36: p. 327-363, 2010.

[66] *ASTM standard specification for coal fly ash and raw or calcined natural pozzolan for use in concrete (C618-05). American Society for Testing Materials.* Annual book of ASTM standards, concrete and aggregates. 4, 2005.

[67] Jensen A. D., et al., *A review of the interference of carbon containing fly ash with air entrainment in concrete.* Progress in Energy and Combustion Science 34: p. 135-154, 2008.

[68] Kopecký L., et al., *Geopolymer materials based on fly ash.* Ceramics - Silikáty 49: p. 195-204, 2005.

[69] Jindřich, P., *After Incineration: The Toxic Ash Problem, Prague - Manchester, 2005.*

[70] *Is fly ash an inferior building and structural material.* Science in Dispute, 2003.

[71] Johnson, J., *The foul side of clean coal.* Chemical & Engineering News. 87: p. 44-47, 2009.

[72] *American Coal Ash Association.* [cited 2011 20 October]; Available from: www.acaa-usa.org.

[73] Altug, S., *A new technique to reduce the radioactivity of fly ash utilized in the construction industry.* Fuel. 90: p. 1612-1617, 2011.

[74] Sear, L. K. A., *UK practice—a review of fly ashes for use in concrete.* Proceedings of the international workshop on novel products from combustion residues: opportunities and limitations, Spain: p. 47-52,2001.

[75] Association, A. C. A., *Coal combustion byproducts survey, USA, 1997.*

[76] Gulten A., et al., *A comparison of basic dye adsorption onto zeolitic materials synthesizedfrom fly ash.* Hazardous Materials. 187: p. 562-573, 2011.

[77] Tara, S., *Usage of Industrial Waste Products in Village Road Construction* Environmental Science and Development. 1: p. 122-126, 2010.

[78] *A team consisting of Washington State University, University of Wisconsin at Madison, and Bloom Companies, High-Volume Use of High-Carbon Fly Ash for Highway Construction - A Case Study.* Sponsored by the U.S. Department of Energy (DOE) and in cooperation with the Minnesota Department of Transportation, 2008.

[79] Mohamed A. M. O., et al., *Role of fly ash and aluminium addition on ettringite formation in lime-remediated mine tailings.* Cement & Concrete Aggregates 25: p. 49-57, 2003.

[80] Petrik L. F., et al., *Utilisation of South African fly ash to treat acid mine drainage, and production of high quality zeolites from the residual solids.* Proceeding of the international ash utilisation symposium, USA, 2003.

[81] Sheetz B. E., et al., *Field applications of cementitious grouts to address the formation of acid mine drainage.* Conference on mining and the environment, Cananda, 1995.

[82] Sheetz B. E., et al., *Design of fly ash based grout for acid mine drainage abatement.* In: Mesch MR, Malin L, editors. Sixteenth annual meeting of the association of abondoned mine lands programs, USA, : p. 53-72, 1994.

[83] Polat M., et al., *Utilization of coal fly ash as a chemical scrubber for acid mine drainage: fixation of heavy metals.* Proceedings of the international workshop on

novel products from combustion residues: opportunities and limitations, Spain: p. 207-216, 2001.

[84] Doye I., et al., *Neutralisation of acid mine drainage with alkaline industrial residues: laboratory investigation using batch-leaching tests.* Appl Geochem 1197, 2003.

[85] Quirol X., et al., *Synthesis of zeolites from fly ash at a pilot plant scale.* Proceedings of the international workshop on novel products from combustion residues: opportunities and limitations, Spain: p. 61-67, 2001.

[86] Canpolat F., et al., *Use of zeolite, coal bottom ash and fly ash as replacement materials in cement production.* Cement & Concrete Research. 34: p. 731-737, 2004.

[87] Sahu S., et al., *Preparation of sulphoaluminate belite cement from fly ash.* Cement & Concrete Research. 24: p. 1065-1072, 1994.

[88] Scheetz B. E., et al., *Utilisation of fly ash.* Ceramic Composite Intergrowths: p. 510-520, 1996.

[89] Saxena M., *Emerging technologies for third millennium on wood substitute andpaint for coal ash.* Proceedings of the second international conference on fly ash disposal and utilisation. 1: p. 26-31, 2000.

[90] Ravikumar K., et al., *Optimization ofprocess variables by the application of response surfacemethodology for dye removal using a novel adsorbent.* Dyes Pigments. 72: p. 66-75, 2007.

[91] Z., E., *Adsorption of reactive black 5 from aqueous solution: equilibrium and kinetic studies.* Desalination. 194: p. 1-10, 2006.

[92] Djwantoro H., et al., *On the Development of Fly ash based geopolymer concrete.* ACI Materials 101: p. 467-472, 2004.

[93] Suresh T., et al., *Acid Resistance of Fly ash based Geopolymer mortars.* International Journal of Recent Trends in Engineering. 1: p. 36-40, 2009.

[94] Djwantoro H., et al., *Develoment and properties of low-calcium fly ash-based geopolymer concrete.* Faculty of Engineering, Curtin University of Technology: Perth, Australia, 2005.

[95] Forss, B., *Process for producing a binder for slurry, mortar, and concrete.* United States Patent 4306912

[96] Gravitt, B. B., et al., United States Patent 4,997,484. 1991.

[97] Jiang, W., *Hydrothermal processing of new fly ash cement.* American Ceramic Society Bulletin. 71: p. 642-647, 1992.

[98] Silverstrim, et al., *Fly ash cementitious material and method of making a product.* united States Patent 5,601,643. 1997.

[99] Silverstrim, et al., *Geopolymeric fly ash cement.* Geopolymer '99 Proceeding: p. 107-108, 1999.

[100] Van Jaarsveld J. G. S., et al., *The potential use of geopolymeric materials to immobilise toxic metals: Part I. Theory and applications.* Minerals Engineering. 10: p. 659-669, 1997.

[101] Van Jaarsveld, J. G. S., et al, *The potential use of geopolymeric materials to immobilise toxic metals: Part II. Material and leaching characteristics.* Minerals Engineering. 12: p. 75-91, 1999.

[102] Palomo A., et al., *Alkali-activated fly ashes A cement for the future.* Cement and Concrete Research. 29: p. 1323-1329, 1999.

[103] Van Jaarsveld J. G. S., et al., *The characterisation of source materials in fly ash-based geopolymers.* Materials Letters 57: p. 1272-1280, 2003.

104 Fernandez J. A., et al., *Characterisation of fly ashes potential reactivity as alkaline cements.* Fuel. 82: p. 2259-2265, 2003.
105 Wallah, S., B. V. R., *Low-calcium fly ash-based geopolymer concrete: long-term properties.* Faculty of Engineering urtin University of Technology Perth, Australia. 2006
106 Gourley, J. T., *Opportunities for Environmentally Friendly Construction Materials.* Materials 2003 Conference: Adaptive Materials for a Modern Society, Sydney. 2003.
107 Swanepoel, J. C., *Utilisation of fly ash in a geopolymeric material.* Applied Geochemistry. 17: p. 1143-1148, 2002.
108 Phair, J. W., *Effect of silicate activator pH on the leaching and material characteristics of waste-based inorganic polymers.* Minerals Engineering. 14: p. 289-304, 2001.
109 Bakharev, T., *Geopolymeric materials prepared using Class F fly ash and elevated temperature curing.* Cement And Concrete Research. 35: p. 1224-1232, 2005.
110 Mingyu, H., *Alkali-activated fly ash-based geopolymers with zeolite or bentonite as additives.* Cement & Concrete Composites. 31: p. 762-768, 2009.
111 Paulo J. M. M., et al., *Bulk modulus of basic sodalite, $Na_g[AlSiO_4]6(OH)_22H_2O$, a possible zeolitic precursor in coal-fly-ash-based geopolymers.* Cement and Concrete Research. 41: p. 107-112, 2011.
112 *Bristish lime association.* [cited 2011 19 October]; Available from: http://www. britishlime. org/edu_limemade01. php.
113 Van Jaarsveld J. G. S., et al., *The characterization of source materials in fly ash-based geopolymers.* Materials Letters. 57: p. 1272-1280, 2003.
114 Hardjito D., et al., *On the development of fly ash-based geopolymer concrete.* ACI Materials 101: p. 467-472, 2004.
115 Xie, Z.H., *Hardening mechanism of an alkaline-activated class F fly as.* Cement and Concrete Research. 31: p. 1245-1249, 2000.
116 Blanco, F., et al. , *Variation in fly ash properties with milling and acid leaching.* Fuel. 84: p. 89-96, 2005.
117 Xiem N. T., et al., *Influence of wet milling of fly ash on compression strength of geopolymer mortar cured at room temperature.* 18th International Conference STRUTEX Structure and Structural Mechanics of Textiles, Czech Republic, 2011.
118 Langley, W., et al., *Structural concrete incorporating high volume of class F fly ash.* ACI Materials Journal. 86: p. 507-514, 1989.
119 Neville, A.M., *Concrete Technology:* Pearson Education Ltd. 456, 1987.
120 Hirschi, T., et al., *Concrete Handbook:* Sika Services AG. 151, 2005.
121 *C143/C143M, Test Method for Slump of Hydraulic-Cement Concrete.*
122 *ASTM C78/C78M - 10, Standard Test Method for Flexural Strength of Concrete (Using Simple Beam with Third-Point Loading).* ASTM: p. 1-4, 2010.
123 *ASTM C348 - 08, Standard Test Method for Flexural Strength of Hydraulic-Cement Mortars.* p. 1-6, 2008.
124 *ASTM C 31/C 31M - 03a, Standard Practice for Making and Curing Concrete Test Specimens in the Field, .* p. 1-5, 2003.
125 *AS 1012.9 - 1999, Methods of testing concrete - Determination of the compressive strength of concrete specimens, 1999.*
*ASTM A370 - 07a, Standard Test Methods and Definitions for Mechanical Testing of Steel Products.* p. 1-47, 2007.

127] *ASTM D5882 - 07, Standard Test Method for Low Strain Impact Integrity Testing of Deep Foundations.* p. 1-6, 2007.
128] Fernandez, J. A. M., et al., *Engineering properties of alkali-activated fly ash concrete.* ACI Materials 103: p. 106-112, 2006.
129] Sofi, M., et al., *Engineering properties of inorganic polymer concretes (IPCs).* Cement and Concrete Research 37: p. 251-257, 2007.
130] Prabir, K. S., *Analysis of geopolymer concrete columns.* Materials and Structures 42: p. 715-724, 2009.
131] *AS 1012.17 - Determination of static chord modulus of elasticity and poisson 's ratio of concrete specimens. Standards Association of Australia, Sydney, Australia. 1997.*
132] *ACI Committee 363, State of the art of high strength concrete. American Concrete Institute, Detroit, USA, 1993.*
133] *AS 3600, Concrete structures, Australian Standards, 2001.*
134] Carrasquillo, R. L., et al., *Properties of high strength concrete subjected to short term loads.* ACI Materials. 78: p. 171-178, 1981.
135] Ahmad, S. H., *Structural properties of high strength concrete and its implication for precastpre-stressed concrete.* PCI Journal. 30: p. 92-119, 1985.
136] Kohei N., et al., *Mesoscopic simulation of failure of Mortar and Concrete by 2D RBSM.* Advanced Concrete Technology. 2: p. 359 - 374, 2004.
137] Zongjin, L., *Advanced Concrete Technology:* John Wiley & Sons, Inc., Cananda. 521, 2011.
138] John, N., *Advanced Concrete Technology: Concrete Properties:* Elsevier Ltd., Science and Technology Rights Department in Oxford, UK. 349, 2003.
139] Turton, C. D., *Plastic cracking of concrete. Paper for publication PP/284.* Cement and Concrete Association, 1981.
140] Paul, J. U., *Plastic Shrinkage Cracking and Evaporation Formulas.* ACI Materials Journal, 95-M3, 1998.
141] Wan Y. Z., et al., *Mechanical, moisture absorption, and biodegradation behaviours of bacterial cellulose fibre-reinforced starch biocomposites.* Composites Science and Technology. 69: p. 1212-1217, 2009.
142] Erdogdu, K., *Effects of fly ash particle size on strength of Portland cement fly ash mortars.* Cement and Concrete Researchs. 28: p. 1217-1222, 1998.
143] Nugtere, H. W., et al., *High strength geopolymers produced from coal combustion fly ash.* Global NEST Journa. 11: p. 155-16, 2009.
144] Chindaprasirt P., et al., *High-Strength Geopolymer Using Fine High-Calcium Fly Ash.* Journal of Materials in Civil Engineering 23: p. 2011.
145] Mohd, M. A. B., et al., *Review on fly ash-based geopolymer concrete without Portland Cement.* Journal of Engineering and Technology Research. 3: p. 1-4, 2011.
146] Kumar, S., et al., *Influence of reactivity o f f l y ash on geopolymerisation.* Advances in Applied Ceramics. 103: p. 120, 2007.
147] Kumar, R., et al., *Towards sustainable solutions for fly ash through mechanical activation.* Resources, Conservation and Recycling. 52: p. 157-179, 2007.
148] Fu, X., et al., *Thephysical-chemical characterization of mechanically treate d CFBC fly ash.* Cement and Concrete Composites. 30: p. 220-226, 2008.
149] THOMOS P. K., et al., *Preparation and Characterisation of Nano Structured Materials from Fly Ash: A Waste from Thermal Power Stations, by High Energy Ball Milling.* Nanoscale Research Letter: p. 397-404, 2007.

[150] Horiuchi S, et al., *Effective use of fly ash slurry as fill material.* Journal of Hazardous Materials. 76: p. 301-37, 2000.
[151] Yang, H.F., *Reuse and Recycle of Solid Waste.* Chemical Industry Press. Press 165: p. 2003.
[152] Habert G., et al., *An environmental evaluation of geopolymer based concrete production: reviewing current rese arch trends.* Journal of Cleaner Production. 19: p. 1229 -1238, 2011.
[153] Vasconcelos, E., *Concrete retrofitting using metakaolin geopolymer mortars and CFRP.* Construction and Building Materials. 25: p. 3213-3221, 2011.
[154] Neville, A. M., *Properties of Concrete.* Fourth Edition (Low Priced Edition), Pearson Education Asia Publishing Limited, England,.Produced by Longman Malaysia: p. 7, 2000.
[155] Monita, O., *Properties of fly ash geopolymer concrete designed by Taguchi method.* Materials and Design. 36: p. 191-198, 2011.
[156] Souradeep, G., *Durability of Flyash Based Geopolymer Concrete.* Civil engineering.
[157] Wallah, S. E., *Creep behaviour of fly ash-based geopolymer concrete.* Civil Engineering Dimension Publisher, 2010.
[158] Davidovits, J., *Personal Communication on Geopolymer Chemistry, 2005.*
[159] [cited 2011 17 June]; Available from: http://www.grace.com/EngineeredMaterials/MaterialSciences/Zeolites/ZeoliteStructure.aspx.
[160] Wallah, S. E., *Low-calcium fly ash-based geopolymer concrete: long-term properties.* Research Report GC 2 Faculty of Engineering Curtin University of Technology Perth, Australia, 2006
[161] Song, X. J., et al., *Durability of fly ash-based Geopolymer concrete against sulphuric acid attack.* 10DBMC International Conference on Durability of Building Materials and Components, Lyon, France. .
[162] Kong, D. L. Y., *Effect of elevated temperaturesgeopolymer paste, mortar and concrete.* Cement Concrete Research. 40: p. 334-339, 2010.
[163] Kong, D. L. Y., *Damage behavior of geopolymer composites exposed to elevated temperature.* Cement Concrete and Composites, (30): p. 986-991, 2008.
[164] Provis, J., *Fire resistance of geopolymer concretes.* Project report - Grant FA23860814096, University of Melbourne, 2010.
[165] Harun, T., *Statistical analysis for mechanical properties of polypropylene fiber reinforced lightweight concrete containing silica fume exposed to high temperature.* Materials and Design 30: p. 3252-3258, 2009.
[166] Reis, J. M. L., *Assessment of fracture properties of epoxy polymer oncrete reinforced with short carbon and glass fibers.* Construction and Building Materials. 18: p. 523-528, 2004.
[167] Gonzalo, M. B., *Mechanical properties of polypropylene-fiber reinforced concrete after gamma irradiation.* Composites 42: p. 567-572, 2011.
[168] Zhijian, L., et al., *Compressive and Flexural Properties of Hemp Fiber Reinforced Concrete.* Fibers and Polymers. 5: p. 187-197, 2004.
[169] *Saint-Gobain Insulation, http://www. isover. com/, accessed 5.10.2011.*
[170] Xiem N. T, et al., *Effects of plasma treatment on mechanical properties of commercial fibers based on geopolymer matrix composites.* 16th Strutex 2009: p. 9, 2009.
[171] Schneider, G. J., *Cutting Tool Applications, 2006.*

[172] Degarmo, E., et al., *Materials andProcesses in Manufacturing (9th ed.). Wiley, 2003.*
[173] Inorganic polymer *http://www.youtube.com/watch?v=ffsHsQUbHVg&feature=relatedhttp://www.gic.co.hu/inorganic_polymer.html.* [cited 2011 16 July].
[174] Van, J. J. G. S., et al., *The potential use of geopolymeric materials to immobilise toxic metals: Part I. Theory and applications.* Minerals Engineering. 10: p. 659-669, 1997.

# APPENDIX A

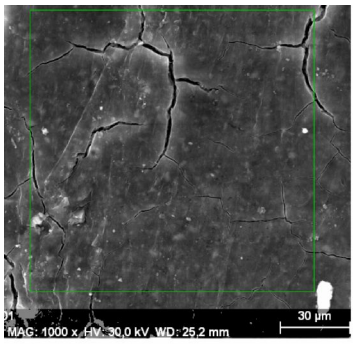
30 µm
MAG: 1000 x HV: 30,0 kV WD: 25,2 mm

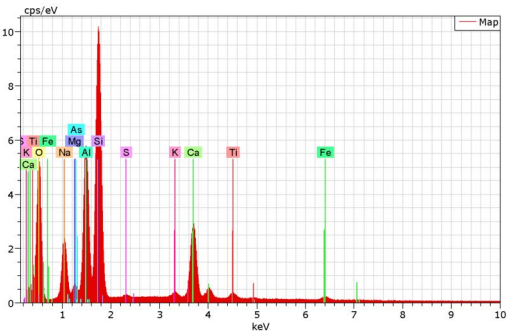
cps/eV
Map
Ti Fe
As
Mg
Si
K O
Na
Al
S
K
Ca
Ti
Fe
Ca
keV

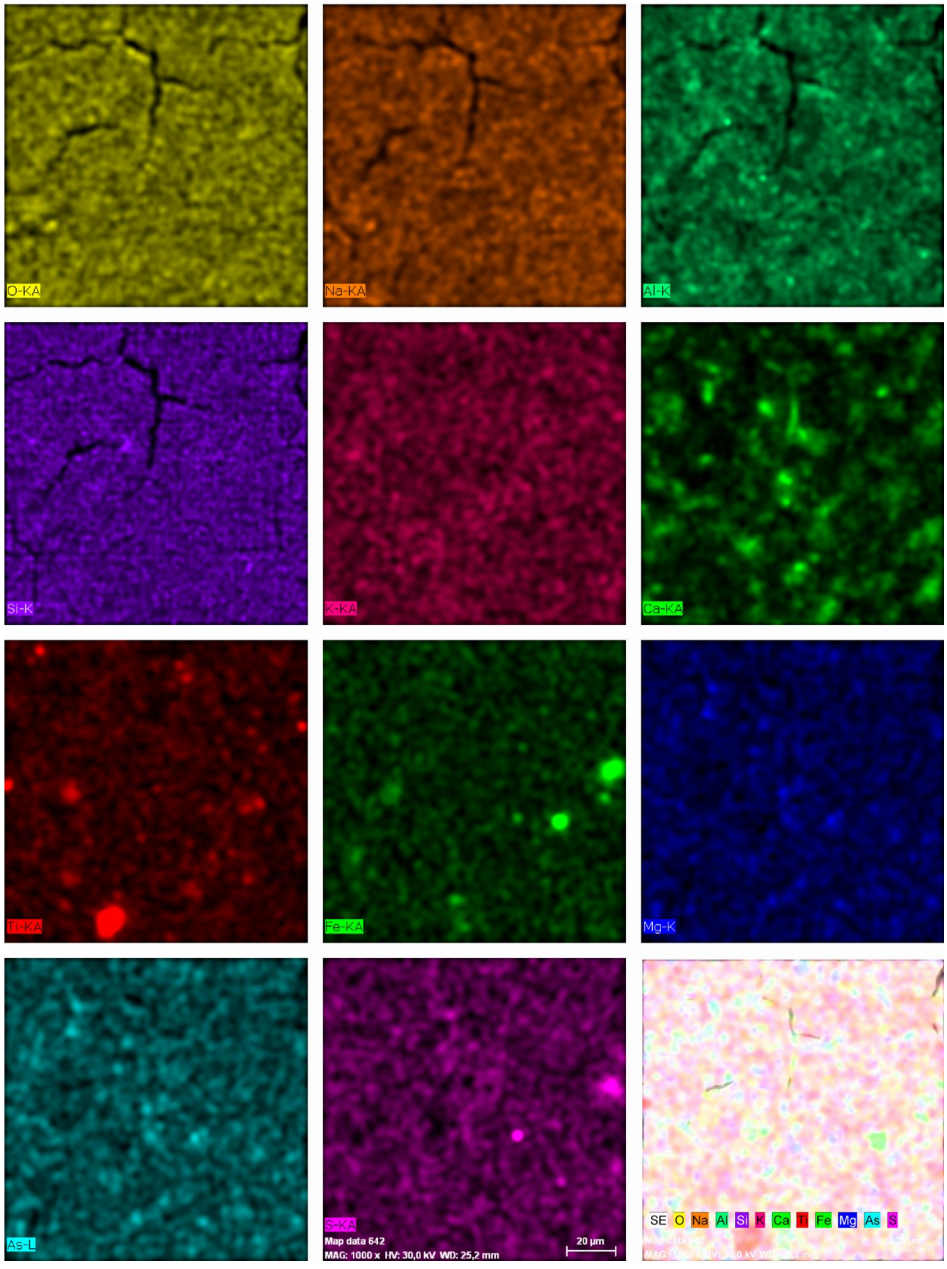
O-KA
Na-KA
Al-K
Si-K
K-KA
Ca-KA
Ti-KA
Fe-KA
Mg-K
As-L
S-KA
Map data 642
MAG: 1000 x HV: 30,0 kV WD: 25,2 mm
20 µm
SE O Na Al Si K Ca Ti Fe Mg As S

# APPENDIX B

**Table 1B** Properties of geopolymer mortar produced by fly ash cured at 60 and 70 °C for 24h

| Type of fly ash | Mixture No | 60 °C, 24 h | | | 70 °C, 24 h | | |
|---|---|---|---|---|---|---|---|
| | | Density P [kg/m$^3$] | Hardness [HV] | Compressive strength [MPa] | Density P [kg/m$^3$] | Hardness [HV] | Compressive strength [MPa] |
| PRT | MT-1 | 1750 | **287** ± 6 | **29.16** ± 1.4 | 1639 | **314** ± 6 | **33.43** ± 0.1 |
| | MT-2 | 1660 | **244** ± 6 | **16.12** ± 0.6 | 1640 | **289** ± 17 | **25.12** ± 0.3 |
| | MT-3 | 1610 | **168** ± 3 | **11.03** ± 0.3 | 1449 | **254** ± 5 | **22.43** ± 0.8 |
| | MT-4 | 1610 | **145** ± 8 | **6.75** ± 0.4 | 1428 | **146** ± 5 | **8.82** ± 0.5 |
| OPE | ME-1 | 1709 | **303** ± 2 | **26.49** ± 4.1 | 1680 | **318** ± 8 | **34.79** ± 2.2 |
| | ME-2 | 1521 | **193** ± 11 | **17.50** ± 2.5 | 1590 | **279** ± 6 | **23.32** ± 2.0 |
| | ME-3 | 1512 | **165** ± 10 | **10.17** ± 1.7 | 1540 | **233** ± 10 | **13.85** ± 1.3 |
| | ME-4 | 1484 | **132** ± 9 | **7.61** ± 0.5 | 1460 | **139** ± 11 | **6.14** ± 0.4 |
| K1 | MK1-1 | 1749 | **301** ± 6 | **27.90** ± 5.1 | 1670 | **311** ± 2 | **31.26** ± 0.2 |
| | MK1-2 | 1657 | **271** ± 1 | **18.98** ± 0.3 | 1591 | **248** ± 3 | **22.14** ± 0.5 |
| | MK1-3 | 1632 | **271** ± 5 | **9.56** ± 0.5 | 1533 | **172** ± 5 | **11.93** ± 0.4 |
| | MK1-4 | 1376 | **222** ± 3 | **1.88** ± 0.1 | 1400 | **136** ± 3 | **1.34** ± 0.1 |
| K3 | MK3-1 | 1721 | **278** ± 4 | **21.98** ± 0.3 | 1631 | **326** ± 4 | **26.55** ± 0.2 |
| | MK3-2 | 1660 | **237** ± 2 | **14.04** ± 0.3 | 1480 | **248** ± 3 | **17.58** ± 0.2 |
| | MK3-3 | 1640 | **220** ± 3 | **13.83** ± 0.2 | 1470 | **185** ± 2 | **7.33** ± 0.2 |
| | MK3-4 | 1440 | **168** ± 3 | **7.31** ± 0.1 | 1430 | **168** ± 3 | **3.95** ± 0.1 |
| K6_LF | MLF-1 | 1690 | **260** ± 5 | **25.80** ± 0.6 | 1631 | **307** ± 4 | **30.32** ± 1.6 |
| | MLF-2 | 1594 | **196** ± 7 | **15.72** ± 0.9 | 1581 | **197** ± 5 | **23.05** ± 0.9 |
| | MLF-3 | 1575 | **136** ± 8 | **7.21** ± 0.6 | 1521 | **159** ± 2 | **8.28** ± 0.6 |
| | MLF-4 | 1502 | **110** ± 5 | **3.01** ± 0.1 | 1388 | **130** ± 9 | **3.11** ± 0.1 |
| K6 | MK6-1 | 1752 | **258** ± 5 | **25.06** ± 0.4 | 1726 | **304** ± 5 | **30.18** ± 1.1 |
| | MK6-2 | 1723 | **191** ± 7 | **15.43** ± 1.3 | 1660 | **270** ± 7 | **24.47** ± 1.0 |
| | MK6-3 | 1573 | **134** ± 6 | **6.69** ± 0.8 | 1524 | **191** ± 5 | **7.76** ± 0.6 |
| | MK6-4 | 1507 | **113** ± 3 | **2.90** ± 0.3 | 1424 | **152** ± 6 | **2.90** ± 0.2 |

# APPENDIX C

## OPE

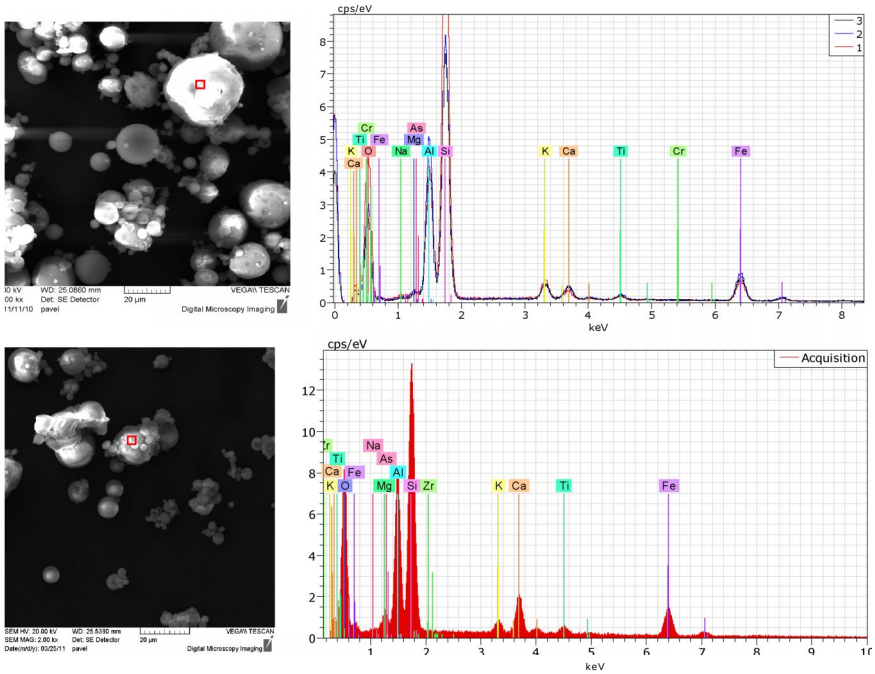


**Fig. 1B** SEM photographs and corresponding energy spectrum of fly ash OPE before (above) and after heating at 1000 $^{o}$C (under)

## PRT

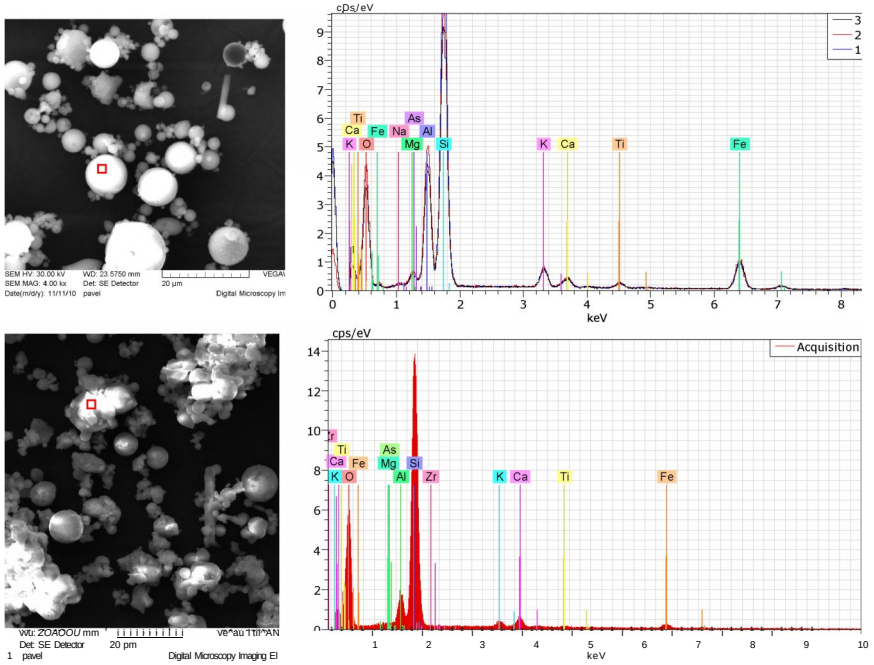


**Fig. 2B** SEM photographs and corresponding energy spectrum of fly ash PRT before (above) and after heating at 1000 $^{o}$C (under)

## K1

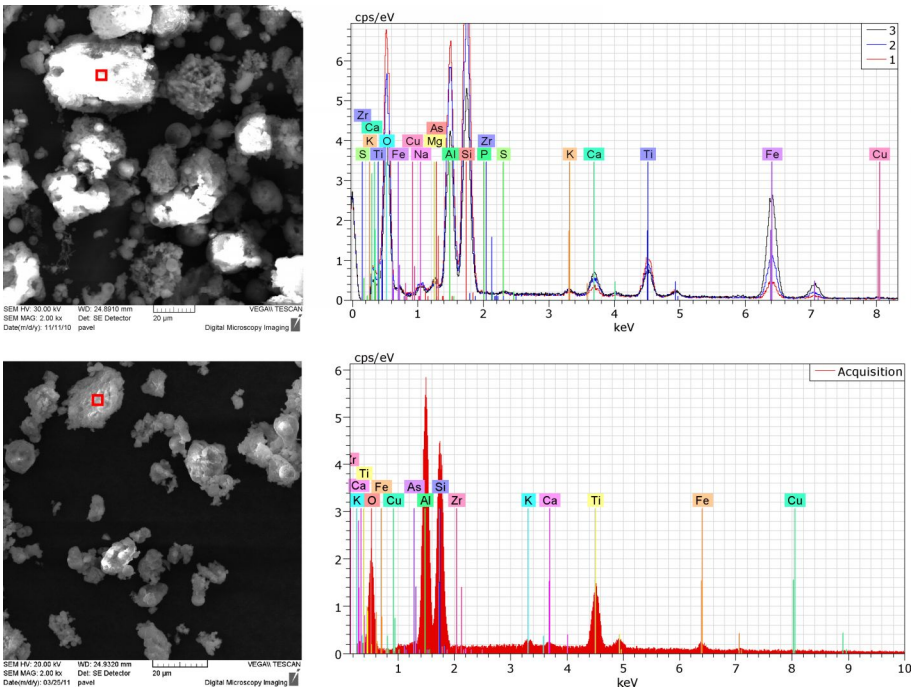


**Fig. 3B** SEM photographs and corresponding energy spectrum of fly ash K1 before (above) and after heating at 1000 $^{o}$C (under)

## K3

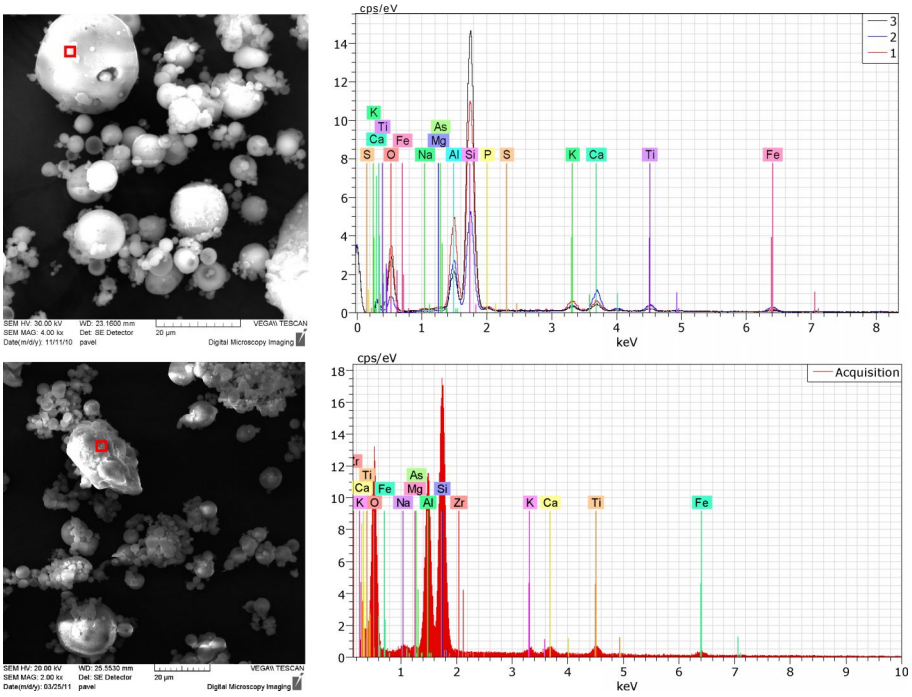


**Fig. 4B** SEM photographs and corresponding energy spectrum of fly ash K3 before (above) and after heating at 1000 $^{o}$C (under)

## K6

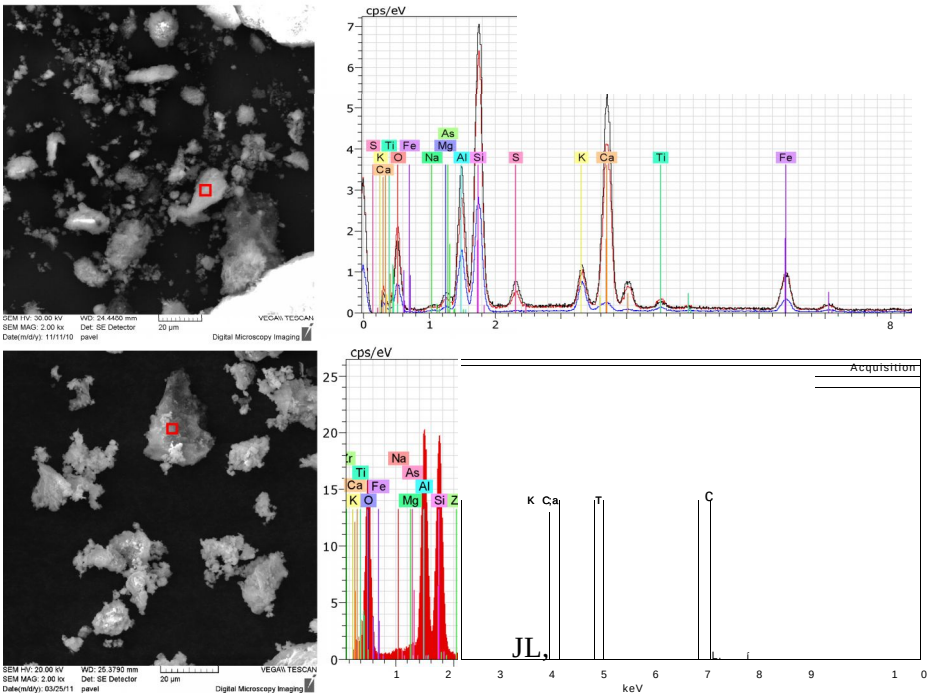


**Fig. 5B** SEM photographs and corresponding energy spectrum of fly ash K6 before (above) and after heating at 1000 $^{o}$C (under)

## K6 LF

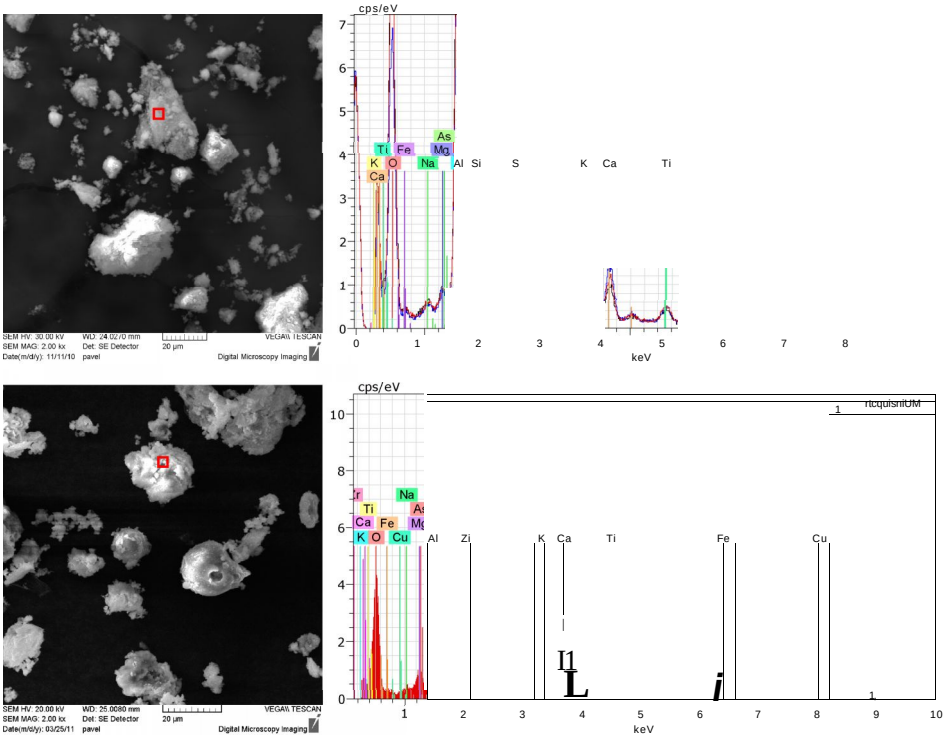


**Fig. 6B** SEM photographs and corresponding energy spectrum of fly ash K6_LF before (above) and after heating at 1000 $^{o}$C (under)

# APPENDIX D

**Table 1D** Impact strength of geopolymer mortar

| Mix No | Number | h [mm] | b [mm] | kpm | J | mJ | h*b [mm] | $mJ/mm^2$ | $mJ/cm^2$ | Average $mJ/cm^2$ | Standard deviation |
|---|---|---|---|---|---|---|---|---|---|---|---|
| MLF'-1 | 1 | 10.9 | 10.3 | 0.0081 | 0.07943 | 79.4339 | 112.27 | 0.708 | 70.75 | 67.14 | 5.11 |
| | 2 | 10.7 | 10.1 | 0.007 | 0.06865 | 68.6466 | 108.07 | 0.635 | 63.52 | | |
| MLF'-2 | 1 | 10.4 | 9.8 | 0.0068 | 0.06669 | 66.6852 | 101.92 | 0.654 | 65.43 | 62.87 | 3.62 |
| | 2 | 11.4 | 9.7 | 0.0068 | 0.06669 | 66.6852 | 110.58 | 0.603 | 60.30 | | |
| MLF'-3 | 2 | 11.45 | 9.4 | 0.0056 | 0.05492 | 54.9172 | 107.63 | 0.510 | 51.02 | 53.59 | 3.62 |
| | 3 | 11 | 9.05 | 0.0057 | 0.0559 | 55.8979 | 99.55 | 0.562 | 56.15 | | |
| MLF'-4 | 1 | 10.8 | 9.58 | 0.005 | 0.04903 | 49.0333 | 103.464 | 0.474 | 47.39 | 49.04 | 2.34 |
| | 2 | 10.4 | 9.3 | 0.005 | 0.04903 | 49.0333 | 96.72 | 0.507 | 50.70 | | |
| MLF'-5 | 1 | 10.3 | 9.9 | 0.0048 | 0.04707 | 47.0719 | 101.97 | 0.462 | 46.16 | 46.67 | 0.72 |
| | 2 | 10.7 | 10.1 | 0.0052 | 0.05099 | 50.9946 | 108.07 | 0.472 | 47.19 | | |
| MLF'-6 | 1 | 11.2 | 10.3 | 0.0067 | 0.0657 | 65.7046 | 115.36 | 0.570 | 56.96 | 51.67 | 5.00 |
| | 2 | 11.3 | 9.9 | 0.0062 | 0.0608 | 60.8012 | 111.87 | 0.543 | 54.35 | | |
| | 3 | 10.85 | 9.5 | 0.0048 | 0.04707 | 47.0719 | 103.08 | 0.457 | 45.67 | | |
| | 4 | 11.55 | 9.91 | 0.0058 | 0.05688 | 56.8786 | 114.46 | 0.497 | 49.69 | | |
| MLF'-7 | 1 | 11.1 | 9.9 | 0.0058 | 0.05688 | 56.8786 | 109.89 | 0.518 | 51.76 | 55.25 | 4.84 |

| | | | | | | | | | | | |
|---|---|---|---|---|---|---|---|---|---|---|---|
| | 2 | 10 | 9.9 | 0.0058 | 0.05688 | 56.8786 | 99 | 0.575 | 57.45 | | |
| | 3 | 10.75 | 8.97 | 0.006 | 0.05884 | 58.8399 | 96.43 | 0.610 | 61.02 | | |
| | 4 | 11.35 | 9.36 | 0.0055 | 0.05394 | 53.9366 | 106.24 | 0.508 | 50.77 | | |
| | 1 | 10.4 | 10.1 | 0.0064 | 0.06276 | 62.7626 | 105.04 | 0.598 | 59.75 | | |
| A/ÍT "Cl O | 2 | 11.7 | 10.3 | 0.0068 | 0.06669 | 66.6852 | 120.51 | 0.553 | 55.34 | 57.92 | 3.26 |
| | 3 | 11.75 | 8.95 | 0.0059 | 0.05786 | 57.8592 | 105.16 | 0.550 | 55.02 | | |
| | 4 | 10.85 | 8.66 | 0.0059 | 0.05786 | 57.8592 | 93.96 | 0.616 | 61.58 | | |
| | 1 | 11.4 | 9.9 | 0.0062 | 0.0608 | 60.8012 | 112.86 | 0.539 | 53.87 | | |
| A/ÍT "Cl Q | 2 | 10.7 | 10.4 | 0.0061 | 0.05982 | 59.8206 | 111.28 | 0.538 | 53.76 | 55.16 | 5.79 |
| | 3 | 11.36 | 9.56 | 0.0055 | 0.05394 | 53.9366 | 108.60 | 0.497 | 49.66 | | |
| | 4 | 11.15 | 10 | 0.0072 | 0.07061 | 70.6079 | 111.5 | 0.633 | 63.33 | | |
| | 1 | 11.1 | 10.2 | 0.0058 | 0.05688 | 56.8786 | 113.22 | 0.502 | 50.24 | | |
| A/TT TH ' 1 n | 3 | 10.9 | 9.8 | 0.005 | 0.04903 | 49.0333 | 106.82 | 0.459 | 45.90 | 48.38 | 4.61 |
| | 4 | 10.75 | 9.65 | 0.0057 | 0.0559 | 55.8979 | 103.738 | 0.539 | 53.88 | | |
| | 5 | 10.74 | 10.08 | 0.0048 | 0.04707 | 47.0719 | 108.259 | 0.435 | 43.48 | | |

**TECHNICKÁ UNIVERZITA V LIBEREC**

**FAKULTA STROJNÍ**

KATEDRA MATERIÁLU

# DISERTAČNÍ PRÁCE

**Ing. Nguyen Thang Xiem**

# POTENCIÁLNÍ VYUŽITÍ GEOPOLYMERNÍCH MATERIALŮ V OBLASTI ZPRACOVÁNÍ ODPADŮ

# THE POTENTIAL APPLICATIONS OF GEOPOLYMER MATERIALS IN WASTE PROCESSING

**ŠKOLITEL: Prof. Ing. Petr Louda, CSc.**

**Liberec, 2011**

Disertační práce byla vypracována v rámci doktorandského studia na Technické univerzitě v Libereci, Fakultě strojní, Katedře materiálu.

Doktorand: Ing. Nguyen Thang Xiem

Školitel: Prof. Ing. Petr Louda, CSc.

Vedoucí katedry: Prof. Ing. Petr Louda, CSc.

Oponenti:

Teze disertační práce byly rozeslány dne

Obhajoba disertační práce se koná dne……před komisí pro obhajoby disertačních prací v oboru strojírenské technologie Fakulty strojní TU v Libereci, v zasedací místnosti č……., v……hodin.

S disertační prací je možné se seznámit na děkanátě Fakulty strojní, TU v Libereci.

ISBN

# TABLE OF CONTENTS

# ABSTRACT

In this research, geopolymer resin was synthesized from shale fly dust burnt in rotary kiln (for 10 hours at 750 $^{o}$C) with Si/Al molar ratio of 2.0 with sodium hydroxide (NaOH) and sodium silicate ($Na_2SiO_3$). The purpose of this research is observing the influence of adding different types of fly ash, fibers in order to obtain the engineering properties (including compressive strength, impact energy, splitting tensile strength, flexural strength and modulus of elasticity) of geopolymer mortar and concrete. Some values of these material properties are not independent but affect each other, and therefore a method for determining the input material properties is developed based on a previous experiment. The optimal curing conditions (both at elevated temperature and at ambient conditions) and different curing time are investigated. In addition, preliminary study about the machinability of geopolymer material on the traditional machine are carried out and ability applications in industry.

# PŘEDMLUVA

V tomto výzkumu byla geopolymerní pryskyřice syntetizována břidličným popílkem z rotační pece (na 10 hodin při 750 °C) s Si/Al o molárním poměru 2,0 s hydroxidem sodným (NaOH) a křemičitanem sodným ($Na_2SiO_3$). Cílem tohoto výzkumu je sledování vlivu různých druhů přidaných popílků a vláken za účelem získání lepších mechanických vlastností (včetně pevnosti v tlaku, v tahu, v ohybu, rázové energie a modulu pružnosti) Geo malty a betonu. Některé hodnoty těchto vlastností nejsou nezávislé a vzájemně se ovlivňují. Proto metoda pro stanovení vlastností vstupního materiálu je založena na základě předchozího experimentu. Byly zkoumány optimální vytvrzovací podmínky (jak při zvýšené teplotě tak za normálních podmínek). Kromě toho je předběžně studována i obrobitelnost geopolymerních materiálů prováděná na tradičních strojích, a možná aplikace v průmyslu.

Today, each one of us and especially factories are generated large quantities of waste materials per day, such as: water, oils, solvents and solid waste (fly ash, glass, stone powder, mine tailings, etc). As a result, solid waste management has become one of the major environmental concerns in the world. Utilization of these materials not only help in getting them utilized in cement, mortar, concrete, and other building materials, it also helps in reducing the cost of manufacturing a product, and also has numerous indirect benefits such as saving in energy, and significantly reducing the emission of green - house gas $CO_2$ released from cement and concrete manufacturing. This is beneficial for resource conservation, environmental protection and ecological damages caused by quarrying and exploitation of the raw materials for making cement [1, 2].

Recently, geopolymers have emerged as a promising new material with environmentally sustainable properties [3-5]. They are a new material for coatings and adhesives, a new binder for fiber composites, and new cement for concrete [6-8]. Geopolymer cements are a class of inorganic polymers formed by the reaction between an alkali-activated and an aluminosilicate source [7]. These materials have a structure that gives geopolymers properties which make them an ideal substitute for Ordinary Portland Cement (OPC) in a whole range of applications. Geopolymers possess many advantages comparing with OPC as the following:

- Abundant raw materials resources [9].
- Energy saving and environment protection: geopolymers do not require large energy consumption. Thermal processing of natural aluminosilicates at relative low temperature (600° to 800°) provides suitable geopolymeric raw materials, resulting in 3/5 less energy assumption than OPC. And as we all know that the manufacture of OPC releases large amount of $CO_2$ to the atmosphere, because the process chemical reaction creates CO2 from the calcinations of limestone (calcium carbonate) at very high temperatures (about 1450 °C) and silica according to the reaction:

  $$5CaCO3 + 2SiO_2 \wedge (3CaO, SiO_2) + (2CaO, SiO_2) + 5CO_2 \quad (1)$$

  The production of one ton of OPC emits approximately one ton of CO2 to the atmosphere [7, 9].
- Simple preparation technique: Geopolymer can be synthesized simply by mixing aluminosilicate reactive with alkaline solutions, then curing at room temperature [9].
- Excellent heavy metal immobilization [10, 11].
- High fire resistant (up to 1000 $^oC$) and high temperature stability, low shrinkage and low thermal conductivity [2, 8, 12, 13].
- Good volume stability, good acid resistance and salt solutions [2, 8, 14].
- Ultra-excellent durability and high compressive strength [2, 8, 9, 15].
- Quick solidification with high strength, high surface definition that replicates mould patterns [8, 15, 16].

Davidovits described four basic forms of silicoaluminate structures corresponding to Si:Al ratios of 1, 2, 3 and greater than 3 as poly(sialate), poly(sialate-siloxo), poly(sialate-disiloxo), and poly(sialate-multisiloxo) [7, 16]. In our study, recommended application of geopolymer cements were synthesized shale fly dust from rotary kiln. And the purpose of this thesis is research about the effect of adding fly ash and other waste materials on mechanical properties of geopolymer mortar and concrete.

## 2 Aims of the research

The present study dealt with the manufacture and structural applications of reinforced fly ash based geopolymer mortar and concrete. The aims of this study were:

- Analysis microstructure and chemical composition of pure geopolymer and fly ash.
- Mechanical properties of geopolymer mortar after modified fly ash particles by high temperature and milling.
- The optimum the percent values by mass of fly ash content in geopolymer mortar and concrete.
- The effect of curing different time and condition on mechanical properties of geopolymer mortar and concrete.
- The effect of high temperature on mechanical properties of geopolymer mortar and concrete.
- The effect of commercial fibers reinforced on the mechanical properties of geopolymer mortar.
- The effect of water and/or alkaline solution to liquids/fly ash ratio in geopolymer mortar and concrete.
- Durability/resistance to degradation: Acid sulfuric attack, freeze-thaw resistance, wet-dry. And effect of chemical reagent on the mechanical properties of pure geopolymer, mortar and concrete.
- The machinability of geopolymer mortar on the traditional machine.
- Ability applications in industry.

## 3. Geopolymer terminology

This section presents a brief literature review of geopolymer terminology and chemistry.

In 1979, the term "geopolymer" was first discovered to the chemical world by a French professor Joseph Davidovits [16], they are inorganic polymeric materials with a chemical composition similar to natural zeolite but containing an amorphous microstructure and possessing ceramic-like in their structures and properties [7, 17-19]. Geopolymer are synthesized and hardened at ambient pressure and temperature, so the science can produce artificial stone at a temperature below 100 $^{o}$C [20, 21]. This material (geopolymer cement) evolved into a mineral-based binder for use as a high strength industrial cement with significantly shorter cure times than OPC [7]. There are two main constituents of geopolymers, namely the source materials and the alkaline liquids. The source materials for geopolymers based on alumina-silicate should be rich in silicon (Si) and aluminium (Al) such as metakaolinite, slag, geological, blast furnace slag, fly ash, rice husk ash, etc. The choice of the source materials for making geopolymers depends on factors such as availability, cost, type of application, and specific demand of the end users. The most common alkaline liquid used in geopolymerization is a combination of sodium hydroxide (NaOH) or potassium hydroxide (KOH) and sodium silicate ($Na_2SiO_3$) or potassium silicate ($K_2SiO_3$) [22, 23].

To discuss the chemical structure of geopolymers, the term 'sialate' is an abbreviation for silicon-oxo-aluminate and is used here to describe the bonding of silicon and aluminium by bridging oxygen. And the term poly(sialate) was suggested as a descriptor of silico-aluminate structure of the type of material [7, 17, 24]. The amorphous to semi-crystalline three dimensional of sialate network consists of $SiO_4$ and $AlO_4$ tetrahedral which are linked alternately by sharing all the oxygens to create basic polymeric Si-O-Al bonds (see in Fig. 2.1) [7, 17], so Prof. Davidovits called it geopolymer. To balance the negative charge of $Al^{3+}$

in IV fold coordination, positive ions sodium (Na+), potassium (K+), lithium (Li+), calcium ($Ca^{2+}$), barium ($Ba^{2}$+), ammonium ($NH_4$ ), hydronium ($H_3O$ ) must be present in the structural spaces [7].

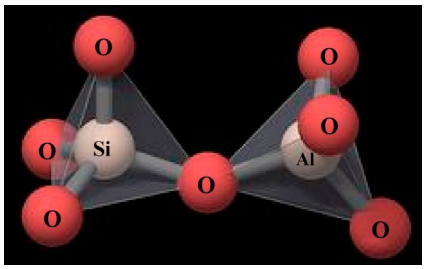


**Fig. 1** Tetrahedral configuration of sialate Si-O-Al-O; Si, Al atoms in white and O atoms in pink [7, 25]

Poly(sialates) are described by the following empirical formula [7, 16, 17, 26, 27]:

$$Mn[-(SiO2)z-AlO2]n.\ WH2O\ , \qquad (2)$$

where M is a monovalent cation such as potassium (K+) or sodium (Na+) , n is the degree of polycondensation and z is either 1, 2, 3 or >> 3. Poly(sialate) are described as chain and ring polymers with $Si^{4}$+ and $Al^{3}$+ in IV-fold coordination with oxygen and range in from amorphous to semi-crystalline.

Davidovits has also distinguished four types of polysialates according to the ratio Si:Al they are of the types:

| | | | |
|---|---|---|---|
| Poly(sialate): | Mn - (- Si-O-Al-O-)n | M-PS | Si:Al=1:1 |
| Poly(sialate-siloxo) | Mn - (-Si-O-Al-O-Si-O-)n | M-PSS | Si:Al=2:1 |
| Poly(sialate-disiloxo) | Mn - (-Si-O-Al-O-Si-O-Si-O-)n | M-PSDS | Si:Al=3:1 |

Poly(sialate-multisiloxo), Si:Al >> 3:1, the polymeric structure results from the cross linking of poly(silicate) chains, sheets or networks with a sialate link (-Si-O-Al-O-) (2D or 3D cross-link).

## 4. Experimental methods

### 4.1 Geopolymer resin

Each mixture geopolymer resin contained only ground aluminosilicate fly dust as the powder binder (Fig. 2) and combination $Na_2SO_3$ solution with NaOH solution to produce alkaline silicate solution with modulus 1.50. The ratio of $H_2O/Na_2O$ used for was 12. Pure geopolymer samples (Fig. 3) for mechanical properties tests, SEM and EDX were prepared with mass ratio of activator/powder equal to 4:5.

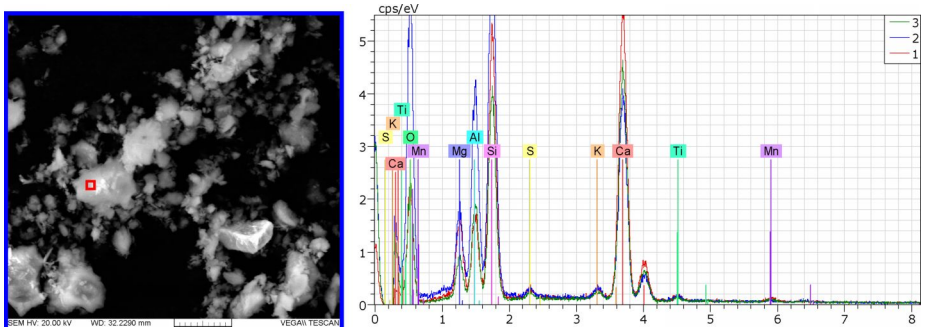


**Fig. 2** SEM image and EDX of geopolymer cement

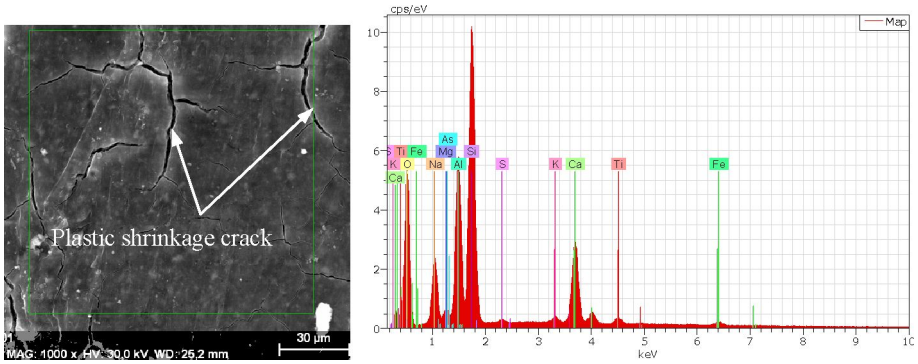


**Fig. 3** SEM and EDX of geopolymer matrix

Aggregates were currently used by the local concrete industry in Czech Republic. Coarse aggregates were obtained in crushed form; majority of the particles were of gravel-type with the size particles ranging from 4.0 to 8.0 mm. The fine sand was obtained from the sand dunes in uncrushed form and particles range in diameter from 0.063 mm to 2.0 mm. All aggregates were in saturated surface dry condition.

### 4.2 Fabrication of the geopolymer mortar - concrete

Several series of samples were prepared to test the influential variables on the compressive strength of hardened geopolymer. The variables include modulus and content of the mixed alkali activator and the sample curing conditions. The technology of sample preparation is as follows. At first, the geopolymer resin was prepared by mixing the alkaline activator with the raw materials. The liquid and solid components were mixed about 5 minutes at room temperature until the solution homogenized. Next, the geopolymer resin mixture was mixed with different fly ash and aggregates (coarse and/or fine) content. The mixing was done in an air conditioned room at approximately 23 $^{o}$C ± 2 $^{o}$C until the well homogenized mixture (about 5 minutes). Directly after mixing, the fresh mortar and concrete was poured in the plastic moulds and vibrated for 2 minutes on the vibration table to remove air voids. Specimens were covered with a plastic bag for 24 hrs after casting. Compressive strength testing of mortar was performed as per AS 1012.9 using (046 x 92) mm diameter cylindrical moulds. ASTM C39 was conducted for compressive strength tests of hardened concrete, using (0100 x 200) mm cylinder moulds. Three cylinders of each sample were tested, with the experimental values being averaged. Testing of the flexural strength indices of the specimens was conducted on (40 x 40 x 160) mm samples in accordance to ASTM C348 - 08.

There are two ways to curing these samples:

(i) These samples were cured at room temperature for 3 days after casting. Next, the samples were removed from the moulds and left in laboratory ambient conditions until the day of test. The sample ages for the latter tests were 7, 14, and 28 days.

(ii) All the mixtures were cured in an oven without delay time at the specific curing temperature for 24 hr and 48 hr ranging from 60 $^{o}$C ^ 90 $^{o}$C. Samples were demoulded after the curing process in the oven and continued curing ambient condition for 2 days.

### 4.3 Testing

#### *4.3.1 Test slump*

The slump test is performed on newly mixed geopolymer concrete. The slump of the concrete is checked in accordance with Test Method for Slump of Hydraulic-Cement Concrete - C143/C143M [28].

#### *4.3.2 Test flexural strength*

The authors are used the Standard Test Method for Flexural Strength of Concrete (Using Simple Beam with Third-Point Loading) - ASTM C78/C78M - 10 and the Standard Test

Method for Flexural Strength of Hydraulic-Cement Mortars - ASTM C348 - 08. These methods are used to determine of the flexural strength of concrete and hydraulic cement mortar by the use of a simple beam with third-point loading [29, 30].

#### *4.3.2 Test compressive strength*

The samples are cured and tested in accordance with the Standard Practice for Making and Curing Concrete Test Specimens in the Field - ASTM C 31/C 31M - 03a and the Methods of testing concrete - Determination of the compressive strength of concrete specimens - AS 1012.9 - 1999 [31, 32]. Values are the averages of four separate tests. Data that deviated more than 10 % were eliminated.

#### *4.3.3 Charpy impact testing*

According to the standard specimen size for Charpy impact testing in the Standard Test Methods and Definitions for Mechanical Testing of Steel Products - ASTM A370 - 07a is (10 x 10 x 55) mm [33] and the Standard Test Method for Low Strain Impact Integrity Testing of Deep Foundations - ASTM D5882 - 07 [34].

#### *4.3.6 Microstructure of geopolymer samples*

In this study, the authors are used a scanning electron microscope (SEM) and Energy Dispersive X-ray Analysis (EDX) on TESCAN VEGA 3XM microscope to analysis the structure and chemical compositions of particles, geopolymer resin, fibers. Examination of the geopolymer material was made on the SEM with the dispersive radiation spectrometer at the maximum magnification of 2500x, using the secondary electron detection, and the Esprit 1.8 software, using 30 kV acceleration voltages.

In addition, geopolymer mortar and concrete are also investigated about the adhesion between geo matrix and particle on optical microscope NIKON EPIPHOT 200 (macroscopic observation) and used the software NIS Elements to take pictures.

#### *4.3.7 Environmental chamber*

The authors are used the environmental test chamber to test the effects of moisture (relative humidity) conditions on geopolymer mortar, concrete and a slightly effect on the mechanical properties and structure of geopolymer materials. The cycles are stopped after 28 days curing (about 120 cycles).

#### *4.3.8 Hardness testing*

MH 180 Portable Leeb Hardness Tester used to measure the hardness of geopolymer mortar. This equipment can test any angle, even upside down. The hardness scales are convertable among hardness units: HRB (Rockwell Hardness B Scale), HRC (Rockwell Hardness C Scale), HV (Vicker), HB (Brinell), HS (Shore), HL (Leeb).

#### *4.3.9 Planetary ball mill*

Planetary ball mill of Fritsch Pulverisette 7 is used to making particles from micro to nano size. The comminution takes place primarily through the high-energy impact of grinding balls. To achieve this, the grinding bowl, containing the material to be ground and grinding balls, rotates around its own axis on a main disk rotating in the opposite direction. At a certain speed, the centrifugal force causes the ground sample material and grinding balls to bounce off the inner wall of the grinding bowl, cross the bowl diagonally at an extremely high speed, and impact on the material to be ground on the opposite wall of the bowl.

#### *4.3.10 Types of moulds*

(i) ASTM C 470/C 470M was conducted for compressive strength tests of hardened concrete, using (0100 x 200) mm cylinder plastic moulds.

(ii) Compressive strength testing of geo mortar was performed as per AS 1012.9 using (046 x 92) mm diameter cylindrical plastic moulds.

(iii) Testing of the flexural strength indices of the specimens were conducted on (40 x 40 x 160) mm samples in accordance to ASTM C78/C78M - 10 and ASTM C348 - 08.

### 4.4 Calculation methods

#### *4.4.1 Compressive strength*

Compressive tests were performed according of the European Standard EN 12390-3: 2009. Three samples of each formulation were tested and the average data were reported. The loading was displacement-controlled at a constant rate of 2.4 mm/min for all the tests.

The compressive strength of mortar ($f_{cm}$) was calculated using equation:

$$f_{cm} \quad F \tag{3}$$

Where:

$f_{cm}$ is compressive strength, MPa;
$F_{max}$ is the maximum applied load indicated by the testing machine, N;
$A_c$ is the original cross-sectional area of a specimen in a compression test, $mm^2$

At least two cylinders are test at the same age and the average strength is reported as the test result to the nearest 0.1 MPa.

#### *4.4.2 Flexural strength*

The flexural strength is expressed as Modulus of Rupture in MPa and is determined by standard test method ASTM C 293 (Using Simple Beam with Center Point Loading) and AASHO T17. The flexural strength was calculated from this test, the flexural strength was calculated using:

$$= \frac{3F}{T} \quad T \tag{4}$$

Where:

$R_{mo}$ is the flexural strength, MPa;

$F_{max}$ is the maximum applied load indicated by the testing machine, N;

b is the average width of specimen, mm;

h is the average depth of specimen, mm;

L is span length, mm.

#### *4.4.3 Modulus of elasticity of geopolymer concrete*

Hardjito et al.[35]:

$$E_c = 2\,7\,0\,7\,f + 5300 \tag{5}$$

The prediction of the modulus of elasticity by Equation (5) is close to the test results and this equation is used to calculate the modulus of elasticity of geopolymer concrete, presented in this study.

#### *4.4.4 Indirect tensile strength*

The splitting tensile strength ($f_{ct}$) of the IPC mixes was experimentally measured following the procedure prescribed by AS 1012.10. The values of splitting tensile strength of geopolymer concrete depend on the basis of their correlation to compressive strength ($f_{cm}$).

There is an agreement on the increasing of splitting tensile strength with the increase in compressive strength of geopolymer concrete.

The modulus of splitting tensile strength of geopolymer concrete was calculated using equation [40]:

$$f_{ct} = 0.4 f \quad , \text{MPa} \tag{6}$$

Where: the value of compressive strength of concrete from 10 MPa to 65 MPa are applied.

## 5. Results and discussion

### 5.1 Effect of the different types of fly ash

Fly ashes used in this study came from different sources in Czech Republic. The fly ashes were already classified into 6 names of city and coded such as: K1 (Kotel 1 Plzeň), K3 (Kotel 3 Plzeň), K6 (Komořany), K6_LF (Komořany Látkový Filtr), PRT (Pražská Teplárenská), OPE (Elna Opatovice). They have many different color brown, light grey to black due to its chemical compositions and contaminants. The SEM images (Figs. 4 ^ 9) present the original fly ash of a series of different sizes particles. All fly ash particles are generally sharp, pointed, and spherical in shape. SEM show that the OPE and PRT fly ashes are finer than other kinds and K6 fly ash has the very coarse particles in all fly ashes.

*(i) Fly ash K1*

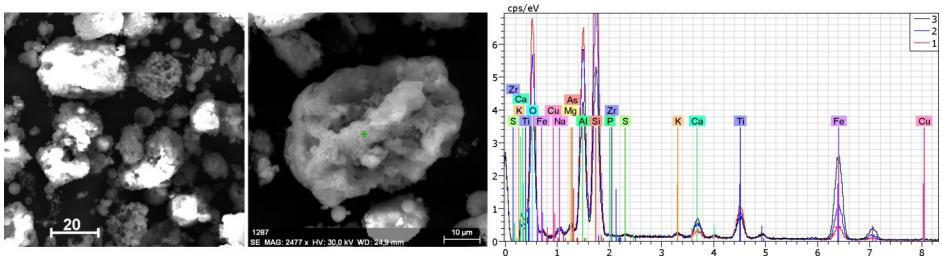


**Fig. 4** SEM photographs and corresponding energy spectrum of fly ash K1

*(ii) Fly ash K3*

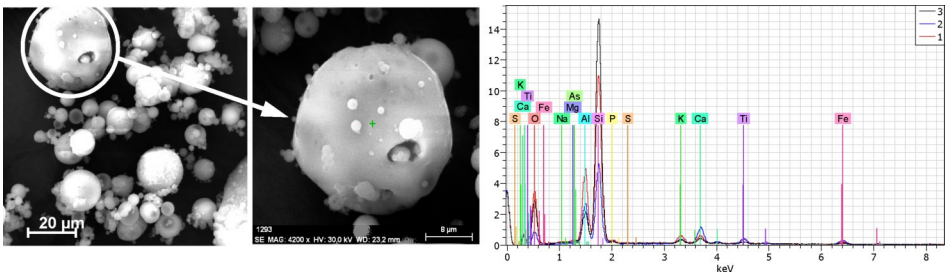


**Fig. 5** SEM photographs and corresponding energy spectrum of fly ash K3

(iii) Fly ash K6

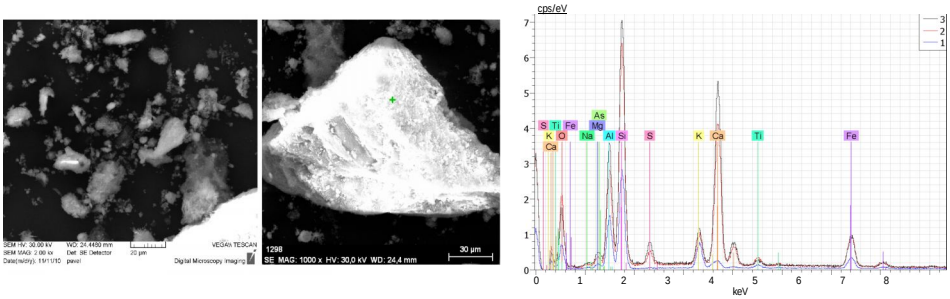


**Fig. 6** SEM photographs and corresponding energy spectrum of fly ash K6

*(iv) Fly ash K6LF*

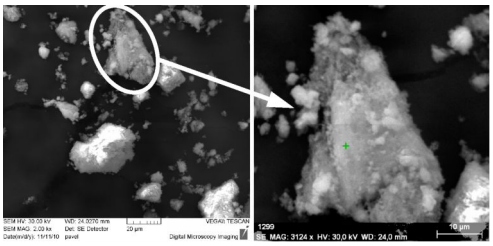

**Fig. 7** SEM photographs and corresponding energy spectrum of fly ash K6_LF

*(v) Fly ash OPE*

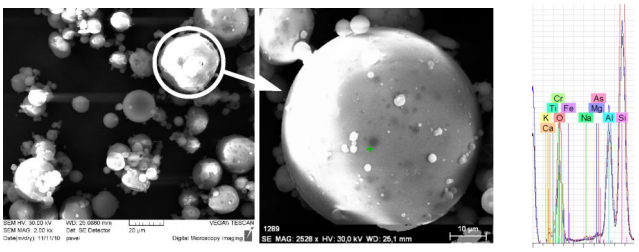

**Fig. 8** SEM photographs and corresponding energy spectrum of fly ash OPE

*(vi) Fly ash PRT*

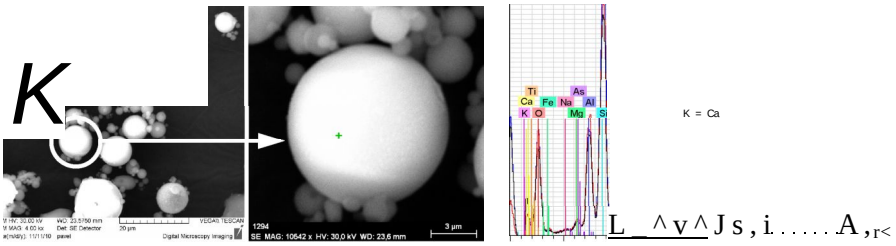

**Fig. 9** SEM photographs and corresponding energy spectrum of fly ash PRT

The experimental shows that geopolymer mortar are prepared with 10 ^ 30 wt% of fly ash exhibited acceptable flowability while more than 40 wt% fly ash containing mortars were stiff and difficult to pack into the plastic moulds. In this section, the mixtures were mixed with extra water.

Geopolymer mortars with varying levels of fly ash were prepared and their mechanical properties studied. The linear regressions of compressive strength value of geopolymer mortar are exhibited on Fig. 10.

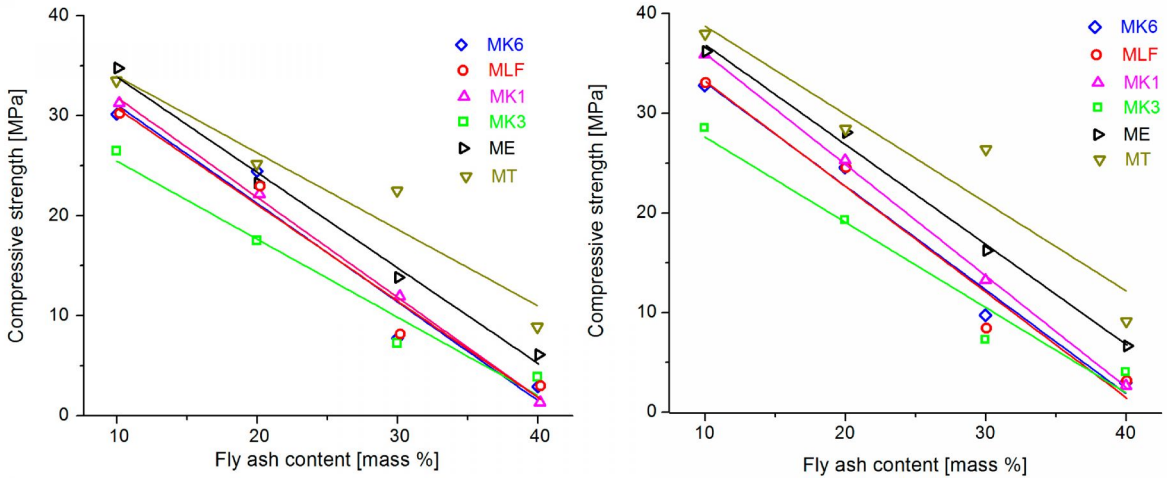


**Fig. 10** Compressive strength of geopolymer mortar samples after curing in the oven at 70 $^{o}$C for 24 hrs (left) and 48 hrs (right)

The results indicate that compressive strength of mortar is a strong relationship between types of fly ash, particle size, and percentage of fly ash in the mixtures. When comparing the compressive strength values of geopolymer mortars which obtained the same percentage fly ash content and curing conditions it can be seen that fly ash PRT in the ratio of 10, 20, 30, and 40% after curing at 70 $^{o}$C for 24 hrs and 48 hrs gives the higher compressive strength and the hardness than mortars produced with other blended fly ash. It has lower particle size than other kinds of fly ash. This result is the same with other researches [41-44]. And the test results showed that, with increasing fly ash content causes a decrease in compressive strength of geopolymer mortar.

### 5.2 Effect of alkaline liquid and water

In OPC mortar and concrete, water in the mixture chemically reacts with the cement to produce a paste that binds the aggregates. In contrast, the water in fly ash-based geopolymer mortar and concrete mixtures does not cause a chemical reaction. Experience showed that water content in the geopolymer concrete mixture affected the properties of concrete in the fresh state as well as in the hardened state. Because the excess water in fresh mixtures which reduces the concentration of activator, the chemical reaction that occurs in geopolymers produces water that is eventually expelled from the binder, leads to a reduced geopolymerization reaction and thus lowers compressive strength.

In this section, authors were concerned about type of fly ash K6_LF. In order to investigate the effect of alkaline liquid and water content in the mixture, the mixtures were divided into two sets. In the first set, the mixtures were mixed with the same components in section 5.1 by extra water. And the second set presents the mixtures by adding alkaline and used code MLF'. The ratio of $H_2O/Na_2O$ and concentrations of NaOH liquid (in Molars) used for this study was 12 and 14 M, respectively.

Fig. 11 shows that water and/or alkaline solution has a significant effect on the compressive strength of geopolymer mortar. And the pictures show that increasing fly ash content can reduce the density of geopolymer mortar.

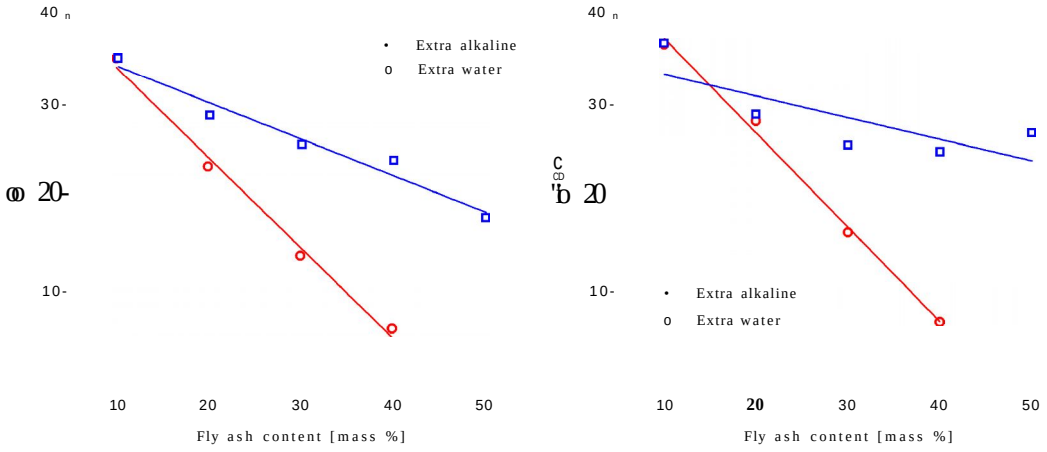


**Fig. 11** Compressive strength of fly ash OPE based geopolymer mortar after curing at 70 $^{o}$C for 24 hrs (left) and 48 hrs (right)

### 5.3 Effect of curing on the compressive strength of geopolyer mortar

Although fly ash based geopolymer mortar can be cured in ambient conditions, heat curing is generally recommended. Both curing time and curing temperature influence the compressive strength of geopolymer mortar and concrete. This section, fresh geopolymer mortar was mixed from 10 % fly ash (K6_LF, OPE, and PRT) together 90 % geopolymer resin.

### *5.3.1 Curing Time*

The curing time is illustrated in Fig. 12 left. The tests cylinders from mixtures MLF-1, ME-1 and MT-1 were heat cured at 70 $^{o}$C in a furnace and continued curing at ambient temperature for 2 days. The curing time varied from 5 hrs to 72 hrs. Longer curing time improved the polymerization process resulting in higher compressive strength. The rate of increase in strength was rapid up to 24 hrs of curing time.

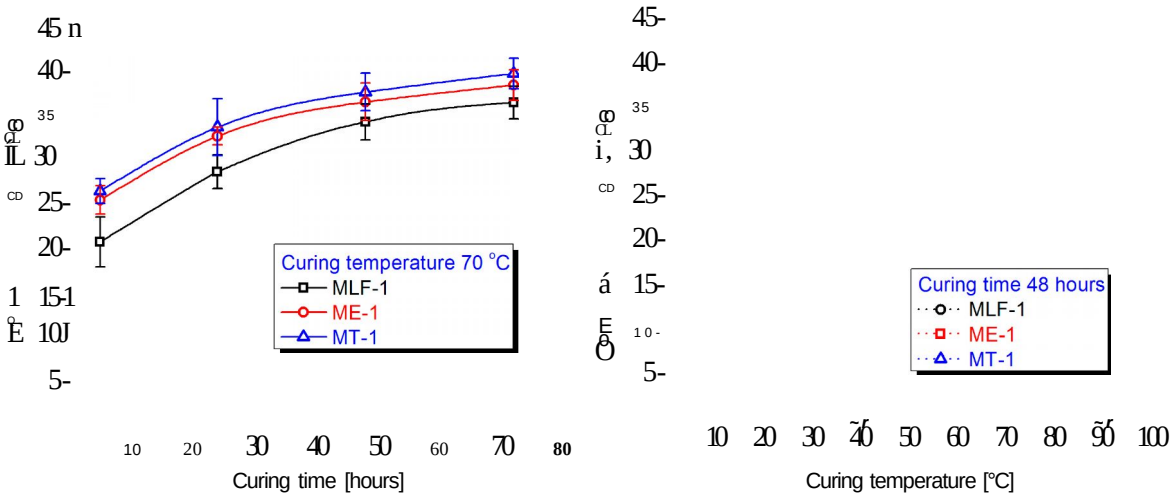


**Fig. 12** Effect of curing time (left) and curing temperature (right) on compression strength of geopolymer mortar

### *5.3.2 Curing temperature*

Fig. 12 right shows the effect of curing temperature on the compressive strength of geopolymer mortar. The tests cylinders from mixtures MLF-1, ME-1 and MT-1 were heat cured in a furnace for 48 hrs and continued curing at ambient temperature for 2 days. Higher curing temperature resulted in larger compressive strength, although an increase in the curing temperature beyond 70 $^{o}$C did not increase the compressive strength substantially. Based on these test trends, a curing temperature of about 70 $^{o}$C is recommended.

## 5.4 Effects of modified fly ash particles by wet milling and high temperature on the properties of geopolymer mortar

### *5.4.1 Wet milling*

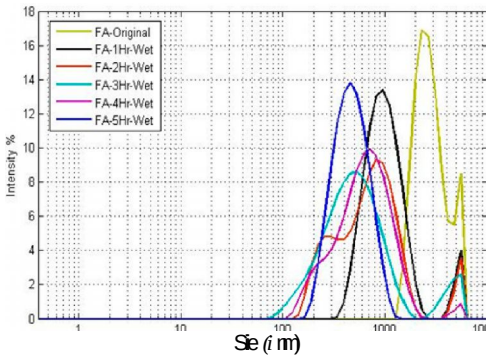


(a) Unmilled and milled fly ash

Fly ash was mechanically activated through particle size refinement from micro to nano scale by milling 1 hr to 5 hr in wet conditions. The milled fly ash was then mixed with geopolymer resin in water dispersion form and in the form of dried particles after evaporation of water. Fig. 13a shows the particle size distribution curves of the unmilled and fly ashes milled for different time 1, 2, 3, 4 and 5 hr. The rate of particle size reduction was greatest during the initial 1hr of milling during which the characteristic particle diameter Z-average reduced from

3547 nm to 989 nm .The particle size gradually decreased with milling time and reached to 493 nm after 5 hrs of wet milling as shown in Figs. 13b and 13c. This shows that the main influence of the mechanical activation of fly ash is to decrease particle size rather than change mineralogical content.

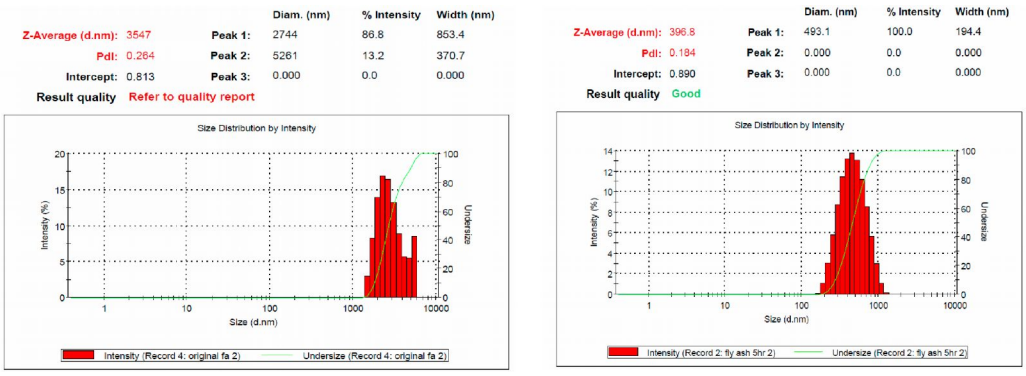


(b) Unmilled fly ash (c) Milled fly ash after 5 hr

**Fig. 13** Particle size distributions of unmilled and milled fly ash

Fig. 14 shows SEM image of unmilled and milled fly ash particles.

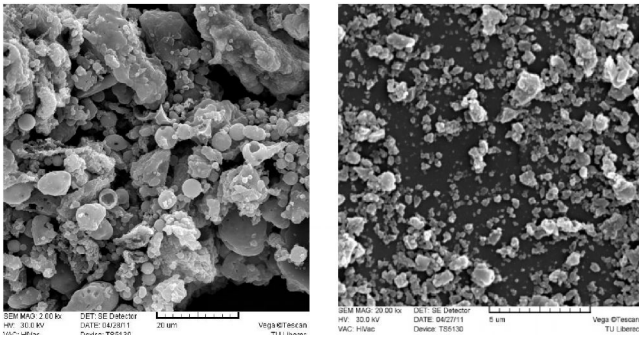

Unmilled original fly ash Milled fly ash

**Fig. 14** SEM image of unmilled and milled fly ash

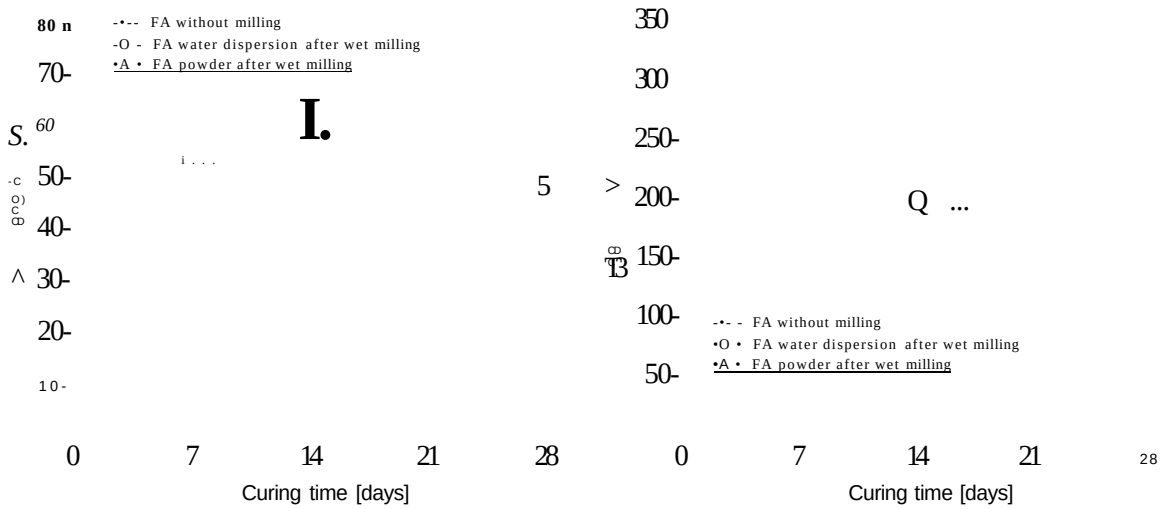


**Fig. 15** Effect of mechanical activation of fly ash on the compression strength (left) and the hardness (right) of geopolymer mortar

Fig. 15 left shows significant improvement in compression strength of geopolymers made from wet milled fly ash which was dried before mixing with geopolymer resin as compared to unmilled fly ash. One of the reasons for improved compressive strength in mechanically activated fly ash mixtures is the high rate of geopolymerization in the sample. Mechanical activation increases the reactivity of the fly ash causing faster dissolution of the fly ash and

rapid setting. Fast setting is the result of improved dissolution of the fly ash into alkaline liquid; leading to improved polymerization and hardening of the gel phase and thus developing compact structure within the geopolymer.

### *5.4.2 Influence of modified fly ash particles by heating*

The purpose of this research is whitening the fly ash to compete with other filler materials. And compared the influence of adding fly ash before and after modified by high temperature in order to obtain the compressive strength and the local hardness of geopolymer mortar is investigated. Experimental results show that high temperature are effective methods to purify fly ash, high whiteness of the particle which increased with the calcination temperature and slightly reduced the local hardness of geopolymer mortar.

Fig. 16 shows the photographs and SEM of fly ash before and after heating at 1000 $^{o}$C. After heating at high temperature, fly ash particles may suffer sever degradation, pitting, buckling, and breakage, which all can eventually regression the mechanical property of matrix. The obvious color difference can be observed by a naked eye.

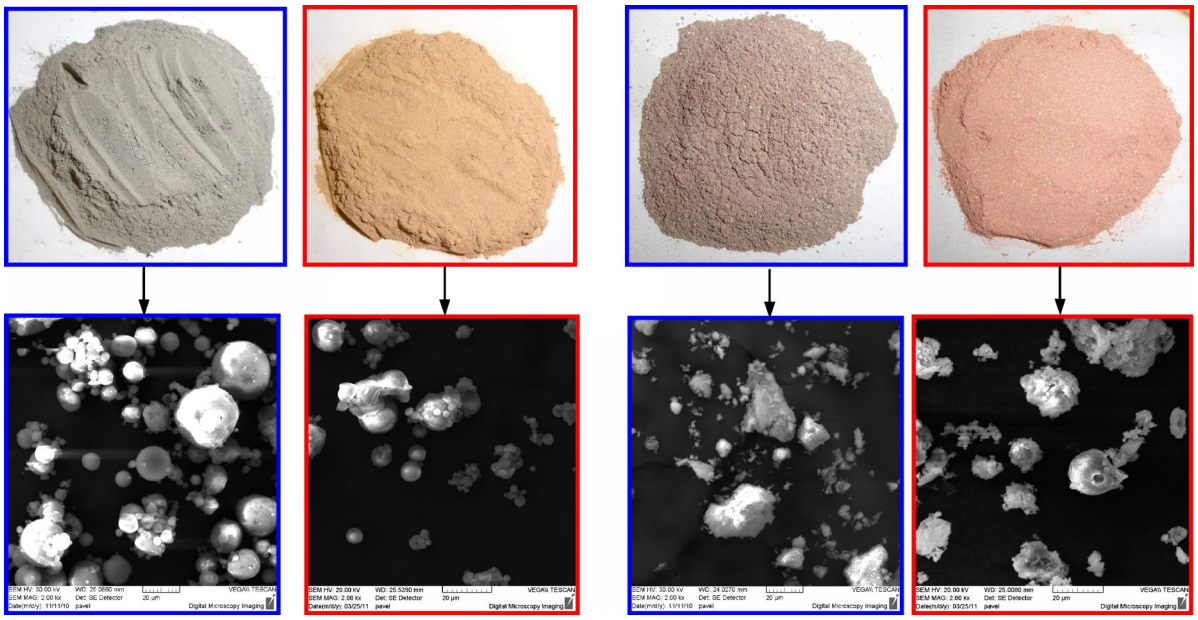

**Fig. 16** The photograph and SEM of OPE and K6_LF before (grey) and after heating at 1000$^{o}$C (brown)

In Figs. 17 and 18 present the photomacrographs of geopolymer mortar based on 40 % fly ash OPE, K6_LF before and after modified particles by heating at 1000 $^{o}$C.

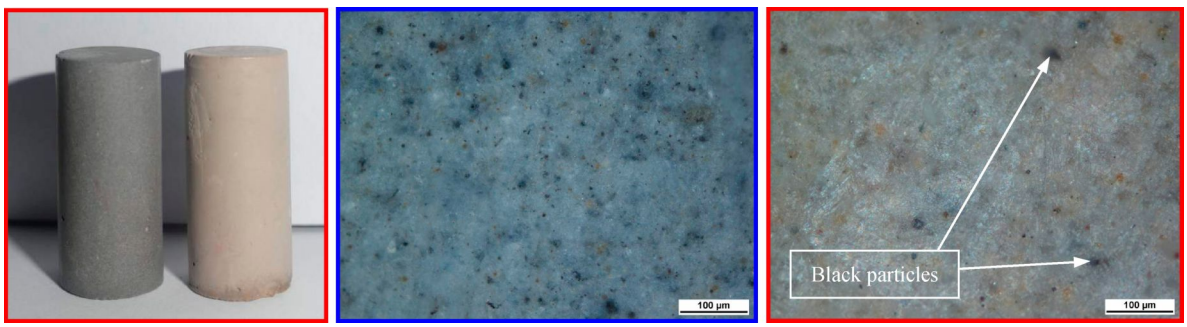


**Fig. 17** Photomacrographs geopolymer mortar based on fly ash OPE before (left) and after heating at 1000 $^{o}$C (right)

In the photomacrographs indicate that the color of geopolymer mortar after heating at 1000 $^{o}$C is brighter than unmodified powder. Because after heating the fly ash at 1000 $^{o}$C removed unburnt carbon from black particles.

Compressive strength [MPa]
Curing 7 days
Curing 14 days
Curing 28 days


Flexural strength [MPa]

Compressive strength [MPa]

Hardness [HV]

**8** Photomacrographs geopolymer mortar based on fly ash K6_LF before (left) and after heating at 1000 °C (right)

Fig. 20 presents linear regression of a fictitious compressive strength and a fictitious flexural strength against ratio of FA / GC. This figure shows that mechanical properties of geopolymer mortar, compressive and flexural strength, are dependent on the ratio of FA / GC which decreasing strength is associated with increasing the ratio of FA / GC.

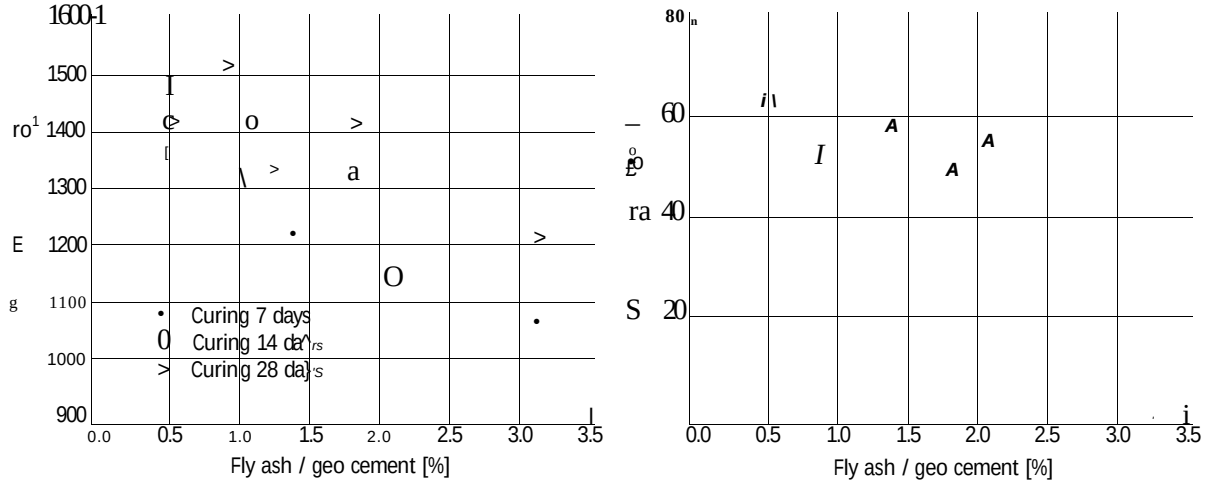


**Fig. 21** Modulus of elasticity (left) and Impact strength (right) of geopolymer mortar

The impact strength test was performed taking average three samples from each mixture after curing 28 days. The results of tests are plotted as Fig. 21. Impact strength and Modulus of elasticity increased with the reducing the ratio FA / GC. And it can be seen that increasing in curing time from 7 to 28 days is increases the elastic modulus.

### *5.5.2 Geopolymer concrete*

The results show that samples cured in the laboratory ambient were measured after 7, 14, 28, and 90 days. After 28 days value of strength is higher than value after curing 7 days presented in Fig. 22. For strength development in time is for cured samples at room temperature typical long time period to reach the final physical-mechanical characteristics. Therefore was measurement focused on compressive strengths after 7, 14, 28 and 90 days, however the results of samples cured at room temperature from 28 days to 90 days was lightly increased or remained unaltered.

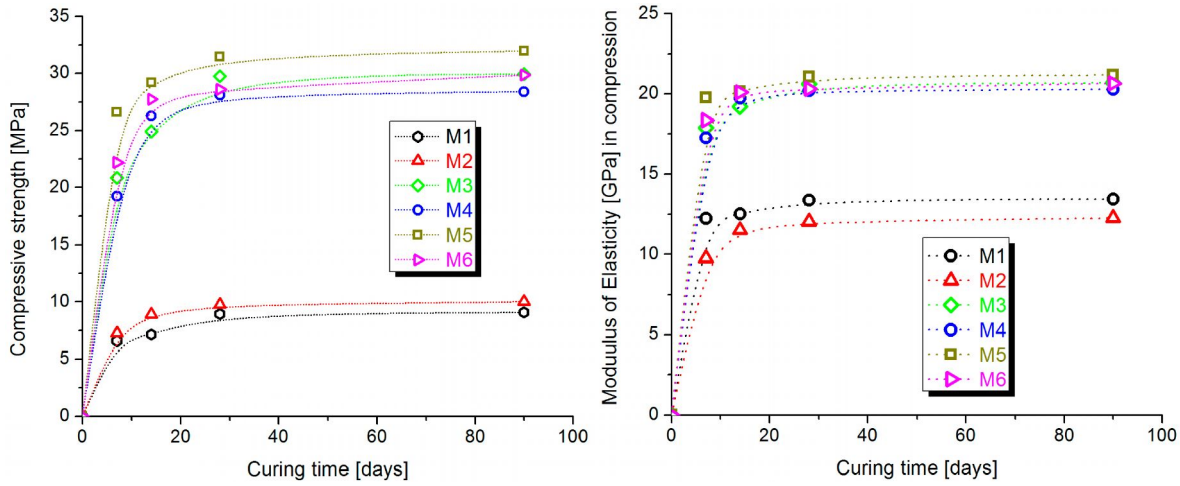


**Fig. 22** Compressive strength (left) and Modulus of elasticity (right) of geopolymer mortar

From the Fig. 22, it can be seen that the above mentioned results of mixtures M1 and M2 is smaller than other mixtures, because of added water in these mixtures to investigate the effect of water on the mechanical properties of geopolymer concrete.

The slump test was chosen to measure the workability of the fresh state concrete. Slump test is useful in detecting the variations in the uniformity of a concrete mixture [47]. Slump values increased as the content of water or alkaline liquid in the mixtures increased, it is one of major effect on the compressive strength of geopolymer concrete.

Fig. 22 shows that the results of the compressive strength of mixture M5 is higher than other mixtures, after 90 days curing at room temperature the mixture M5 present the compressive strength approximately 32 MPa and elastic modulus about 21 GPa.

Table 1 shows that the flexural strength of geopolymer concrete increases with age in the order of about 30 % from 7 days to 14 days and remained almost constant after that.

**Table 1** Flexural strength of geopolymer concrete M5 cured at room temperature

| Mixture | Flexural strength $R_{mo}$ [MPa] | | | Relative deformation [%] | | |
|---|---|---|---|---|---|---|
| | 7 days | 14 days | 28 days | 7 days | 14 days | 28 days |
| M5 | **4.80** ± 0.13 | **6.88** ± 0.98 | **7.09** ± 0.58 | 0.81 | 1.14 | 0.71 |

### 5.6 Effects of high temperature and environmental conditions on mechanical properties of geopolymer mortar and concrete

#### *5.6.1 Effect of high temperature*

Geopolymer mortars after heating from 200 °C to 1000 °C can see by a naked eye that branched cracks appear over the whole surface of the samples after heating up to 600 °C, which is causes the mechanical properties of geopolymer mortar and concrete significantly reduce after thermal exposure up to high temperature.

The weight loss, shrinkage and compressive strength of geopolymer mortar and concrete were determined during the experiment. It can see from Fig. 24 that the weight loss of mortar is increased about 20 % when the temperature up to 400 °C and remained up to 1000 °C, while concrete is also increased but smaller than mortar approximately 12 % at 1000 °C.

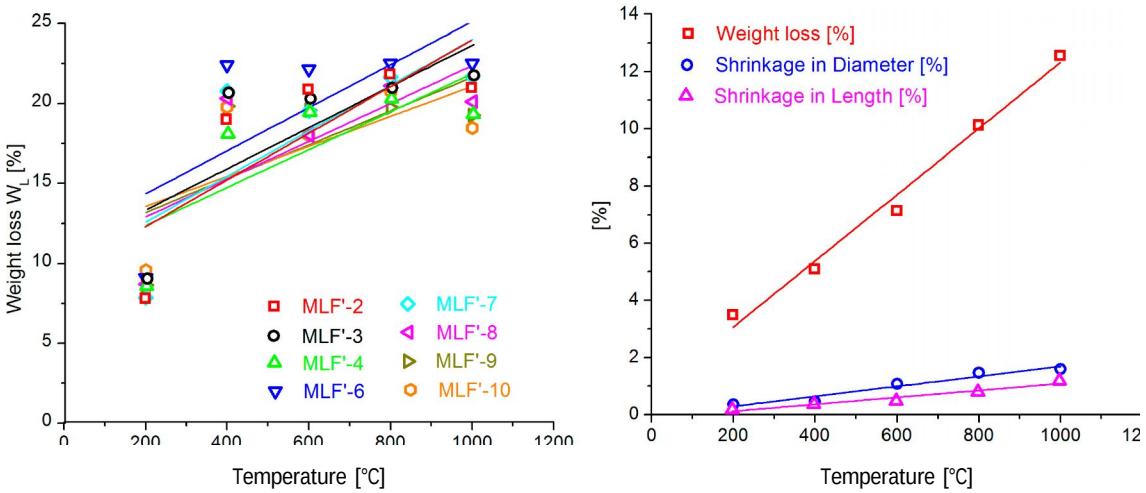


**Fig. 24** The weight loss of mortar (left), the weight loss and shrinkage of concrete (right) after heating from 200 °C to 1000 °C

Shrinkages in length and in diameter (Figs. 24 and 25) are the reduction in volume which is primarily caused by loss of water contained in the alkaline and burnt some particles on the surface of samples during the heating process. Percentage of shrinkage of samples was also depended about temperature and aggregates content. While the aggregate plays the important role in affecting shrinkage of concrete. Indeed, most aggregates restrain concrete shrinkage because they are less elastic than the cement paste to which they are bonded. Concretes with

higher aggregate contents shrink substantially less than cement-rich mixes all else being equal [48, 49].

Davidovits had given the concept that the smaller drying shrinkage strain of fly ash-based geopolymer concrete may be explained by the block polymerization. According to this concept, the Si and Al atoms in the fly ash are not entirely dissolved by the alkaline liquid. The polymerization that takes place only on the surface of the atoms is sufficient to form the blocks necessary to produce the geopolymer binder. Therefore, the insides of the atoms are not destroyed and remain stable, so that they can act as micro-aggregates in the system and this could increase the aggregate content in concrete [48, 50, 51]. The below Fig. 26 shows the shrinkage of fly ash geopolymer mortar after heated at 800 $^{o}$C.

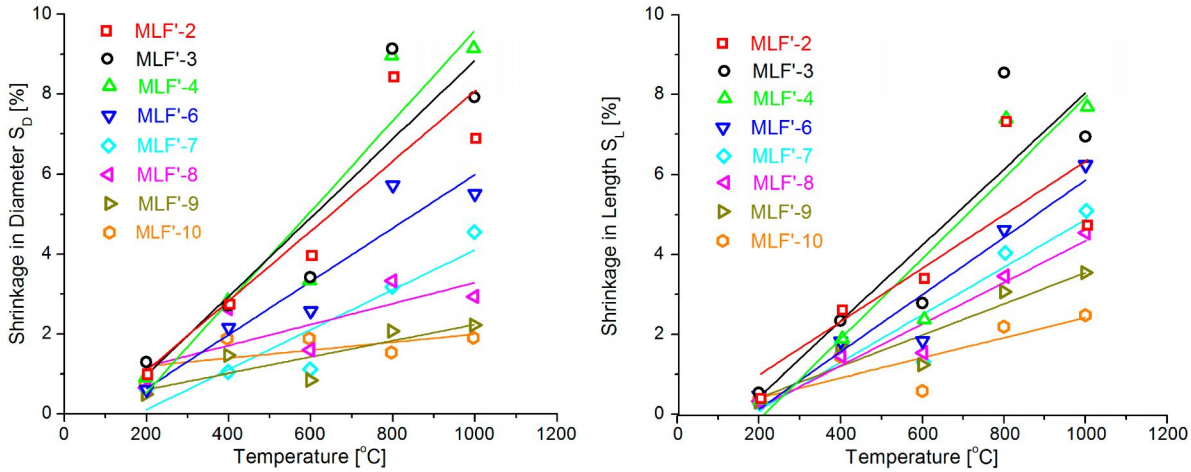


**Fig. 25** Shrinkage in Diameter (left) and in Length (right) of mortar at high temperature

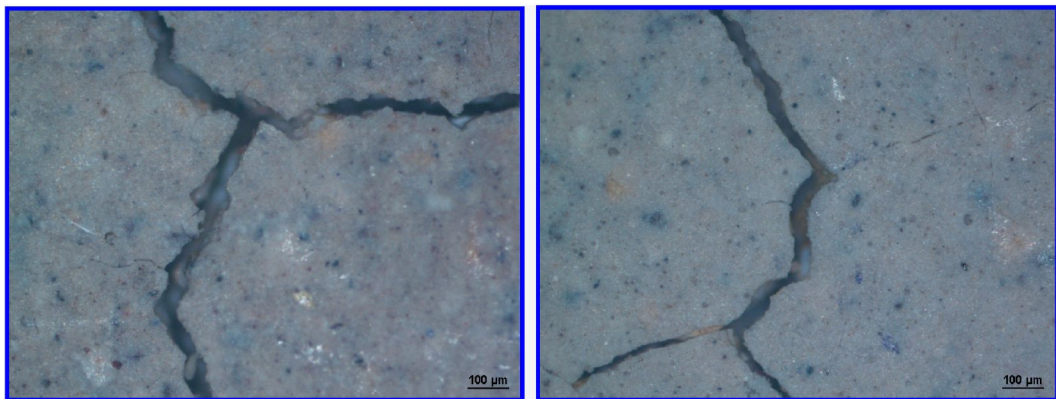


**Fig 26** Influence of sand on the shrinkage performance after heated at 800 $^{o}$C: 0 % (left) and 50 % (right)

Fly ash based geopolymer mortar and concrete can sustain when exposed to considerably high temperature. It can see from Fig. 27 that the highest compressive strength is obtained when the temperature is 200 $^{o}$C, but they exhibit a decreasing tendency afterwards. The strength starts dropping once temperature over 400 $^{o}$C and slightly reduces at higher temperatures. The lowest values of the residual strength were observed in the temperature range of 600 to 800 $^{o}$C; they were due to the presence of the melt that started forming. While OPC concrete degrades and degenerates at high temperature, it has been found from different study that fly ash geopolymer concrete can maintain its desired compressive strength even at 400 $^{o}$C [48], the residual strengths of the OPC concrete are very low, on the order a few MPa.

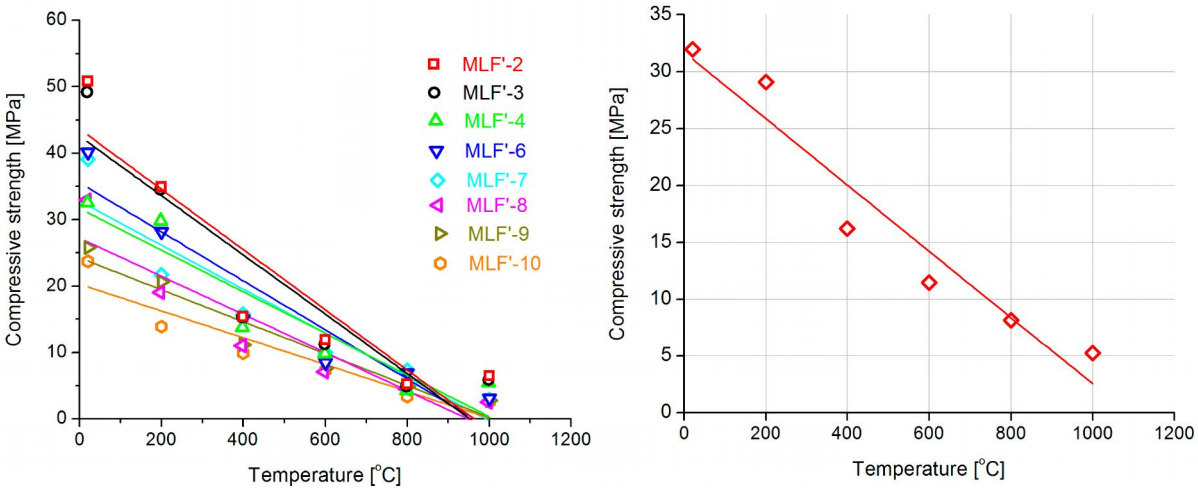


**Fig. 27** Influence of high temperature on the compressive strength of mortar (left) and concrete (right)

### *5.6.2 Effect of envirionmental conditions*

*(i) Freeze - Thaw / Wet - Dry test*

After freeze-thaw and wet-dry test were determined water absorption, weight loss, shrinkage and compressive strength of geopolymer mortar (Fig. 28). This figure presents the results of geopolymer mortar for 3 environments such as ambient conditions, freeze-thaw, and wet-dry.

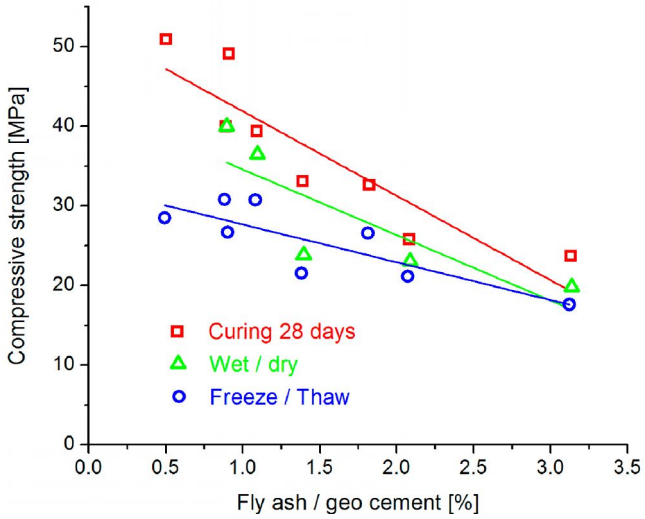


**Fig. 28** Compressive strength of geopolymer mortar after freeze/thaw and wet/dry cycle, comparison with initial strength at 28 days

*(ii) Acid resistance test*

Acid resistance test was conducted on geopolymer mortar. In this study, the specimens were soaked in sulfuric acid solution with selected concentrations ranging from 1% to 3% with the measured pH about 1.0. In each case, three samples were immersed in the sulfuric acid solutions until 28 days. The acid resistance of geopolymer mortar was then evaluated based on the change in compressive strength and the change in mass after acid exposure.

The concentration of $H_2SO_4$ solution was also significantly effect on the compressive strength of mortar, if increasing the concentration was reduced the strength and concomitant the weight loss of samples was also increased.

### 5.7 Effects of commercial fibers reinforced on the mechanical properties

The results of geopolymer mortar containing 0 %, 1 % Isover granulate and 2 % basalt fibers are shown in Figs. 29 and 30. The flexural strength of unreinforced and synthetic reinforced geopolymer mortar is compared. Commercial fibers reinforced geopolymer mortar has higher flexural strength than unreinforced mortar. The test results showed that optimum content of fibers (1 % for Isover and 2 % for short basalt fibers) results in ca the same flexural strength (6.95 and 6.91 MPa) after curing 28 days at room temperature. An increase in the flexural strength of ca 36 % for both fiber reinforcement is observed when compared with unreinforced geopolymer mortar.

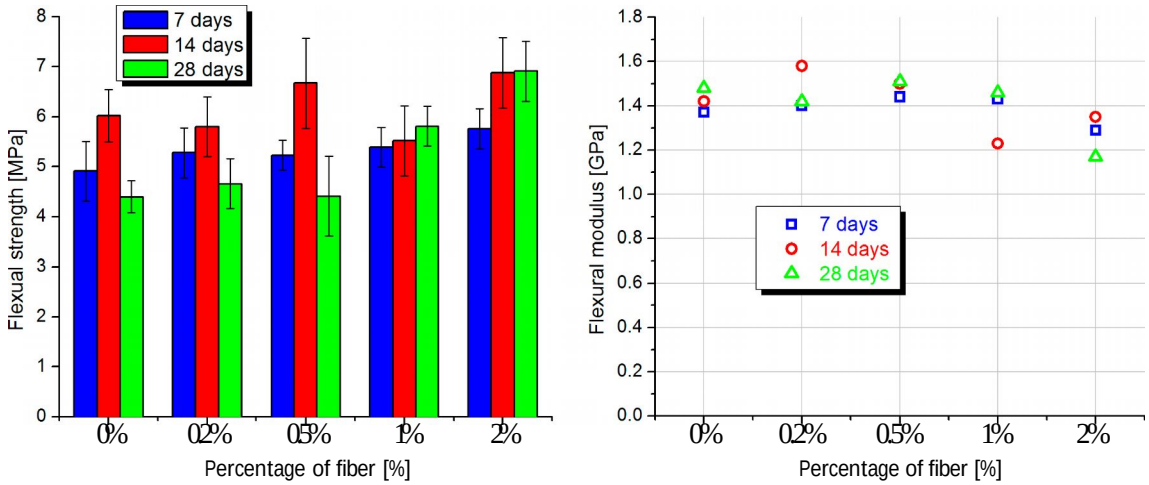


**Fig. 29**The flexural strength (left) and flexural modulus (right) of short basalt fiber reinforced geopolymer mortar

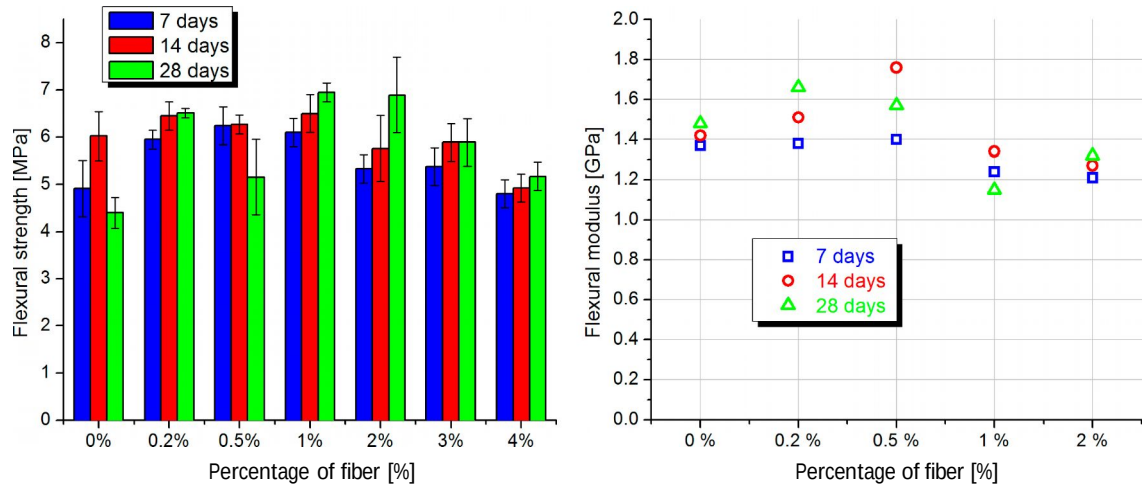


**Fig. 30** The flexural strength and flexural modulus of Isover granulate fiber reinforced geopolymer mortar

### 5.8 Machinability of geopolymer mortar

All samples had a cylindrical shape with a diameter $D_o$ = 120 mm and a length $l_o$ = 45 mm. We used 3 kinds of powder (fly ash K6_LF, stone and shale) as a filler to produce geopolymer mortar. Test specimens were made using geopolymer mortar from mixture MLF'-4 (40 % filler).

Figs. 31 ^ 33 illustrate the SEM image and EDX of a polished cross-section of the fly ash, stone powder and shale based geopolymer. The main components of fly ash geopolymer are $Al_2O_3$ and $SiO_2$. In this study, the mole ratio of Si to Al directly determines the molecular configuration types of the products type at Si/Al = 7, 10, 8 respectively fly ash, stone and

shale geopolymer. With this type geopolymer are obvious excellent fire-resistance and high bonding [7, 52]. Thus, the mole ratio of Si to Al is one very key parameter for the synthesis of geopolymer with fly ash, stone and shale powder.

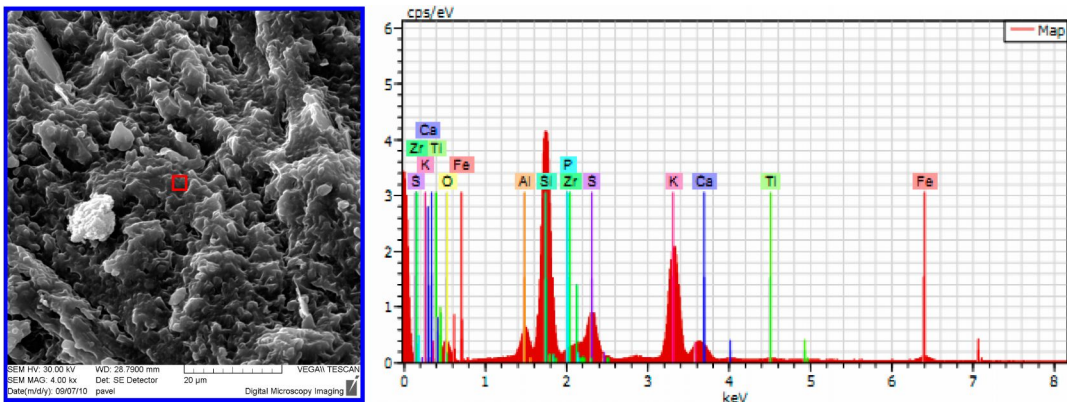


**Fig. 31** SEM image and EDX of fly ash geopolymer

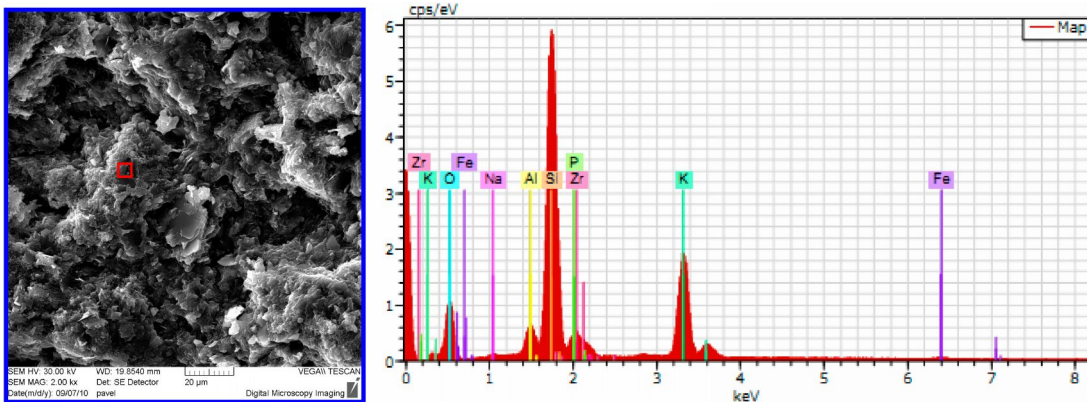


**Fig. 32** SEM image and EDX of stone geopolymer

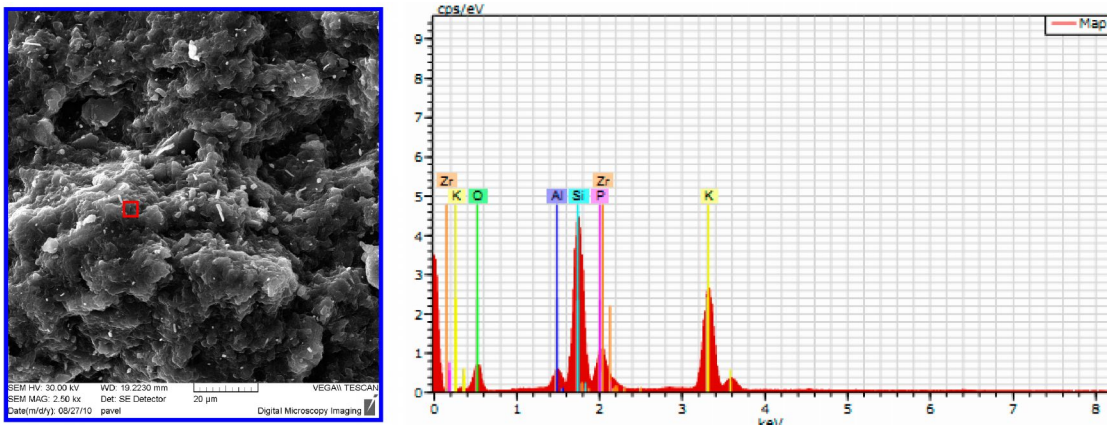


**Fig. 33** SEM image and EDX of shale geopolymer

Fig. 34 shows geopolymer mortar with fly ash filler is the best tool life under the same cutting conditions. Geopolymer mortar with stone and shale filler expresses very low durability. Geopolymer mortar with fly ash filler has 10 times higher durability than geopolymer mortar with stone and shale filler. Geopolymer mortar with stone and shale filler shows very abrasive effects. It was done only approximately measurements without repetition (experimental duration about 4 hours).

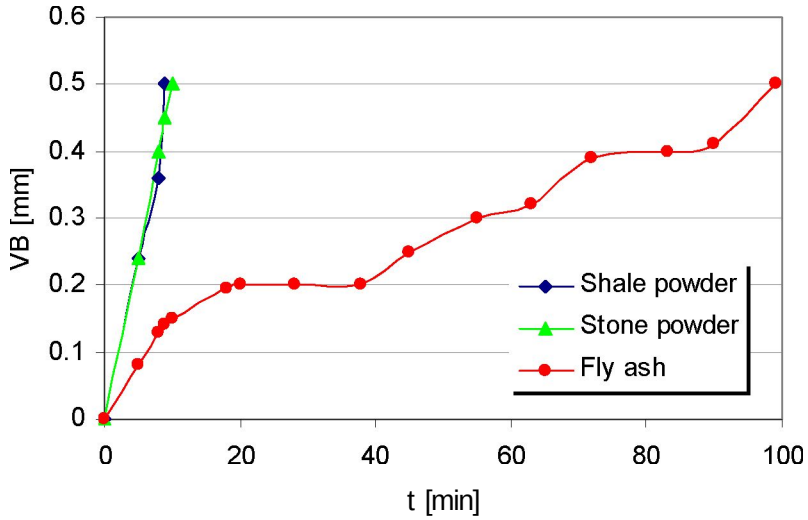


**Fig. 34** The time course of cutting edge wear

Fig. 35 shows that geopolymer mortar with shale filler need the largest cutting force during machining by drilling. Medium needed for cutting force of geopolymer mortar with stone filler. The smallest cutting force is the geopolymer mortar with fly ash filler. It was done only approximately measurements without repetition (experimental duration about 1 hour).

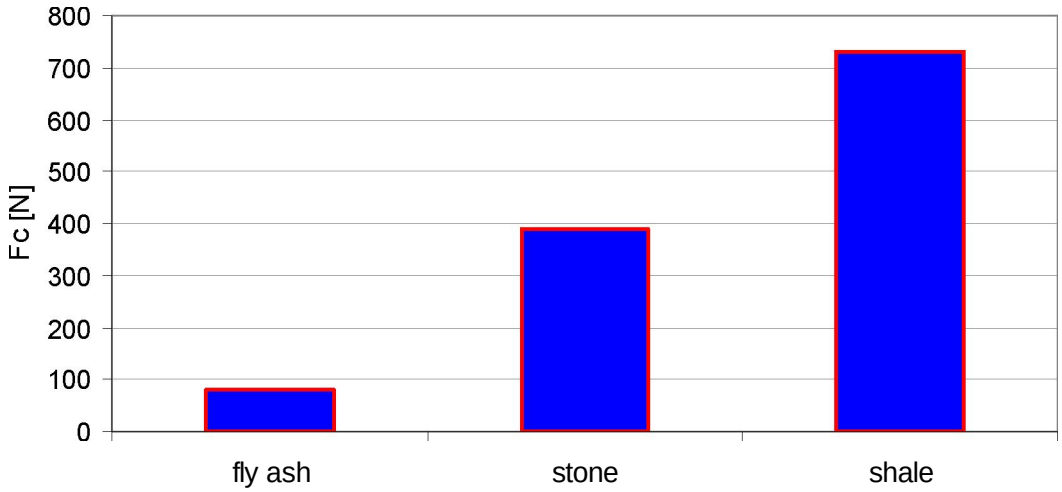


**Fig. 35** Comparison of cutting force Fc

Fig. 36 shows that increasing cutting speed is decreases tool life. This chart shows three lines of constant displacements, where the highest durability is with the constant shift of 0.025 mm.

Fig. 37 shows a very significantly effect of cutting speed on tool life, it is also clear that at high cutting speed ($v_c$ = 6.28 m-min"[1]) the change of the shift value has the minimal influence on the tool life. But the change of shift at low cutting speed ($v_c$ = 1,13 m-min"[1]) has far more significantly effect on tool life, thus with increasing value of shift with low cutting speed, tool life decreases rapidly.

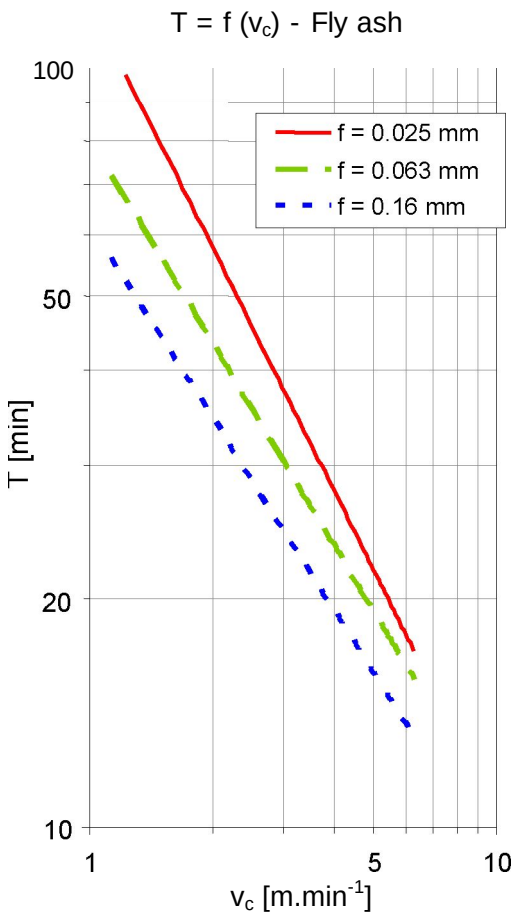


**Fig. 36** Dependence of durability for cutting speeds for three different shifts - geopolymer mortar with fly ash filler

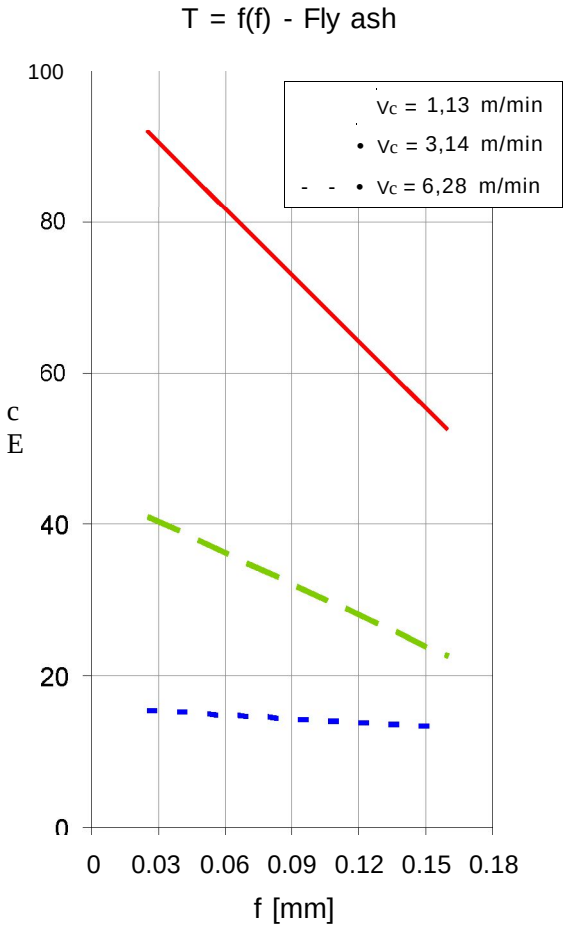


**Fig. 37** Dependence of durability for shift for three different cutting speeds - geopolymer mortar with fly ash filler

The effects of cutting speed and shift to the $F_c$ were assessed while experiments.

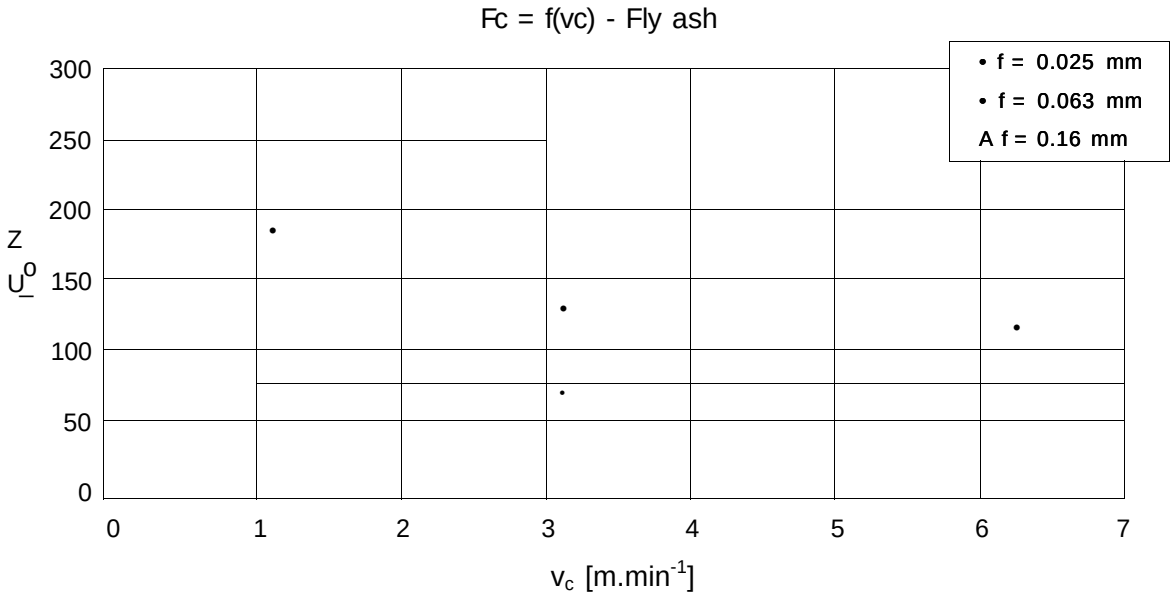


**Fig. 38** Dependence of cutting force on the cutting speed for three different shifts - geopolymer mortar with fly ash filler

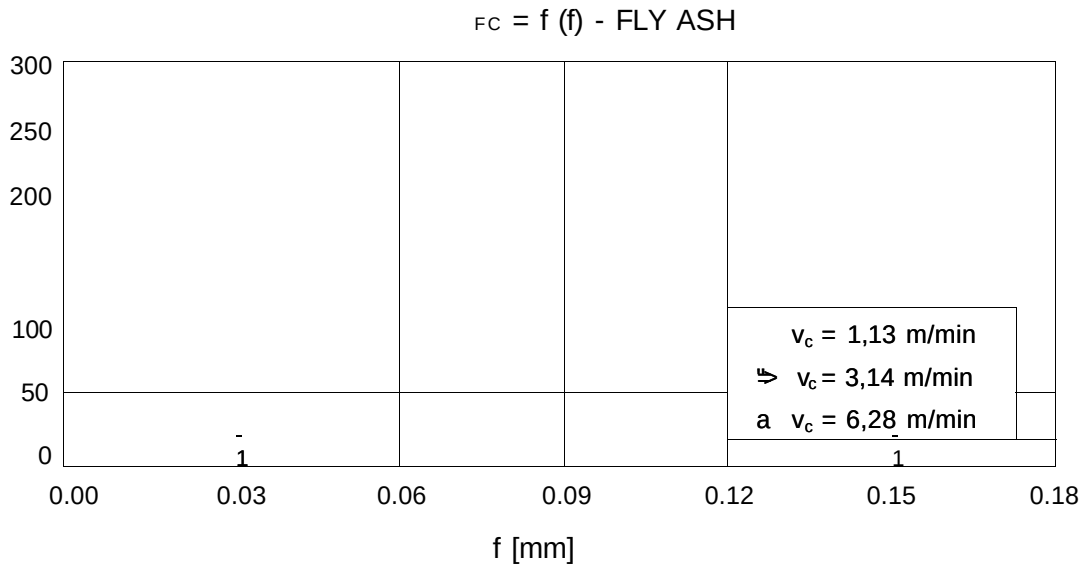


**Fig. 39** Dependence of cutting force on the shift for three different cutting speeds - geopolymer mortar with fly ash filler

Fig. 38 shows that increasing cutting speed gradually decreases the value of cutting forces. This is most pronounced in case of the line with constant shift f = 0.16 mm/turn and f = 0.063 mm/turn.

Fig. 39 shows that increasing shift increases the value of cutting forces. This progression is evident in all curves of constant cutting speeds.

### 5.9 Potential applications

The atomic ratio Si:Al in the poly(sialate) structure determines the properties and application fields. In my thesis, recommended application of geopolymer resin was synthesized shale fly dust from rotary kiln (for 10 hours at 750 $^{o}$C) with Si/Al molar ratio of 2.0 with sodium hydroxide (NaOH) and sodium silicate ($Na_2SiO_3$). From 2009 to present, we have been produced some productions that are made mainly from fly ash as following:

# Bricks, ceramic tiles, artificial stone

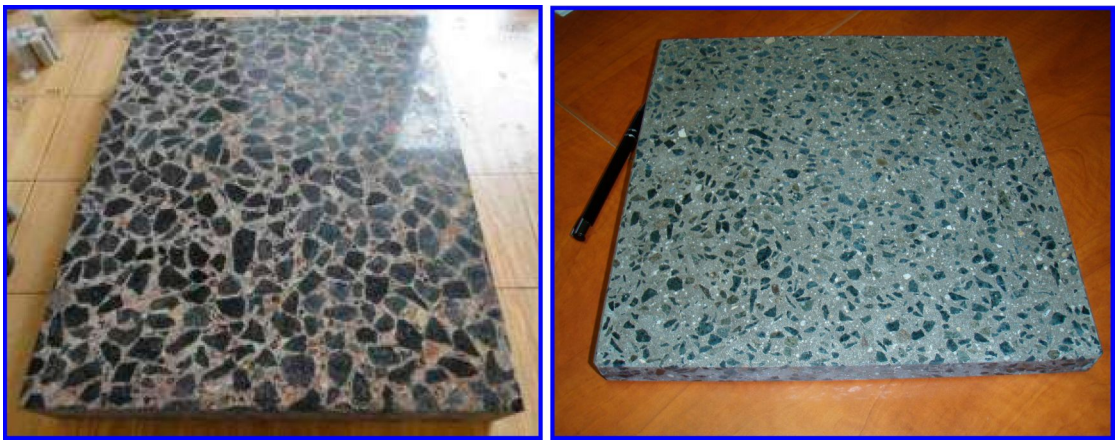

**Fig. 40** Artificial stone

# Backfilling the road and embankment


**Fig. 41** Backfilling the road by fly ash based geopolymer concrete in United Energy company

# We have been used pure geopolymer and fly ash based geopolymer mortar for fire resistant coatings for some materials, such as: polystyrene, wood, plastic, and concrete.

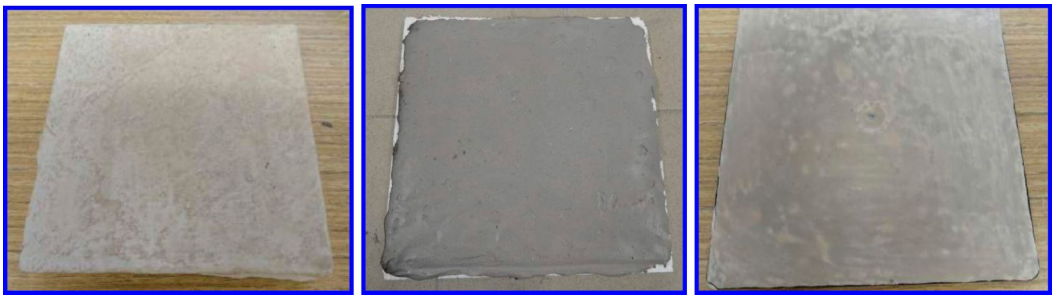

(a) (b) (c)

**Fig. 42** Polystyrene coated by pure geopolymer (a), geopolymer mortar (b) and plastic coated by pure geopolymer (c)

**Fig. 43** Portland concrete coated by pure geopolymer before (left) and after heated 600 $^{o}$C


**Fig. 44** The box (200 x 200 x 200) mm heated by flame up to 374 $^{o}$C

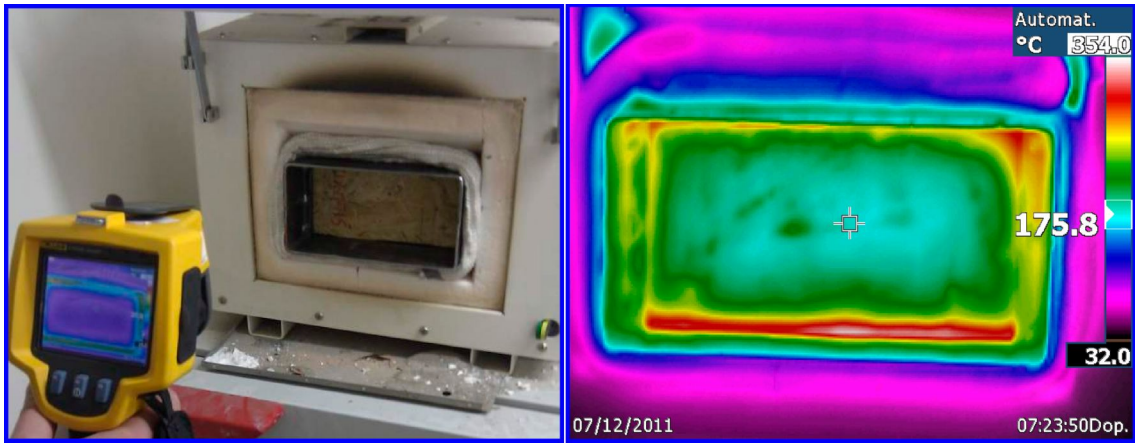


**Fig. 45** Wood coated by geopolymer mortar before (left) and after heated 354 $^{o}$C in the oven, outside only 175.8 $^{o}$C

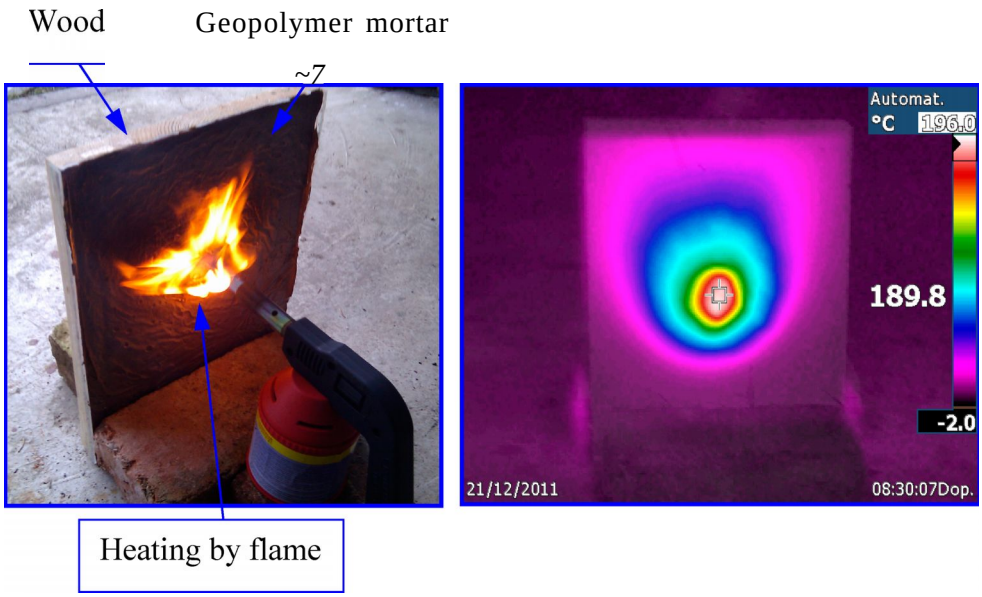


**Fig. 46** Wood coated by geopolymer mortar heating by flame (left) and measured local temperature (right)

# Tanks to contain acid solution


**Fig. 47** Tank made from geopolymer mortar

# Optimal colors

**Fig. 48** Geopolymer mortar with different colors

# Logo of Technistone Company

**Fig. 49** Samples made from fly ash + stone powder + geopolymer

## 6. Conclusions

In this research, geopolymer binders were synthesized from shale fly dust from rotary kiln with a molar Si:Al ratio of 2.0 combined with alkaline silicate solution ($Na_2SO_3$ + NaOH) and using geopolymer binders to produce geopolymer mortar and concrete. Geopolymer binders have many advantages in comparison with than OPC, due to their excellent fire resistance, excellent mechanical properties, environmentally friendly nature and good acid resistance. However the cost of geopolymer mortar and concrete especially geopolymer cement and alkaline is still high, so the main purpose of this study was reduced the cost of geopolymer binders by additive more waste material as fly ash, stone with rich content of Si and Al and extra water in the mixtures but mechanical properties of mortar and concrete is still good enough to meet essential requirements of industries.

Results show that the mechanical properties of geopolymer mortar and concrete are dependant on the chemical composition, types of fly ashes, ratio fly ash / geopolymer cement, curing conditions, addition fibers and other fillers. Using SEM/EDX analysis was carried out to analysis the shape, chemical composition of fly ash particles and microstructure of geopolymers. We can easy see that the strength of geopolymers after milling fly ash and combination with commercial fibers is higher than unmilled fly ash particles and without fibers. They are analyzed detailed as follows:

The chemical composition and properties of all types of fly ash coming from many power station of Czech Republic were investigated. They are different color brown, light grey to black due to its chemical compositions and contaminants. Fly ash particles are generally sharp, pointed, and spherical in shape and range in size from 1 |im to 30 |im. From chapter 6 to 10, the authors were used K6_LF to study, because United Energy Company were supported this material for our research.

We were recognized that extra water lead to decrease amount of alkaline and in the mixtures was significantly reduced the mechanical properties of geopolymer mortar from 30 % to 80 %

with the same curing conditions and components. Based on these test trends, a curing temperature of about 70 $^{o}$C is recommended. In additions, curing time with ranging from 5 to 72 hrs, the rate of increase in strength was rapid up to 48 hrs of curing time. Therefore, heat curing time need not be more than 48 hrs in practical applications for fly ash based geopolymer mortar.

The scope application of fly ash is very limited due to fly ash is grey or black in color. For this reason, a heating method (1000 $^{o}$C) is necessary to increase the whiteness of fly ash. However, the particles after heated 1000 $^{o}$C are reduced mechanical properties of the geopolymer mortar about 20 %. Thus, authors recommended this method use in fine art sculpture, architecture, especially where color is more important than the mechanical properties.

Modification of fly ash particles from micro to nano scale by milling method is significantly increase about 20 % the compressive strength of fly ash based geopolymer with the same component.

For each type of test, after 28 days the compressive strength did not change significantly.

The effect of high temperature on the mechanical properties of geopolymer mortar and concrete are investigated. After heating up to 600 $^{o}$C, the branched cracks appear over the whole surface of the samples. Increasing the percentage of fine sand of mortar or coarse aggregate of concrete will be reduced the shrinkage and micro-cracks.

For environmental conditions testing, geopolymer mortars were immersed in sulfuric acid solution with selected concentrations ranging from 1% to 3% with the measured pH about 1.0. The weight loss, shrinkage and compressive strength are investigated. And the effects of freeze-thaw testing are also reduced about 45 % and 8 % in wet-dry of the compressive strength of geopolymer mortar.

Optimal percentage of Isover granulate (1 %) and basalt (2 %) fibers reinforced geopolymer mortar are given highest results of the flexural properties, however concrete is still remained.

The machinability of fly ash based geopolymer mortar is good with small temperatures generated, cutting force and high durability.

We believe that geopolymer may apply in building and other fields. And utilization of these materials is the energy and resource saving process and it is also indirectly reduce the emission of green - house gas $CO_2$ released from cement manufacturing. This is beneficial for resource conservation and environmental protection.

## 7. References


[1] Rafat, S., *Waste Materials andBy-Products in Concrete.* 2008: Springer, German.

[2] Duxson P., et al., *Geopolymer technology: the current state of the art.* Journal Material Science. 42: p. 2917-2933, 2007.

[3] Palomo, A., *Alkaline activation of metakaolin and calcium hydroxide mixtures: influence of temperature, activator concentration and.* Materials Letters. 47: p. 55-62, 2001.

[4] Rangan, R. V., *Low-calcium fly ash based geopolymer concrete.* Concrete construction Engineering handbook, New York 2007. 2$^{nd}$ ed.

[5] Hardjito D., R. B. V., *Development and properties of low-calcium fly ash-based geopolymer concrete:* Australia p. 103, 2005.

[6] Shuzheng Z., et al., *Novel modification method for inorganic geopolymer by using water soluble organicpolymers.* Lsevier B.V. 58(7-8): p. 1292 - 1296, 2004.

[7] Davidovits, J., *Geopolymer chemistry & application,* ed. Second. 2008: Institute Géopolymer - France. 587.

[8] Duxson P., et al., *The role of inorganic polymer technology in the development of 'green concrete.* Cement and Concrete Research 37: p. 1590 - 1597, 2007.

[9] Zongjin L., et al., *Development of sustainable cementitious materials.* International Workshop on Sustainable Development and Concrete Technology, China: p. 55-76, 2004.

[10] Provis J. L., et al., *Geopolymers for immobilization of $Cr^{6}$+, $Cd^{2}$+, and $Pb^{2}$+.* Hazardous Materials. 157: p. 587-598, 2008.

[11] Provis J. L., et al., *The role of sulfide in the immobilization of Cr(VI) in fly ash geopolymers.* Cement and Concrete Research. 38: p. 681-688, 2008.

[12] Duxson P., et al., *Thermal conductivity of metakaolin geopolymers used as a first approximation for determining gel interconnectivity.* Ind. Eng. Chem. Res. 45(23): p. 7781 - 7788, 2006.

[13] Cheng T. W., et al., *Fire-resistant geopolymer produced by granulated blast furnace slag.* Minerals Engineering 16: p. 205-210, 2003.

[14] Palomo A., et al., *Chemical stability of cementitious materials based on metakaolin.* Cement Concrete Research. 29 (7): p. 997 - 1004, 2004.

[15] Lee W. K. W., et al., *The effect of ionic contaminants on the early-age properties of alkali-activated fly ash-based cements.* Cement Concrete Research. 32 (4): p. 577 - 584, 2006.

[16] Davidovits, J., *Chemistry of Geopolymeric Systems, Terminology.* 2nd International conference 'Géopolymere': p. 9 - 40, 1999.

[17] Davidovits, J., *Geopolymers: Inorganic polymeric new materials.* Journal of Thermal Analysis. 37: p. 1633 - 1656, 1991.

[18] Pereira, C. F., *Waste stabilization/solidification of an electric arc furnace dust using fly ash-based geopolymers.* Fuel. 88: p. 1185-1193, 2009.

[19] Davidovits, J., *30 Years of Successes and Failures in Geopolymer Applications - Market trends and Potential breakthroughs.* Geopolymer 2002 Conference: Melbourne, Australia, 2002.

[20] Carlos A. R. R., et al., *A comparative study of two methods for the synthesis of fly ash-based sodium andpotassium type zeolites.* Fuel. 88: p. 1043-1416, 2009.

[21] Newman J., B. S. C., *Advanced Concrete Technology Processes.* 2003, Elsevier. p. 699.

[22] Lioyd, N. A., *Geopolymer concrete with fly ash.* 2nd International Conference on Sustainable Construction Materials and Technologies. 3: p. 1493 - 1504, 2010.

[23] Ahmed, M. F., *Compressive Strength and Workability Characteristics of Low-Calcium Fly ash-based Self-Compacting Geopolymer Concrete.* World Academy of Science, Engineering and Technology 74, 2011.

[24] Van J., et al., *The effect of composition and temperature on the properties of fly ash-andkaolinite-basedgeopolymers.* Chemical Engineering Journal 89: p. 63 - 73, 2002.

[25] *Chemical properties of quartz.* [cited 2011 20 October]; Available from: http://www.quartzpage.de/gen_chem.html.

[26] Davidovits, J., *Geopolymer chemistry and sustainable Development. The Poly(sialate) terminology: a very useful and simple model.* The International Workshop on Geopolymer Cements and Concrete for the promotion and understanding of green-chemistry, Australia, 2005.

[27] Duxson P., et al., *Structural ordering in geopolymers derived from metakaolin.* Geopolymer chemistry and sustainable Development. 21-25, Australia, 2005.

[28] *C143/C143M, Test Method for Slump of Hydraulic-Cement Concrete.*

[29] *ASTM C78/C78M - 10, Standard Test Method for Flexural Strength of Concrete (Using Simple Beam with Third-Point Loading).* ASTM: p. 1-4, 2010.

[30] *ASTM C348 - 08, Standard Test Method for Flexural Strength of Hydraulic-Cement Mortars.* p. 1-6, 2008.

[31] *ASTM C 31/C 31M - 03a, Standard Practice for Making and Curing Concrete Test Specimens in the Field,* . p. 1-5, 2003.
[32] *AS 1012.9 - 1999, Methods of testing concrete - Determination of the compressive strength of concrete specimens, 1999.*
[33] *ASTM A370 - 07a, Standard Test Methods and Definitions for Mechanical Testing of Steel Products.* p. 1-47, 2007.
[34] *ASTM D5882 - 07, Standard Test Method for Low Strain Impact Integrity Testing of Deep Foundations.* p. 1-6, 2007.
[35] Hardjito D., et al., *The stress-strain behaviour of fly ash-based geopolymer concrete.* Developments in mechanics of structures and materials.: p. 831-834, 2005.
[36] *AS 3600, Concrete structures, Australian Standards, 2001.*
[37] Carrasquillo, R. L., et al., *Properties of high strength concrete subjected to short term loads.* ACI Materials. 78: p. 171-178, 1981.
[38] Ahmad, S. H., *Structural properties of high strength concrete and its implication for precastpre-stressedconcrete.* PCI Journal. 30: p. 92-119, 1985.
[39] *ACI Committee 363, State of the art of high strength concrete. American Concrete Institute, Detroit, USA, 1993.*
[40] Kohei N., et al., *Mesoscopic simulation of failure of Mortar and Concrete by 2D RBSM.* Advanced Concrete Technology. 2: p. 359 - 374, 2004.
[41] Erdogdu, K., *Effects of fly ash particle size on strength of Portland cement fly ash mortars.* Cement and Concrete Researchs. 28: p. 1217-1222, 1998.
[42] Nugtere, H.W., et al., *High strength geopolymers producedfrom coal combustion fly ash.* Global NEST Journa. 11: p. 155-16, 2009.
[43] Chindaprasirt P., et al., *High-Strength Geopolymer Using Fine High-Calcium Fly Ash.* Journal of Materials in Civil Engineering 23: p. 2011.
[44] Mohd, M.A.B., et al., *Review on fly ash-based geopolymer concrete without Portland Cement.* Journal of Engineering and Technology Research. 3: p. 1-4, 2011.
[45] Horiuchi S, et al., *Effective use of fly ash slurry as fill material.* Journal of Hazardous Materials. 76: p. 301-37, 2000.
[46] Yang, H.F., *Reuse and Recycle of Solid Waste.* Chemical Industry Press. Press 165: p. 2003.
[47] Neville, A. M., *Properties of Concrete.* Fourth Edition (Low Priced Edition), Pearson Education Asia Publishing Limited, England,.Produced by Longman Malaysia: p. 7, 2000.
[48] Souradeep, G., *Durability of Flyash Based Geopolymer Concrete.* Civil engineering.
[49] John, N., *Advanced Concrete Technology: Concrete Properties:* Elsevier Ltd., Science and Technology Rights Department in Oxford, UK. 349, 2003.
[50] Wallah, S.E., *Creep behaviour of fly ash-based geopolymer concrete.* Civil Engineering Dimension Publisher, 2010.
[51] Davidovits, J., *Personal Communication on Geopolymer Chemistry, 2005.*
[52] Davidovits, J., *Geopolymer Chemistry and Properties* First European Conference on Soft Mineralurgy, France, 1988.

## 8. Publications of author

### A. Book chapter

Tran Doan Hung, Petr Louda, Dora Kroisová, Oleg Bortnovsky, **Nguyen Thang Xiem,** "New Generation of Geopolymer Composite for Fire-Resistance", Advances in Composite Materials - Analysis of Natural and Man-made Materials, Editor Pavla Tesinova, pp. 73 - 92, Published by InTech, Croatia 2011. ISBN 978-953-307-449-8.

**B. Journals**

1. **Xiem Nguyen Thang,** Petr Louda, Dora Kroisova, Trung Nguyen Duc, Thien Nguyen, "The influence of modified fly ash particles by heating on the compressive strength of geopolymer mortar", Journal of Chemiské listy, accepted. ISSN 0009-52770.
2. **Xiem Nguyen Thang,** Petr Louda, Dora Kroisova, Vladimir Kovaci, Hiep Le Chi, Nhut Luu Vu, "Effects of commercial fibers reinforced on the mechincal properties of geopolymer mortar", Journal of Chemiské listy, accepted. ISSN 0009-52770.
3. **Xiem Nguyen Thang,** Petr Louda, Dora Kroisova, "Thermophysical properties of woven fabrics reinforced geopolymer composites", World Journal of Engineering, submitted for publication.
4. Vijay Baheti, **Xiem Nguyen Thang,** Jiri Militky, Petr Louda, "Influence of wet milling of fly ash on compression strength of geopolymer mortar cured at room temperature", World Journal of Engineering, submitted for publication.
5. **Xiem Nguyen Thang,** Dora Kroisová, Petr Louda, Oleg Bortnovsky: "Microstructure and Flexural Properties of Geopolymer Matrix-Fiber Reinforced Composite with Additives of alumina (Al2O3) Nanofibres", World Journal of Engineering, volume 7 Supplement 1, 2010, ISBN: 1708-5284.
6. **Xiem Nguyen Thang,** Dora Kroisová, Petr Louda, Oleg Bortnovsky, Petra Prokopčáková, Petra Zdobinská, Pavel Kejzlar: "Moisture and Chemical Resistant of Geopolymer Composites", World Journal of Engineering, volume 7/4, 2010, ISBN: 1708-5284.
7. **N. T. Xiem,** D. Kroisová, P. Louda, T.D. Hung, Z. Rozek (Czech Republic): "Effects of temperature and plasma treatment on mechanical properties of ceramic fibres". Journal of Achievements in Materials and Manufacturing Engineering, JAMME. Volume: 37/2, December 2009, pp. 526-531, ISBN: 1734-8412.

**C. Czech republic patents**

1. Petr Louda, Dora Kroisová, Tran Doan Hung, **Thang Xiem Nguyen,** "Vysokopevnostní geopolymerní kompozit", Publish No: 2011-24194.
2. Petr Louda, Dora Kroisová, Tran Doan Hung, **Thang Xiem Nguyen,** "Vysokopevnostní geopolymerní kompozit", Publish No: 2011-24195.
3. Petr Louda, Dora Kroisová, Tran Doan Hung, **Thang Xiem Nguyen,** "Vysokopevnostní geopolymerní kompozit", Publish No: 2011-24196.
4. Petr Louda, Dora Kroisová, Tran Doan Hung, **Thang Xiem Nguyen,** "Vysokopevnostní geopolymerní kompozit", Publish No: 2011-24197.
5. Petr Louda, Dora Kroisová, Tran Doan Hung, **Thang Xiem Nguyen,** "Vysokopevnostní geopolymerní kompozit", Publish No: 2011-24198.

**D. Conferences**

1. **Xiem Nguyen Thang,** Petr Louda, Dora Kroisova," Thermophysical properties of woven fabrics reinforced geopolymer composites", 18th International conference STRUTEX 2011, Czech Republic (CD version). ISBN-978-80-7372-786-4.
2. Vijay Baheti, **Xiem Nguyen Thang,** Jiri Militky, Petr Louda, "Influence of wet milling of fly ash on compression strength of geopolymer mortar cured at room temperature", 18th International conference STRUTEX 2011, Czech Republic (CD version). ISBN-978-80-7372-786-4.

3. **Xiem Nguyen Thang,** Petr Louda, Dora Kroisova, Trung Nguyen Duc, Thien Nguyen, "The influence of modified fly ash particles by heating on the compressive strength of geopolymer mortar", 8th International Conference LMP 2011, Oloumoc - Czech Republic, pp. 82, ISBN: 978-80-244-2889-5.

4. **Xiem Nguyen Thang,** Petr Louda, Dora Kroisova, Vladimir Kovaci, Hiep Le Chi, Nhut Luu Vu, "Effects of commercial fibers reinforced on the mechincal properties of geopolymer mortar", 8th International Conference LMP 2011, Oloumoc - Czech Republic, pp. 83, ISBN: 978-80-244-2889-5.

5. Linh Trinh Thi, Dora Kroisova, Petr Louda, **Nguyen Thang Xiem,** Pavel Kejzlar, "Compressive strength of fly ash based geopolymer adding nanofiber", Workshop pro doktorandy FS a FT TUL, September 2011, Czech Republic, pp. 253 - 257, ISBN: 978-80-7372-765-9.

6. **N. T. Xiem,** P. Louda, D. Kroisová, L. C. Hiep, L. V. Nhut, N. D. Trung, N. V. Q. Thien, "Možnosti průmyslového využití geopolymerních materialů v konstrukce", Workshop pro doktorandy FS a FT TUL, September 2011, Czech Republic, pp. 288 - 293, ISBN: 978-80-7372-765-9.

7. **N. T. Xiem,** P. Louda, D. Kroisová, "Effect of curing on the mechanical properties of geopolymer mortar incorporating different fly ash content", IXth International Conference Preparation of Ceramic Materials, June 2011, Slovakia, pp. 89 - 93, ISBN: 978-80-553-0678-0.

8. **N. T. Xiem,** P. Louda, D. Kroisova, O. Bortnovsky: "Effects of high temperature on the mechanical properties of fly ash and stone powder based geopolymer materials", 18th International Students' Day of Metallurgy, March 2011, Austria, pp. 460 - 467, ISBN: 978-3-200-02155-6.

9. **Xiem Nguyen Thang,** Dora Kroisová, Petr Louda, Oleg Bortnovsky: "Influence of chemical reagent on flexural properties of geopolymer composites", the 9th Workshop on Polymer Processing. December 2010, Hanoi - Vietnam. Publishing licence No: 215-2010/CXB/146.1-17/KHKT.

10. **Xiem Nguyen Thang,** Dora Kroisová, Petr Louda, Oleg Bortnovsky: "Microstructure and Flexural Properties of Geopolymer Matrix-Fiber Reinforced Composite with Additives of alumina ($Al_2O_3$) Nanofibres" 7th Textile science International Conference (TEXSCI 2010). Liberec - Czech Republic, September 2010, ISBN: 978-80-7372-635-5 (CD version).

11. **Xiem Nguyen Thang,** Dora Kroisová, Petr Louda, Oleg Bortnovsky, Petra Prokopčáková, Petra Zdobinská, Pavel Kejzlar: "Moisture and Chemical Resistant of Geopolymer Composites" 7th Textile science International Conference (TEXSCI 2010). Liberec - Czech Republic, September 2010, ISBN: 978-80-7372-635-5 (CD version).

12. **N. T. Xiem,** D. Kroisová, P. Louda, Z. Rozek, and O. Bortnovsky: "Influence of Plasma Treatment on the Flexural Properties of Geopolymer Composites", 2nd RMUTP International Conference: Green Technology and Productivity. Bangkok, Thailand, pp. 253-259, June 2010, In press.

13. **Xiem Nguyen Thang,** Dora Krosová, Petr Louda, Hung Tran Doan, Zbigniew Rožek, Oleg Bortnovsky: "Effects of plasma treatment on mechanical properties of commercial fibers based on Geopolymer matrix composites", 16th International Conference Strutex structure and structural mechanics of textiles. Liberec - Czech Republic, December 2009, ISBN: 978-80-7372-542-6 (CD version).

14. Hung Tran Doan, Dora Kroisová, Petr Louda, **Xiem Nguyen Thang,** Oleg Bortnovsky, Petr Bezucha: "Effect of temperature of curing on flexual properties of thermal silica

based geopolymer-carbon fiber as reinforcement. 4th International Conference on Vacuum and Plasma Surface Engineering (VaPSE 2009). Liberec - Czech Republic, Octorber 2009, pp. 43, ISBN 978-80-7372-524-2 (CD version).

15. **Xiem Nguyen Thang,** Dora Kroisová, Petr Louda, Hung Tran Doan, Zbigniew Rozek, "Effects of temperature and plasma treatment on mechanical properties of ceramic fibers". 4th International Conference on Vacuum and Plasma Surface Engineering (VaPSE 2009). Liberec - Czech Republic, Octorber 2009, pp. 59, ISBN 978-80-7372-524-2.

16. Hung, T. D., Kroisová, D., Bortnovsky, O., Louda, P., and **Xiem, N. T.** "Primary abilities of thermal sustainment of composites based on geopolymer matrices". 3rd International Conference on Vacuum and Plasma Surface Engineering (VaPSE 2008). Liberec - Czech Republic, October 2008, pp. 69, ISBN 978-80-7372-398-9.